USGS science for a changing world

CGS CALIFORNIA GEOLOGICAL SURVEY

The Search for Geologic Evidence of Distant-Source Tsunamis Using New Field Data in California

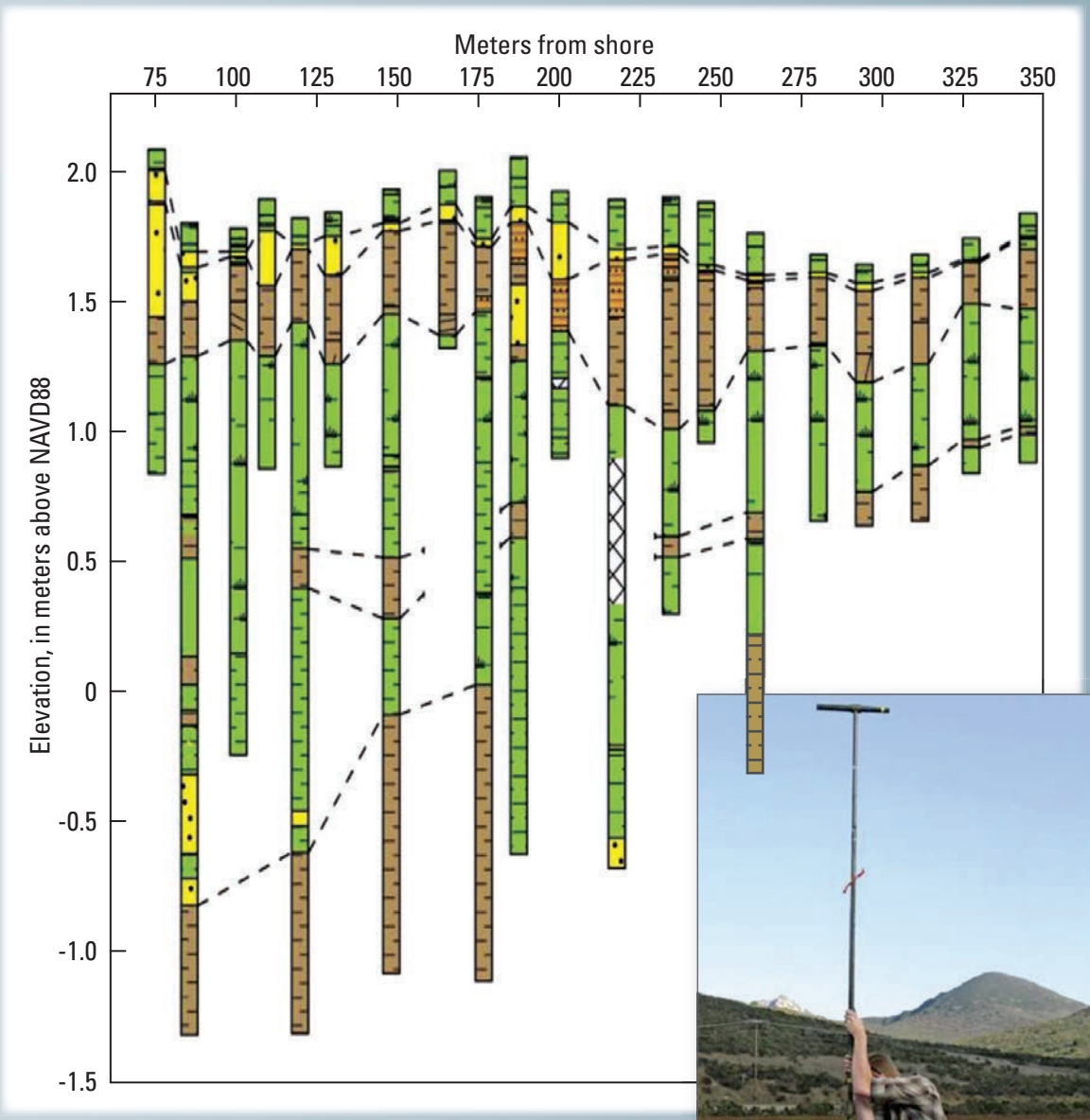

Open-File Report 2013–1170–C
California Geological Survey Special Report 229

U.S. Department of the Interior
U.S. Geological Survey

FRONT COVER: A photograph of two scientists collecting gouge core samples in the field, a photograph of a core containing the 1946 tsunami deposit (upper sand unit) at Half Moon Bay, and a figure showing correlations between layers in cores along a transect.

The SAFRR (Science Application for Risk Reduction) Tsunami Scenario

Stephanie Ross and Lucile Jones, Editors

The Search for Geologic Evidence of Distant-Source Tsunamis Using New Field Data in California

By Rick Wilson, Eileen Hemphill-Haley, Bruce Jaffe, Bruce Richmond, Robert Peters, Nick Graehl, Harvey Kelsey, Robert Leeper, Steve Watt, Mary McGann, Don Hoirup, Catherine Chagué-Goff, James Goff, Dylan Caldwell, and Casey Loofbourrow

Open-File Report 2013-1170–C

California Geological Survey Special Report 229

U.S. Department of the Interior
U.S. Geological Survey

U.S. Department of the Interior
SALLY JEWELL, Secretary

U.S. Geological Survey
Suzette M. Kimball, Acting Director

U.S. Geological Survey, Reston, Virginia 2014

Suggested citation:
Wilson, R., Hemphill-Haley, E., Jaffe, B., Richmond, B., Peters, R., Graehl, N., Kelsey, H., Leeper, R., Watt, S., McGann, M., Hoirup, D., Chague-Goff, C., Goff, J., Caldwell, D., and Loofbourrow, C., 2014, The search for geologic evidence of distant source tsunamis using new field data in California, chap C of Ross, S.L., and Jones, L.M., eds., The SAFRR (Science Application for Risk Reduction) tsunami scenario: U.S. Geological Survey Open-File Report 2013-1170-C, 122 p., http://dx.doi.org/10.3133/ofr20131170c.

ISSN 2331-1258 (online)

STATE OF CALIFORNIA
EDMUND G. BROWN, JR.
GOVERNOR

THE NATURAL RESOURCES AGENCY
JOHN LAIRD
SECRETARY FOR RESOURCES

DEPARTMENT OF CONSERVATION
MARK NECHODOM
DIRECTOR

CALIFORNIA GEOLOGICAL SURVEY
JOHN G. PARRISH, Ph.D.
STATE GEOLOGIST

Page intentionally left blank

Contents

Figures

Tables

The Search for Geologic Evidence of Distant-Source Tsunamis Using New Field Data in California

By Rick Wilson,[1] Eileen Hemphill-Haley,[2] Bruce Jaffe,[3] Bruce Richmond,[3] Robert Peters,[4] Nick Graehl,[5] Harvey Kelsey,[2] Robert Leeper,[3] Steve Watt,[4] Mary McGann,[3] Don Hoirup,[6] Catherine Chagué-Goff,[7] James Goff,[8] Dylan Caldwell,[2] and Casey Loofbourrow[2]

Abstract

A statewide assessment for geological evidence of tsunamis, primarily from distant-source events, found tsunami deposits at several locations, though evidence was absent at most locations evaluated. Several historical distant-source tsunamis, including the 1946 Aleutian, 1960 Chile, and 1964 Alaska events, caused inundation along portions of the northern and central California coast. Recent numerical tsunami modeling results identify the eastern Aleutian Islands subduction zone as the "worst-case" distant-source region, with the potential for causing tsunami runups of 7–10 m in northern and central California and 3–4 m in southern California. These model results, along with a review of historical topographic maps and past geotechnical evaluations, guided site selection for tsunami deposit surveys. A reconnaissance of 20 coastal marshlands was performed through site visits and coring of shallow surface sediments to determine if evidence for past tsunamis existed. Although conclusive evidence of tsunami deposits was not found at most of the sites evaluated, geologic evidence consistent with tsunami inundation was found at two locations: Three marshes in the Crescent City area and Pillar Point marsh near Half Moon Bay. Potential tsunami deposits were also evaluated at the Carpinteria Salt Marsh Reserve in Santa Barbara County. In Crescent City, deposits were ascribed to tsunamis on the basis of stratigraphic architecture, particle size, and microfossil content, and they were further assigned to the 1964 Alaska and 1700 Cascadia tsunamis on the basis of dating by cesium-137 and radiocarbon methods, respectively. The 1946 tsunami sand deposit was clearly identified throughout Pillar Point marsh, and one to two other similar but highly discontinuous sand layers were present within 0.5 m of the surface. A tsunami-origin interpretation for sand layers at Carpinteria is merely consistent with graded bedding and unsupported by diatom or foraminiferal assemblages. Additional studies, including age dating, grain-size, and microfossil analyses are underway for the deposits at Crescent City, Pillar Point marsh, and Carpinteria, which may help further identify if other tsunami deposits exist at those sites. The absence of evidence for tsunamis at other sites examined should not preclude further work beyond the reconnaissance-level investigations at those locations.

[1]California Geological Survey.
[2]Humboldt State University.
[3]U.S. Geological Survey.
[4]U.S. Geological Survey (contractor).
[5]Humboldt State University; now Lettis Consultants International.
[6]California Department of Water Resources.
[7]University of New South Wales and Australian Nuclear Science and Technology Organisation.
[8]University of New South Wales.

Introduction

A key element to determining the impact from a possible large, distant-source tsunami similar to the Science Application for Risk Reduction (SAFRR) tsunami scenario is evaluating the evidence and impacts from past tsunamis. Developing a better understanding of the number and size of past events will improve the ability of scientists to determine how often tsunamis are likely to occur in California in the future. Although analysis of historical records can demonstrate the severity of particular tsunamis along specific portions of the coast, California's documented history only goes back to the time of establishment of the Spanish missions in the late 1700s. Prehistoric geological evidence of tsunamis would provide better constraints on the magnitude and frequency of these past events.

As part of the SAFRR scenario project, both historical and prehistoric tsunamis were evaluated. Specialists from the U.S. Geological Survey (USGS), Humboldt State University (HSU), California Geological Survey (CGS), and other organizations conducted a statewide assessment of known tsunamis and field investigations to find geological evidence of tsunamis, primarily distant-source events. A significant amount of work has been completed and cataloged for areas north of Cape Mendocino, where deposits from tsunamis generated by great (*M*8–9) local earthquakes along the southern Cascadia subduction zone are captured in coastal marshes that characteristically have undergone tectonic subsidence coincident with the earthquake (Abramson, 1998; Garrison-Laney, 1998; Patton, 2004; Peterson and others, 2011). In California, tsunami deposits typically consist of laterally extensive sand deposits or other evidence indicative of high-energy coastal flood events, buried within peat and mud deposits normally found in low-energy, coastal marsh settings. Microfossil assemblages and grain-size distribution and provenance of the sand are also key indicators of tsunami deposits. The relation between buried (subsided), wetland soil layers and overlying tsunami deposits is one of the classical ways scientists are able to confirm that these sands were indeed generated by a local-source tsunami.

Tsunamis generated far from California, in such areas as Alaska or the Aleutian Islands, can be more difficult to identify from sand sheets in California marshes because these marshes do not subside during the distant earthquake in the tsunami source area. Tsunami sands have less chance to be captured and preserved at marshes in areas of the coast south of Cape Mendocino, where local earthquakes that cause tectonic subsidence is are absent. In addition, there are few documented examples of long-lasting sandy deposits that were deposited by a tsunami on shores far from its source. Disruption of the natural coastal marsh sediments by development and other human influences also reduces the potential for undisturbed tsunami deposits to be found. For these reasons, there have only been a limited number of studies looking specifically for tsunami deposits in central and southern California, where large local sources are not as prevalent and generally do not involve subsidence. This investigation, which is part of the SAFRR project, with Wilson, Hemphill-Haley, Jaffe, and Richmond as co-principal investigators, is currently the most comprehensive California study to be undertaken.

The objective of this report is to review the tsunami history of California and present findings from new field investigations in search for evidence of past tsunamis, particularly deposits from Aleutian-Alaska tsunami sources. Although there may be other local (offshore thrust faults and submarine landslides) and distant (Chile, Japan, Kuril Islands, and others) tsunami sources capable of causing tsunami deposits in California, relating suspect tsunami deposits to known Aleutian-Alaska seismic/tsunami events is here a priority. A thorough evaluation of large tsunami events over the past several hundred years was initiated in order to determine where distant-source tsunami deposits might be present along California's coast. Numerical tsunami inundation model results, literature review, coastal imagery, and historical topographic data were used to determine the most promising sites for reconnaissance fieldwork. Based on this initial evaluation, several coastal wetland locations were identified for detailed site investigations and sample analysis. Although all analyses and interpretations have not been completed, the initial findings of the project are presented in this report. It should be noted

that most of the findings presented herein are the result of consensus amongst all the project coauthors, with multiple hypotheses provided where appropriate.

Significant Historical Tsunamis

Though California has a limited historical written record (~200 years), more than 80 tsunami events have been described and (or) recorded since the early 1800s (McCulloch, 1985; Lander and others, 1993; California Seismic Safety Commission, 2005; Wilson and others, 2013). Although most of these tsunamis were relatively small and only documented by tidal gauges, at least 14 were reported to have caused damage and (or) casualties in California. Because of the dramatic increase in the coastal population and construction in the State over the past 70 years, there has also been an increase in the occupation and vulnerability of waterfront areas. During these seven decades, eight distant-source tsunamis have caused damage and (or) casualties. Table 1 provides information about these eight events for five locations in California. Among these eight events are three tsunamis (1946, 1957, and 1964) that originated along the Aleutian-Alaska subduction zone, the same region of the SAFRR tsunami scenario source.

Table 1. Historical tsunami impacts in California from significant distant-source events over the past 70 years.
[NGDC, National Geophysical Data Center; *M*, earthquake magnitude; M, million]

Significant Historical Distant Source Tsunamis (year-magnitude-source location)	Tsunami Amplitudes for Historical Events, from NGDC Database (in meters above normal tide conditions; "-" means no data available)					Effects in California (damage value is presented in constant dollars, not adjusted for inflation)
	Crescent City	San Francisco	Half Moon Bay	Port of Los Angeles	San Diego Bay	
1946 *M*8.1 Eastern Aleutian Islands	0.9	0.3	2.6	0.4	0.2	One fatality; significant inundation in Half Moon Bay; damage approached several million dollars
1952 *M*9.0 Kamchatka	0.9	0.5	-	0.3	0.3	Damage approached a million dollars
1957 *M*8.6 Western Aleutian Islands	0.7	0.3	-	0.2	0.5	Damage was minimal
1960 *M*9.5 Chile	2.0	0.5	2.2	0.5	1.2	Two fatalities; inundation in Crescent City; damage approached several million dollars
1964 *M*9.2 Alaska	4.8	1.1	2.0	0.5	2.0	Thirteen fatalities; significant inundation in Crescent City; damage approached $20M
2006 *M*8.3 Kuril Islands	0.9	0.2	-	0.1	0.1	Damage to docks in Crescent City approached $20M
2010 *M*8.8 Chile	0.6	0.3	0.6	0.4	0.6	Damage to 12 harbors approached $3M
2011 *M*9.0 Japan	2.5	0.6	0.7	0.5	0.9	One fatality; damage to 27 harbors approached $100M
Numerical Modeling of SAFRR Aleutians Scenario	4.3	2.2	4.4	1.2	1.4	Projected: Inundation widespread; damage exceeds several billion dollars

Historical tsunamis known to have caused inundation in California could also have produced tsunami deposits in coastal marshes. Five events, two from local earthquake sources and three from distant source events, were considered significant in this evaluation:

January 26, 1700.—An earthquake with an estimated magnitude of 9 probably ruptured most if not all of the 1,100-km length of the Cascadia subduction zone, including segments offshore of California north of Cape Mendocino (Satake and others, 2003). Though there were no local written accounts, scientists originally recognized the event from geological evidence and oral histories from the Native American people in the area (Ludwin and others, 2005). This information was cross-referenced with Japanese documents describing an "orphan" tsunami that was not accompanied by a large earthquake in Japan (Atwater and others, 2005). The exact date and time of this earthquake are known because of a combination of tsunami deposit evidence, ^{14}C and tree-ring dating, tsunami modeling, and the historical Japanese information. Paleoseismic and paleotsunami deposits from this event have been found in a number of marshes, ponds, and lakes from Cape Mendocino north to British Columbia. In California, these locations include Lagoon Creek Pond and several marshes in and around Crescent City (Abramson, 1998; Garrison-Laney, 1998; Peterson and others, 2011). Reference-level and detailed databases of these tsunami deposits have been developed by SAFRR project participants (Peters and others, 2003; Wilson and others, 2010 and 2012).

December 21, 1812.—A tsunami struck the Santa Barbara and Ventura County coastline in southern California shortly after a large earthquake (M>7) was felt in the area. Although reports of the size of this tsunami have been debated, the event was large enough to inundate lowland areas and cause damage to nearby ships (Trask, 1856; Lander and others, 1993). One theory is that the tsunami was caused by a nearby submarine landslide triggered by the earthquake (Greene and others, 2006). Several wetlands along the Santa Barbara and Ventura coastlines might have been inundated by this tsunami.

April 1, 1946.—A Pacific-wide tsunami was generated by tectonic displacement and potential added displacement of a large-scale landslide mass associated with a magnitude 8.1 earthquake just south of the Aleutian Islands (Fryer and others, 2004; López and Okal, 2006). The 1946 tsunami killed 159 people in Hilo Bay, leading to the formation of the Pacific Tsunami Warning Center in Hawaii. It also caused damage and one fatality along the coast of California and inundated more than 300 m inland at Half Moon Bay on the central coast of California (Lander and others, 1993). Chagué-Goff and others (2012) discovered tsunami deposits from the 1946 event in Pololu Valley on the northeast coast of the Island of Hawaii.

Figure 1 shows a number of photographs taken at Half Moon Bay shortly after the 1946 tsunami, each helping demonstrate the possibility of tsunami deposit production (Orville Magoon, private photo collection). Figure 1*A* shows tsunami surge levels on a house near the bay, supporting reports that tsunami flood levels were 2 to 4 m in places. Figure 1*B* shows large pieces of rock and debris that were moved from the shoreline inland. Figure 1*C* shows that beaches were denuded of sands, which presumably provided the sediment for landward deposition in the marsh. Figure 1*D* shows a fishing boat and debris that were deposited on the seaward side of Pillar Point marsh within Half Moon Bay. Locations and view angles for the photographs in figure 1 are shown in the post-tsunami aerial photograph, figure 2. Note that debris and possibly sand from the tsunami still appear in figure 2 (taken approximately 3 months after the tsunami) and that there are drainage channels apparent on the upper beach.

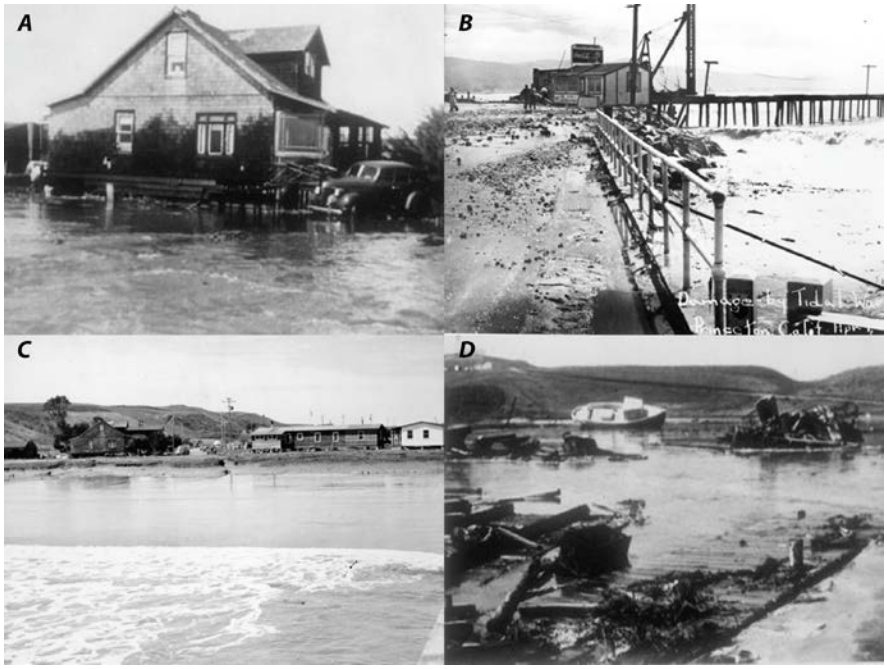

Figure 1. Photographs of the Half Moon Bay area following the April 1, 1946, tsunami (Orville Magoon, private photo collection). The view angles of the photos are shown in figure 2. *A*, Showing tsunami surge levels on a house near the bay. *B*, Large pieces of rock and debris that were moved from the shoreline inland. *C*, A beach denuded of sand. *D*, Ships and debris moved inland near Pillar Point Marsh within the bay.

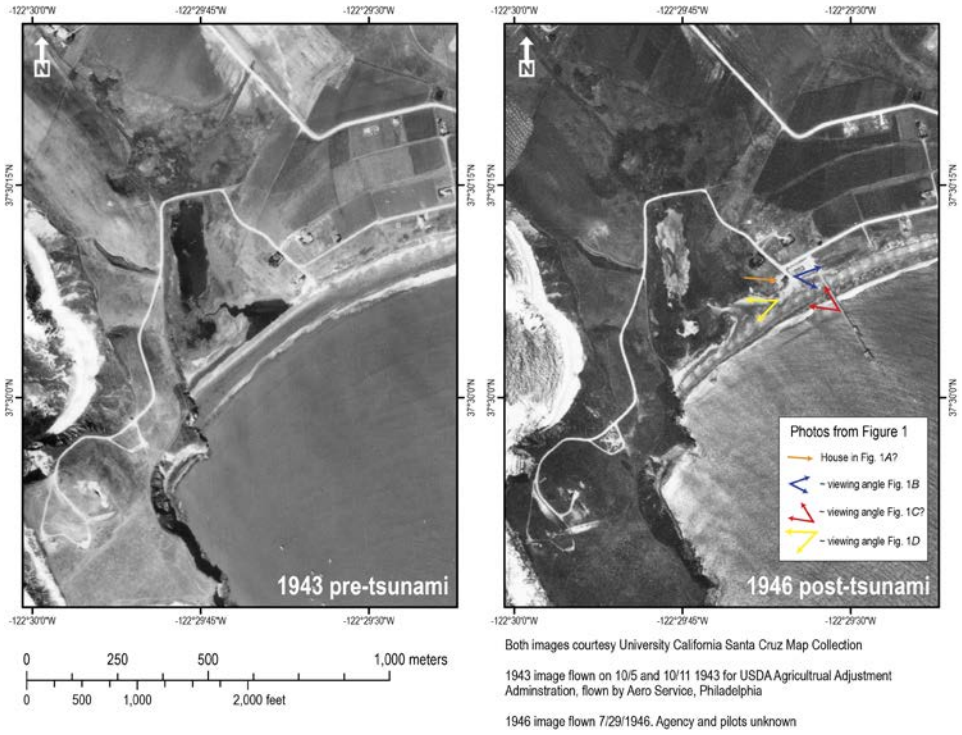

Figure 2. Aerial photographs taken at Half Moon Bay before and after the 1946 tsunami. Locations and view angles for photographs shown in figure 1 are shown in the post-tsunami photograph. Note that there appears to be sand in the lagoon and pond in the post-tsunami photograph (taken approximately 3 months after the tsunami) and that there are drainage channels apparent on the upper beach.

May 22, 1960.—The largest recorded historical earthquake, a magnitude 9.5 occurring off the coast of Chile, triggered a tsunami that traveled across the Pacific Ocean. The teletsunami energy was focused in a northwesterly direction, resulting in 61 deaths in Hawaii and 138 deaths in Japan (Atwater and others, 1999). In California, the tsunami caused damage to harbors along the entire coast (Lander and others, 1993). Figure 3 is a photograph (Orville Magoon archives) taken during the tsunami showing inundation of waterfront areas in Crescent City. Peterson and others (2011) found a silty debris layer in Anchor Way Marsh in Crescent City at a depth consistent with deposition from the 1960 tsunami, indicating that coastal wetlands in Crescent City may have been flooded by this event.

Figure 3. Photograph of Crescent City Wharf during the 1960 tsunami (Orville Magoon, private photo collection).

March 27, 1964.—A magnitude 9.2 earthquake occurred in the region offshore from and under Alaska, generating a tsunami that arrived in California about 4 hours later. This destructive tsunami flooded 29 city blocks in Crescent City (fig. 4; Orville Magoon archives) and damaged harbors and port facilities statewide. The event was responsible for 13 deaths in California. Peterson and others (2011) identified debris and possible sand deposits from this event within coastal marshes near Crescent City. Deposits from the 1964 tsunami were also identified in Seaside, Oregon (González and others, 2009), and Clague and others (1994) identified a sand layer deposited by the 1964 tsunami in Port Alberni, British Columbia.

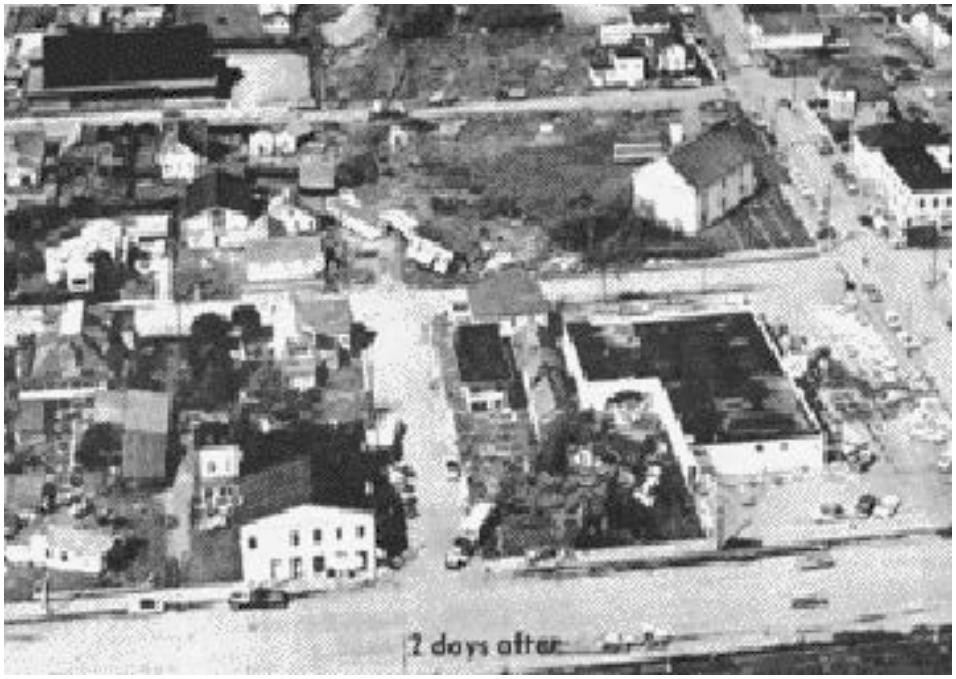

Figure 4. Aerial photograph of Crescent City following the 1964 tsunami (Orville Magoon, private photo collection).

One other potential significant historical event is the eastern Aleutian Islands earthquake and tsunami of July 11, 1788. Soloviev (1968) suggested that, based on the reports of strong ground shaking and local tsunami heights ranging from 5 to 30 meters, the fault rupture appears to have been 600 kilometer long, rivaling that of the SAFRR scenario source. Recent paleoseismic and paleotsunami-deposit studies in the Aleutian Islands have not yet confirmed the extent and impact of the 1788 tsunami, though those studies are still in early stages (Alan Nelson, Harvey Kelsey, Guy Gelfenbaum, and Rob Witter, written commun., 2013; Nelson and others, 2012). Although there is no mention of the 1788 tsunami in Spanish mission records in California, the size and location of the earthquake and tsunami source demonstrate the potential for producing a large distant-source tsunami along the coast of California. Due to its similarity to the source region of the SAFRR scenario, the 1788 tsunami became a potential target event for tsunami-deposit work in this study.

Tsunami Deposit Investigation

Because of the relatively short historical record, a statewide tsunami-deposit investigation was initiated in an attempt to: (1) extend the record of tsunami events, (2) evaluate the severity of tsunamis along the coast, and (3) determine if evidence of large Aleutian-Alaska Island source tsunamis exists in the paleorecord. As previously mentioned, distant-source tsunami deposits are more difficult to find because of the lack of coseismic subsidence, distinct buried soils, and other factors. However, the distant-source tsunamis of 1946 and 1964 demonstrated that significant tsunami inundation and strong, forceful surges can be generated by events originating from the Aleutian-Alaska subduction zone. This type of information is not only important to substantiate the significance of the Aleutian Island-Alaska tsunami source region, it is also vital to understanding the long-term vulnerability of the California coast.

Site Selection

A significant challenge for this project was to find the ideal locations along the coast where distant-source tsunami deposits could be found. Many wetlands along California's coast have been altered or disturbed by coastal development. A careful evaluation of the coastal wetlands was conducted to determine appropriate locations for fieldwork. The field localities for the study were selected using several criteria, including past geological and geotechnical investigations, numerical inundation modeling results, proximity of the marsh to the shoreline, and extent of undisturbed wetlands.

Existing Geological and Geotechnical Literature

We reviewed reports from previous geological and geotechnical investigations within California coastal marshlands. Although most of these investigations were not focused on tsunami deposits from distant-source events, subsurface explorations at these sites provided a baseline for determining if the site was appropriate for tsunami-deposit exploration. These reports included: (1) Peterson and others' (2011) evaluation of large Cascadia source events in marshes around Crescent City; (2) tsunami deposit work by Hoirup (2006) in Drake's Bay near Point Reyes; (3) Knudsen and others' (2002) investigation of the San Andreas Fault Zone in Bolinas Bay and Bodega Bay; (4) Koehler and others' (2004) evaluation of the San Gregorio Fault Zone near Half Moon Bay; (5) Watson and others' (2011) paleoclimate study in Elkhorn Slough; and (6) Peters and others' (2008) paleotsunami-deposit work in a wetland near Carpinteria in southern California. Of these locations, Crescent City, Drake's Bay, Half Moon Bay, and Carpinteria were given higher priority for further evaluation because they provided the greatest potential for evidence of paleotsunami deposits from distant sources.

Aleutian-Alaska Subduction Zone III (AASZ III) Numerical Tsunami Model

Numerical tsunami model results from the statewide inundation mapping project identified which locations along the coast were most susceptible to inundation from a large Aleutian Islands-Alaska event (Wilson and others, 2008). The premise behind incorporating these data was that, all other factors (tide stage, sediment supply, preservation) being equal, the larger the modeled tsunami heights, the greater the potential that tsunami deposits could be generated. There is consensus among modelers that tsunamis generated from the Aleutian Island-Alaska subduction zone represent the "worst case" conditions in California from a distant source (Wilson and others, 2008; Uslu, 2008; Barberopoulou and others, 2009; Thio, 2010).

The results of the Aleutian-Alaska Subduction Zone III (AASZ III) model provided a starting point for planning the reconnaissance field studies. The model assumes a *M*9.2 earthquake in the central Aleutians subduction zone with a rupture area 800 km by 100 km and stretching from Kodiak to the Shumagin Islands, with an average of 25 m of slip. Although the AASZ III scenario is considered an extreme, upper-bounds event used for evacuation planning purposes (Wilson and others, 2008; Barberopoulou and others, 2009), the use of these modeling results are only meant to provide a basis for relative comparison of tsunami potential along California's coast. The AASZ III model results show tsunami wave heights of 5–10 m in a number of locations along the northern and central California coast, but only 2–4 m along the southern California coast. Wetland areas in northern and central California with the greatest predicted wave heights, therefore, were given a higher priority for tsunami deposit exploration.

Additional Reference Data

After assessing information from previous studies and numerical tsunami modeling, several other digital datasets were used to determine more precise locations for the reconnaissance field studies. In some locations, post-tsunami photos from the 1946, 1960, and 1964 tsunamis helped identify flooded

wetlands along the coast (figs. 1–4). These ground-level photos were cross-referenced with aerial orthophotographs taken before and after the tsunamis to help determine if beach sands had been transported inland. The orthophotographs along with historical topographic maps were compared with modern remote imagery to identify the amount of manmade disturbance that had occurred within the coastal wetlands. Locations where disturbance was minimal or absent were given a higher priority for reconnaissance fieldwork for tsunami deposits.

Tsunami Deposit Identification

Identification of tsunami deposits in cores, channel cutbanks, and trenches at the sites evaluated in this study was based on a set of sedimentary characteristics derived from studies of modern, historical, and prehistoric tsunami deposits. Previous studies have documented tsunami-deposit characteristics and developed identification criteria based on both modern tsunami deposits (Nanayama and others, 2000; Kortekaas and Dawson, 2007; Morton and others, 2007; Bourgeois, 2009; Peters and Jaffe, 2010a; Jagodowski and others, 2012) and paleotsunami deposits (Nelson and others, 1996; Dawson and Shi, 2000; Schlichting and Peterson, 2006; Peters and others, 2007). Goff and others (2012) and Chagué-Goff and others (2011) describe advances in tsunami-deposit identification techniques using multiproxy analyses. Tsunami deposit characteristics have been derived from inverse modeling of tsunami depositional processes (Jaffe and Gelfenbaum, 2007; Moore and others, 2007; Soulsby and others, 2007, Jaffe and others, 2012). Other potential sources for coarse-grained deposits, such as large coastal storms, need to be considered in this evaluation. Several studies have addressed the issue of distinguishing tsunami deposits from storm deposits (Nanayama and others, 2000; Goff and others, 2004; Tuttle and others, 2004; Kortekaas and Dawson, 2007; Morton and others, 2007). Based on these studies, we adapted a set of tsunami-deposit identification criteria to be used on the California coast.

Sedimentary characteristics used in the identification of tsunami deposits include the following:

Coarse-Grained Sediments.—Transport and deposition of sand is characteristic of high-energy processes, including tsunamis. If coarser grained sediments are available, such as gravel or boulders, tsunamis may be capable of transporting and depositing these as well (Richmond and others, 2011). In coastal marshes, ponds, or lagoons, anomalous sand layers contrast with the peat and mud that typically characterizes deposition in these low-energy environments. Tsunamis also transport and deposit fine-grained sediments, and mud may be present within a tsunami deposit, between layers of a tsunami deposit, or as a cap at the top of the tsunami deposit. A tsunami deposit may consist entirely of mud (Richmond and others, 2012). However, a tsunami deposit consisting of mud may be difficult to distinguish from the fine-grained sediments typical of low-energy environments.

Geometry.—Large tsunamis typically deposit sediment in extensive, landward-thinning sheets (Peters and Jaffe, 2010a; Richmond and others, 2012). In a smaller tsunami, the tsunami deposit may be limited in extent or present only on or near tidal channel banks. In Seaside, Oregon, deposits from the 1964 Alaska tsunami were only preserved near the banks of the Necanicum River and Neawanna Creek (Gonzalez and others, 2009).

Lateral Continuity.—Sheet-like deposition results in lateral continuity, and the deposit will be present in adjacent cores. When a sand layer is found that is potentially a tsunami deposit, cores are taken nearby to trace the extent and lateral continuity of the deposit. As with geometry, lateral continuity may also be limited in a smaller tsunami.

Sharp or Erosional Basal Contact.—A sharp basal contact suggests an event-driven process. An erosional contact indicates a high-energy process. Tsunamis are high-energy events capable of erosion. Peters and Jaffe (2010a) in developing tsunami-deposit identification criteria based on a database of modern tsunamis (Peters and Jaffe, 2010b), found that a sharp basal contact was the only sedimentary characteristic that all of the tsunami deposits had in common.

Thickness.—The thickness of tsunami deposits typically ranges from <1 cm to 30 cm thick. Tsunami deposit thickness may exceed 20 cm, particularly in swales or depressions, but tsunami deposits greater than 30 cm thick are less common (Peters and Jaffe, 2010a; Richmond and others, 2012).

Normal Grading/Suspension Grading.—Sediments that become finer grained upwards are termed "normally graded." Normal grading is commonly found in both paleo- and modern tsunami deposits (Shi and others, 1995; Minoura and others, 1997; Gelfenbaum and Jaffe, 2003; Jaffe and others, 2003; Jaffe and others, 2006; Szczuciński and others, 2006; Moore and others, 2006; Peters and others, 2007; Hawkes and others, 2007; Hori and others, 2007; Morton and others, 2007; Choowong and others 2008; Bourgeois, 2009, and references therein; Fujino and others, 2010; Peters and Jaffe, 2010a, and references therein). Suspension grading, a specific type of normal grading that forms as sediments settle out of turbulent suspension, is found in tsunami deposits and discussed below in the section on "Suspension Grading in Tsunami Deposits."

Landward Fining.—The grain size of sediments deposited by tsunamis typically fines landward. Landward fining results from the decreasing velocity of the tsunami as it moves inland (Moore and others, 2007; Peters and Jaffe, 2010a).

Composition.—Tsunamis may entrain sediment from many environments, including the nearshore, beach, dune, channels, and the marsh itself. Tsunami deposits will contain sediment from one or more of the environments where sediment was entrained. A deposit containing sediment from coastal or nearshore environments indicates a marine source, consistent with tsunami deposition.

Angularity.—Rounded grains are typical of dunes and other coastal systems where the sand has been transported long distances and reworked in a high-energy environment. Angular grains are consistent with short transport in a fluvial system. However, beach systems may also contain angular grains. Comparison of grain angularity with sediments from possible sediment sources may help determine the provenance of the candidate tsunami sediments.

Rip-Up Clasts.—Rip-up clasts are clasts of muddy substrate torn up by a tsunami that are preserved in a sand layer. Rip-up clasts have been observed in several modern tsunami deposits (Peters and Jaffe, 2010a). Rip-up clasts are less likely to be preserved in a storm deposit, because prolonged re-working by waves breaks down the mud clasts.

Organics.—Organic material is often present within a tsunami deposit or capping the top of the deposit (Peters and Jaffe, 2010a; Richmond and others, 2011). This may consist of wood or other plant material entrained and transported by the tsunami. Marsh plants or coastal grasses buried by sand may also be present at the base of a tsunami deposit, sometimes bent over in the direction of flow (Morton and others, 2011).

Microfossils.—Tsunami deposits may contain coastal or marine diatoms or foraminifera (Hawkes and others, 2007; Hemphill-Haley, 1996; Sawai and others, 2009), but in some instances, marine or coastal diatoms and foraminifera may be rare or absent in a tsunami deposit (Pilarczyk and others, 2012, Szczuciski and others, 2012). Microfossils in a tsunami deposit are indicative of the sediment sources. Therefore, the presence of marine or coastal microfossils indicates a marine or coastal sediment source, consistent with a tsunami, but the absence of marine or coastal microfossils does not necessarily exclude tsunami deposition.

Tsunami deposits may meet one or more of these criteria, but may not show all of the characteristics consistent with tsunami deposition. In addition, many of the sedimentary characteristics consistent with tsunami deposition may also be consistent with other depositional processes.

Storm deposits have many features that are shared with tsunami deposits. Storm and tsunami deposits are derived from similar sediment sources, may be similar in composition and texture, and may contain similar microfossils as well. Storms and tsunamis also both are high-energy events that leave deposits having sharp or erosional basal contacts. Distinguishing tsunami deposits from storm deposits

requires interpreting a combination of deposit geometry and sedimentary characteristics. Storm deposits are often deposited in fans or ridges closer to shore in comparison to the landward-thinning sand sheets typical of tsunami deposits (Morton and others, 2007). Although storm deposits can be thicker than is common for tsunami deposits (Morton and others, 2007, Tuttle and others, 2004), their thickness may also be in the same range as tsunami deposits (Nyman and others, 1995, Donnelly and others, 2001). Storm deposits often are composed of numerous thin layers or laminations (Tuttle and others, 2004; Morton and others, 2007). Tsunami deposits typically contain 1–5 layers (Morton and others, 2007; Peters and others, 2010a). These layers may take the form of couplets of sand overlain by finer grained sediments. Tsunami deposits can also be massive or contain multiple thin layers or laminations (Peters and others, 2010a, Richmond and others, 2012). Layering patterns within tsunami and storm deposits can overlap, but the number of layers and the style of layering may be used to distinguish tsunami from storm sediments when the number of layers within a deposit and the style of layering have distinctive forms, such as sand-mud couplets. Normal grading is common in tsunami deposits but is rarely observed in storm deposits.

Flood deposits also may have several characteristics in common with tsunami deposits. Flood deposits generally have sharp basal contacts, and their thickness may also be in the range reported for tsunami deposits. Sediment provenance can be used to distinguish tsunami deposits from deposits resulting from flooding due to fluvial overwash, alluvial fan, or debris flow deposits. Tsunami deposits may contain sediment or microfossils indicating a nearshore or coastal origin, while fluvial, alluvial, or debris flow deposits only contain sediment from an inland source.

Suspension Grading in Tsunami Deposits

Suspension grading is a distinctive type of normal grading formed by suspended sediment settling out of the water column from a high-speed flow as it slows rapidly. It is found in modern tsunami deposits—for example, 1998 Papua New Guinea (Jaffe and Gelfenbaum, 2007), 2009 Samoa (Jaffe and others, 2011), and 2011 Tohoku-oki, Japan (Jaffe and others, 2012). It is also found in paleotsunami deposits— for example, 1700 Cascadia deposits in Oregon (Witter and others, 2012). Suspension grading is characterized by a shift in the entire grain-size distribution to finer sizes upward in a suspension graded interval. The shift occurs because of the timing of when larger and smaller grains are deposited. Grains with higher settling velocities (larger particles for a given density and shape) deposit first and are therefore absent in the water column during the later stages of deposition. The grains with lower settling velocities, which take longer to reach the bed, are absent from the bottom of the suspension-graded interval and present in the top of it (Jaffe and others, 2012).

Although suspension grading may ultimately prove to be a strong discriminator between tsunami and other event deposits, there is still much research needed to establish that this is the case. Not all tsunami deposits are suspension graded, and commonly only a portion of a tsunami deposit may be suspension graded—depositional processes other than falling out of suspension also occur in tsunamis (Shanmugan, 2012). When a tsunami deposit contains more than one layer, each layer may be suspension graded or contain a suspension-graded interval. Suspension grading has also been found in turbidites (Kuenen and Minard, 1952; Middleton, 1967). We have analyzed storm overwash deposits to look for suspension-graded intervals and have found them to be rare. We know of no studies searching for suspension grading in fluvial deposits, debris flows, and other types of deposits. As such, with the current state of knowledge, the presence of suspension grading does not rule out formation by depositional agents other than tsunami.

Whether an interval of a deposit is formed by sediment falling out of suspension (that is, suspension graded) can be tested using sediment transport modeling. The vertical variation in grain-size distributions of the suspension-graded interval of the candidate tsunami deposit is reconstructed and compared to the actual distributions of the tsunami deposit sampled in the field. The reconstruction

follows the methods of Jaffe and Gelfenbaum (2007) and as applied by Witter and others (2012 to Cascadia paleotsunami deposits in Oregon and by Jaffe and others (2011, 2012) to deposits formed in the 2009 Samoa and 2011 Japan tsunamis. The reconstruction is simple—a sample of the candidate tsunami-deposit sediment is placed in suspension and allowed to settle, and the amount settling in each size class is tracked as the deposit accretes (details in the appendix of Jaffe and others, 2012).

If the grading of the reconstructed deposit matches that of the observed deposit reasonably well, then the assumption that the sediment was deposited from suspension is supported (Jaffe and Gelfenbaum, 2007). We quantify the fit between the reconstructed and observed suspension-graded interval as the average of the root square error (RSE) between the observed and modeled grain-size distribution for all subintervals (usually 1-cm samples). The units of RSE are weight percent (Jaffe and others, 2012). An RSE of 0 indicates a perfect match between the modeled and observed grain-size distributions for all subintervals. RSE can be as high as 100 when modeled and observed distributions do not match at all (the extreme case for a process other than sediment falling out of suspension forming the deposit). For 2011 tsunami deposits on the Sendai coastal plain of Japan, RSE is between 2 and 5 for two-thirds of the suspension-graded intervals and between 5 and 10 for one-third of the suspension-graded intervals (Jaffe and others 2012). For massive portions of the 2011 tsunami deposit that we interpret to be formed by sediment transport convergences, not falling out of suspension, the RSE is 15 or higher (Jaffe and others, 2012).

Reconnaissance Fieldwork

Figure 5 shows the field sites that were selected for reconnaissance fieldwork, and later for detailed fieldwork. Fieldwork during this stage of the project consisted of both site visits in order to visually assess surface conditions and 1–2 days of subsurface exploration using shallow subsurface coring and sampling at the sites. In order to procure field data, hand-driven 30-mm diameter and 60-mm diameter gouge corers were used along transects of varying lengths. Cores were described and documented, photographed, and either subsampled or sampled in entirety in the field for subsequent laboratory analyses. Hand-held GPS devices or real-time kinematic (RTK) survey units were used to record coring-site locations.

Prior to going into the field, permits were obtained from the agencies and organizations controlling access to the reconnaissance site areas. In some cases, field access was limited by the presence of sensitive animal species in protected wetlands or by potential for buried, unexploded ordinance on military bases. Team members also implemented a protocol, which supported consistent field coring methods, sampling techniques, and note taking, before deploying for fieldwork.

Between July 2011 and July 2012, team members completed reconnaissance field studies at a total of 20 localities along the California coast to determine: (1) if the sites had characteristics conducive for deposition/preservation of prehistoric tsunami deposits and (2) if candidate paleotsunami deposits were evident in the recent stratigraphic record (that is, the uppermost few meters of deposits below modern marsh surfaces). Table 2 lists the field locations, site information, and a summary of the results from the reconnaissance work. In total, 7 localities were visually evaluated for the feasibility or usefulness of attempting detailed work at those sites, and another 13 localities were so evaluated in greater detail using hand-driven cores to examine subsurface deposits. For most of the localities, this study constitutes the first concerted effort to search for tsunami deposits and to analyze the reasons why a particular locality may or may not possess a late Holocene stratigraphic record of tsunami inundation.

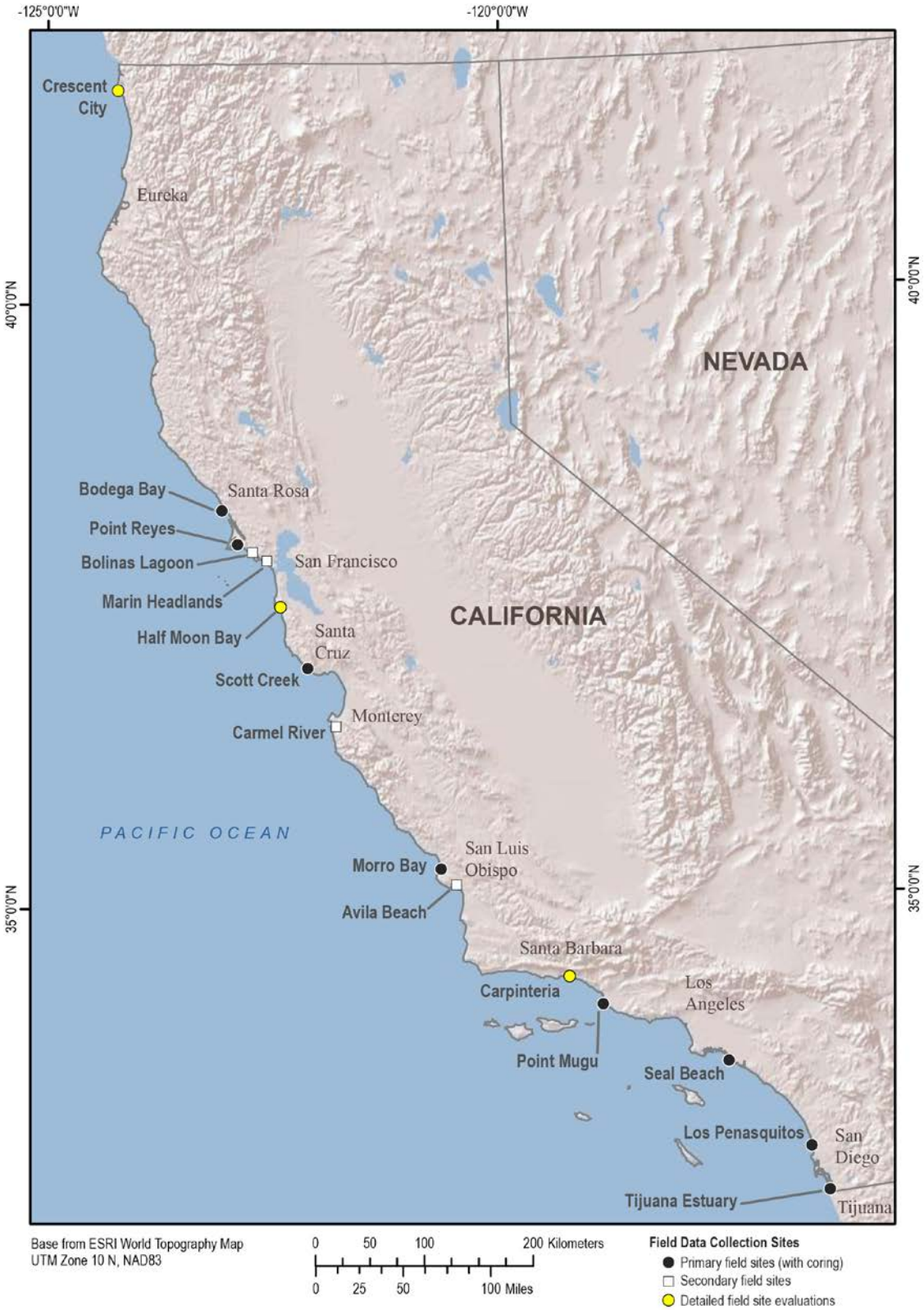

Figure 5. Map of California showing localities for reconnaissance and detailed field work in this study.

Table 2. Background information about the field areas that were evaluated in this study.

[MSL, mean sea level; dates in m/d/yy format; -, no data]

SITE LOCATION–NAME OF WETLAND	PRELIMINARY EVALUATION		RECONNAISSANCE AND DETAILED SITE WORK				COMMENTS
	Maximum tsunami amplitude from Aleutians-Alaska Source (meters above MSL)	Reference for previous subsurface work	Field study type (1=visual recon 2=sample recon 3=detailed analysis)	Dates of field Investigation	Number of cores collected	Sample analysis (D = diatom F = foraminers G = grain size A = age dating X = x-ray of core P = provenance)	
NORTHERN CALIFORNIA							
Crescent City; McNamara Marsh	6–7		3	6/9/12 to 6/11/12; 9/30/12	19	D, G, A, X	A.D. 1700 deposit verified by C-14; other analyses in progress
Crescent City; Elk Creek Marsh	6–7	Yes	2	6/10/12; 9/27/12	10	D	No evidence for paleotsunami deposits between 1964 and A.D. 1700
Crescent City; Sand Mine Marsh	6–7	Yes	3	6/10/12; 9/28/12 to 9/30/12	16	D, G, A, X	1964 deposit verified by Cs-137; other analyses in progress
Redwood Creek; Orekw Marsh			2	11/4/12 11/4/12	3 3	D, G, A D, G, A	Possible AD 1700 deposit; other sand units equivocal; analyses in progress
Bodega Bay; Doran Marsh	5–6	Yes	2	7/28/11	6	D, P	No anomalous deposits observed
Drakes Bay; Barries Bay Marsh	2–3		2	7/26/11	3	D	No anomalous deposits observed
Drakes Bay; Home Bay Marsh	2–3	Yes	2	7/27/11	6	D, G	No anomalous deposits observed; previously proposed tsunami deposits identified as debris flow and upland runoff
Bolinas; Bolinas Lagoon	4–5	Yes	1	7/26/11	-		Previous study indicated marsh area strongly impacted by past landslides and storms
Marin County; Rodeo Lagoon	8–9		1	7/26/11	-		Natural lagoon environment strongly impacted by past land-use/dredging

Table 2—Background information about the field areas that were evaluated in this study.—Continued

SITE LOCATION–NAME OF WETLAND	PRELIMINARY EVALUATION		RECONNAISSANCE AND DETAILED SITE WORK				COMMENTS
	Maximum tsunami amplitude from Aleutians-Alaska Source (meters above MSL)	Reference for previous subsurface work	Field study type (1=visual recon 2=sample recon 3=detailed analysis)	Dates of field Investigation	Number of cores collected	Sample analysis (D = diatom F = foraminers G = grain size A = age dating X = x-ray of core P = provenance)	
CENTRAL CALIFORNIA							
Half Moon Bay; Pillar Point Marsh	8–9	Yes	3	10/26/11 8/7–9/12 8/16/12 10/9/12 2/27/13 3/8/13 3/26/13	63	D, F, G, A, X, P	1946 deposit verified by Cs-137; other analyses in progress
Davenport; Scott Creek	4–5		2	8/30/12	8	G, P	No anomalous deposits observed
Moss Landing; Elkhorn Slough	3–4	Yes	1		-		Previous study indicated lack of sand deposits
Carmel; Carmel River Lagoon	3–4		1		-		Area flooded; no access to watercraft
Morro Bay; Los Osos Creek	2–3		2	10/22/11	2	D, G	No anomalous deposits observed
Morro Bay; Sweet Springs Reserve	2–3		2	10/23/11	4	D, G, P	No anomalous deposits observed
Morro Bay; Morro Bay Wetlands/ Chorro Creek	2–3		2	10/21-23/11	10	D, G	No anomalous deposits observedat up-estuary sites; graded deposit observed near marina
Avila Beach; Avila Creek	9–10		1	10/23/11	2	P	Significant grading and site disturbance; samples from Avila Beach and San Luis Obispo Creek for provenance

Table 2—Background information about the field areas that were evaluated in this study.—Continued

SITE LOCATION–NAME OF WETLAND	PRELIMINARY EVALUATION		RECONNAISSANCE AND DETAILED SITE WORK				COMMENTS
	Maximum tsunami amplitude from Aleutians-Alaska Source (meters above MSL)	Reference for previous subsurface work	Field study type (1=visual recon 2=sample recon 3=detailed analysis)	Dates of field Investigation	Number of cores collected	Sample analysis (D = diatom F = foraminers G = grain size A = age dating X = x-ray of core P = provenance)	
SOUTHERN CALIFORNIA							
Carpinteria; Carpinteria Marsh	2–3	Yes	3	2/13–22/08 2/4–7/12 10/22–23/12	114	D, F, G, A, X, P	Semi-continuous sand layers younger than 1600s verified by C-14; origin of sands not certain
Point Mugu; Point Mugu Marsh	1–2		2	2/3/12 2/6/12	19	G, P	Significant terrestrial influence
Seal Beach; Seal Beach Marsh	2–3		2	2/28/12	8	G	No anomalous deposits observed
Del Mar; Los Penasquitos Wetlands	2–3		2	9/17–18/12	16	G, P	No anomalous deposits observed
Imperial Beach; Tijuana River Estuary	3–4		2	9/6–7/12	10	G	Initial findings are estuary has significant terrestrial influence

A number of reconnaissance sites had continuous or semi-continuous sand layers that could have a tsunami origin. For these locations, the extent and spatial variability of the thickness of the sand layers, a strong discriminator between tsunami deposits and those formed by other processes (for example, storms), was explored by gouge coring. In addition, preliminary laboratory work was performed on samples of or related to potential tsunami deposits. Laboratory analyses included microfossil identification, grain-size distribution, and provenance to aid in the stratigraphic and depositional analysis. For the microfossil analyses, about 140 surface or down-core subsamples were collected and processed for diatoms, and an additional 50 samples were processed for foraminifers. The microfossil data are particularly useful for reconstructing past depositional environments, differentiating marine from freshwater deposits, and identifying evidence of a tsunami where sand layers may not be present. For grain-size analyses, sediment samples consisting mostly of sand-size material were submitted to the USGS sediment laboratory for determining particle-size distribution. The grain size is particularly useful for indicating depositional process, such as falling out of suspension for a high speed flow as would occur during some phases of tsunamis (Jaffe and others, 2012). For provenance analysis, we examined both surface samples to characterize modern environments and subsurface samples from cores for comparison purposes.

During the course of this reconnaissance work, the project collaborators sought feedback from a range of science professionals. The results of the reconnaissance work were presented as posters at the 2011 annual meetings of the Southern California Earthquake Center in Palm Springs (Leeper and others, 2011), the American Geophysical Union (AGU) in San Francisco (Hemphill-Haley and others, 2011), and at a National Science Foundation-funded workshop for international tsunami studies held in San Francisco the week prior to AGU. Presentations were also made to the National Tsunami Hazard Mitigation Program at its 2011 annual meeting in San Diego, and the California Tsunami Steering Committee that met in San Francisco in June of 2011. A field trip was arranged for a group of international tsunami experts from the U.S., Japan, and Australia to evaluate deposits at Pillar Point marsh (Half Moon Bay), a suspected promising locality for detailed site evaluation. The field trip participants provided valuable insight regarding potential paleotsunami deposits at the site.

Reconnaissance Field Sites North of Point Conception, 2011–2012

Coastal northern and central California extends for approximately 650 km from the Oregon border south to Point Conception (fig. 5). Two tectonic regimes exist in this area: the Cascadia subduction zone north of Cape Mendocino and the San Andreas transform fault system to the south. As previously mentioned, the Cascadia subduction zone has produced large local tsunamis that have been observed in the geological record (Abramson, 1998; Garrison-Laney, 1998; Patton, 2004; Peterson and others, 2011).

Along the coast that parallels the San Andreas Fault, the potential for large local-source tsunamis is significantly less because of the transform nature of the San Andreas and related faults—they exhibit predominantly strike-slip (horizontal) motion, with little vertical displacement. However, the region may be subject to tsunamis generated by vertical displacement of the seafloor during earthquakes on offshore faults that trigger submarine landslides (Wilson and others, 2008; Barberopolou and others, 2009). More than a dozen tsunamis occurred along the central and northern California coast between 1806 and 2011 (Lander and others, 1993; National Geophysical Data Center, 2013). Outside of the region directly adjacent to the Cascadia subduction zone, very few data exist on prehistoric tsunamis occurring in the region. However, numerical model results from large distant-source tsunami scenarios indicate that earthquakes on the Aleutian-Alaska subduction zones may produce relatively large tsunami runups (10 m) for some portions of this coastline, making it an important region for tsunami-deposit fieldwork (table 2; Wilson and others, 2008; Barberopolou and others, 2009). Reconnaissance fieldwork in northern and central California centered on the marshes at Bodega Bay, Point Reyes, Bolinas Lagoon, Rodeo Lagoon (Marin Headlands), Half Moon Bay, Scott Creek, Carmel River, Morro Bay, and Avila Beach (fig. 5).

Bodega Bay (Doran Marsh)

The Doran Marsh study area is located in Doran Regional Park, at the north end of Bodega Bay and along the southeast shore of Bodega Harbor (fig. 5). The marsh occupies a trough between a graben-bounding fault at the base of Pleistocene marine terraces on the east edge of the marsh, and the San Andreas Fault a few hundred meters to the west (Knudsen and others, 2002; especially their figure 3). The 1906 rupture of the San Andreas Fault offset the sand spit at Doran Beach, located about 200–300 m west of the marsh (Lawson, 1908). For this study, we evaluated sedimentary deposits below a broad salt marsh on the northwest side of Doran Beach Road (“NW field area” in fig. 6) and a salt marsh to freshwater wetland on the southeast side of the road adjacent to the Links at Bodega Harbor golf club (“SE field area” in fig. 6). The marsh/wetland in the SE field area is separated from the Pacific Ocean and a broad sandy beach (Doran Beach) by a vegetated dune field about 30–40 m wide and reaching estimated elevations of 5–7 m relative to mean high water (MHW).

Figure 6. Vertical aerial photograph showing locations of gouge cores collected and described at Doran Marsh, Bodega Beach Regional Park, Bodega, California.

We chose Doran Marsh as a site to search for paleotsunami deposits for several reasons: (1) it is one of the few low-lying marshes along a mostly rocky stretch of the California coast; (2) the modeling results from the State's large Aleutian sources scenario (AASZ III) showed moderately high (~ 4 m MHW) wave heights for the north end of Bodega Bay; and (3) Knudsen and others (2002) reported anomalous coarse-grained deposits in the upper 1 m of the subsurface stratigraphy at their core sites on the golf course approximately 75 m to the southeast of the SE field area.

We collected four gouge cores (DM1–DM4) from the *Salicornia*-dominated salt marsh in the NW field area and two cores (DM5, DM6) from the marsh/wetland in the SE field area between Doran Beach Road and the golf course. From the observations on these and a number of additional test cores,

we found no compelling stratigraphic evidence for tsunami deposits within about 2 m of the modern sediment surface. The cores in the NW field area contain a 3–10 cm thick veneer of salt-marsh peat capping several meters of muddy and sandy mud deposits, indicating that the NW field area existed as an intertidal to shallow subtidal inner-bay environment until the recent past, and therefore any paleotsunami deposits formed there would have had a high likelihood of being reworked and not preserved. In the SE field area, which we interpret as the former vegetated head of the inner bay, we found no evidence for coarse-grained deposits being washed in from the direction of the open ocean. However, we found evidence for multiple sandy beds that thickened inland in the direction of the former inner bay (towards the northwest), which would be consistent with deposition at the transition of the marsh and tidal flat at the edge of the embayment. We identified an abrupt change from peat to overlying mud in the subsurface of the SE field area, consistent with observations by Knudsen and others (2002), who concluded that offset along the San Andreas Fault triggered coseismic subsidence, possibly associated with liquefaction, at this location.

Point Reyes 1 (Barries Bay)

Barries Bay is a narrow embayment in southwestern Drakes Estero at Point Reyes National Seashore (fig. 7). The salt marsh at the head of Barries Bay (informally named “Barries Bay marsh” for this study) is relatively small and flat, extending approximately 200 m inland from the shore of Drakes Estero and with a maximum breadth of about 90 m (fig. 8). The adjacent tidal flat is soft, muddy, and broadly mounded because of a filamentous algae growth that forms a thin, dense surface layer, and contributes to anoxic conditions directly below the surface. The marsh may be extensively submerged during highest tides, as suggested by the elevation of high-tide staining on rocks bordering the south side of the lower marsh and adjacent tidal flat.

Barries Bay marsh was included in the reconnaissance evaluation for several reasons: (1) the site is less than 3,500 m from the mouth of Drakes Estero where the AASZ III modeling results showed relatively high tsunami wave heights (~5 m); (2) it is a low-lying wetland along a predominantly rocky stretch of the coast; (3) there are ample sources for sandy deposits seaward of the marsh that could have been relocated by a tsunami (coarse-grained deposits from the open estero as well as from the barrier sand spits forming the southern boundary of the estero; and (4) previous work by Hoirup (2006) had reported the possible occurrence of paleotsunami deposits in another arm of Drakes Estero (Home Bay; see next section).

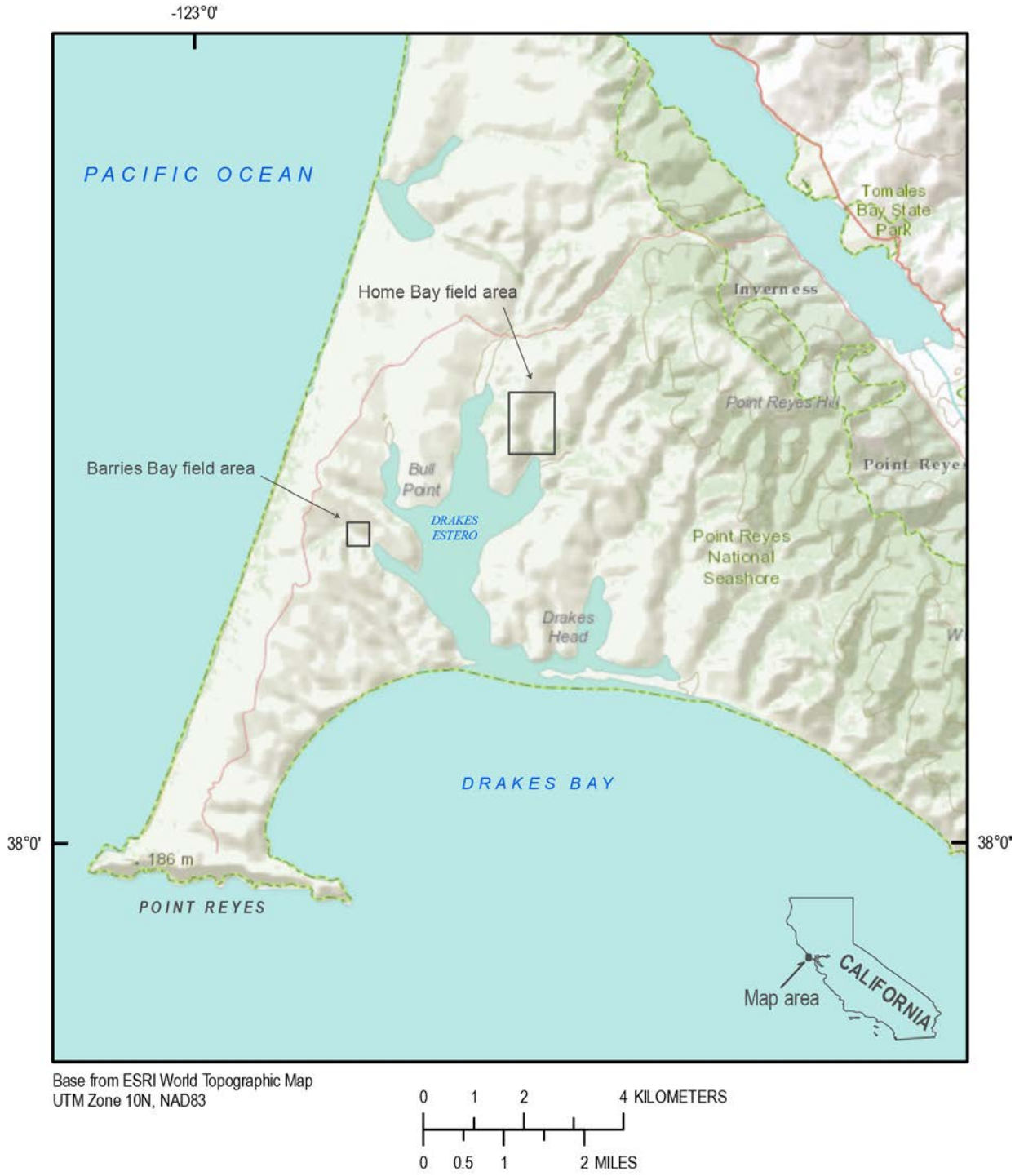

Figure 7. Map showing locations of the Barries Bay Marsh and Home Bay Marsh field localities in Drakes Estero, Point Reyes National Seashore, California.

Figure 8. Vertical aerial photograph showing locations of gouge cores collected and described at Barries Bay Marsh, Point Reyes National Seashore.

We collected and described three gouge cores (BB1, BB2, and BB3) along a shore-normal transect near the center of Barries Bay marsh (figs. 8, 9). We positioned our core transect as distant as possible from a slough channel cutting through the marsh, as well as from the steep hillslopes on the northeast side of the marsh. The hillslopes bordering the marsh are composed of highly erodible late Tertiary mudstones, siltstones, and sandstones of the Purisima Formation (Clark and Brabb, 1997), as evidenced by pale yellowish brown alluvial deposits at the base of slope in some locations, particularly below the bluffs at the seaward edge of the marsh. In addition, a large alluvial fan is present at the termination of drainages at the landward edge of the marsh. Our coring strategy, therefore, was to estimate the best location for sampling marsh/marine deposits and avoiding contamination from alluvial material. In addition to the cores described in detail, we inspected (but did not log) several cores within a few tens of meters of core BB3 to evaluate possible lateral continuity of some subsurface deposits.

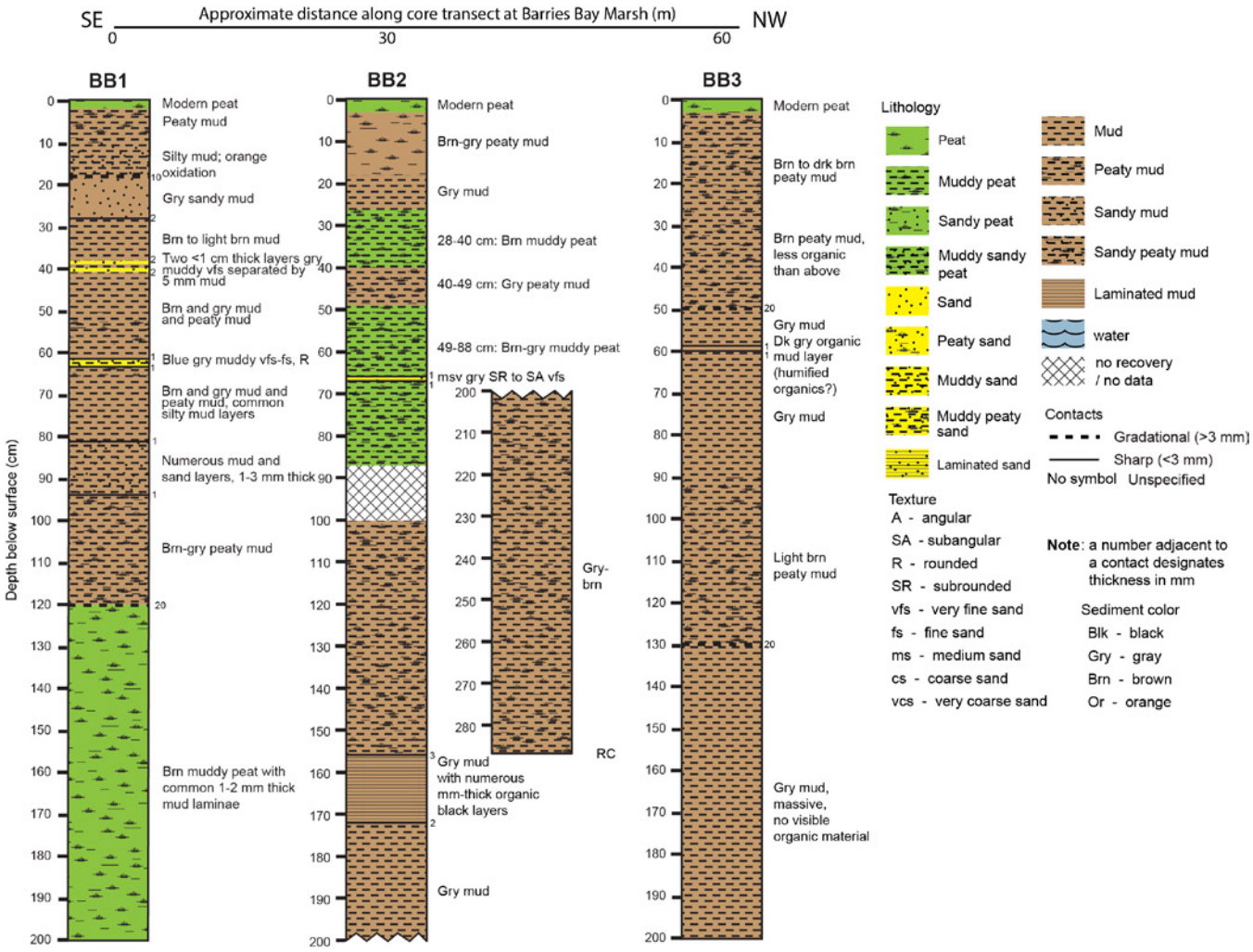

Figure 9. Core logs of Barries Bay cores BB1, BB2, and BB3.

Analysis of the three cores logged at Barries Bay marsh shows that the subsurface stratigraphy down to 2-m depth is heterogeneous over short distances. Evidence for gradual submergence and later emergence of a marsh environment is evident in cores BB1 and BB2, but a former episode of marsh drowning is not evident in core BB3. Silt and fine sand are prominent in some muddier sections of the cores, present as irregular interbeds with indistinct contacts. Of particular interest, however, are occurrences of a thin gray sand unit near depths of 62 to 67 cm in each of cores BB1 and BB2 (fig. 9). In core BB1, the unit is 2 cm thick, between 62 and 64 cm depth. Based on field observations, it is composed of gray, fine-grained, subangular to subrounded sand. The unit contains fragments of peat at the base, and there is no observable grading. It forms sharp basal and upper contacts with the surrounding mud. In core BB2, the comparable fine-grained gray sand unit is between 66 and 66.4 cm depth. It is massive (that is, no visible evidence for grading in the thin unit), and forms a sharp basal contact with underlying brown muddy peat. In both cores BB1 and BB2, the color and texture of the sand layers stand out in contrast to surrounding mud or muddy peat deposits. In the most landward core, BB3, no similar sand layers are observed, but there is a dark gray organic mud layer near the same subsurface depth (59–59.4 cm) as the sand units in BB1 and BB2. This layer stands out in contrast to the gray-brown peaty mud, and field observations suggest it is more consistent with accumulation of humified organic material than post-depositional anoxic staining or banding that is common in tidal flat

deposits. Quickly inspected test cores collected about 10–20 m to the west of BB3 similarly lacked any recognizable sand layers, and although the overall downcore stratigraphy was comparable between BB3 and the test cores, a comparable thin organic layer near 60 cm depth was not evident.

Thin deposits consisting of sand to organic mud in the three cores about 60–65 cm below the modern marsh hint at the possibility of a single landward-thinning, laterally continuous deposit. Whether these units correlate could be resolved by observations from additional closely spaced cores. From the current core data it can be determined that sand deposition did not extend as far as 90 m inland from the (modern) tidal flat, and the depositional environment—as indicated by the lithology surrounding the units in the three cores—would probably have been a muddy low marsh or tidal flat. If the units near 60–65 cm depth are widespread and correlatable, this would represent an anomalous depositional event, as no other comparable, unusual-looking sandy deposits were obvious in the cores. Whether such a deposit would record a past tsunami or a storm would be a challenge to ascertain, but its uniqueness in the stratigraphic record would rule out deposition by tidal processes, which would be more frequent. We conclude that further work at this locality is warranted and should include more detailed research into any unusual or anthropogenic sources of sediment input into Barries Bay to rule out nonnatural impacts to the stratigraphic record.

Point Reyes 2 (Home Bay)

Home Bay is the northeastern arm of Drakes Estero, on the south side of the Point Reyes Peninsula (fig. 7). Two stream systems feed into the head of Home Bay, separated by a high ridge formed by Tertiary rocks of the Purisima Formation and Monterey Formation. Field observations were completed in the stream valley at the north end of Home Bay, which is about 100 m wide between moderately steep hillslopes. A well-developed salt marsh (informally named "Home Bay marsh" for this study) covers the valley floor approximately 450–500 m inland from the shore of the estero, where it transitions to a freshwater wetland (fig. 10). The southern (bayward) end of the valley is approximately 4.5 km from the present day mouth of Drakes Estero at the Pacific Ocean.

Home Bay marsh was chosen for study for several reasons: (1) the AASZ III modeling results showed relatively high runups (~5 m) for the mouth of Drakes Estero); (2) in a previous study in Home Bay Marsh, Hoirup (2006) reported anomalous sandy deposits below the marsh surface that he interpreted as possible tsunami deposits; (3) historical information showed that the marsh has been relatively undisturbed by ranching activities; and (4) although somewhat distant from the mouth of Drakes Estero (~4.5 km), the marsh is also far enough from extensive dune fields in western Point Reyes to avoid abundant wind-blown sand deposition that would obscure the stratigraphic record.

We completed fieldwork in two separate areas in Home Bay marsh: the southern (bayward) marsh and adjacent tidal flat, and in an area of well-developed salt marsh about 400–500 m upvalley. In addition to being less susceptible to impact from storm surges, the upvalley field area includes the localities previously reported by Hoirup (2006).

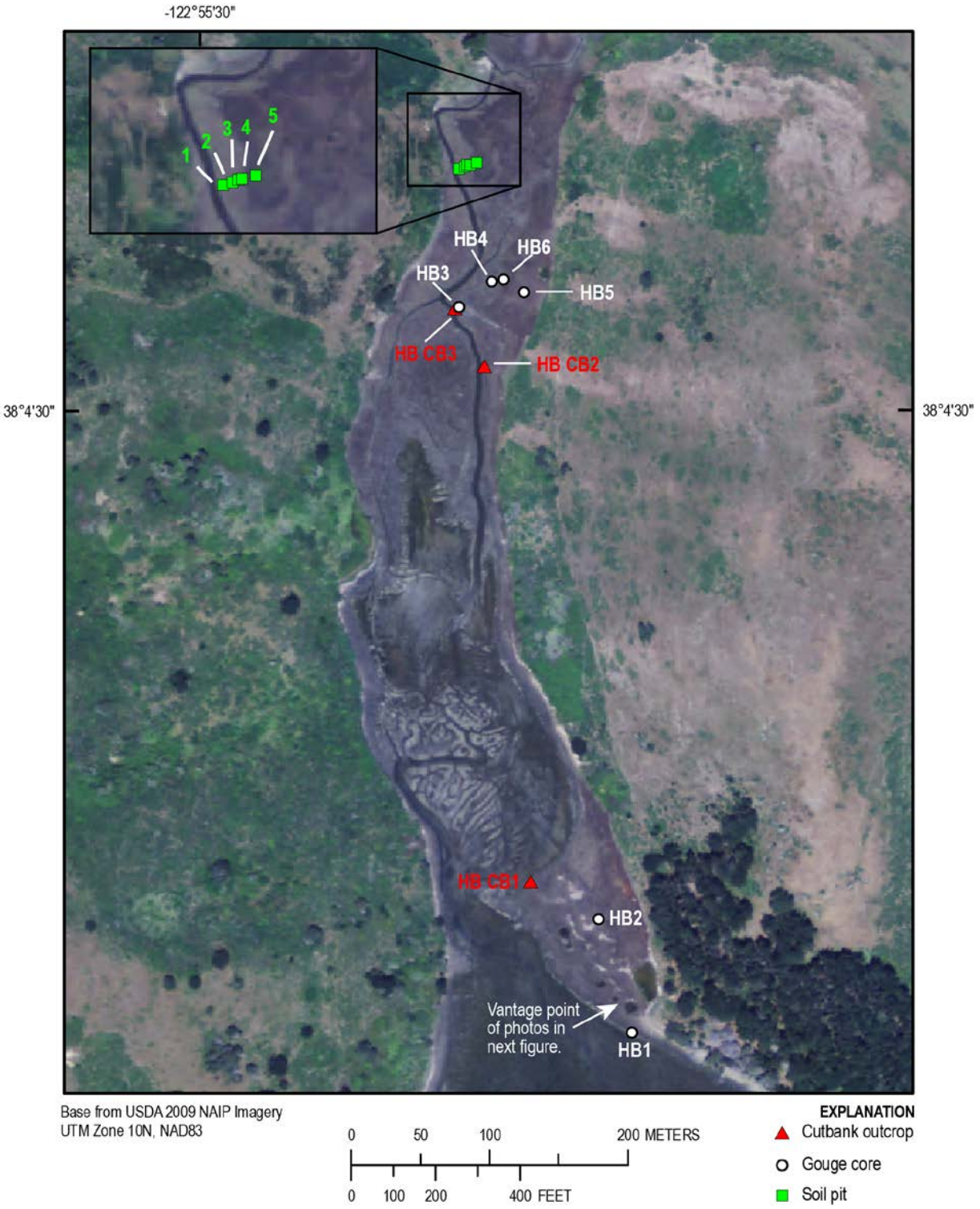

Figure 10. Vertical aerial photograph showing locations of gouge cores, tidal stream cutbank outcrops, and soil pits examined at Home Bay Marsh.

We found no evidence for anomalous deposits in two gouge cores and a channel cutbank outcrop evaluated at the southern end of the valley. The tidal flat in this area is thoroughly bioturbated and nearly impossible to traverse. The ~1-m tidal flat core consisted of massive gray mud with discontinuous layers of gray sand, as well as concentrations of indurated mudstone clasts likely originating from outcrops of Tertiary rocks along the shores of the estero. The marsh core and tidal streambank outcrop showed predictable sections of salt-marsh peat overlying massive to sandy mud. Considering the extensive bioturbation of the tidal flat deposits, the overall massive appearance of deposits exposed in the streambank, and the dense network of crab burrows (fig. 11), bioturbation could be a problem in obscuring the depositional record.

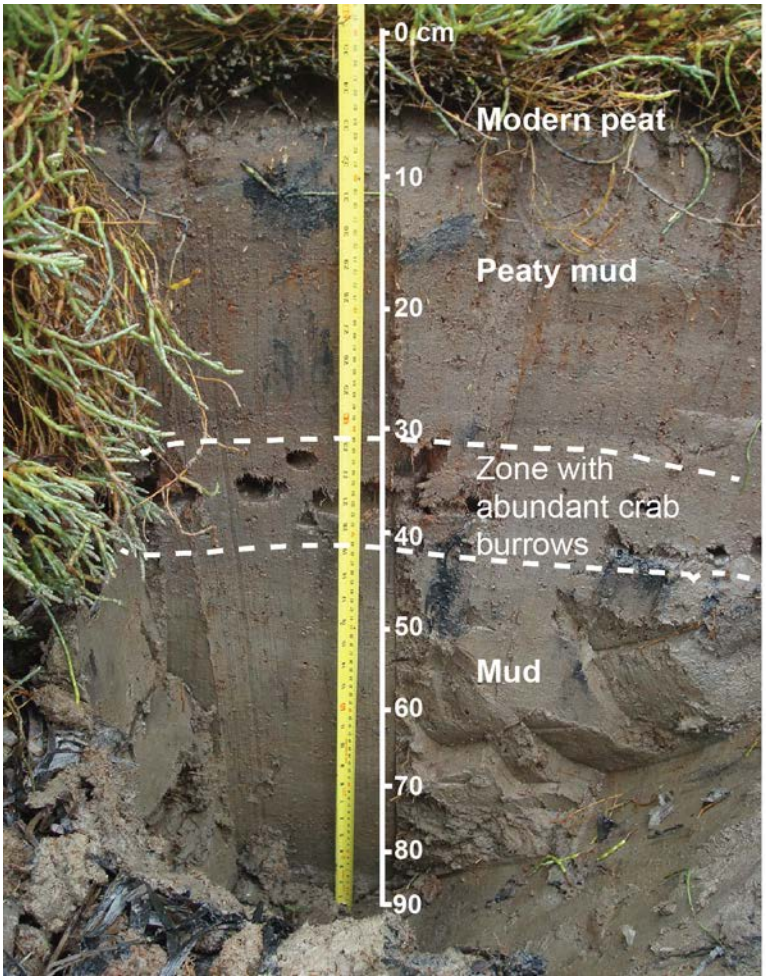

Figure 11. Photograph of cutbank outcrop CB1 at Home Bay marsh, showing the subsurface stratigraphy to 90-cm depth exposed during low tide. Holes about halfway down the exposure are from burrowing crabs populating a narrow zone at the transition from underlying inorganic mud deposits to overlying peaty mud to peat deposits.

Although the upvalley field area was distant enough from the mouth of the estero (>5 km) to make preservation of tsunami deposits even less likely than at the downvalley sites, we were compelled to examine cores, cutbank outcrops, and soil pits in this area because of the previous work by Hoirup (2006). In that study, Hoirup observed subsurface sandy deposits in two localities that he speculated might be evidence for past tsunami deposition. Hoirup joined us in the field and directed us to his previous study sites. With the assistance of a larger field crew to complete a more thorough core transect and evaluation of additional slough-bank outcrops, it became evident that the coarse-grained units he

had identified had very limited distributions and were likely the result of two different terrestrial depositional events: an older, local hillslope failure, and a relatively recent upland runoff associated with a fire (likely the "Vision Fire" that burned several thousand acres above Home Bay in 1995; Forrestel and others, 2011). The limited distribution of the slump deposits was established by evaluating a series of soil pits extending from near the base of the hillslope towards the center of the valley (fig. 12). The cores collected on the adjacent marsh indicate that the postfire deposits were confined to point bars of the stream channel and are not part of the long-term record for the marsh. These deposits also showed cross-bedding consistent with downstream flow, as well as abundant charcoal and rare freshwater diatoms (fig. 13). The cores collected near the center of the valley showed no unusual deposits, but rather a predictable transition from mineral-rich lower intertidal/subtidal deposits to organic-rich marsh deposits within the upper ~0.5–1.2 m of the stratigraphic record (fig. 14). Therefore, in conclusion, we found no evidence in the Home Bay marsh area of sand layers with characteristics that could be attributed to deposition by a tsunami. This lack of evidence for past tsunami deposits for Home Bay marsh could, in part, be explained by the relatively great distance from the mouth of the estero, which is >5 km for the northernmost, upvalley sampling locations.

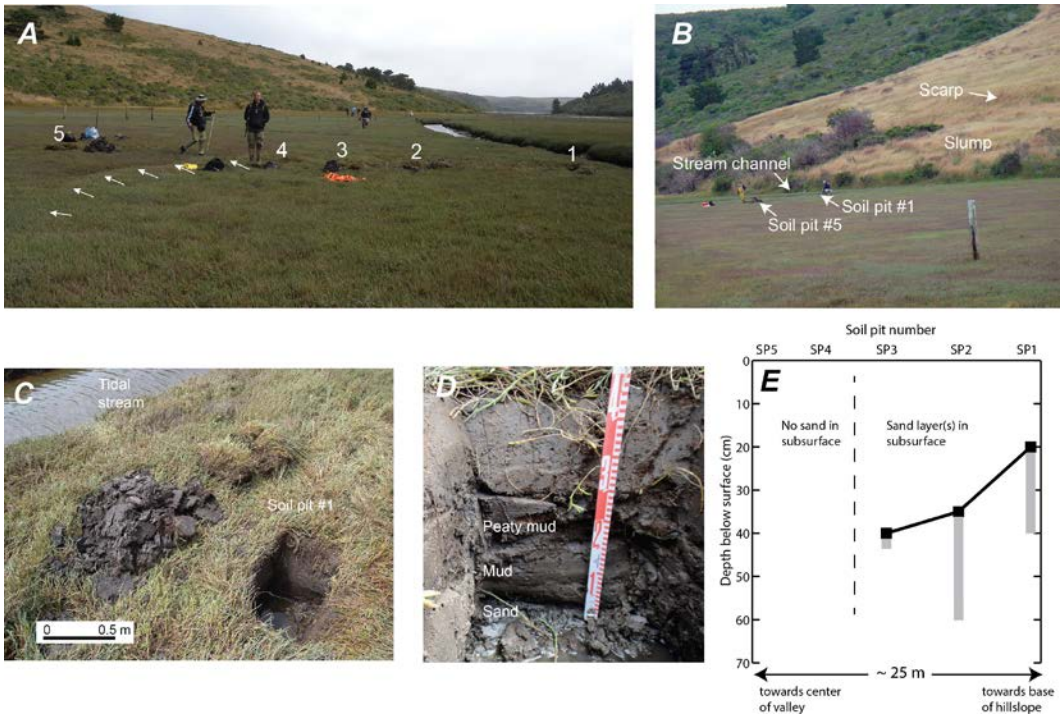

Figure 12. Photographs and cross-section plot of soil pits excavated at Home Bay marsh to evaluate the depth and lateral extent of an anomalous subsurface sand deposit. *A*, View to south; Drakes Estero visible in the distance. Five soil pits were excavated several meters apart along a line perpendicular to a tidal stream (visible in the upper right of photo) and hillslope (to right, out of frame; see image *B*) on the west side of the marsh. The sand layer is visible in pits 1–3, thinning away from the hillslope. Numbers indicate soil pits in order from west to east; arrows show topographic remnant interpreted as the toe of a slump from the adjacent hillslope. *B*, View to west from near the center of the valley towards the soil pit excavation area. The tidal stream channel is at the base of the hillslope; a slump deposit and scarp are visible on the lower hillslope. *C*, View of soil pit 1. Discontinuous patches of gray, fine-grained sand in a mud matrix are present between 20 and 40 cm depth. *D*, View of soil pit 3. A distinct, 2-cm-thick gray sand deposit is present at ~40 cm below the surface. *E*, Plot showing depths to the tops of sandy subsurface deposits (black squares) and approximate thickness of deposits (gray vertical rectangles). No subsurface sand deposits were found in pits 4 and 5.

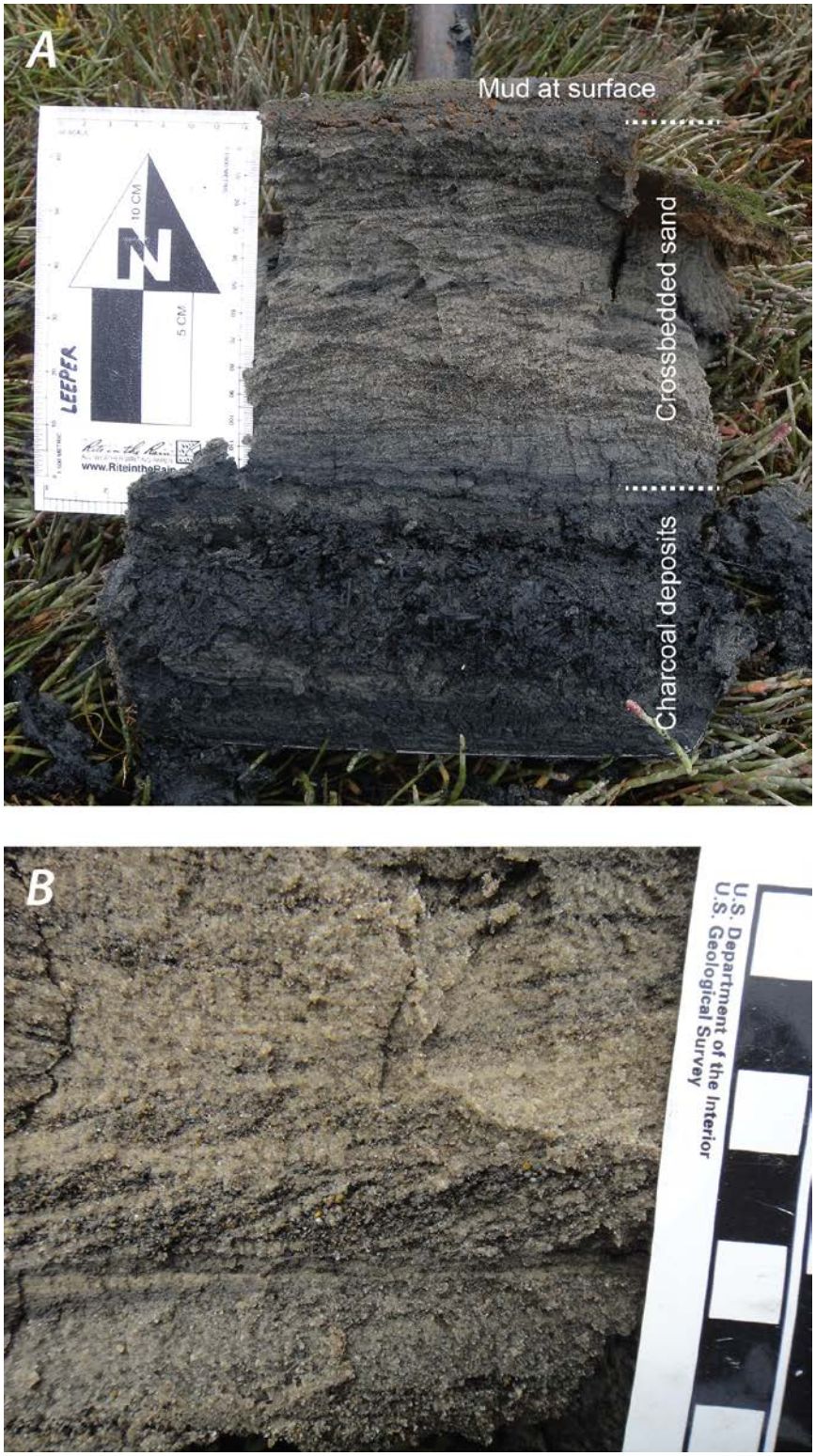

Figure 13. Photographs showing point bar deposits from the stream channel at the base of outcrop CB3 at Home Bay marsh. *A*, Black, coarse-grained charcoal deposits and clean crossbedded sand are likely the results of upland runoff associated with the 1995 Vision Fire at Point Reyes. *B*, Closeup view of crossbedding in sand collected a short distance from the sample shown in *A*.

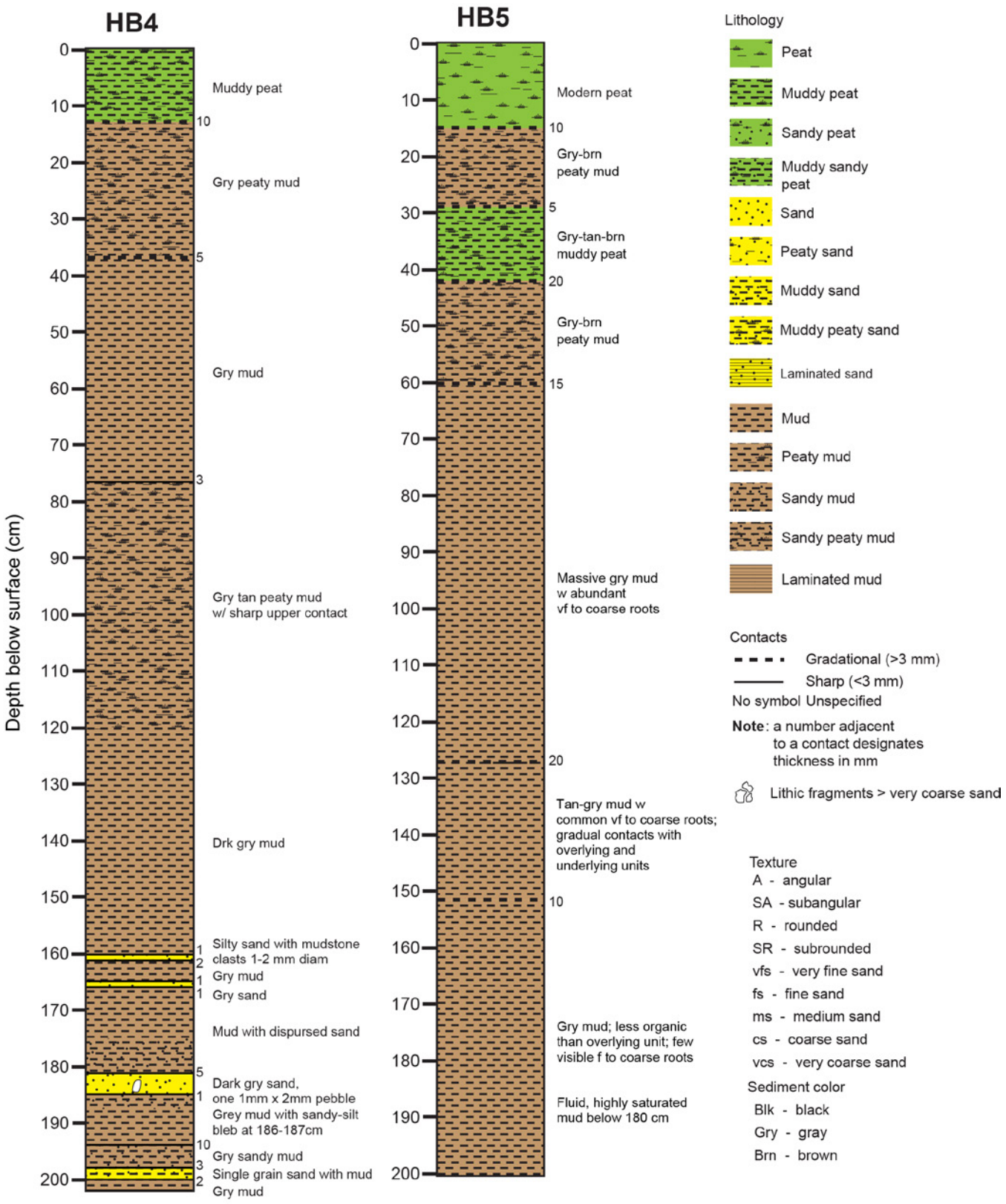

Figure 14. Core logs of cores HB4 and HB5 at Home Bay marsh. Core HB5, collected closer to the margin of the valley, shows about 60 cm of peaty deposits capping massive to rooty mud. Core HB4 shows some sandy layers consistent with lower intertidal or subtidal deposition, comparable to deposits in nearby core HB6.

Bolinas Lagoon

Bolinas Lagoon is a shallow, narrow embayment approximately 20 km north of the Golden Gate of San Francisco Bay (figs. 5, 15). The Bolinas Lagoon area has been the focus of a number of tectonic or paleoseismologic studies because of its location at the complex junction of the San Andreas and San Gregorio Faults and its historical record of deformation during the 1906 rupture of the northern San Andreas Fault (Lawson, 1908; Galloway, 1977; Berquist, 1978; Zoback and others, 1999; Knudsen and others, 2002).

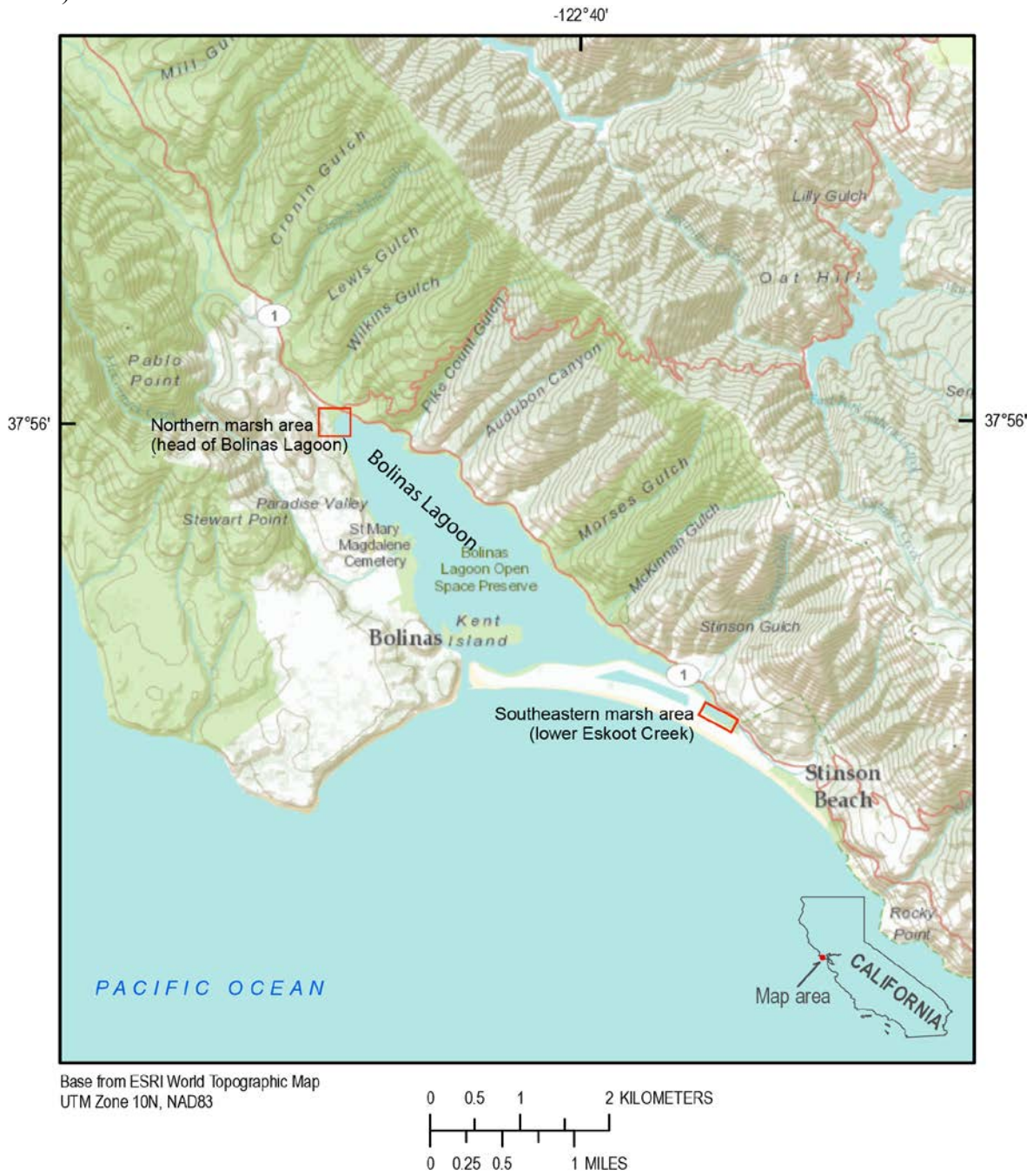

Figure 15. Map of Bolinas Lagoon. Small red boxes show approximate locations of historical (pre-1850s) salt marshes.

Although the AASZ III model predicts relatively high tsunami wave heights (~5–6 m) for the mouth of Bolinas Lagoon, for the purposes of this study the area ranked low for finding preserved paleotsunami deposits. The reason for this is twofold: (1) there are few locations of long-lived, undisturbed marshes along the shores of the lagoon, and (2) there is well-documented evidence for high sedimentation rates from both natural processes (storms, seismically induced landslides) and anthropogenic land-use practices that would skew the recent stratigraphic record (Berquist, 1978; unpublished 1996 Bolinas Lagoon Management Plan Update, prepared for the Marin County Open Space District; Knudsen and others, 2002; U.S. Army Corps of Engineers, 2002; Byrne and others, 2006). According to Byrne and others (2006), sedimentation rates peaked in the late 1880s during a period of aggressive redwood logging in watersheds above the northern lagoon, but even into the mid-1900s there is documented evidence for development of new intertidal flats and marshes in the lagoon. Historical maps from the 1800s show that emergent marshes were confined to the southeast area of the lagoon along the lower reach of Eskoot Creek and at the northwestern end (head) of the lagoon (fig. 15).

Based on a literature review and field visit/visual inspection of these two marsh localities, we concluded that neither would likely provide reliable stratigraphic evidence for past tsunami deposition. The southeastern marsh area, along lower Eskoot Creek, occupies a confined wedge of land averaging less than 150 m wide, bounded on its northeast side by Highway 1 and steep hillslopes, and otherwise surrounded by residential and commercial development. Although its location near the coast, just behind a barrier spit ~4.5–6.5 m high MHW, makes it an intriguing location for locating possible tsunami deposits, we excluded it from this reconnaissance study because of unknown, but likely, impacts from past land development.

The northern location, at the head of Bolinas Lagoon, was previously extensively studied by Knudsen and others (2002) for evidence of coseismic subsidence associated with past rupture of the San Andreas Fault and by the Byrne Lab at U.C. Berkeley[9] for changes in sedimentation rates associated with past land-use practices. Knudsen and others (2002) collected a series of cores across the marsh that, in addition to showing evidence for abrupt land-level changes during fault rupture, show thick, widely distributed fluvial flood deposits associated with past seismic shaking, logging, and even high stream discharge from storms during the 1983 El Niño/Southern Oscillation. Because of the absence of predominantly fine-grained, undisturbed marsh deposits at the site, and the predominance of fluvial debris deposits, we concluded that this was a poor locality to pursue our reconnaissance paleotsunami deposit investigation.

In summary, we evaluated two long-extant marsh localities in Bolinas Lagoon as possible sites for deposition and preservation of paleotsunami deposits. The southeastern site, along lower Eskoot Creek, is located adjacent to the coast behind a barrier spit, but is a small, confined wetland in the midst of dense land development. The northern site at the head of the lagoon is less affected by road construction and other development, but has been exceptionally impacted by high sedimentation rates from both natural and anthropogenic causes. Therefore, we excluded the Bolinas Lagoon sites for further evaluation, focusing our efforts instead on other localities along the California coast in more natural settings and with lower likelihoods of unusually high sedimentation rates.

Rodeo Lagoon

Rodeo Lagoon is a small (~900×250 m) brackish lagoon to freshwater wetland on the southwest shore of the Marin Headlands, in the Golden Gate National Recreation Area (fig. 16). It is separated from the Pacific Ocean by a broad sand spit (Rodeo Beach); it is otherwise surrounded by steeply eroded hillslopes primarily composed of folded and faulted metamorphic rocks of the Franciscan Assemblage.

[9]Byrne Lab for Quaternary Research, University of California, Berkeley; Available from: http://geography.berkeley.edu/paleoecology/research.html

Freshwater input to the lagoon is via groundwater and surface inflow primarily from Rodeo and Gerbode Creeks (Striplen and others, 2004). Until 1937, the lagoon consisted of a single, open brackish waterbody behind a barrier sand spit, but a weir and culverted road built across the lagoon to support operations for Fort Cronkhite effectively divided the area into a lower (western) shallow brackish lagoon, and an upper (eastern) densely vegetated freshwater wetland, currently termed "Rodeo Lake" (fig. 17). Striplen and others (2004; especially their figure 3) provide an analysis of two U.S. Coast Survey topographic sheets from 1850 (T-321) and 1853 (T-400) that show a lagoon area about 20 percent larger than at present, positioned behind a wide beach and dunes with a confined outlet on the north side of the lagoon. An extensive "wet meadow" area inland from the lagoon along the lower reaches of Rodeo Creek was also identified. The maps show that prior to the mid-1800s there was little anthropogenic impact to the lagoon. This is in contrast to later conditions, in which local development and runoff from upstream ranching operations have impacted the lagoon both in terms of sedimentation and organic influx.

Figure 16. Map showing location of Rodeo Lagoon, a natural brackish lagoon on the southwest shore of the Marin Headlands, within the National Park Service Golden Gate National Recreation Area. Red arrows show locations and directions of view of photographs in figure 17.

Figure 17. Photographic images of Rodeo Lagoon. *A*, View of the open brackish lagoon looking west from the weir/bridge that separates the lagoon into west and east sections. The sand spit separating the lagoon from the Pacific Ocean is visible in the distance. *B*. View looking south of the freshwater wetland ("Rodeo Lake") above the bridge. Unlike the open lower lagoon, Rodeo Lake is densely vegetated. Structures in the distance are historical buildings of Fort Cronkite, a World War II Army outpost.

Rodeo Lagoon was chosen as a reconnaissance evaluation site for tsunami deposits for several reasons: (1) it is one of the few low-lying sites along a stretch of steep sea cliffs along the shore north of the Golden Gate (that is, the Marin Headlands); (2) it has a substantial sand source from the beach and low dunes at the seaward end of the lagoon; and (3) the ASZIII model predicted large tsunami wave heights (~8.5 m) at the mouth of the lagoon.

Based on a literature review, interviews with National Park Service (NPS) personnel[10], and our on-site observations, however, we determined that reconnaissance coring for tsunami deposits at Rodeo Lagoon would not be feasible. The main problems were: (1) anthropogenic/land use impacts on sediment input into the lagoon; (2) lack of natural areas of fringing marsh or long-extant freshwater ponds; and (3) restrictions for access to the lagoon because of protected species and water-quality and health-hazard issues. For example, results of initial studies for restoration efforts in the Rodeo Creek watershed showed sedimentation accumulation in the Rodeo Lake area—a location we targeted for possible coring—to be strongly impacted by ranching during the past century (Striplen and others, 2004). In addition to anthropogenic impacts, the naturally dynamic lagoon environment, with regular seasonal breaching of the barrier sand spit (Hill, 1970) and episodic freshwater flooding and sedimentation during periods of high rainfall[11], further made Rodeo Lagoon an impractical location for identifying tsunami deposits in the stratigraphic record. Although deep coring from a boat in the lagoon might be considered for future sampling, we conclude that the stratigraphic record accessible with coring equipment on land would be disturbed and difficult to interpret.

Scott Creek

Scott Creek marsh is a small marsh at the mouth of Scott Creek, approximately 21 km north of Santa Cruz, California (Figure 18). The site was included in the tsunami deposits reconnaissance study because: (1) it is one of the few low-lying wetlands along a mostly rocky section of the Central California coast between Half Moon Bay and northern Monterey Bay; and (2) the ASZIII model predicts tsunami wave heights of ~3-4 m for the coast at Scott Creek, great enough to inundate at least the lower estuary and possibly leave a sedimentary record.

The main channel of Scott Creek has been engineered with artificial levees so that it passes underneath the Highway 1 bridge. It divides the marsh into north and south sections. Our investigation focused on the marsh to the north of Scott Creek, which is a relatively flat marsh crossed by several channels (fig. 19). We also investigated the marsh area south of the creek channel, which included a small lagoon surrounded by dense stands of cattails, but the marsh surface at the time of the study was too dry to extract any cores.

[10]We appreciate the information and advice provided by NPS scientists at the Golden Gate National Recreation Area, including Darren Fong (Aquatic Ecologist), Sue Fritzke (Plant Ecoogist), and Tamara Williams (Hydrologist).

[11]For example, flooding during the 1983 ENSO event was so intensive that additional drainage culverts were installed at the outlet of the lagoon to contain the overflow lagoon (Stilpen and others, 2004, especially their figure 8).

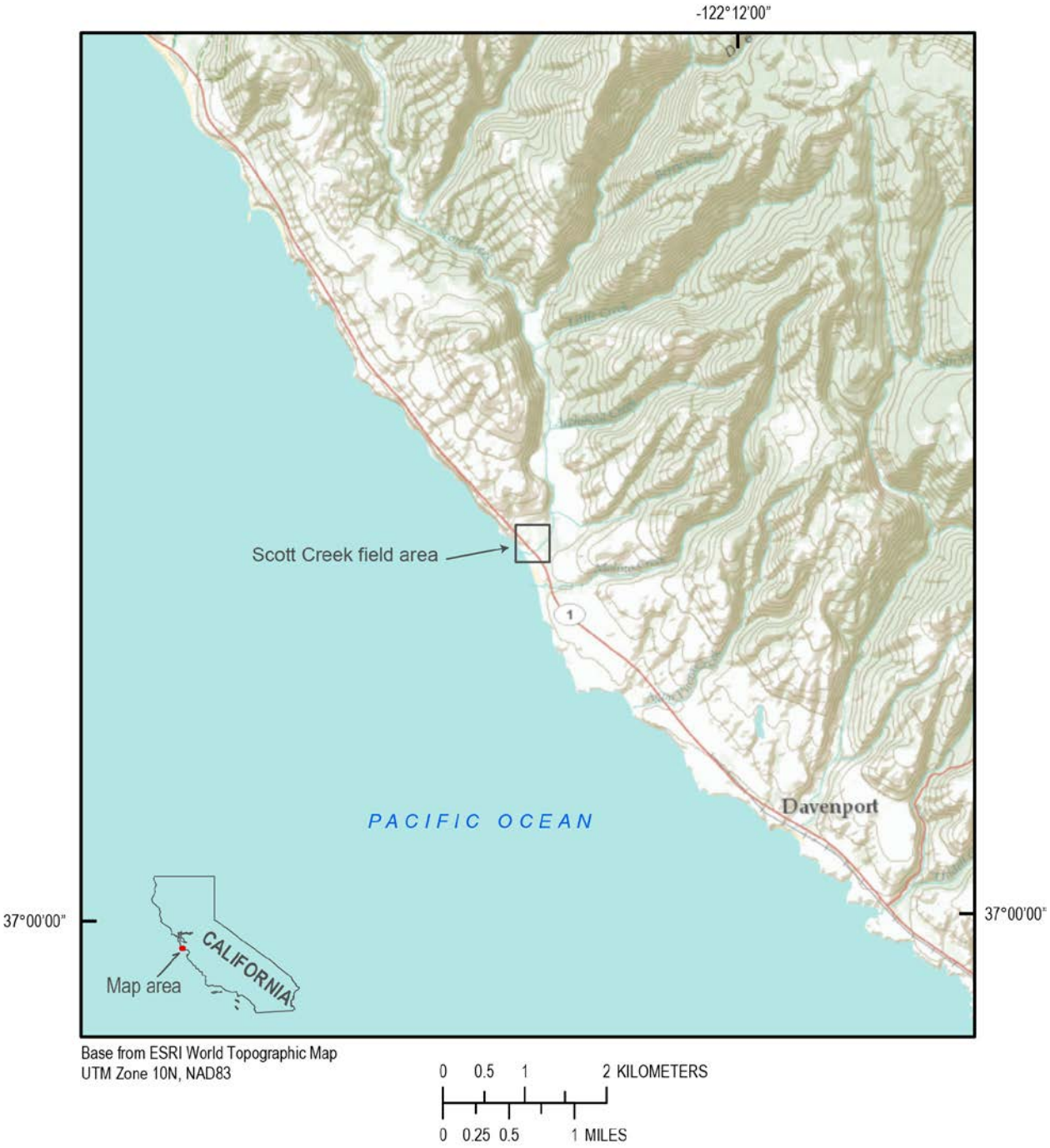

Figure 18. Map showing location of the Scotts Creek study area, on the Central California coast about 21 km north of Santa Cruz.

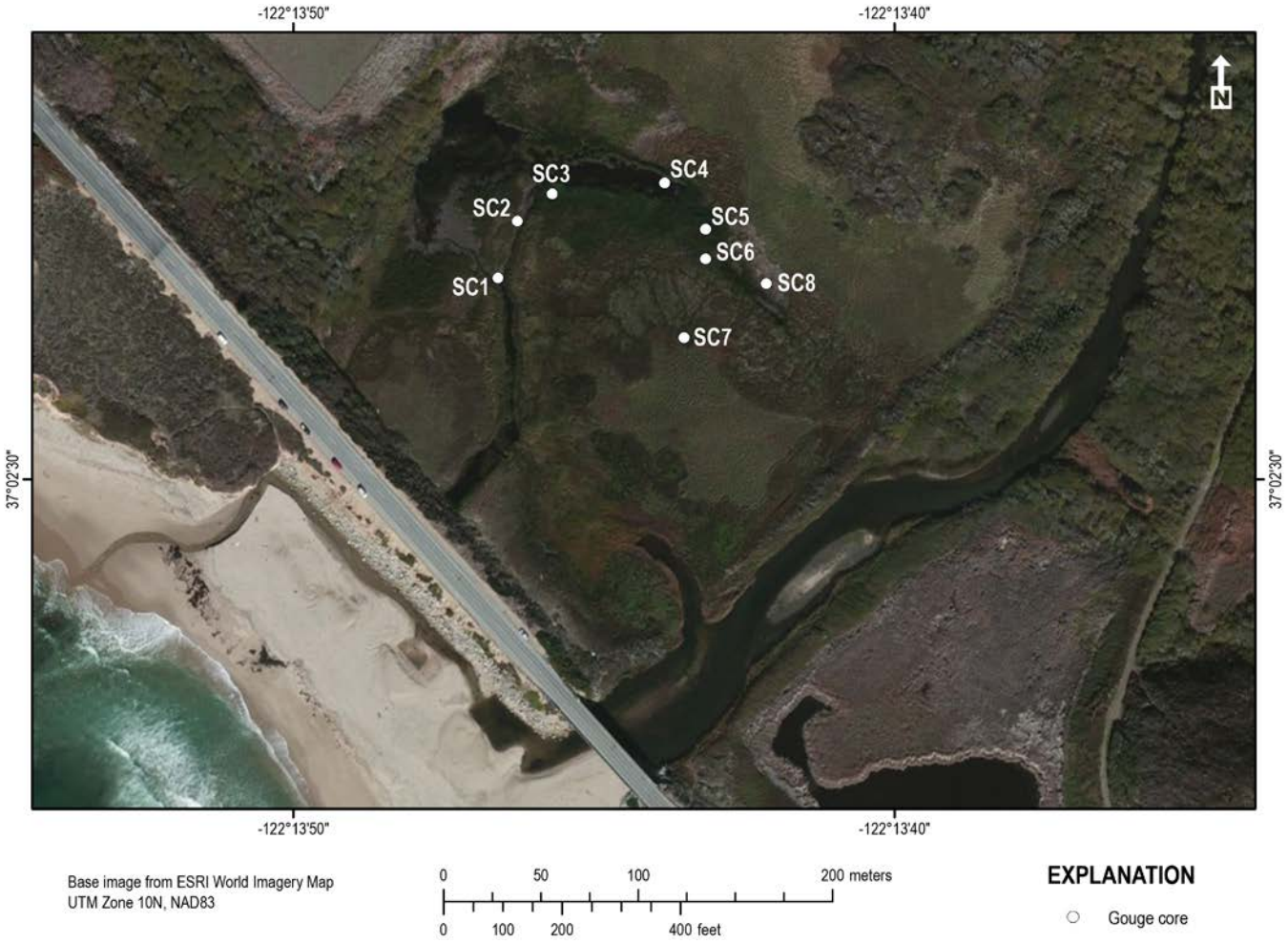

Figure 19. Vertical aerial photograph showing distribution of gouge cores collected and described from the marsh on the north side of lower Scotts Creek. The marshes on either side of the creek channel are susceptible to flooding by freshwater when the beach builds up and blocks outflow of the creek to the ocean.

A sand bar typically forms at the mouth of Scott Creek during summer and fall, converting the lower Scott Creek estuary into a freshwater lagoon that floods the marshes on either side of the creek (Hayes and others, 2008). When the bar is breached and the creek flows out to the ocean, the marsh drains and dry conditions prevail in many of the channels. At the time of our investigation, Scott Creek was flowing out to sea. As in the marsh on the south side of the creek, the surface was hard and dry over much of the northern marsh area, making core penetration and recovery difficult. We had the best success with core penetration and recovery in lower, wetter areas where the dominant vegetation was cattails. These areas primarily surrounded the marsh channels, which, except for a small stagnant pool in a channel near SC4 and for a short distance along the main channel near Scott Creek and Highway 1, were dry and mud-cracked at the time of the survey. Dry portions of the cores often fell out of the core barrel and were unrecoverable.

As part of the field investigation, numerous modern sediment samples were collected and examined from the channel of Scott Creek adjacent to the marsh, upstream of the marsh area from Little Creek (a tributary of Scott Creek), and seaward of the marsh in the surf zone, beach, and dunes. Although the variability in mineral composition, grain size, and sorting was great among the samples, a significant observation was that the upstream samples included greater amounts of mica and mudstone

fragments than the beach deposits, which were of variable size range and sphericity, but dominantly consisted of quartz.

During coring, we encountered hard, often sandy, strata at approximately 1-m depth that were impenetrable by our gouge cores. The most landward core, SC4, was the longest at 121 cm (figs. 20 and 21).

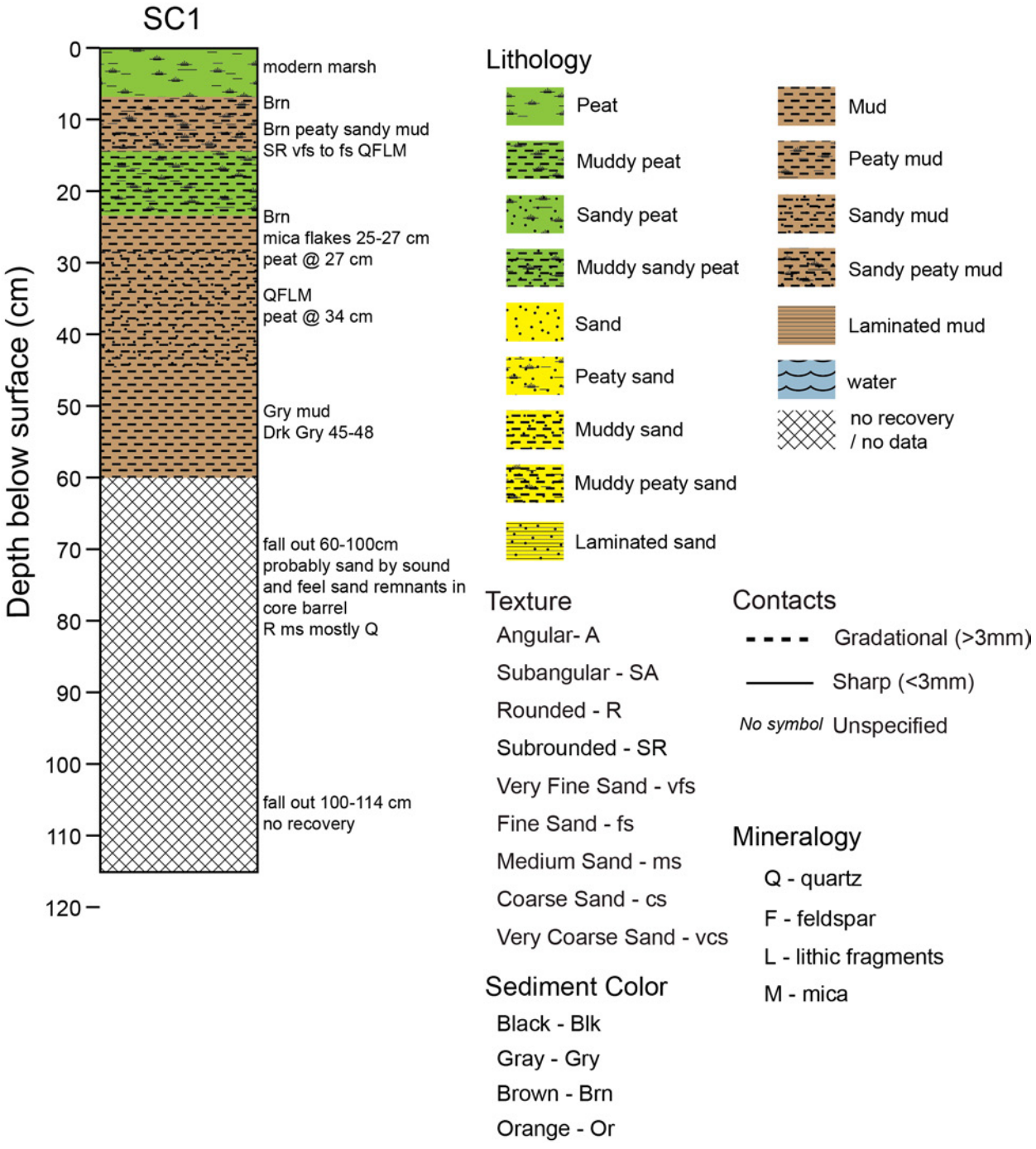

Figure 20. Core log of gouge core SC1, from Scotts Creek marsh. Dry surface conditions at the marsh prevented deep core penetration and recovery.

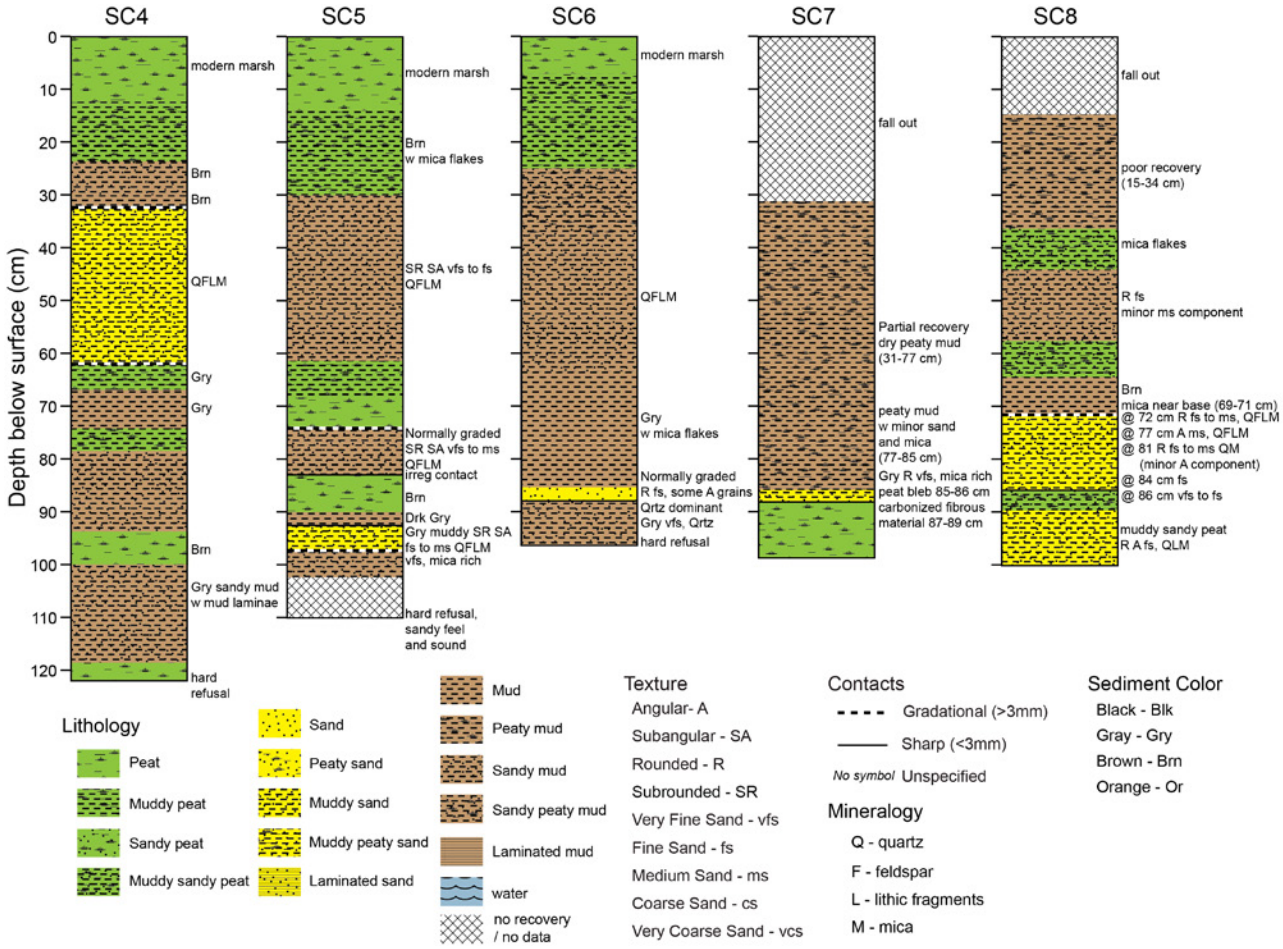

Figure 21. Correlation core logs from gouge cores SC4 through SC8, Scotts Creek marsh. A sand or muddy sand layer between 70 and 90 cm depth is interpreted as a laterally continuous deposit among the cores, which sediment provenance analysis indicates was most likely deposited by freshwater flooding.

No sandy deposits consistent with tsunami deposition were observed in cores SC1, SC2, and SC3, taken from along a large channel on the north side of the marsh (figs. 19, 20). The deposits in the cores consisted largely of peat, mud, and sandy mud.

Sandy deposits were recovered in cores SC4, SC5, SC6, and SC8, from a cattail-dominated inland area of the marsh, and SC7, collected near the center of the wetland in a small patch of *Salicornia* (pickleweed). In addition to peat and mud, each of these cores contains one or more layers of sand or muddy sand with sharp basal contacts. Mica is present throughout most of the cores in the sand, mud, and peat.

Of particular interest at the Scott Creek locality is a possibly correlative layer of sand and muddy sand about 70–90 cm below the surface, which was observed in cores SC4–SC8 (fig. 21), as well as near 1-m depth in an additional unlogged core. The presence of the layer in these six cores suggests lateral continuity over at least 60 m. It includes some physical characteristics consistent with deposition by a tsunami: (1) grading: normal grading was observed in core SC5, and inverse grading (81–86 cm) giving way to normal grading (72–77 cm) in core SC8 (fig. 21); (2) sharp basal contacts of the sand unit in each of cores SC4–SC8; and (3) a possible peat rip-up clast at 85–86 cm in core SC7.

The sand deposits between 70 and 90 cm in the cores show more similarities with upstream sediments than with modern sands from the swash zone, beach, and dunes. Compositionally, the sand is similar to beach and dune sand except that mica is abundant in the sand layer in the cores, but largely

absent from the beach and dune sands. The sand samples from the upper Scott Creek drainage basin are derived from plutonic and metamorphic rocks of the Salinian Block, Santa Margarita Sandstone, and Santa Cruz Mudstone. They contain a large component compositionally similar to the core deposits and are mica rich. Texturally, the sand units in the cores do not include coarse sand as is found in the berm and back beach, and the very fine component of the core sands is not present on the beach or dunes. Sand grains in the core deposits have a well-rounded component dissimilar to what is observed in most of the upstream sediment sources evaluated for the study, with the exception of sands derived from the Santa Margarita Sandstone, which were observed to be very fine grained and well rounded. The Santa Margarita Sandstone was the only source sediment sampled that had a very fine-grained component. There is a consistent occurrence of very fine rounded sand and mica throughout the cores – in some mud and peat units as well as sandy deposits—which shows that fine rounded sand and mica are regularly deposited on the marsh through non-tsunami processes.

In summary, the stratigraphic record easily accessible at Scott Creek is short, with most core penetration less than 1 m. Six cores with sandy deposits at about 70–90 cm below the surface of one area of the marsh have some characteristics consistent with tsunami deposition. This includes lateral continuity, sharp basal contacts, normal grading (evident in two cores), and a rip-up clast (present in one core). However, the mica present in the deposits indicates an upstream source and the very fine rounded sand was only present in sediment sampled from the channels and upstream. Microfaunal analyses might provide additional insight into the conclusion, by evaluating whether a marine and freshwater source for the deposit is more evident. Detailed grain-size analyses of normally graded sands could help determine if the grading resulted from sediment settling out of suspension. Employing one or more age dating techniques could help with correlations and help determine the length of the record sampled. More work could be attempted in the marsh area south of the creek channel, although it is likely that at least part of that area was altered in conjunction with highway construction, and we suspect that the subsurface record would not be more extensive than what is seen beneath the marsh north of the channel.

Carmel River Lagoon and Wetland Natural Preserve

The Carmel River Lagoon and Wetlands Natural Preserve covers an area of about 300 acres at the mouth of the Carmel River, immediately south of the city of Carmel-by-the-Sea (fig. 22). The lagoon and wetland form an ecologically dynamic area where environmental factors (area of surface water, water depth, salinity, sediment deposition, and turbidity) vary both seasonally and annually and are attributed to both natural processes and anthropogenic impacts (Monterey Peninsula Water Management District, 2013). At the time of our field investigation, the barrier sand spit was intact, and standing water as deep as ~1 m prevented access and coring in the northern, tule marsh area where we had planned to work (fig. 23).

Figure 22. Map showing location of the Carmel River Lagoon and Wetland Preserve, on the Central California coast south of the city of Carmel-by-the-Sea.

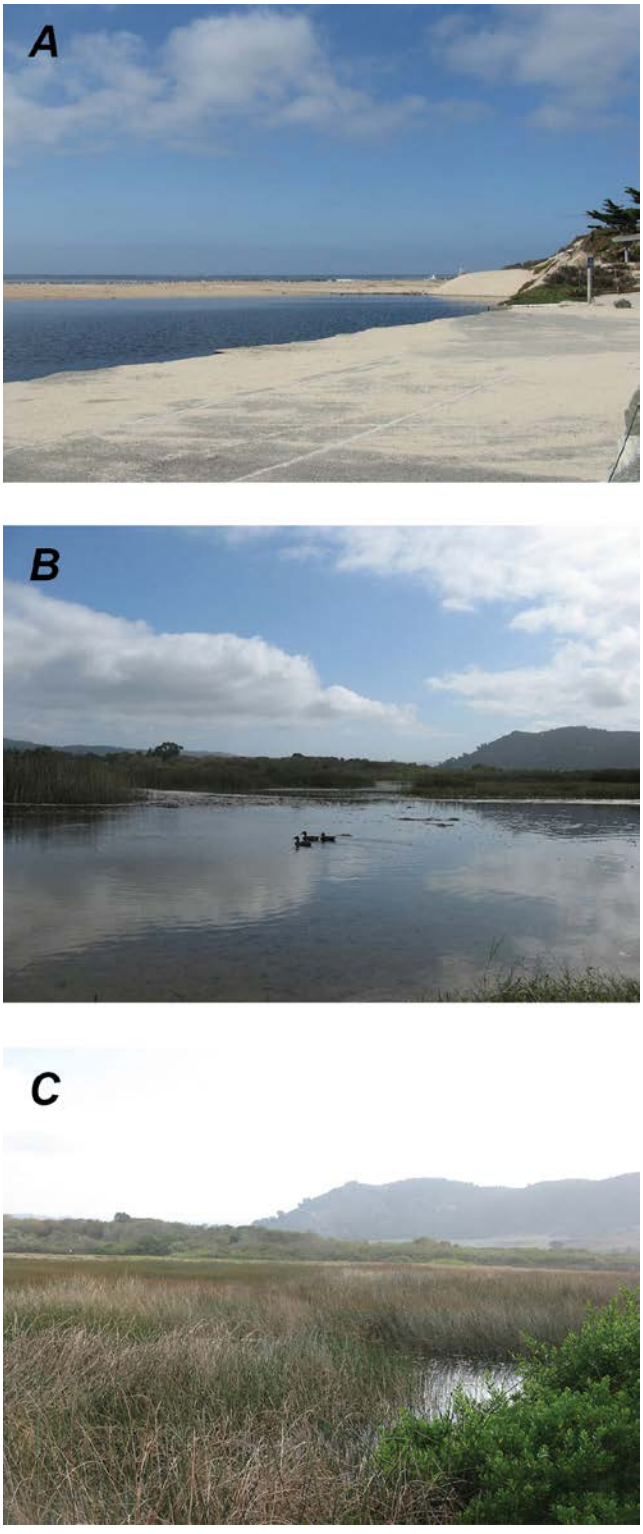

Figure 23. Photographs of the barrier beach and interior of the Carmel River Lagoon. *A*, View of the north end of the barrier beach from the visitor's parking area. At the time of the field visit, the barrier was intact, resulting in more than 1 m of standing water in the proposed coring locations, as well as near encroachment on private properties adjacent to the preserve. *B*, View to the southeast of the river channel / open lagoon area. *C*, View to the east at the densely vegetated wetland flooded by ~ 1 m of water backed up from the lagoon.

The Carmel River Lagoon and Wetlands Nature Preserve was included as a reconnaissance site for this study primarily because it is low-lying wetland along a stretch of the Central California coast dominated by rocky terraces and broad sandy beaches. The ASZIII model predicted moderately high (~3–4 m) tsunami wave heights in the vicinity of Carmel Lagoon, presumably great enough to inundate at least the lower Carmel River estuary.

However, based on a literature review, interviews with California State Parks personnel[12], and our on-site observations, we determined that the likelihood of preservation—and identification—of paleotsunami deposits in this setting would be low. This conclusion is primarily based on previous work and historical observations in the area documenting the natural variability of the marsh and lagoon environments, including extensive flooding from the Carmel River as well as inundation from storm surges that in past have crossed the entire wetland to affect adjacent residential areas (Casagrande and Watson, 2003; Larson and others, 2005; Casagrande, 2006; Monterey Peninsula Water Management District, 2013). Anthropogenic impacts are also a major consideration, including artificial breaching of the barrier sand spit for flood control, a near-annual practice started in the early 20th century (Monterey Peninsula Water Management District, 2013). Therefore, because of the influence of dynamic natural processes and effects of local land-use practices, we conclude that the Carmel River Lagoon area is likely a low-probability site for recording past inundation by tsunamis.

Los Osos Creek (Morro Bay)

Los Osos Creek is one of three localities, along with Sweet Springs Nature Preserve and Morro Estuary Natural Preserve, investigated for possible paleotsunami deposits along Morro Bay (fig. 24). The AASZ III model predicts wave heights of ~5 m MHW for the coast near the current mouth of Morro Bay, and ~2 m in the interior of the bay.

Los Osos Creek flows into southeastern Morro Bay ~0.5 km northeast of the town of Los Osos (fig. 24). It is one of the main tributaries to Morro Bay, draining a watershed area of about 60 km^2 (Gillespie and others, 2011). The study site, a marsh along lower Los Osos Creek, is ~4.3 km from the current mouth of Morro Bay, and ~3.5 km due east of the central reach of the Morro Bay Sand Spit, which separates Morro Bay from the Pacific Ocean.

Lower Los Osos Creek was chosen as an evaluation site for possible paleotsunami deposits because of the presence of long-extant salt marshes, evident on historical topographic sheets, or T-sheets (Forney, 1883–84), and its distance from residential or commercial development. Salt marshes cover the floor of the low-gradient, lower stream valley of Los Osos Creek for hundreds of meters upstream from the current mouth of the creek at Morro Bay (figs. 24, 25, and 26).

[12]We particularly appreciate information about environmental conditions at Carmel River Lagoon provided by Amy Palkovic, the Monterey District Environmental Scientist for California State Parks.

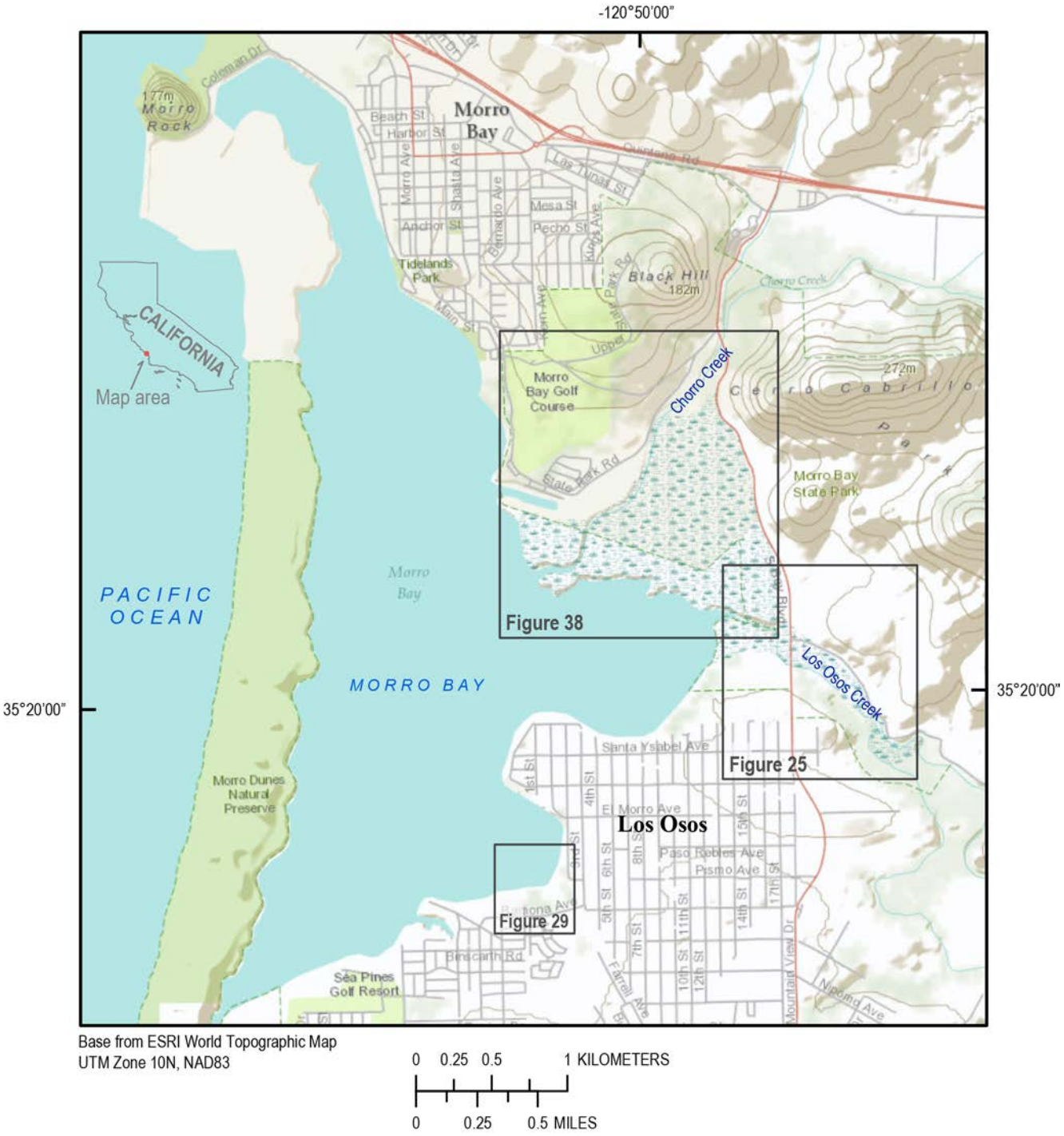

Figure 24. Map showing locations of the three field localities for Morro Bay: Morro Estuary Natural Preserve (see fig. 38), Los Osos Creek (see fig. 25), and Sweet Springs Nature Preserve (see fig. 29).

Figure 25. Vertical aerial photograph showing distribution of gouge cores examined at the Los Osos Creek study site.

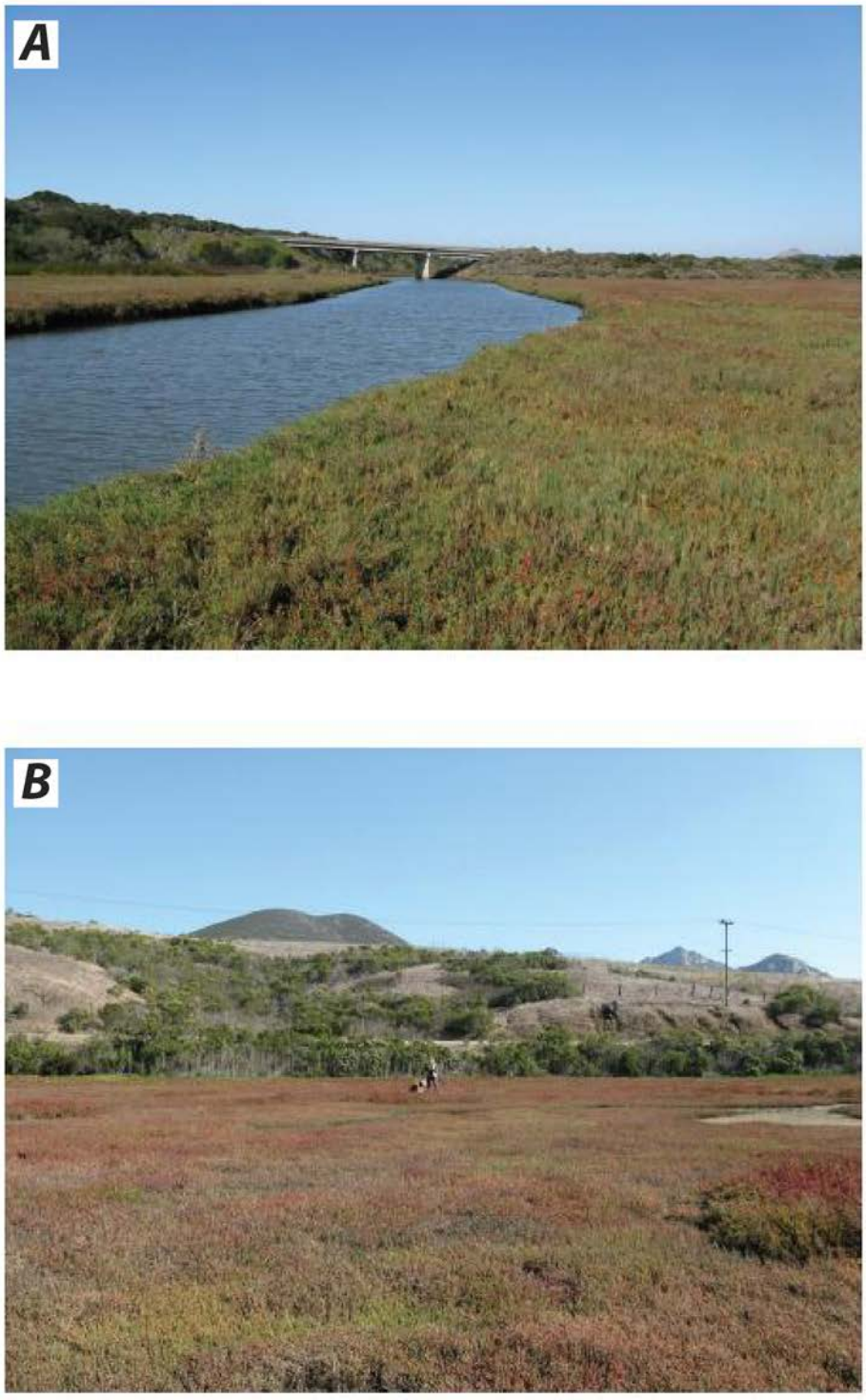

Figure 26. Photographs of the Los Osos Creek field locality. *A*, View to the west-northwest (downstream) in the direction of Morro Bay. *B*, Same vantage point as in *A* but looking to the north towards core site LO1.

Two gouge cores (LO1, LO2) were extracted and described from the marsh on the north bank of lower Los Osos Creek (fig. 25). Core site LO1 is about 125 m north of the present creek channel and about 20 m landward of a saltpan 50–60 m wide. Core site LO2 is about 20 m from the creek channel and roughly equidistant between the saltpan and a slough draining the marsh.

The stratigraphy in core LO1, from the inner marsh, shows a gradual change over time from intertidal flat or slough to marsh. Dominantly peat-rich deposits in the upper core are consistent with historical maps that show long-extant salt marshes at this location (fig. 27). Diatoms support the interpretation of a brackish-marine environment throughout the core, and they dominantly include taxa typical of low salt marshes (*Gyrosigma eximium*, *Nitzschia scapelliformis*) or muddy intertidal flats (*Caloneis westii*, *Tryblionella navicularis*, and *Surirella fasciculata*).

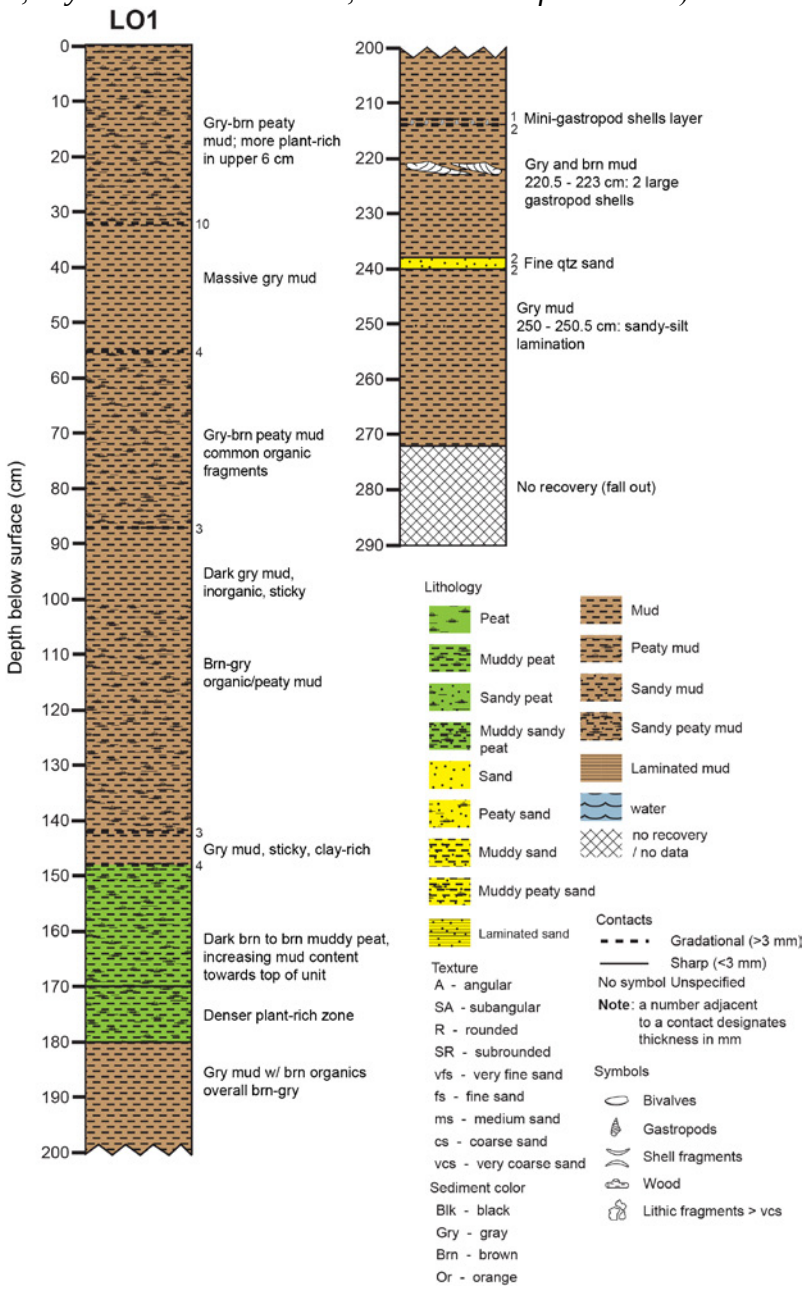

Figure 27. Core log of gouge core LO1 from the Los Osos Creek study site. The stratigraphy shows an overall trend from lower intertidal flat or slough to tidal flat to marsh, consistent with long-extant marshes shown on historical maps.

In comparison, the environment indicated by deposits in LO2 is dominantly muddy intertidal or subtidal, showing that the present emergent marsh is a relatively recent environment for the core site (fig. 28). Fine sand is a prominent component throughout LO2, both in inorganic muddy deposits in the lower core and organic-rich, peaty deposits shallower than about 40-cm depth. Peat between 26 and 31 cm contains a visibly greater concentration of fine sand, but similar deposits were not observed in test cores collected within a few meters of LO2, showing that the deposit is not laterally extensive. Both cores LO1 and LO2 bottomed out in sand at subsurface depths of about 280–290 cm.

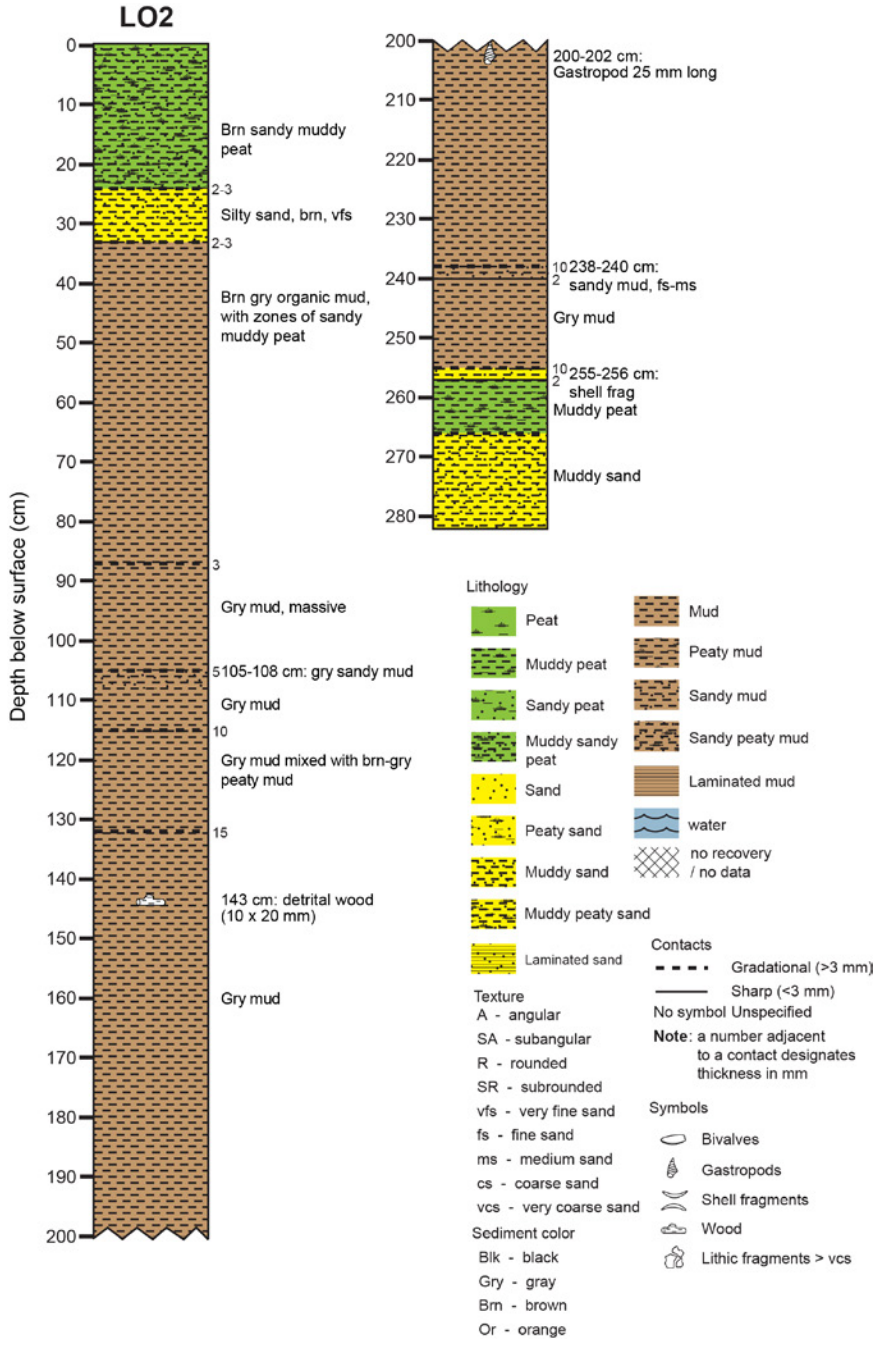

Figure 28. Core log of gouge core LO2, Los Osos Creek marsh. Organic-rich/peaty deposits are primarily found shallower than ~40 cm, indicating a relatively recent development of an emergent marsh area at the core site.

Although we found no anomalous deposits consistent with tsunami deposition at the LO1/LO2 study site on the north side of lower Los Osos Creek, it might be informative to investigate additional marsh areas on the south side of the channel that are still proximal to the mouth of creek and within the area of historically extant marshes.

Sweet Springs Nature Preserve (Morro Bay)

Sweet Springs Nature Preserve is a 24-acre property owned by the Morro Coast Audubon Society on the south shore of Morro Bay (figs. 24, 29). For this study, we focused on the salt marsh to freshwater wetland that borders the bay on the eastern part of the property, part of which has been emergent since at least 1884 based on the historical T-sheet (Forney, 1883–84). The marsh is located about 2 km east-southeast of the southern reach of the Morro Bay Sand Spit and roughly 4.1 km from the present entrance to the bay.

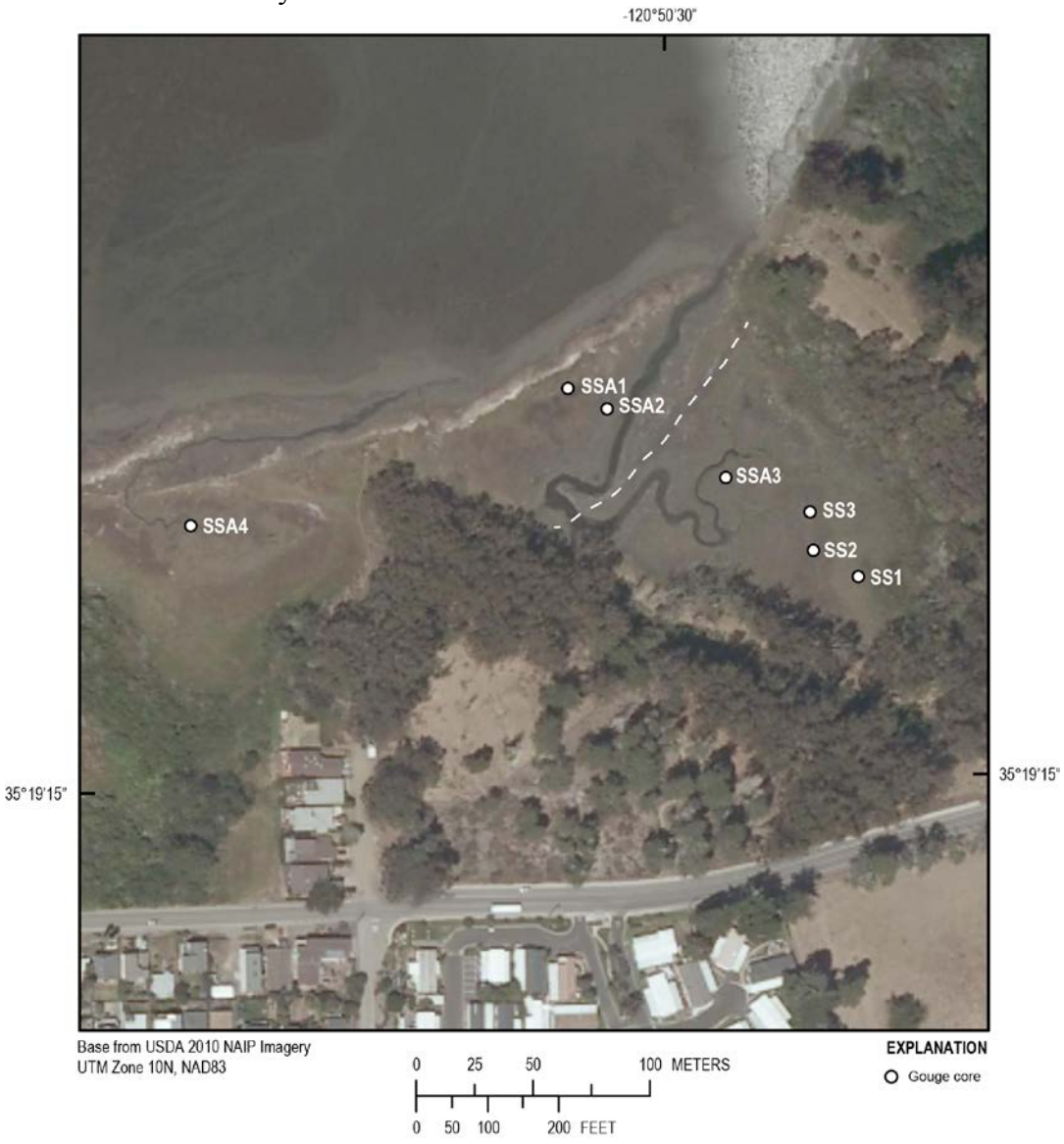

Figure 29. Vertical aerial photograph showing locations of gouge cores examined at the Sweet Springs Preserve study site. White dashed line is the approximate bayward extent of the historical emergent marsh based on gouge core data.

Two field teams collected and described six gouge cores on a shore-normal, southeast-northwest transect in the eastern marsh area (figs. 29, 30). An additional gouge core (SSA4) was collected in a small marsh area close to the margin of the bay about 200 m west of the transect.

From southeast to northwest (bayward) along the transect, the four most landward cores—SS1, SS2, SS3, and SSA3—show thick sections (>150 cm) of dense, fibrous peat to peaty mud, consistent with a long-extant marsh at the site (figs. 30–34). No coarse-grained or mineral-rich deposits are found within the peaty units above 150-cm depth in SS1 or SS2, or above 200-cm depth in SS3 and SSA3. Several thin beds of poorly sorted, quartz-dominant sand are found intercalated in peaty mud below 200-cm depth in both SS3 and SSA3.

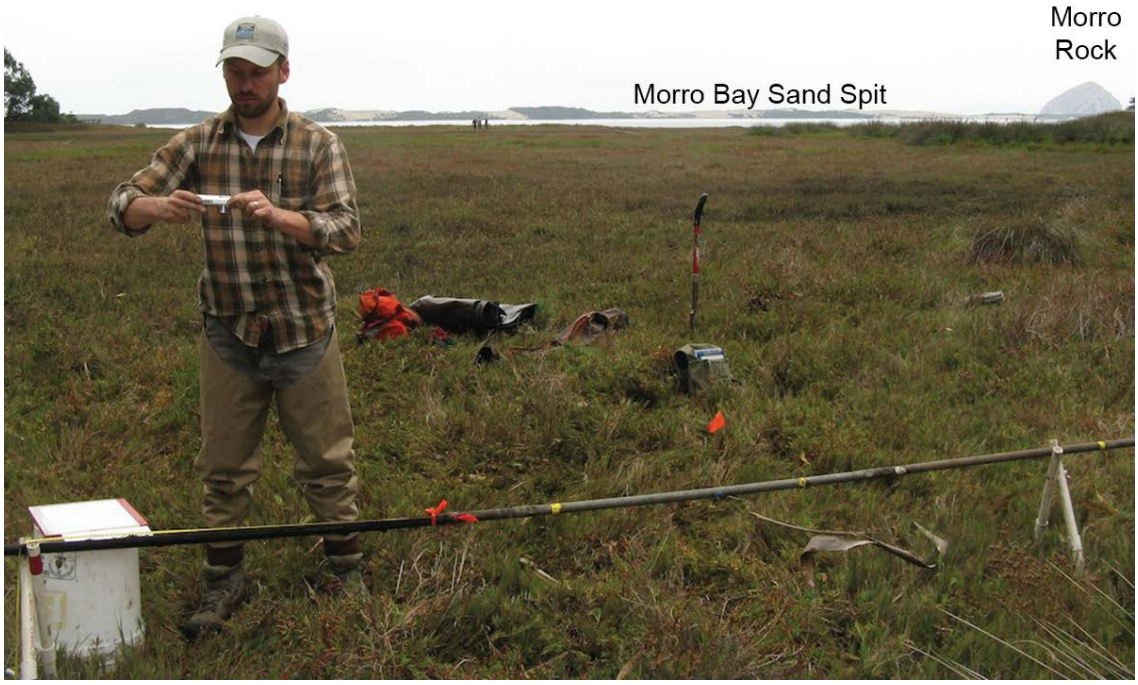

Figure 30. Photograph of coring operations at Sweet Springs Nature Preserve, on the south shore of Morro Bay. View is to the northwest from the location of core SS1, across the marsh towards Morro Bay. The approximate middle reach of Morro Bay Sand Spit is visible in the distance, as is Morro Rock at the entrance to the harbor. In foreground is Humboldt State University research assistant Nick Graehl; team members from the USGS and Cal State University Fullerton are visible in the distance at core site SSA1.

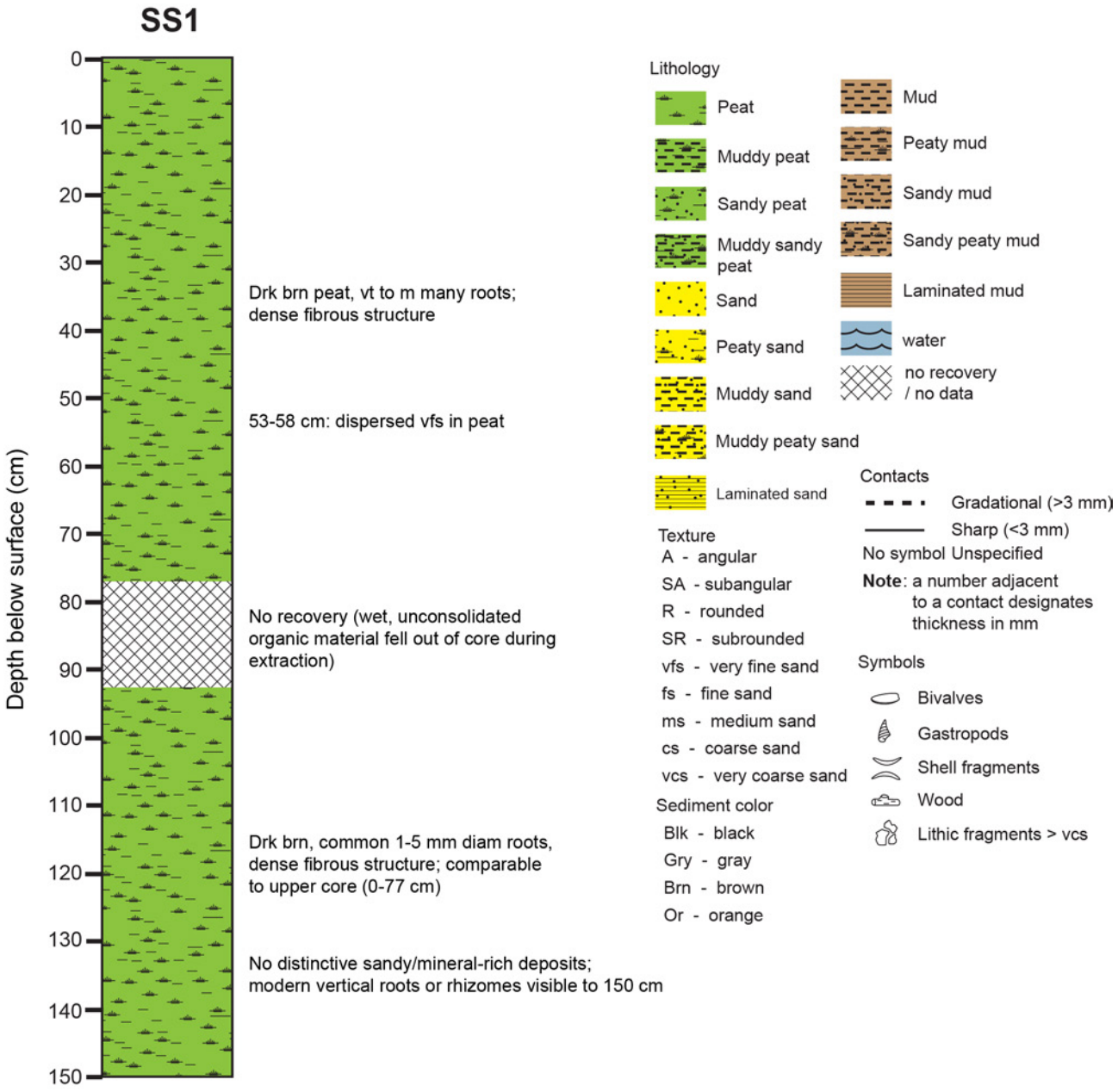

Figure 31. Core log for gouge core SS1, Sweet Springs Nature Preserve

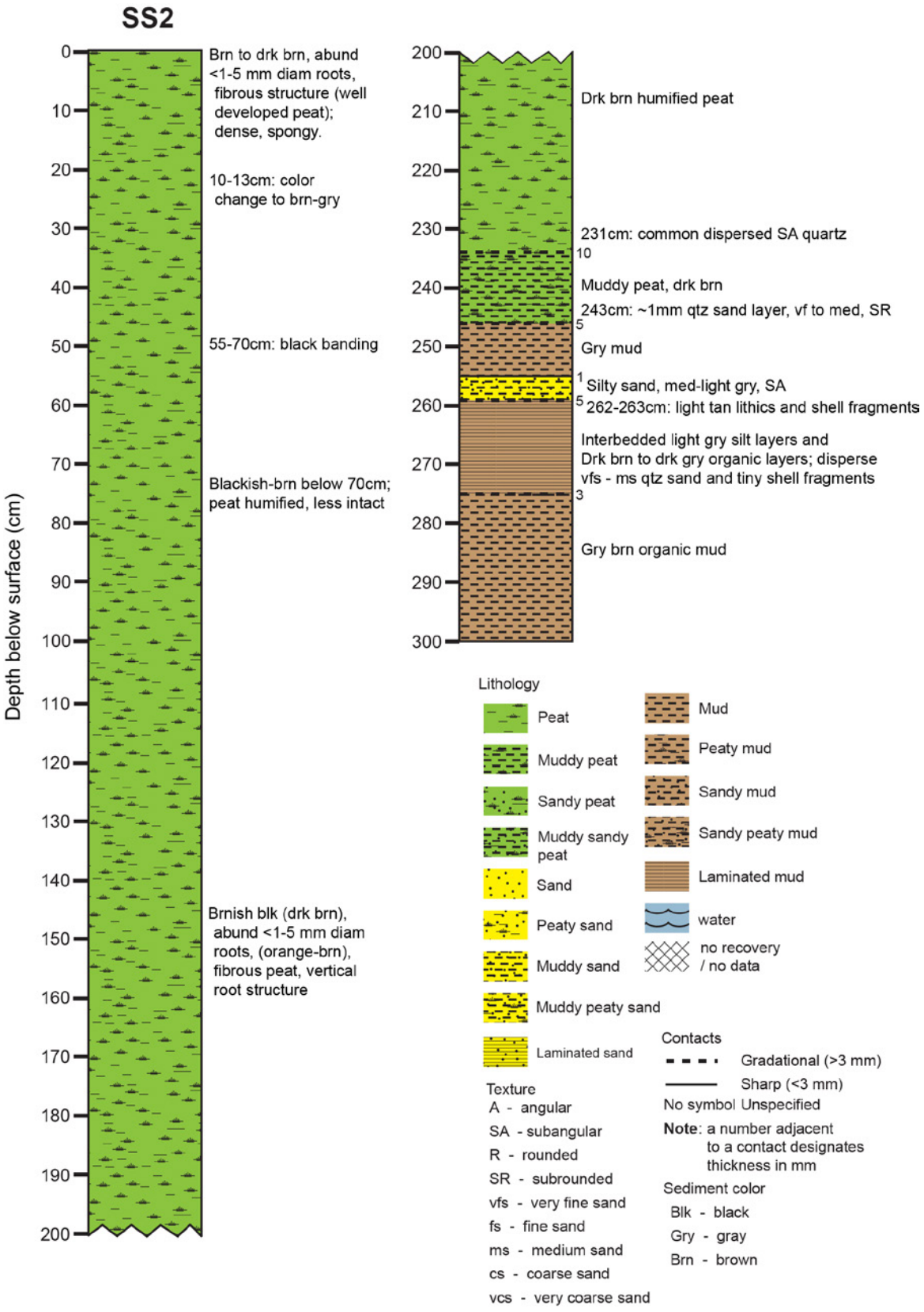

Figure 32. Core log for gouge core SS2, Sweet Springs Nature Preserve.

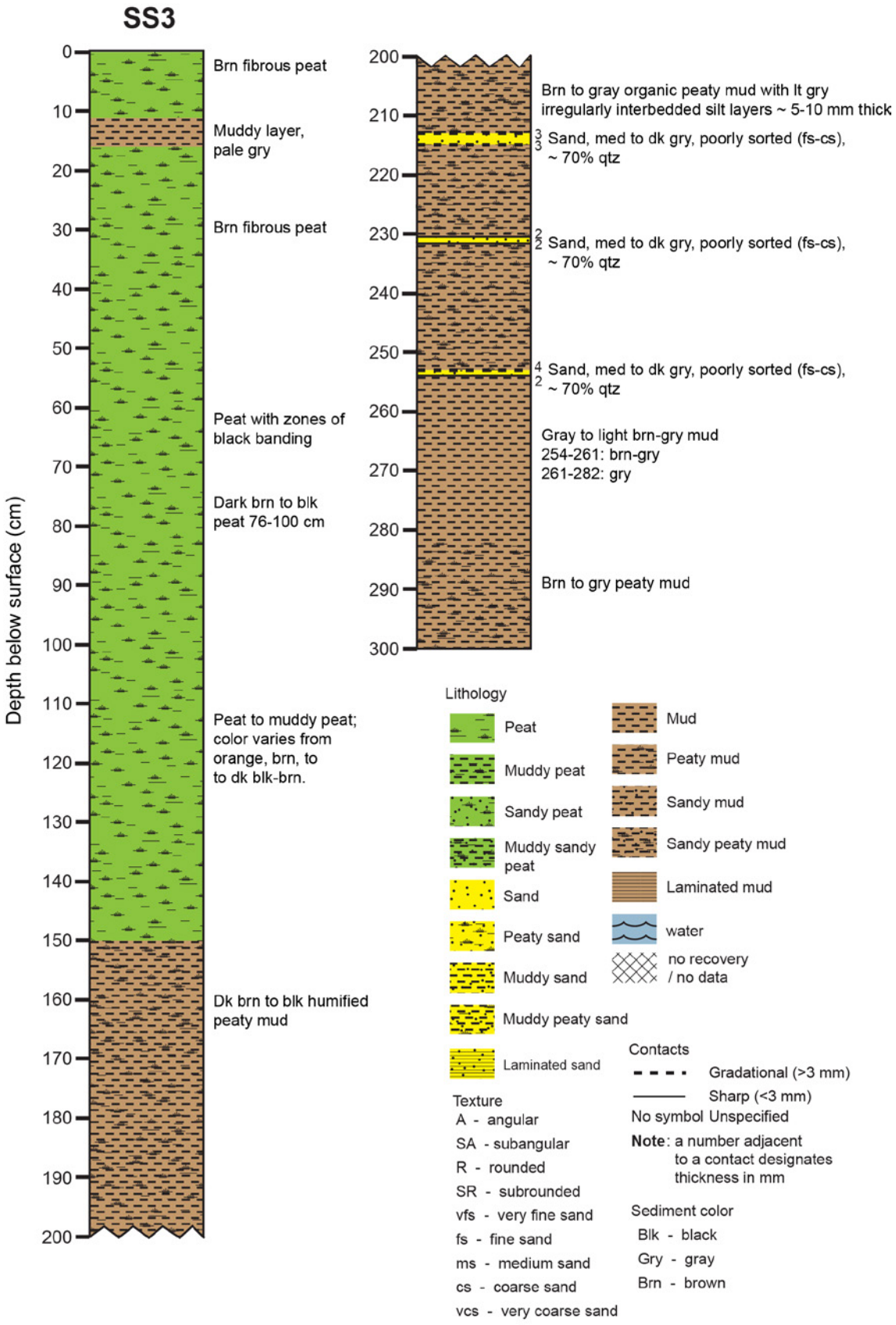

Figure 33. Core log for gouge core SS3, Sweet Springs Nature Preserve.

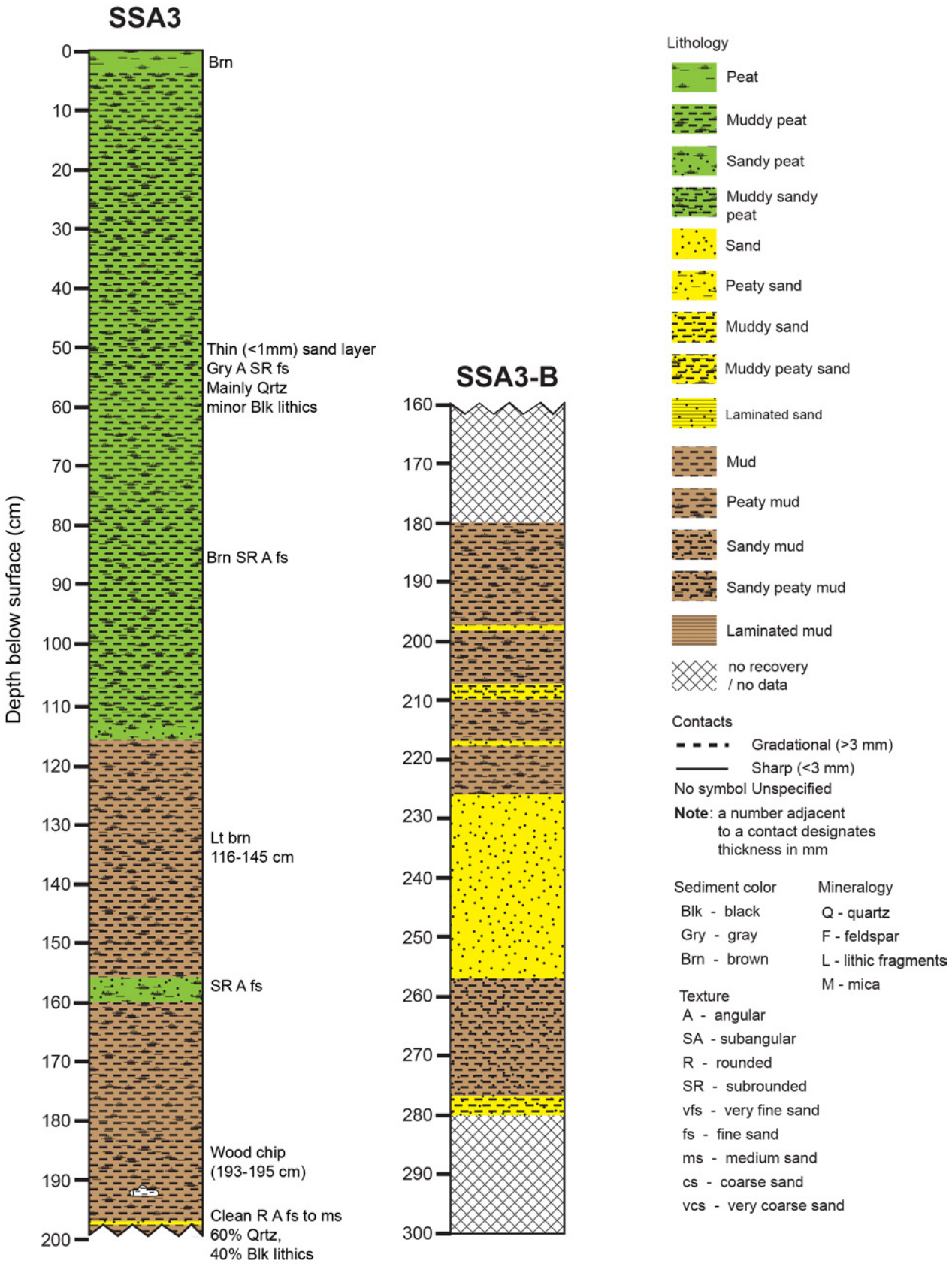

Figure 34. Core log for gouge core SSA3, Sweet Springs Nature Preserve.

Cores SSA1 and SSA2 are located bayward of a large slough draining the marsh; SSA1 is about 10 m from the present narrow beach at the shore of the bay; SSA2 is about 40 m inland from the shore (figs. 35, 36). The cores primarily contain massive, fine- to medium-grained, quartz-rich sand consistent with coastal (beach or dune) deposits. The sand units are overlain by a bayward-thinning wedge of mud and peaty mud, which is then capped by about 15 cm of modern salt marsh peat. Core SSA4, collected in the marsh area about 200 m to the west, similarly contains thin deposits of organic-rich mud to peat capping a thick section of fine- to medium-grained sand to the base of core (fig 37).

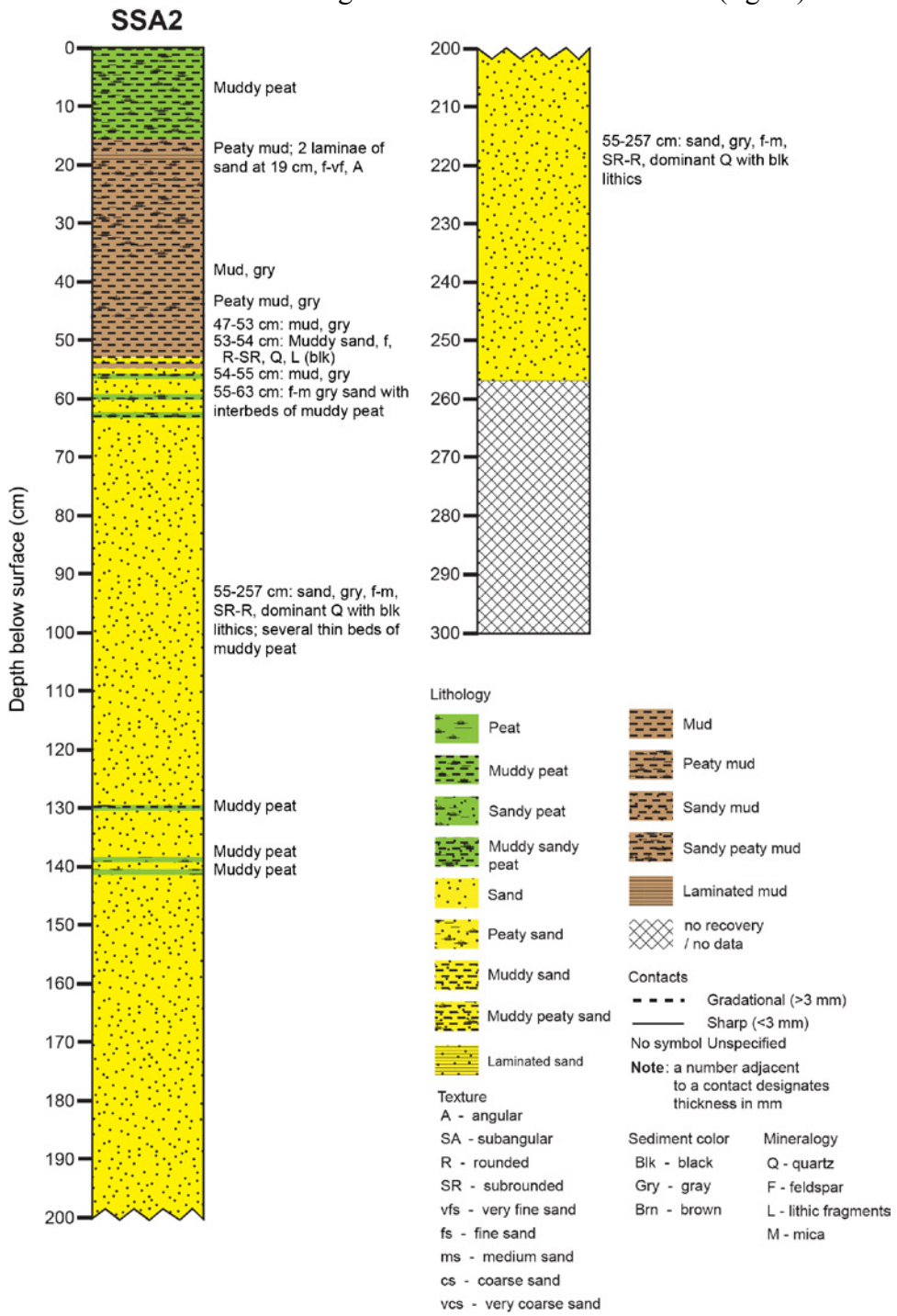

Figure 35. Core log for gouge core SSA2, Sweet Springs Nature Preserve.

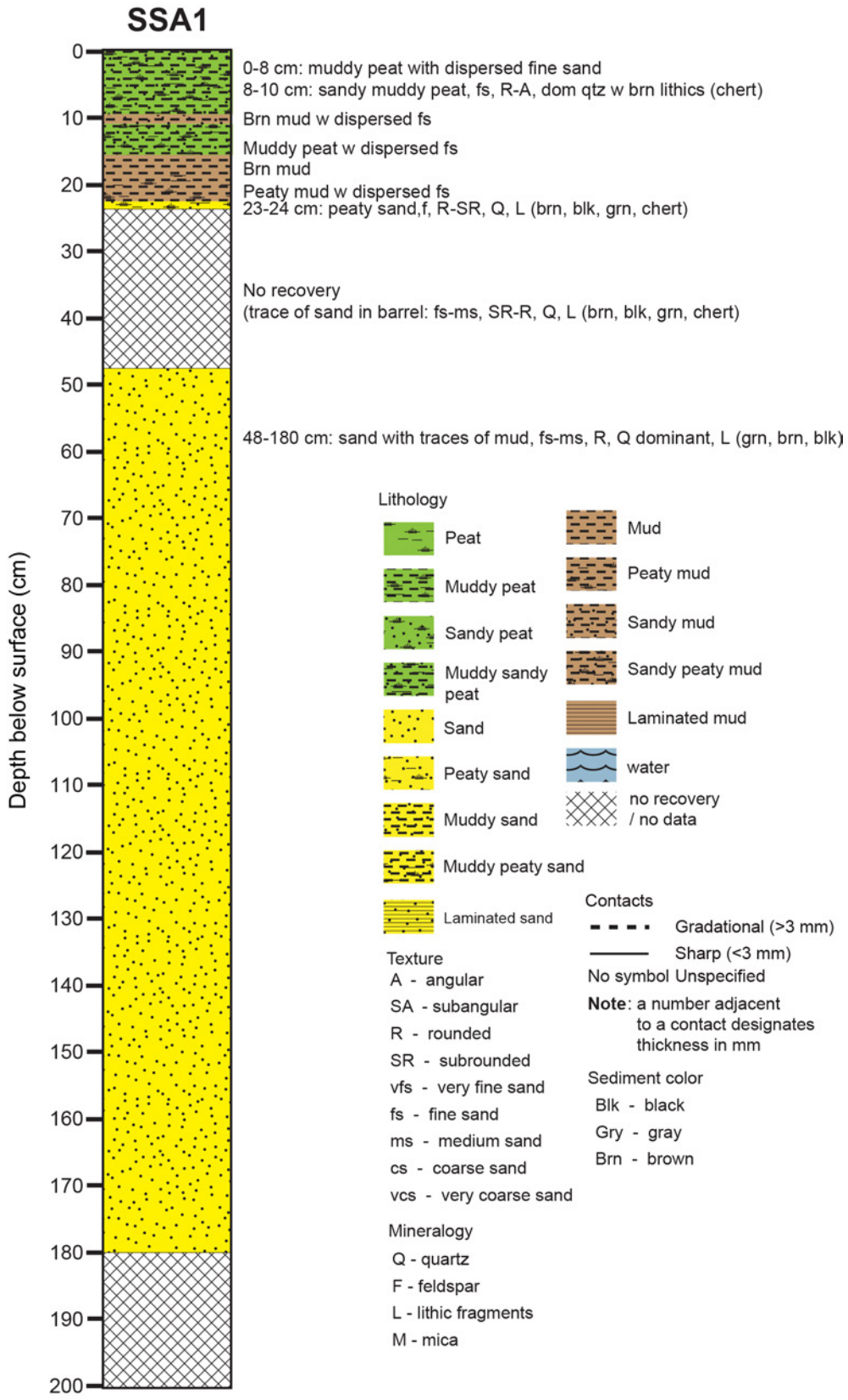

Figure 36. Core log for gouge core SSA1, Sweet Springs Nature Preserve.

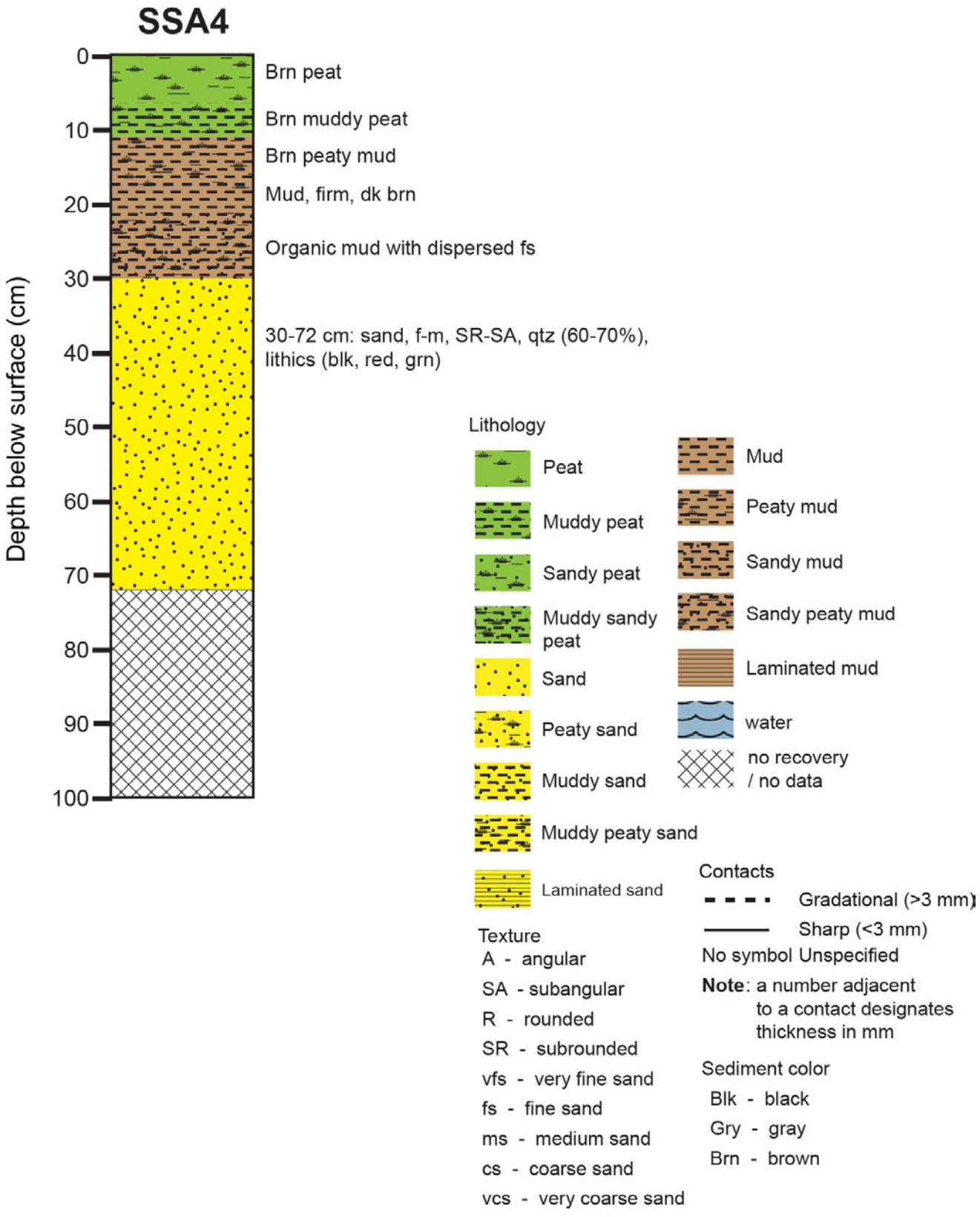

Figure 37. Core log for gouge core SSA4, Sweet Springs Nature Preserve.

The lateral transition along the core transect from dominantly sandy (that is, possible beach or dune) deposits to organic-rich peaty deposits shows that only the most landward four cores are from the area of long-extant marsh. A possible former beach strand is visible on aerial imagery in this area about 10–20 m landward of the slough channel between cores SSA2 and SSA3 (fig. 29, dashed white line). Therefore, an emergent marsh in the vicinities of SSA1, SSA2, and SSA4 is a relatively recent feature, having aggraded since the 1869 T-sheet survey, comparable to other nearshore areas of Morro Bay (for example, the extensive tidal flats and emergent marsh areas at the outlets of Chorro and Los Osos Creeks). The absence of any visible coarse-grained, mineral-rich deposits in the upper peaty sections of the landward cores suggests that inundation from the bay—from storms or tsunami—has not been recorded at those core sites for some time. It would be informative to acquire accurate elevation data for the core sites at this location to compare the changes in lithology relative to sea level.

Morro Estuary Natural Preserve (Morro Bay)

The Morro Estuary Natural Preserve (MENP) is an 800-acre wetland within Morro State Park in northeastern Morro Bay (figs. 24, 38). The MNEP consists of emergent salt marshes and tidal sloughs formed on the delta of Chorro Creek, an area of well-documented excessive sediment loading during the 20th century (Haltiner, 1988; Central Coast Regional Water Quality Control Board, 2002; Gillespie and others, 2011). The localities cored within the MENP for this study are located about ~2–3 km from the present entrance to the bay and about ~1.4–1.9 km east of the central reach of the Morro Bay Sand Spit.

Figure 38. Vertical aerial photograph showing locations of gouge cores examined in the Morro Estuary Natural Preserve, including a series of cores near the Morro Bay Marina. The dashed lines show the extent of emergent salt marshes (white line) and tidal flat (black line) as depicted on the 1869 T-Sheet, prior to excessive sediment accumulation at the terminus of Chorro Creek caused by erosion from upstream ranching and agricultural practices.

Based on the U.S. Coast Survey T-sheet from 1883 (Forney, 1883–84), emergent marshes now extend westward to areas that were previously intertidal flats or shallow bay floor, extending ~400 m farther than the boundaries shown for the late 1800s (fig. 38). Although it was likely that recent high sedimentation loading would complicate efforts to locate possible paleotsunami deposits in this area, the MNEP represented one of the few locations along the shores of Morro Bay with evidence from historical maps for long-extant salt marshes. Therefore, the MENP locality was included in the reconnaissance survey to determine if a pre-1900s stratigraphic record could be identified, and if that record might provide evidence for anomalous deposits.

Two field teams collected and described a total of 11 gouge cores from salt marshes in the MENP: 3 cores (MP1–MP3) in the northeastern area of the preserve; and 8 cores (MBM1–MBM8) from the southwestern area near the Morro Bay Marina and the lower channel of Chorro Creek (fig. 38). Cores MP1, MP2, and MP3 were collected along a southwest-northeast transect in an area of marsh dissected by deep slough channels, and densely vegetated with bushy stands of halophytes (*Salicornia* sp. ?) suggesting high soil salinity (figs. 39, 40). Using hand-driven gouge cores, we were able to penetrate only through ~2 m of mostly muddy and sandy deposits below the modern marsh surface.

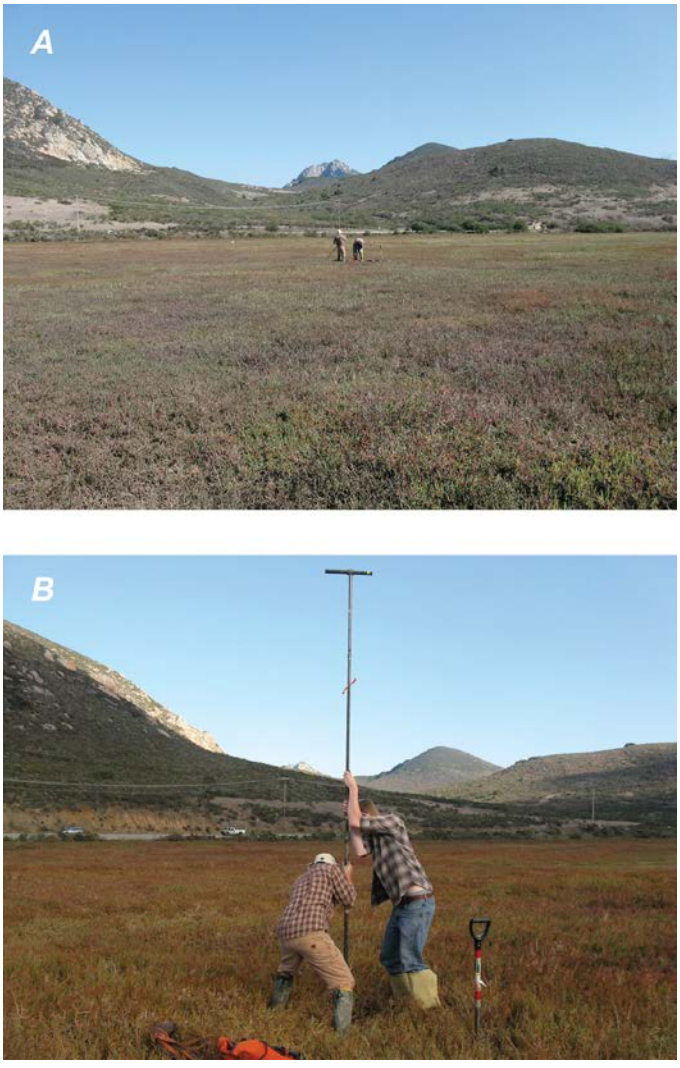

Figure 39. Photographs of coring operations at core site MP3, Morro Estuary Natural Preserve. *A*, View to the east-northeast across the flat, densely vegetated marsh towards core site MP3 in the northeastern part of this field area. *B*, Humboldt State University geologist Nick Graehl and student assistant extracting gouge core MP3.

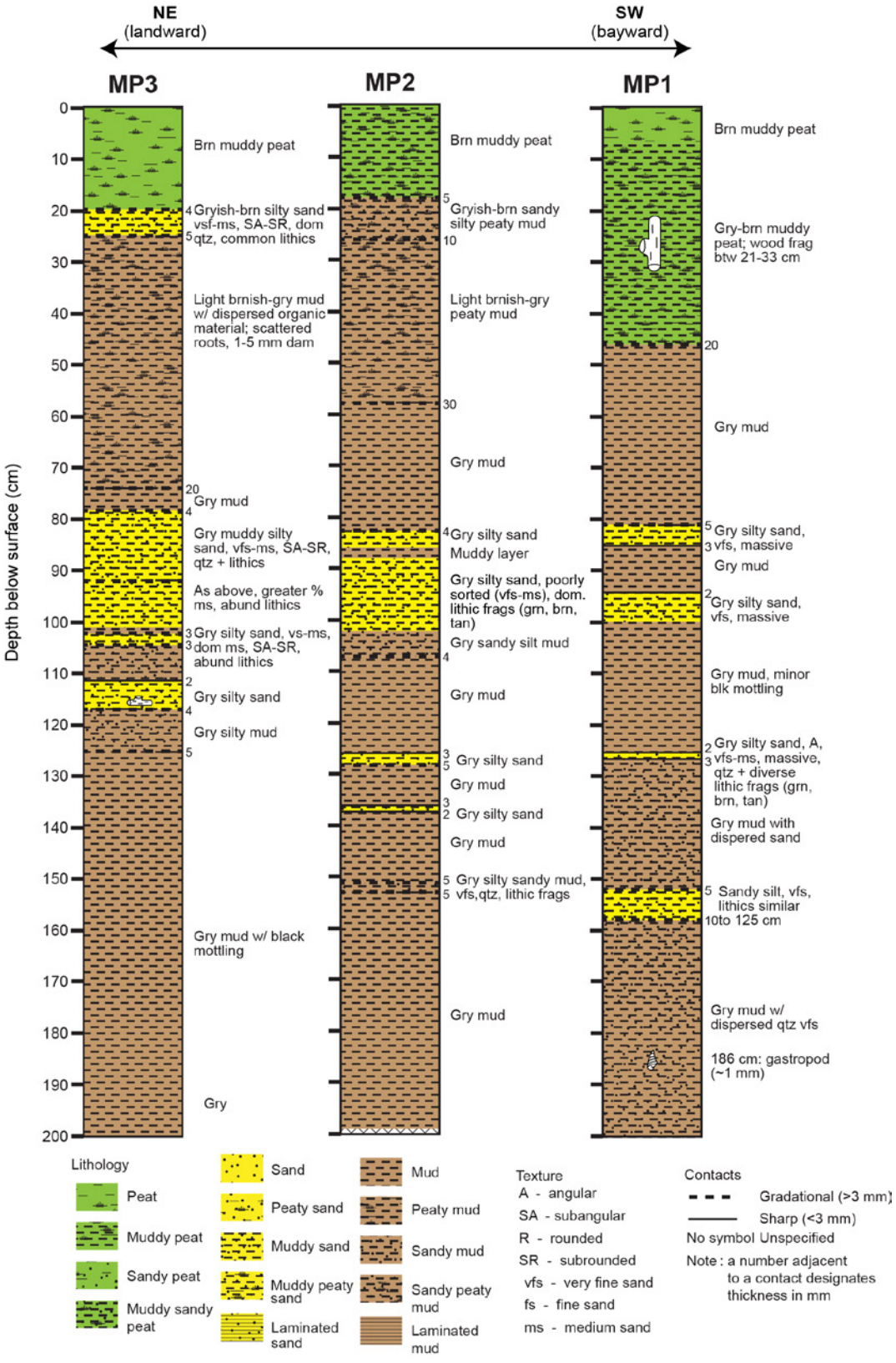

Figure 40. Core logs for cores MP1, MP2, and MP3 from the northeastern Morro Estuary Natural Preserve study area. Gray muddy sand deposits near 80-100 cm are lithic-rich and thicker in a landward direction, indicating a fluvial source.

In each of these cores, the uppermost few decimeters consist of muddy peat, consistent with accumulation of modern marsh deposits. Overall, muddy peat and organic/peaty mud deposits thin in a bayward direction. Only inorganic mud and sand deposits are found in the core records below the capping organic-rich deposits. Likely correlatable units of muddy sand near 80-cm depth in each core are lithic rich and thicken in a landward direction, consistent with fluvial deposits. A comparable though less distinct deposit visible in cores MP2 and MP3 near 20-cm depth is also interpreted as fluvial in origin. We interpret the stratigraphy to ~2-m depth in cores MP1, MP2, and MP3 as recent deposits associated with high rates of upstream erosion since the early 20th century. We conclude that it would require machine-driven coring equipment in this area to reach and penetrate through the pre-1900s marsh surface to evaluate the older stratigraphy for any anomalous deposits.

Cores MBM1, MBM2, and MBM3 were collected from the marsh area west of the main lower channel for Chorro Creek, near the Morro Bay Marina, and are the three most bayward cores evaluated for the MENP study area (fig. 41). MBM1 is located along the lower area of salt marsh shown on the 1869 T-sheet. The sites for cores MBM2 and MBM3, also collected in the marsh area, would have been in the open bay prior to the late 1800s. MBM3 shows a few decimeters of brown muddy peat to gray peaty mud capping sand-rich sections to the base of core. Overall there is a trend of greater sand concentration among the three cores in a bayward direction.

Cores MBM4 through MBM8 were collected from the salt marsh area on the northwest side of the lower channel of Chorro Creek, about 300 to 700 m northeast of the Morro Bay Marina (figs. 42, 43). Cores MBM4, MBM5, and MBM7 bottom out in muddy quartz-rich sand, comparable to the sand deposits in the lower section of core MBM1. Two 3-cm-thick layers of sand in MBM4 between 30- and 40-cm depth consist of clean, fine- to medium-grained tan sand with angular to rounded grains. The sand layers are not laterally continuous in adjacent cores. Basal contacts are sharp. The upper sand layer shows normal grading, the lower unit exhibits no clear grading, and both have sharp basal contacts. The composition and texture of both sand layers in MBM4 are distinct from sand sampled locally from the lower Chorro Creek channel. Grains-size and mineralogical analyses to better estimate the provenance and mode of deposition for these sand layers are currently underway.

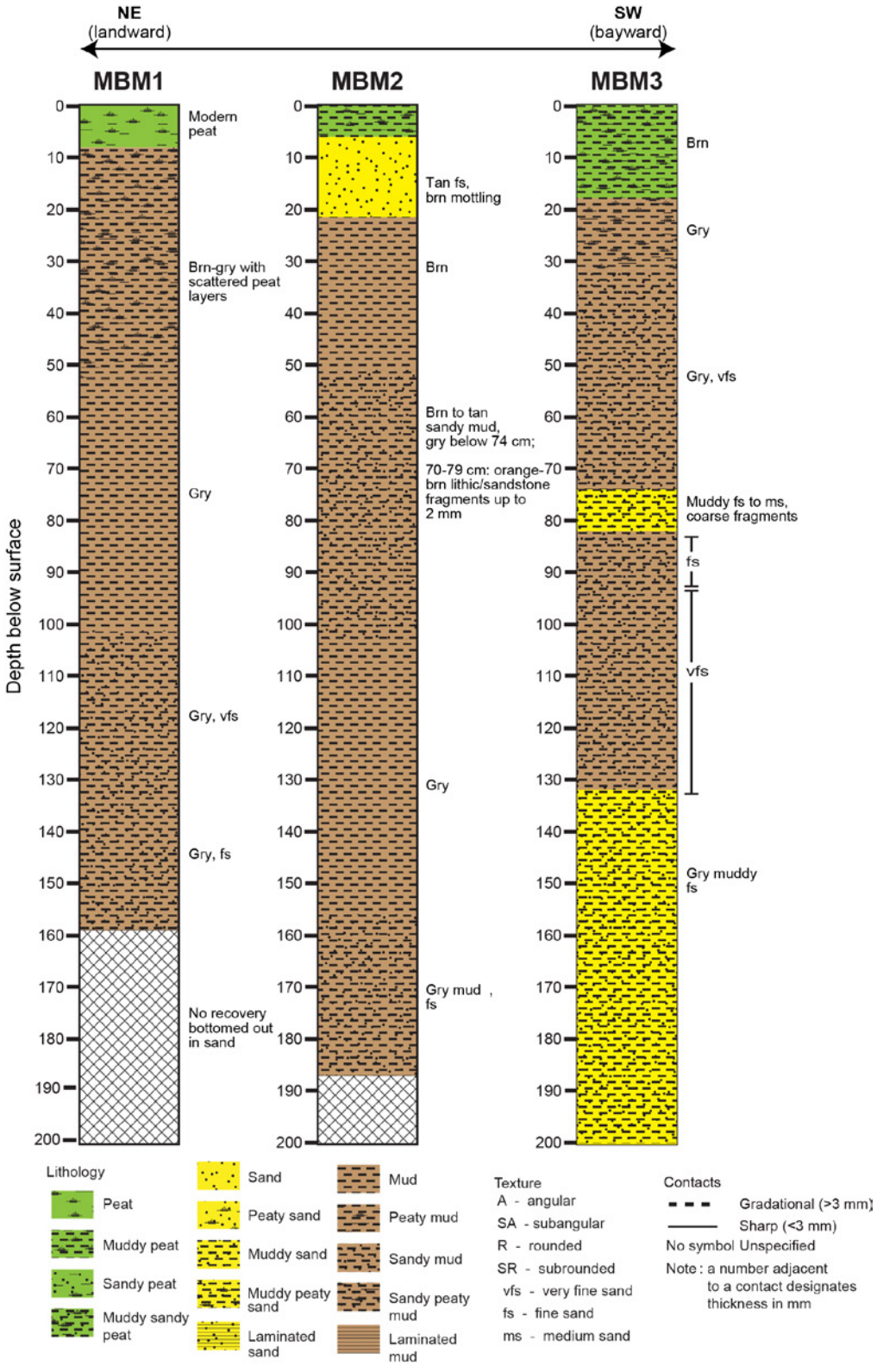

Figure 41. Core logs for cores MBM1, MBM2, and MBM3, from the lower delta of Chorro Creek near the Morro Bay Marina. The recent accretion of emergent marshes at the core sites is indicated by thin deposits of peat or peaty mud in the upper few decimeters of each core, capping progressively sandier delta or tidal flat deposits in a bayward direction.

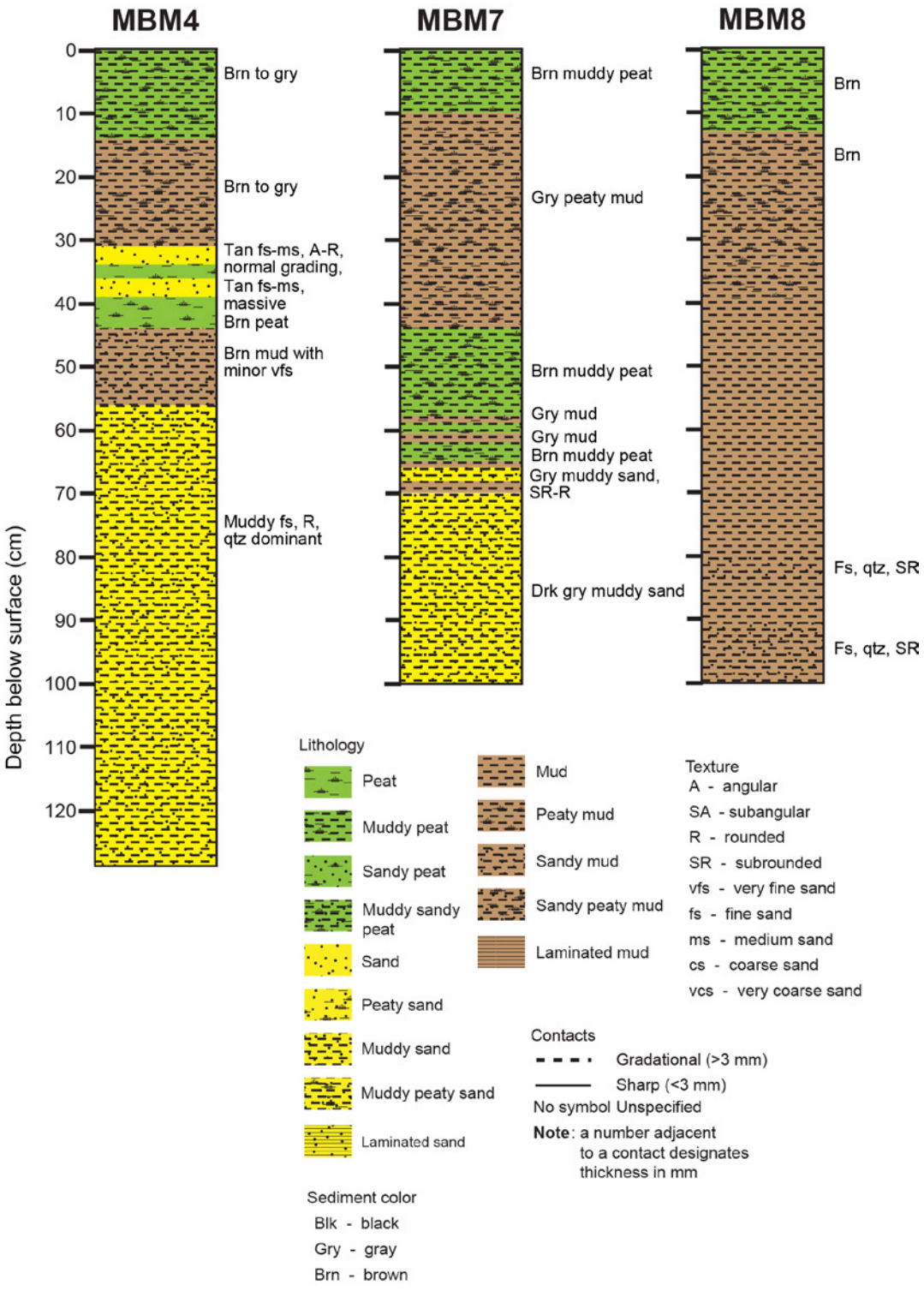

Figure 42. Core logs for cores MBM4, MBM7, and MBM8, from a salt marsh area on the northwest side of the lower channel of Chorro Creek, about 300 m northeast of the Morro Bay Marina.

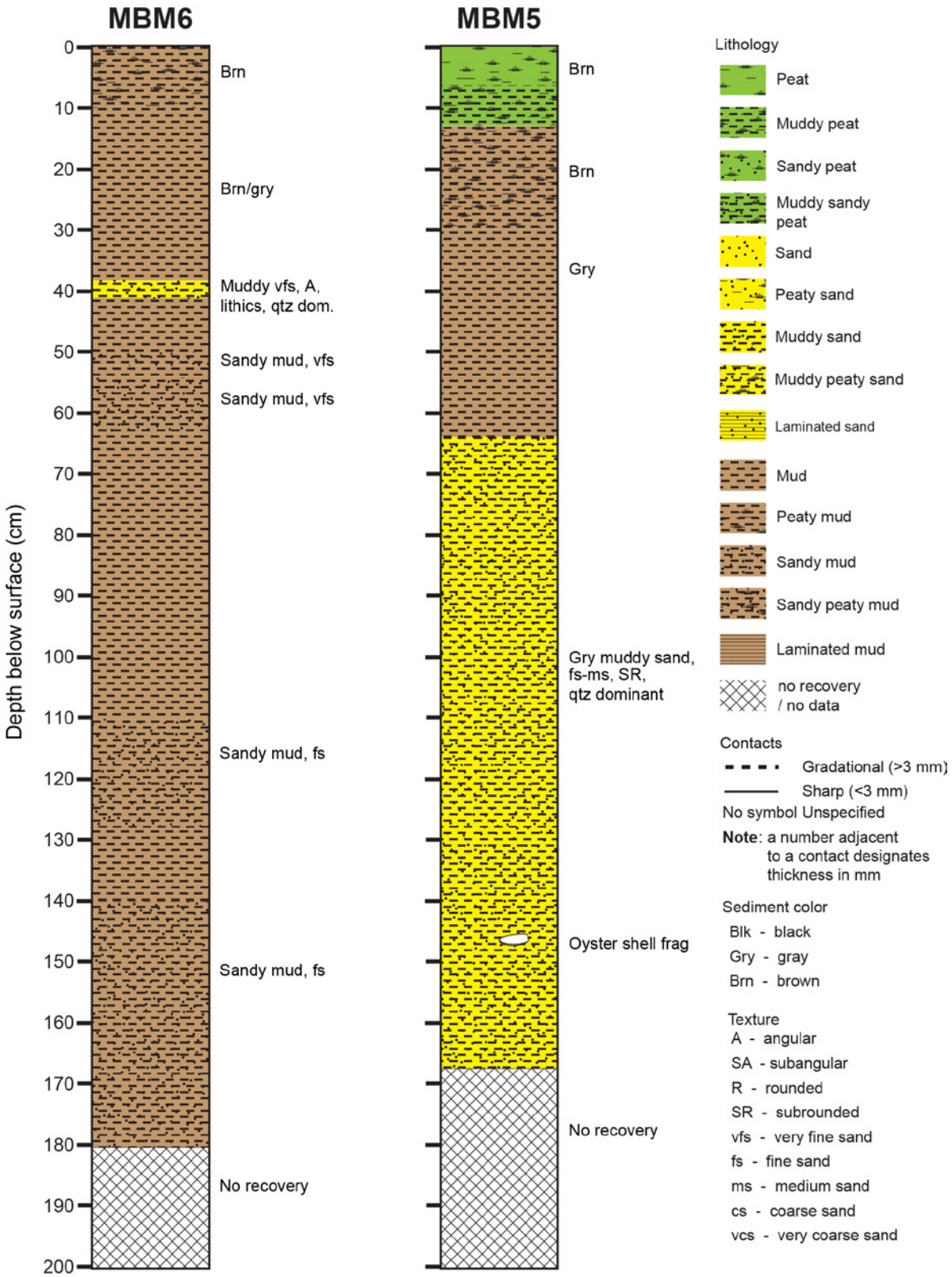

Figure 43. Core logs for cores MBM5 and MBM6 from a salt marsh area on the northwest side of the lower channel of Chorro Creek, about 650 m northeast of the Morro Bay Marina.

Based on analysis of the series of cores collected for this study, any further work in the MENP to evaluate the stratigraphic record older than the 20th century should be undertaken with coring equipment capable of deeper drilling than is possible with hand-driven gouge cores. If possible, future investigations should focus on locations estimated to have minimal fluvial impact from Chorro Creek.

San Luis Obispo Creek (Avila Beach)

San Luis Obispo Creek meets the Pacific Ocean at the town of Avila Beach, on the south-facing north shore of San Luis Obispo Bay on the central California coast (figs. 44, 45). Avila Beach is about 9 km northwest of Pismo Beach and is the closest community to the Diablo Canyon Nuclear Power Plant, which is located about 11 km northward along the coast.

Figure 44. Map showing location of the San Luis Obispo Creek / Avila Beach study area.

Figure 45. Vertical aerial photograph of the San Luis Obispo Creek / Avila Beach study area. The bright green area is a golf resort built over former marsh areas along the lower estuary and on the floor of a low-contour valley north of the estuary.

The San Luis Obispo Creek estuary was chosen as a reconnaissance evaluation site for tsunami deposits for several reasons: (1) the ASZIII model predicted large tsunami wave heights (~11 m) for the coast at Avila Beach; (2) San Luis Obispo Creek is one of the few low-lying estuarine sites along a stretch of coast primarily formed of steep sea cliffs or wide sandy beaches; (3) historical maps showed large marsh areas along the north and south margins of the lower creek; and (4) in addition to the northeastward-trending lower stream valley, there is a low-gradient valley leading northward from the mouth of the estuary that could be a possible depositional site for large tsunami. Although it was evident from aerial photos that former marsh areas of the lower estuary had been reclaimed first for agricultural uses and then for a golf resort, we completed a field reconnaissance at the site to ascertain if there might be any remnant natural wetland areas, either upstream from the main resort area or along the margins of the northward-trending valley.

We concluded that there were no remaining wetland areas to be explored in the lower estuary or northward-trending valley, and that all formerly flat marsh surfaces had been most recently reclaimed, graded, and contoured to make the Avila Beach Golf Resort. We are grateful for the help of Mr. Rob Rossi, the resort owner, who briefed us on the historical changes to Avila Beach—including the huge oil-spill remediation and reconstruction of the town during 1998–2002 by Unocal (Union Oil Company of California, since 2005 part of Chevron Corporation)—and gave us permission to explore the golf course property with gouge cores. We attempted coring at several locations to determine if we could penetrate through the surface vegetation and fill to reach the former wetland deposits, but it was not feasible to penetrate the dry surface and underlying gravel fill with hand-driven coring equipment (fig. 46). Although it is possible that borehole coring might reach paleo-estuarine deposits at depth beneath the golf course, it is likely that the latest Holocene record is too disrupted to provide any stratigraphic information about possible past tsunami deposition at this locality.

Figure 46. Photographs of areas investigated for possible coring on the golf course property in the San Luis Obispo Creek / Avila Beach study area. *A*, In the northward-trending valley. *B*, At the farthest upstream creek terrace (former wetland area) on the south side San Luis Obispo Creek.

Reconnaissance Field Sites South of Point Conception, 2012

Coastal southern California extends for approximately 450 km from Point Conception south to the Mexican border. Situated along the northeastern edge of the tectonically complex inner California Continental Borderland (see, for example, Baher and others, 2005), the region is subject to local-source tsunamis generated by vertical displacement of the seafloor during earthquakes on offshore faults and submarine landslides, and also to distant-source tsunamis (Ross and others, 2004; Wilson and others, 2008; Barberopolou and others, 2009). Ten significant tsunamis occurred along the southern California coast between 1806 and 2011 (Lander and others, 1993; National Geophysical Data Center, 2013). Very few data exist on prehistoric tsunamis occurring in the region. Although numerical modeling of distant-source tsunami scenarios indicates that tsunami runups would be small to moderate (2–4 m) in southern California (table 2), the large coastal population and major maritime assets of the region make it highly vulnerable to any tsunamis that inundate dry land (Wood and others, 2013; Porter and others, 2013) and, therefore, important for tsunami deposit fieldwork. Reconnaissance fieldwork in southern California centered on the marshes at Pt. Mugu, Seal Beach, Los Penasquitos, and the Tijuana River estuary (fig. 5).

Point Mugu

Point Mugu is located in southern Ventura County approximately 96 km northwest of Los Angeles on the Point Mugu unit of the U.S. Naval Base Ventura County. This estuarine intertidal system is the largest in southern California. Point Mugu marsh is designated as a Federal Nature Preserve and provides a safeguarded research location with limited historical anthropogenic influence. Coastal southern California T-sheet data show beach ridge erosion and progradation of the marsh intertidal flat and vegetated wetlands since the mid to late 1800's (San Francisco Estuary Institute, 2009). Marsh vegetation is dominated by pickleweed and seepweed (see, for example, U.S. Fish and Wildlife Service, 2013). Calleguas Creek and Revolon Slough feed the wetlands, and the estuary's water regime is irregularly flooded. Situated approximately 6 km south of the estuary is the offshore section of the Malibu Coast sinistral-oblique reverse fault (see, for example, Petersen and others, 1996 and U.S. Geological Survey, 2004). Results of numerically modeled tsunami flow depths during the Aleutian-Alaska tsunami scenario event show depths of 1.12 m are possible in this area.

Eighteen gouge cores were collected along three northeast-trending transects (fig. 47). Transect A–A' extended approximately 725 m, with 75-m core spacing and penetrable depths between 63 and 128 cm. Transect B–B' stretched roughly 625 m, with 75-m core spacing and penetrable depths between 40 and 220 cm. Transect C–C' comprised two cores spaced 225 m apart that penetrated depths of 152 cm and 275 cm. Core spacing was dependent on marsh topography, which occasionally hindered accessibility to certain locations along each transect.

No stratigraphic evidence supporting the deposition of sand by tsunamis was seen at Point Mugu. In transect A to A', the upper stratigraphic unit in the cores was modern marsh, which capped mud or muddy sand of varying thickness (fig. 48). The third stratigraphic unit at depth varied from very fine sand to coarse sand interbedded with mud or sandy mud. Cores in transects B to B' and C to C' are composed of alternating mud and sand layers of varying thicknesses (not shown). The sand layers do not appear to be of tsunami origin and are most likely a result of alluvial processes. Samples from cores in Point Mugu have been submitted for laboratory analysis.

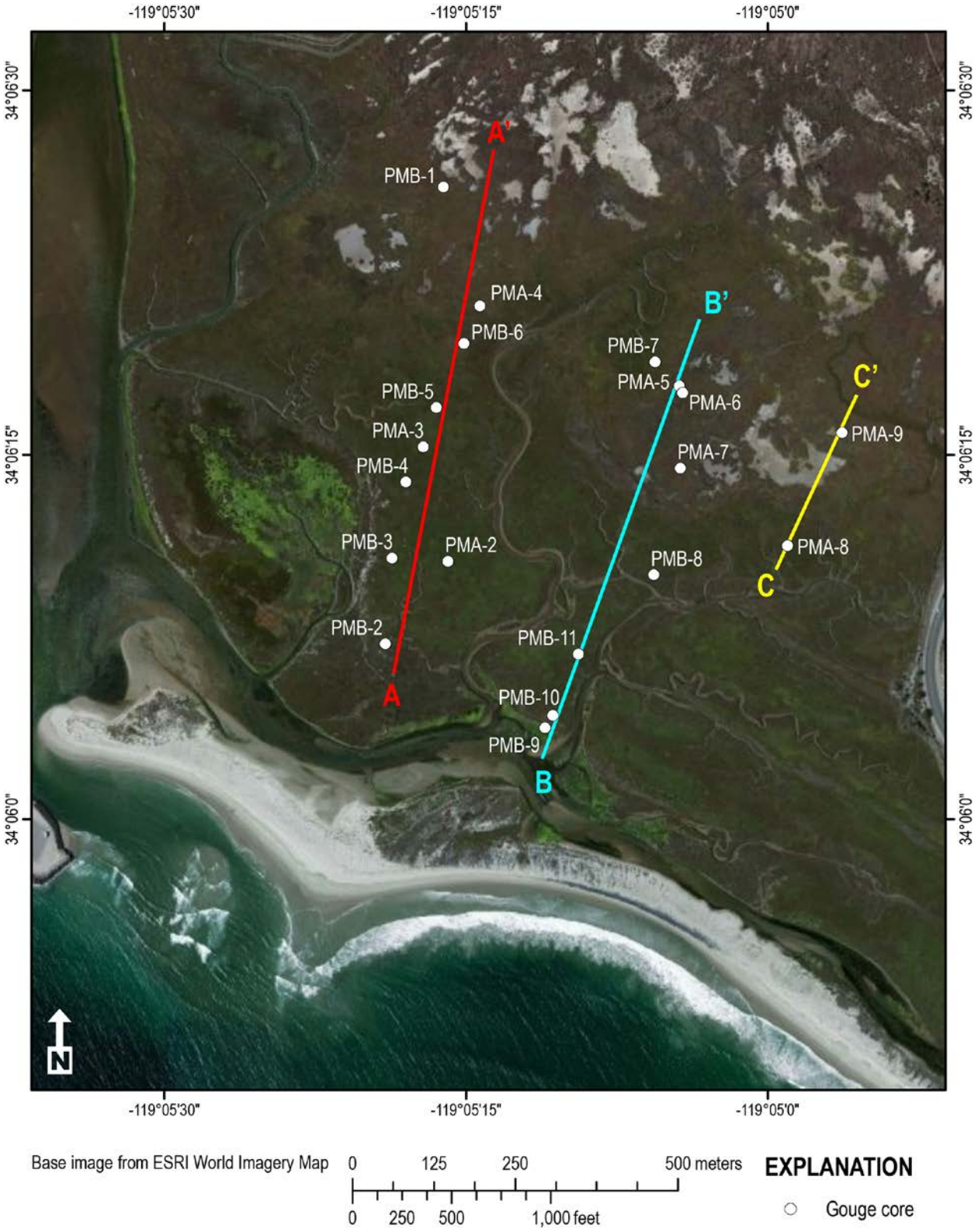

Figure 47. Vertical aerial photograph of the Pt. Mugu research site showing gouge core locations along three northeast to southwest-trending transects.

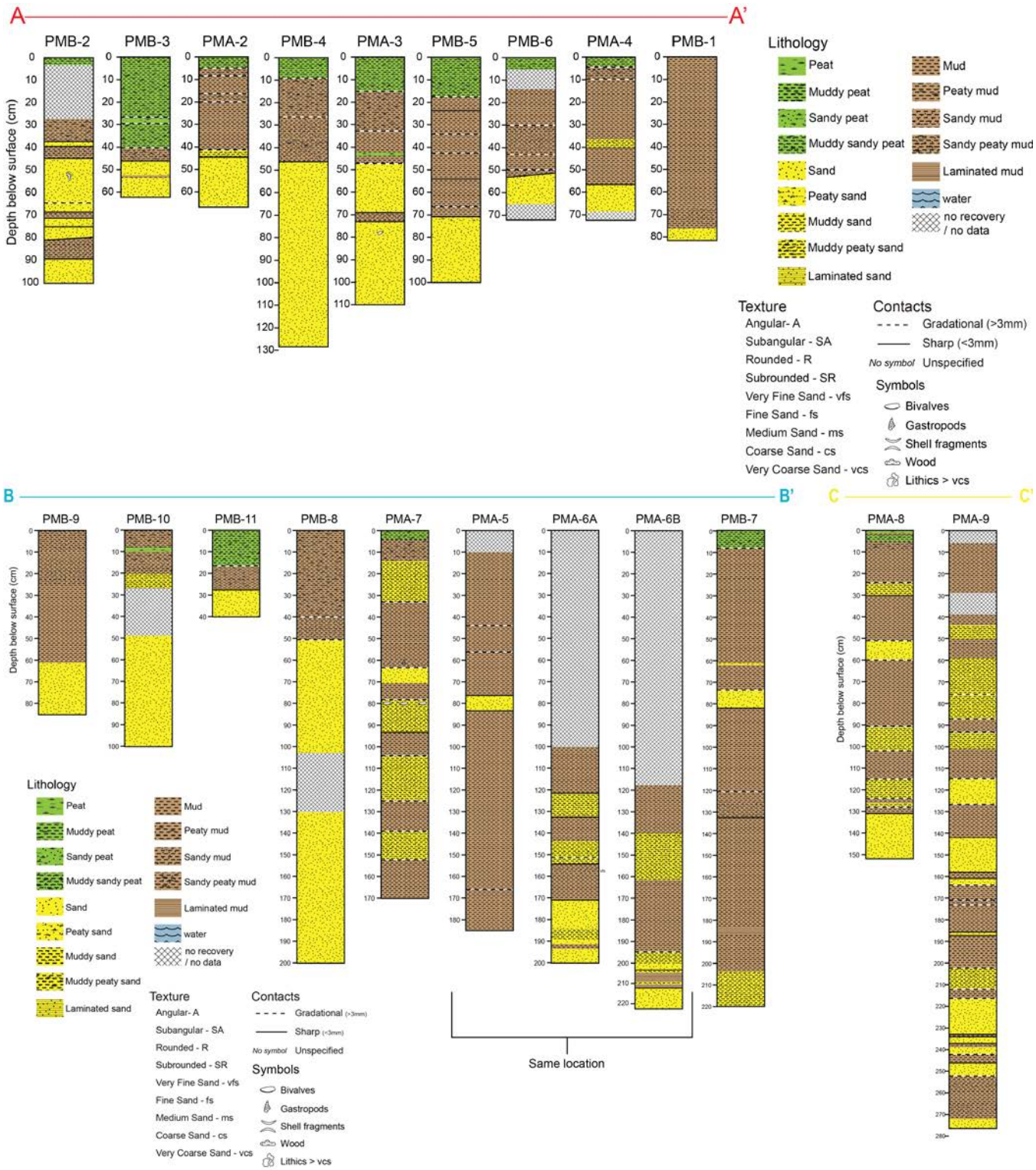

Figure 48. Gouge core logs along transect A-A' at the Pt. Mugu research site (see fig. 47 for location).

Seal Beach

The estuarine intertidal system situated at Seal Beach in northern Orange County, approximately 37 km southeast of Los Angeles on the U.S. Naval Weapons Station Seal Beach, is designated as a National Wildlife Refuge. The estuary's water regime is regularly flooded, and the marsh is dominated by pickleweed and saltwort (see, for example, U.S. Fish and Wildlife S, 2013). The wetland is part of the larger Anaheim Bay estuary and is located atop the northwest-striking right-lateral Newport-Inglewood Fault Zone (see, for example, Bryant, 1988; Wright, 1991). Coastal southern California T-sheet data show very little change in the Seal Beach marsh intertidal flat and vegetated wetlands since the mid to late 1800s (San Francisco Estuary Institute, 2009). Results of numerically modeled tsunami flow depths during the Aleutian-Alaska Tsunami Scenario event show depths of 1.56 m are possible near this area.

Eight gouge cores were taken at Seal Beach along a south- to southwest-trending transect (A–A') (fig. 49). The transect covered approximately 1,150 m, with core sites separated by roughly 200 m and penetrable depths ranging from 153 to 287 cm. In most of the cores, the upper stratigraphic unit is a 10–30–cm layer of the modern marsh capping peaty muds and muddy peats of varying thickness (fig. 50). The underlying third stratigraphic unit varies from mud to muddy peat and peaty mud, which caps muddy peat and muddy sand.

Figure 49. Vertical aerial photograph of Seal Beach research site showing gouge core locations along a south to southwest-trending transect (A-A').

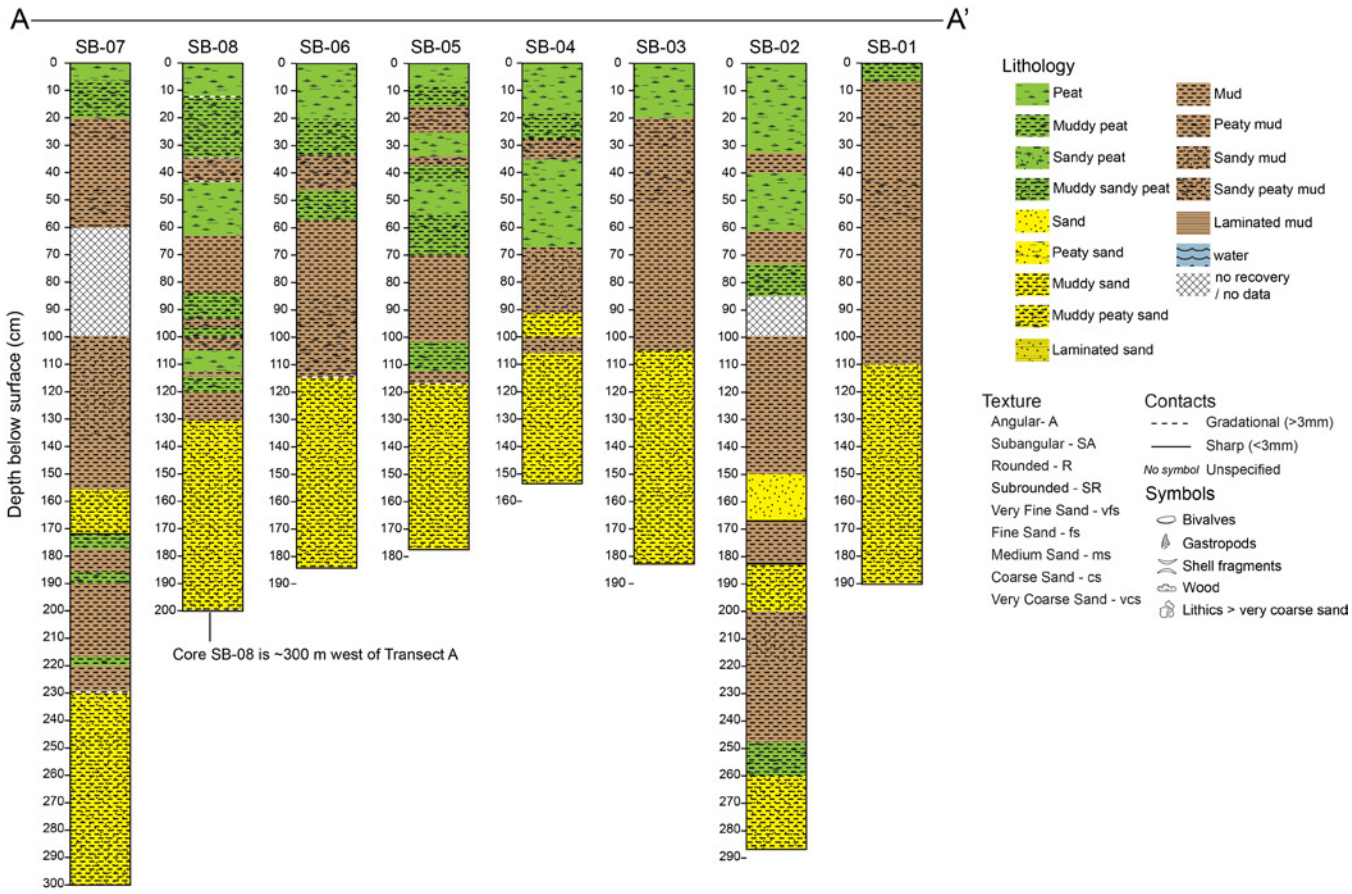

Figure 50. Gouge core logs along transect A-A' at the Seal Beach research site (see fig. 49 for location).

A sand layer at a depth of 156–172 cm in core SB-07 overlies muddy peat and underlies mud. The sand layer has a sharp basal contact and consists of very fine to fine grained muddy sand with no apparent grading (fig. 50). This core is located closest to shore along the transect but is close to where major channels converge. The presence of this sand layer overlying muddy peat in only one core along the transect suggests that this sand layer is not extensive. There is little evidence at present to suggest a tsunami origin for this sand layer, although additional work may be useful to trace its lateral extent and to look for correlative sand layers in other portions of the marsh. Five samples were taken from this sand layer and underlying sediments for grain size and provenance analyses. Results from these analyses are not yet available.

Los Penasquitos

Los Penasquitos marsh is located 25 km north of San Diego at the mouth of the Los Penasquitos River. High sea level and river flooding down Los Penasquitos Canyon at the end of the glacial period resulted in the formation of the modern marsh (Torrey Pines State Nature Reserve, 2013). The site's water regime is an irregularly flooded estuarine intertidal system characterized by cordgrass, pickleweed, and alkali heath vegetation (U.S. Fish and Wildlife Service, 2013). Coastal southern California T-sheet data show very little change in the marsh intertidal flat and vegetated wetlands since the mid to late 1800's (San Francisco Estuary Institute, 2009). Results of numerically modeled tsunami flow depths during the Alaska-Aleutian Tsunami Scenario event show depths of 1.64 m are possible in this area.

Sixteen gouge cores (PEN–01 to PEN–16) were taken along three transects located south of the southern main channel (fig. 51). Along transect A–A', core PEN–03 included two sand layers 6–8 cm thick, which appeared to be normally graded, separated by 14 cm of stiff gray mud. In order to sample for grain size and provenance analysis, a 50 cm long × 6 cm diameter sample was collected from PEN-03. Results of these analyses are still pending (fig. 52). Two sand layers are also present in cores PEN–02, PEN–10, and PEN–12; however, these sand layers are much thicker, and the base of the lower sand layer is much deeper, than in core PEN–03. Moreover, the basal contacts of both sand layers are gradual in cores PEN–10 and PEN–12. In core PEN-04, there are two thin sand layers at 58–60 cm and 62–63 cm, separated by mud. The lower sand overlies 2 cm of mud, which in turn overlies thick impenetrable sand. There is only evidence for one sand deposit in core PEN–09, extending from 53-cm depth to the base of the core at 1 m.

Figure 51. Vertical aerial photograph of Los Penasquitos research site showing gouge core locations along three transects.

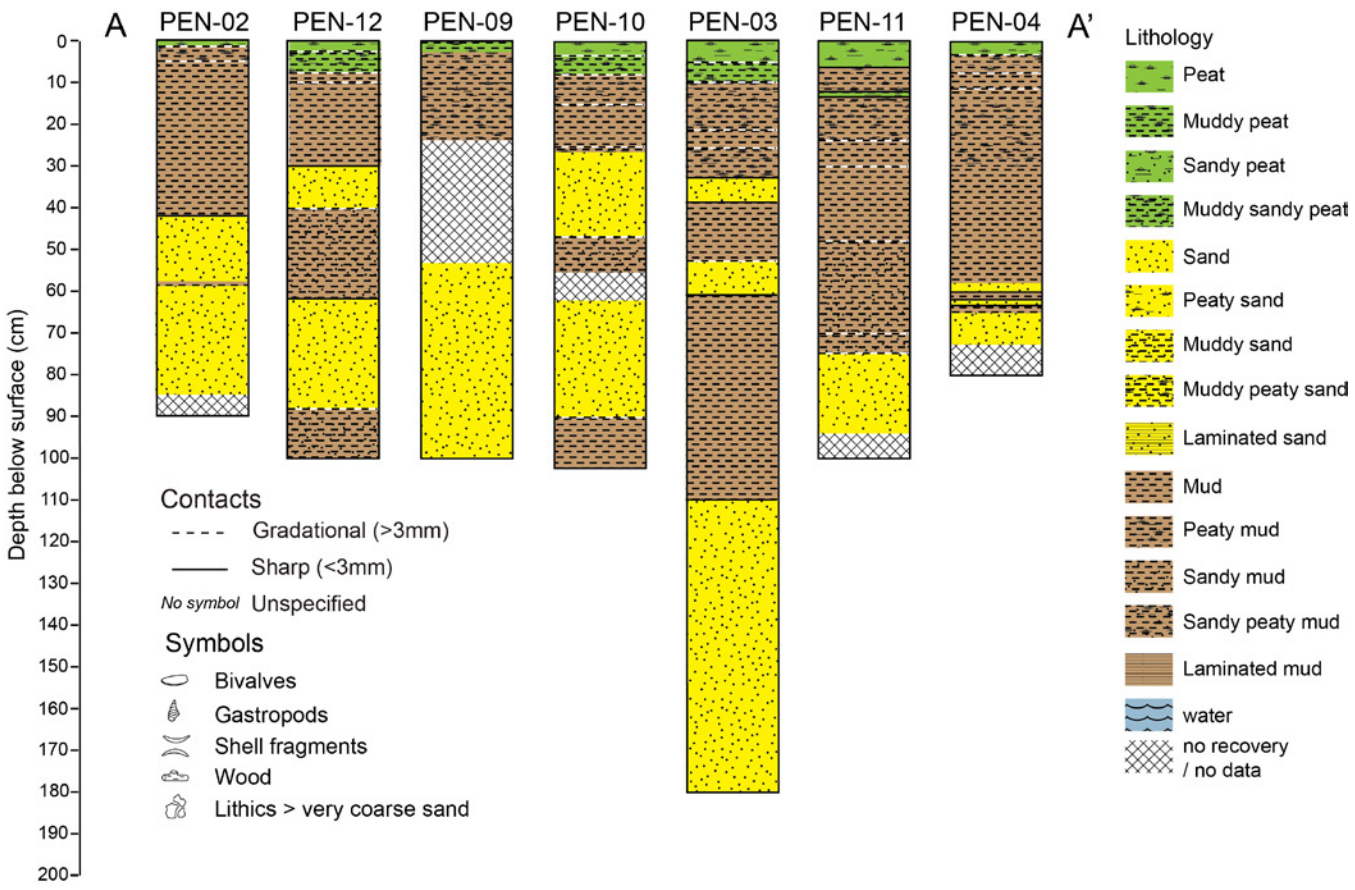

Figure 52. Gouge core logs along transect A-A' at the Los Penasquitos research site (see fig. 51 for location).

Along the transect B–B', core PEN-14 included a sand layer from 35 to 52 cm that appeared normally graded and contained scattered mud. This sand layer has been subsampled at 1-cm intervals for grain-size and provenance analyses. Results of these analyses are still pending. Core PEN–15 had a sand layer from 40 to 60 cm. Core PEN–08 had a sand layer from 97 to 99 cm, and core PEN–16 had a thin sand layer from 35.5 to 36.5 cm.

Cores along transect C–-C' contained no sand layers consistent with tsunami deposition, but often bottomed out in dense sand, which was shallow near the shoreline but deepened to more than 2 m east of the major side channel.

The sand layers in the cores from transects A–A' and B–B' are not laterally continuous. The gradual basal contacts in cores PEN–10 and PEN–12 are not consistent with tsunami deposition. In summary, at this time there is no evidence for tsunami deposition in cores from transects B–B' and C–C', though some test results are still pending. However, based on thickness, basal contacts, and lateral continuity, it is not likely that the sand layers documented at Los Penasquitos had a tsunami origin.

Tijuana Estuary (Tijuana River National Estuarine Research Reserve; Oneonta Slough)

The Tijuana Estuary field site is located in Oneonta Slough, which is part of the Tijuana River National Estuarine Research Reserve in southern San Diego County (fig. 5). The reserve comprises about 2,500 acres and includes salt marsh, riparian habitat, sandy beach, dunes, and upland areas in the floodplain of the Tijuana River near the U.S.—Mexico border. Our study site is located in Oneonta Slough at the northwest corner of the reserve and is bounded to the north and west by housing and Imperial Beach, to the south by the Tijuana River, and to the east by Tijuana Estuary Visitors Center,

housing, and the Naval Outlying Landing Field (NOLF) Imperial Beach. The area is underlain by the late Pleistocene Bay Point Formation, which is composed mostly of marine and nonmarine, poorly consolidated, deposits (Kennedy, 1975). The deposits consist of reddish-brown, moderately permeable, mostly poorly sorted siltstone, sandstone, and conglomerate of beach, dune, estuarine, and colluvial origin. The estuary is bounded to the west by the Rose Canyon Fault Zone, and to the east by the La Nacion Fault Zone.

The work in Tijuana Estuary was a "study of opportunity" in collaboration with a group of biologists and geologists who are studying the effects of sea-level rise and extreme events on California coastal habitats. We coordinated our work with a group led by principal investigators John Takekawa (USGS/Western Ecological Research Center) and Glenn MacDonald (University of California Los Angeles), who made arrangements to core, sample, and establish monitoring sites in the estuary during September 2012.

For our paleotsunami study we collected eight gouge cores (TJ–12–01 to TJ–12–08) from the vegetated wetland areas in the northwest area of Oneonta Slough (fig. 53). Most of the cores were composed of three units: (1) an upper dark brown peat or muddy peat generally less than 10 cm thick; (2) a gray or tan-colored mud and (or) peaty mud unit that ranged between 8 and 167 cm thick; and (3) a gray, tan, or reddish-brown basal sand and (or) muddy sand unit, generally massive in appearance. Many of our cores ended in a reddish brown, mildly consolidated, moderately well sorted sandstone composed of angular to sub-angular sand grains of either probable fluvial origin or possibly the upper weathering surface of the Bay Point Formation. Core TJ–12–02 was located adjacent to a tidal channel and contained scattered gastropod shells (fig. 54). Core TJ–12–07 was our most seaward core and contained multiple sand layers of unknown origin at depths below about 120 cm (fig. 55).

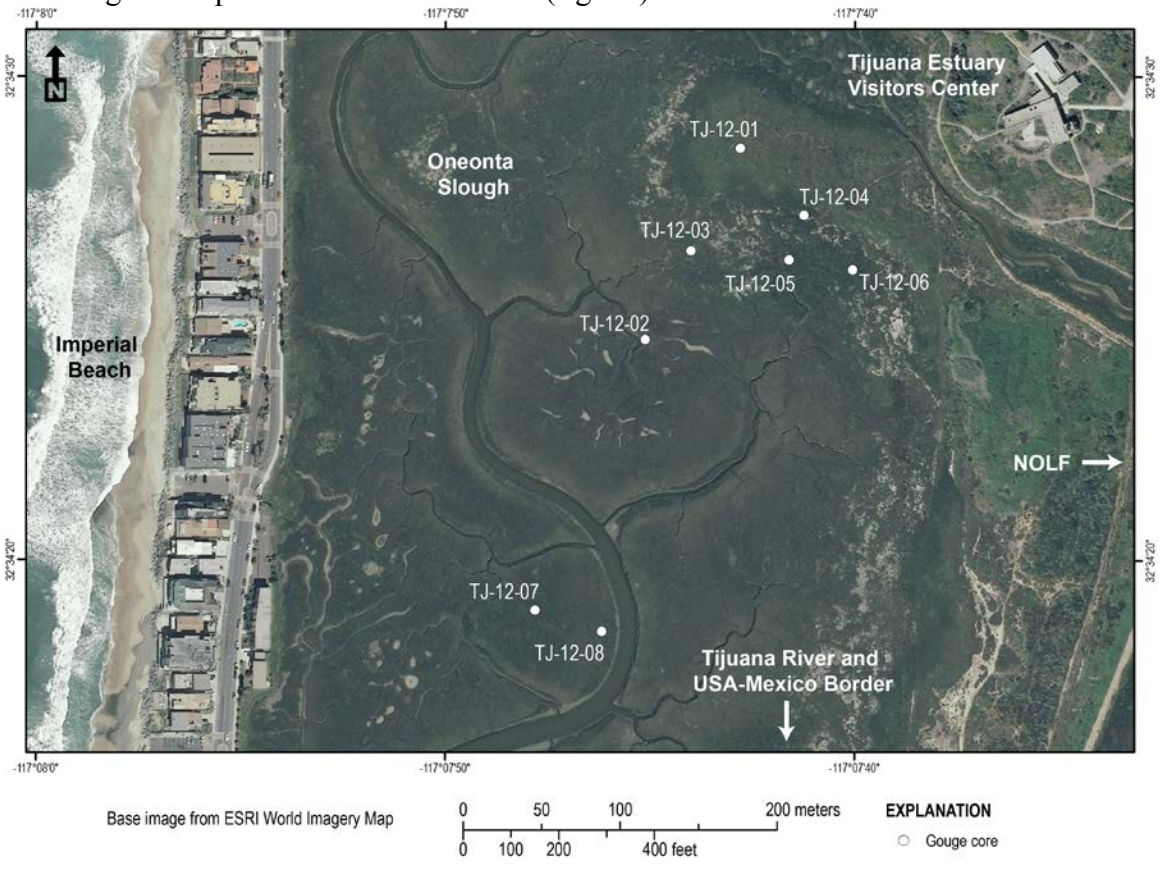

Figure 53. Vertical aerial photograph of Tijuana Estuary showing gouge core locations in the Oneonta Slough area of the Tijuana River National Estuarine Research Reserve.

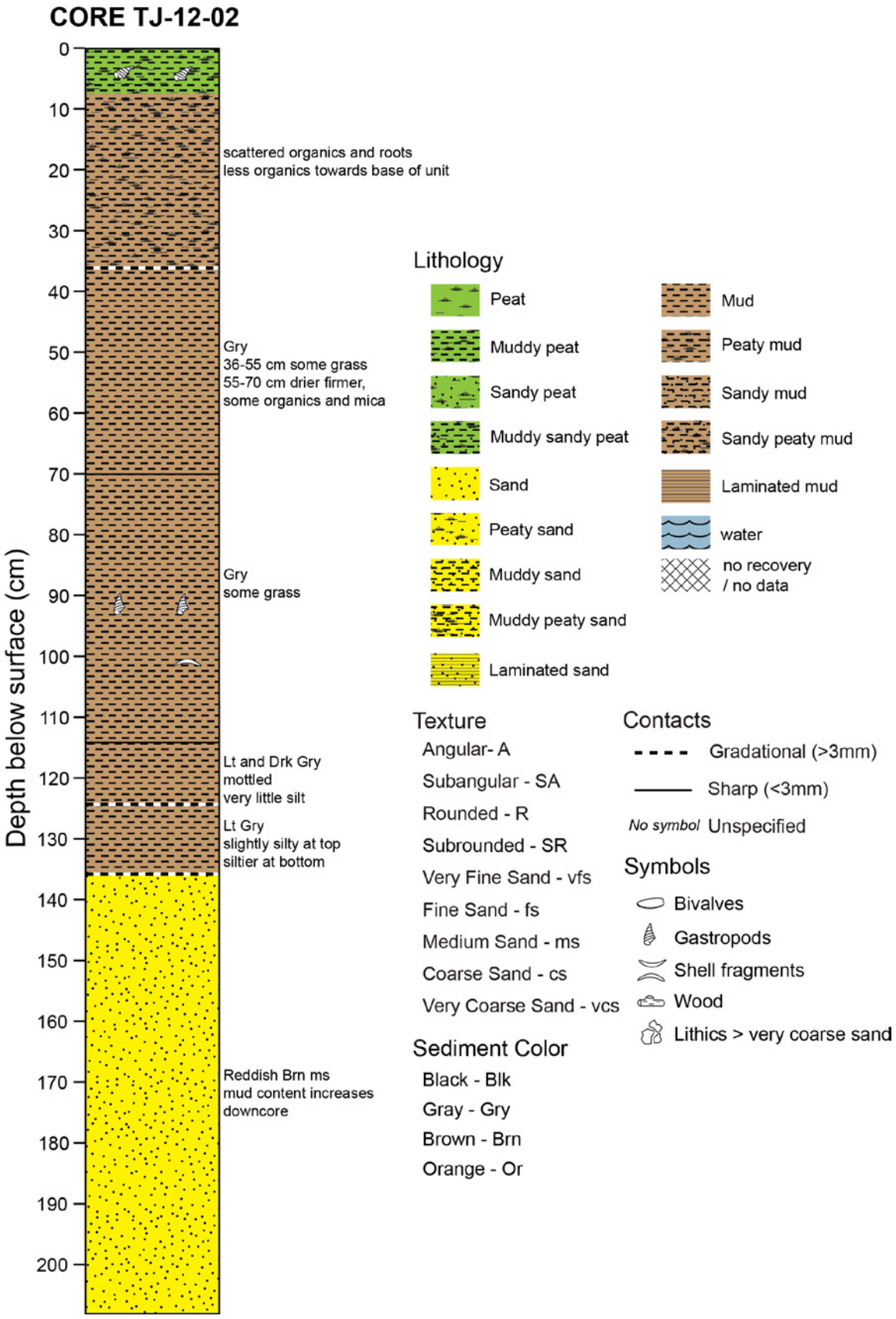

Figure 54. Log for gouge core TJ-12-02 at the Tijuana Estuary site.

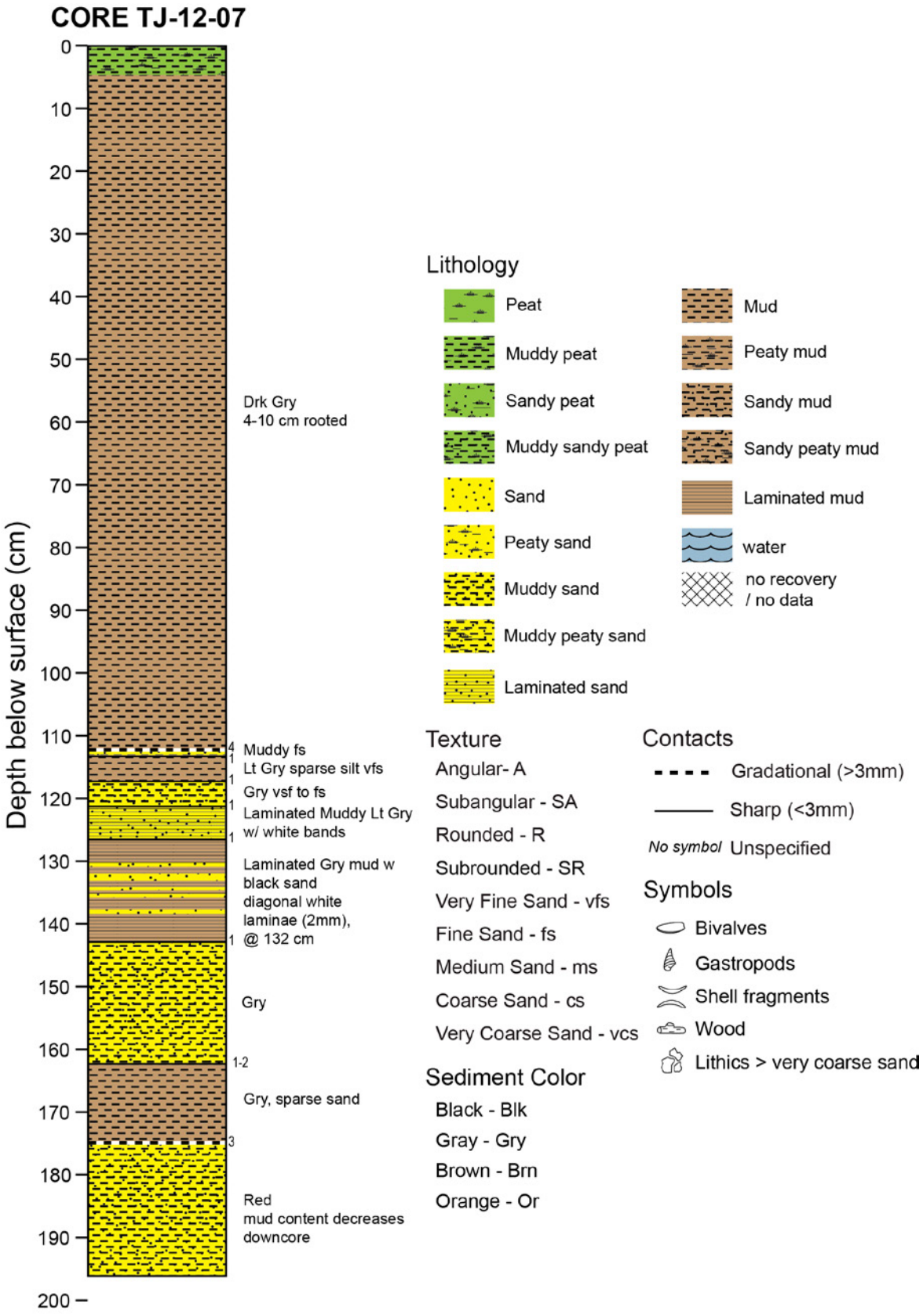

Figure 55. Log for gouge core TJ-12-07 at the Tijuana Estuary site.

Detailed Site Evaluations

Based on the reconnaissance fieldwork and evaluation of other background information, three locations, Crescent City, Half Moon Bay, and Carpinteria, represented the best opportunities to evaluate deposits from tsunami inundation from distant-source tsunami events. Previous work at Crescent City provided evidence that a tsunami deposit from 1964 and several other older, anomalous deposits were present. Preliminary evidence from Pillar Point at Half Moon Bay suggested that a preserved near-surface deposit could reflect the 1946 tsunami, and other deeper anomalous sands could represent older, similar events. Additional cores and samples collected at the Carpinteria wetland supported the potential for tsunami deposits at the site. Detailed fieldwork plans were developed and implemented for these localities in the summer and fall of 2012. The following sections describe the work and initial findings of the detailed site evaluations.

Crescent City Marshes (primary summary by Eileen Hemphill-Haley)

Introduction

Crescent City, on the far north coast of California, has been termed a "tsunami magnet"[13] for good reason: since 1933, some 34 distance-source tsunamis have been recorded, including 12 with wave heights exceeding 1m, and 5 that have caused serious damage (Dengler and others, 2008; Admire and others, 2012; University of Southern California Tsunami Research Center, 2013). The largest historical tsunami, in March 1964, struck the southwest-facing shore of Crescent City with wave heights of 6–7 m, causing extensive structural damage and claiming 10 lives. In addition to distant-source tsunamis, Crescent City is also episodically struck by near-field tsunamis generated by earthquakes in the Cascadia subduction zone (CSZ). Geologic evidence for past CSZ tsunamis—anomalous sand deposits capping buried marsh soils—is found in subsurface deposits at several wetland localities in the Crescent City area, based on previous studies led by Dr. Gary Carver of Humboldt State University (1998, unpublished, Investigation of paleotsunami evidence along the north coast of California, prepared for Pacific Gas and Electric Company), and Dr. Curt Peterson of Portland State University (Peterson and others, 2011). These researchers also identified deposits from the 1964 distant-source tsunami, although such deposits occur at fewer locations and with more limited distributions.

Crescent City was excluded from the 2011–2012 California-coast reconnaissance fieldwork because paleotsunami deposits had already been documented for the area. With most of statewide reconnaissance work completed, attention was turned back to Crescent City to look closely for evidence of non-CSZ, distant-source tsunamis in addition to the 1964 event. The new fieldwork at Crescent City builds on the previous investigations cited above and includes coring at new sites and additional age-dating, microfossil, and particle-size analyses.

Field Localities

Fieldwork was focused on three locations with the potential to preserve deposits from distant-source tsunamis in the Crescent City area: McNamara marsh, Elk Creek marsh and Sand Mine marsh (fig. 56). Each of these localities is currently a fresh to fresh-brackish wetland or marsh. Inundation from the 1964 tsunami was documented for both Elk Creek and Sand Mine marshes (Peterson and others, 2011).

[13] The term "tsunami magnet" is a 2011 quote from Humboldt State University Professor Lori Dengler, which has been widely repeated in the media. Factors influencing why Crescent City is unusually susceptible to damage from distant-source tsunamis include refraction of wave energy at the Mendocino escarpment coupled with local amplification of wave height over a shallow submarine shelf (Kowalik and others, 2008).

Field data were collected using hand-driven gouge corers. The cores were either described, photographed, and subsampled in the field, or they were returned to the lab for analysis and subsampling. All core locations and elevations were recorded in the field using a real-time kinematic (RTK) Global Positioning System (GPS) survey unit.

Figure 56. Map showing Crescent City area field localities: McNamara Marsh, Elk Creek Marsh, and Sand Mine Marsh.

McNamara Marsh.—McNamara marsh[14] is a fresh to fresh-brackish wetland in the lower stream valley of Marhoffer Creek, about 1 km northwest of the Crescent City limits (fig. 56). Based on lidar data and our leveling measurements, the marsh is positioned more than 1 m above extreme high water, and preliminary microfossil analyses show that a fresh or fresh-brackish environment has persisted at this site for centuries.

McNamara marsh was chosen as one of our primary study sites because of its proximity to the ocean (fig. 57) and because the elevation (~3.5 m) is above regular storm inundation but within the range of larger distant-source tsunamis. For example, numerical modeling predicts a maximum tsunami amplitude from an Aleutian-Alaska source (AASZ III model) of 5–6 m for Crescent City, comparable to the 1964 event (Wilson and others, 2008; Barberopoulou and others, 2009). The model takes into account a shallow submarine shelf off the southeast-facing shore of Crescent City, which amplifies wave heights. Even though the offshore bathymetry along Pebble Beach between McNamara marsh and Crescent City does not include an extensive shallow shelf, inundation could occur at McNamara marsh by tsunami or storm surges with wave heights greater than about 4 m.

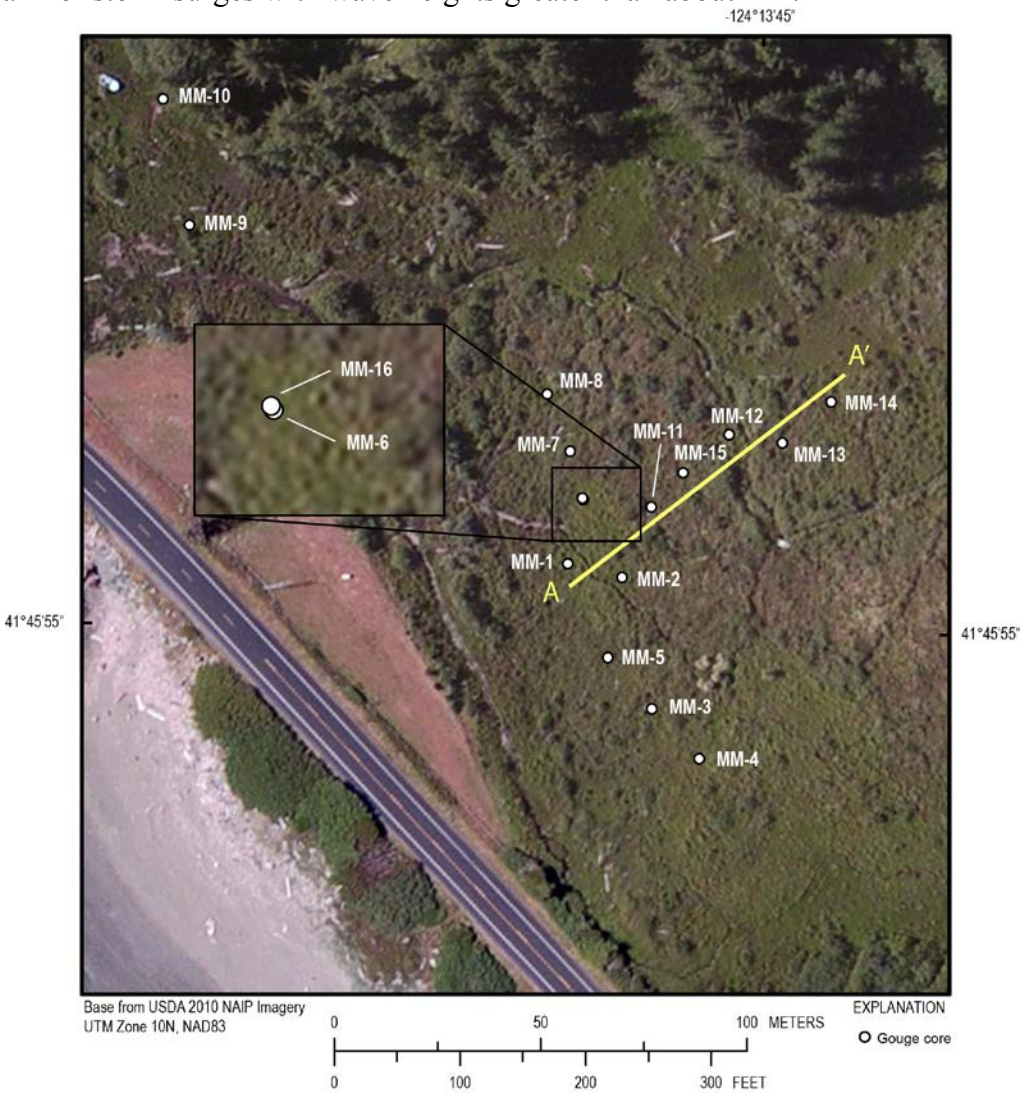

Figure 57. Vertical aerial photograph of McNamara marsh showing gouge core locations and core correlation transect A-A'.

[14] "McNamara marsh" is informally named for the landowners who granted us access to the site.

A total of 18 gouge cores were collected along shore-normal and shore-parallel transects (fig. 57), including replicate cores at site 16 (cores MM-16A, 16B, 16C) for grain size, microfossil, and age determinations. The subsurface lithology to at least 2-m depth dominantly consists of peat, but distinct sand units are found in all cores, including a widely correlatable sand unit near 1-m depth seen in most cores (fig. 58). Accelerator mass spectrometry (AMS) ^{14}C ages for seed pods and woody detritus extracted from immediately below the sand in 3 cores (table3; fig. 58) support the interpretation that this is the tsunami deposit from the earthquake of January 26, 1700 (Atwater and others, 2005). The more seaward cores show two to four anomalous sandy deposits younger than the A.D. 1700 sand, but only the A.D. 1700 deposit is observed farther than about 100 m from the modern beach, that is, inland from core MM-15 (fig. 58).

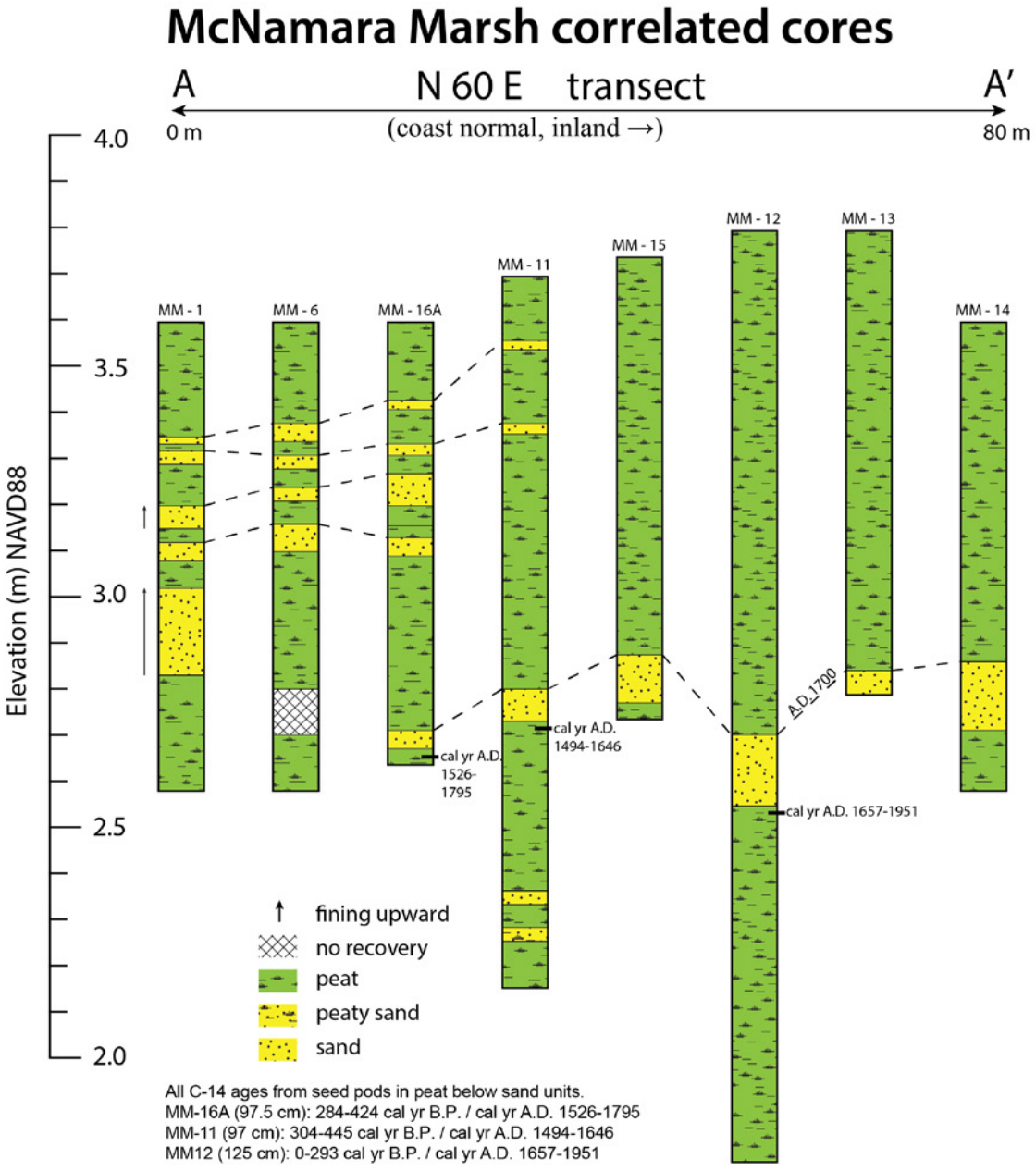

Figure 58. Stratigraphic correlation of core logs along a coast-normal transect line A-A' at McNamara marsh (see fig. 57 for location).

Table 3. Accelerator mass spectrometry (AMS) 14C ages for samples from Sand Mine Marsh core SM11 and McNamara Marsh cores MM11, MM12, and MM16.

[B.P., before present (1950). For each core, seed pods and (or) woody detritus were used for the analysis]

Core ID	Sample depth interval (cm)	Lab ID[a]	Conventional ^{14}C age (yr B.P.)[b]	$\partial^{13}C$	Calibrated calendric age (cal yr A.D.)[c]	Organic material used in analysis	Notes
SM11	42–43	OS-99972	235 ± 20	-25.10	1643–1951	Woody plant material	Dark brown rooted peat above sand layer
SM11	42–43	OS-99973	170 ± 15	-26.30	1667–1952	Wood fragment	Dark brown rooted peat above sand layer
SM11	99–100	OS-99971	150 ± 20	-28.92	1666–1953	Seeds, wood pieces	Dark brown rooted peat below sand layer
MM11	97–98	OS-97870	310 ± 20	-26.27	1494–1646	Seed pods	Black humified to fibrous peat below sand
MM12	125–126	OS-97871	195 ± 20	-26.82	1657–1951	Seed pods	Dark brown peaty soil below sand
MM16	97.5–98.5	OS-97872	265 ± 20	-26.69	1526–1795	Seed pods	Dark brown fibrous peat below sand

[a]All analyses completed by the NOSAMS facility at Woods Hole Oceanographic Institute.

[b]Conventional lab-reported radiocarbon age with ± 1 sigma error.

[c]Calibrated calendric age range (± 2 sigma) in calibrated years A.D., calculated with the CALIB 6.0 program (http://calib.qub.ac.uk/calib/).

Analyses for grain size, microfossils, and dating by ^{210}Pb and ^{137}Cs methods are currently underway to help evaluate the likely depositional mechanism for the post-A.D. 1700 deposits. The results of ^{137}Cs analyses will help to show whether or not the uppermost sand unit was deposited by the 1964 tsunami. These analyses will be especially helpful at McNamara marsh because post-tsunami inundation mapping in 1964 was not completed as far north up the coast as McNamara marsh.

Elk Creek Marsh.—The Elk Creek marsh study area is within Elk Creek Wetland Wildlife Area, a U.S. Fish and Wildlife Service property along the lower reaches of Elk Creek and bordering downtown Crescent City (figs. 56 and 59). The wildlife area currently consists of freshwater marshes, swamps, and ponds, including reclaimed millponds. The modern freshwater environments of lower Elk Creek are not natural, but rather the result of land reconstruction and development in the early 1900s to support timber and livestock production. Prior to that time, the lower valley was an intertidal estuarine environment, as documented both by our core data and previous observations of Peterson and others (2011).

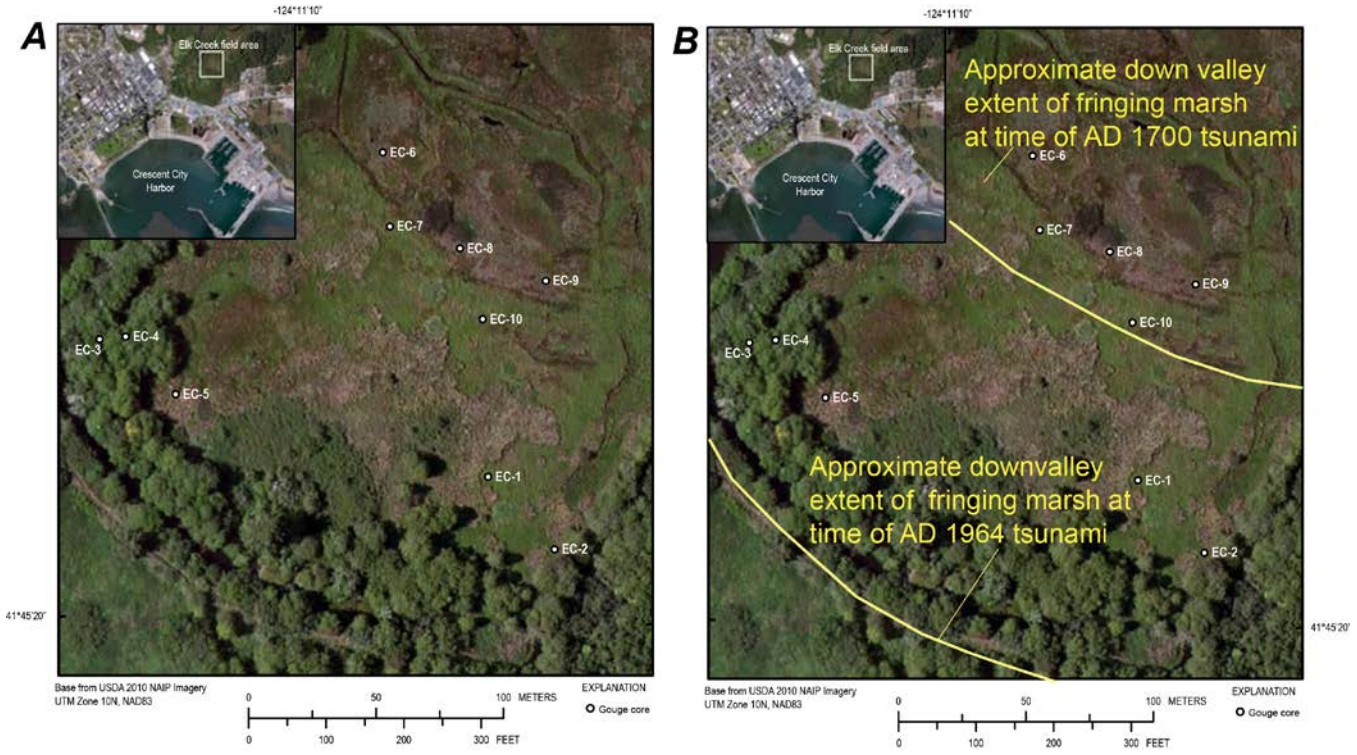

Figure 59. Vertical aerial photographs of Elk Creek marsh field area. *A*, Gouge core locations. *B*, Approximate downvalley extent of fringing marshes in 1964 compared to 1700.

Because the Elk Creek valley is low-lying and relatively flat (average elevations of about 2.3–2.4 m at our core sites), inundation by the 1964 tsunami extended about 1.5 km inland. Furthermore, Peterson and others (2011) found thin sand deposits at least 0.7 km upvalley from the modern coastline. One hypothesis, therefore, is that distant-source tsunamis with wave heights and energy comparable to the 1964 tsunami could have similarly flooded the Elk River valley, possibly leaving a comparable sedimentary record. It was determined, both from previous work by Peterson and others (2011) and the rapid field reconnaissance for this project, that the stratigraphy within about 400–500 m of the modern coastline consists of a thin veneer of modern freshwater peat overlying meters of gray muddy silt and sand that are deposits of the former estuarine embayment or lagoon. Preservation of paleotsunami deposits is not likely in lower intertidal environment or shallow subtidal environments (that is, tidal flats and channels), and therefore the goal was to locate, through reconnaissance coring, former fringing salt marshes where paleotsunami deposits would have a better chance of being preserved.

The 1964 and A.D. 1700 tsunami deposits were located, through a series of gouge cores, in the densely vegetated marsh and swamp approximately 600–950 m from the modern coastline (fig. 59*A*). The stratigraphy revealed in the cores showed, using these two marker dates, the approximate transition from paleoembayment to paleomarsh (fig. 59*B*).

Similar to the approach of Peterson and others (2011), in the absence of ^{14}C or ^{137}Cs data, stratigraphic position and anomalous lithology were used to identify the 1964 and A.D. 1700 deposits. The 1964 tsunami sand deposit is identifiable as a unit 1–2 cm thick unit about 10–15 cm below the modern marsh surface, but only in the more seaward part of the field area that is underlain by paleoembayment deposits (for example; core EC2; see figs. 59 and 60). In contrast, the probable A.D. 1700 deposit is observed in paleomarsh deposits about 0.5 m below the modern surface, but upvalley beyond the extent of sand deposition by the 1964 tsunami (for example; core EC9; see figs. 59 and 60).

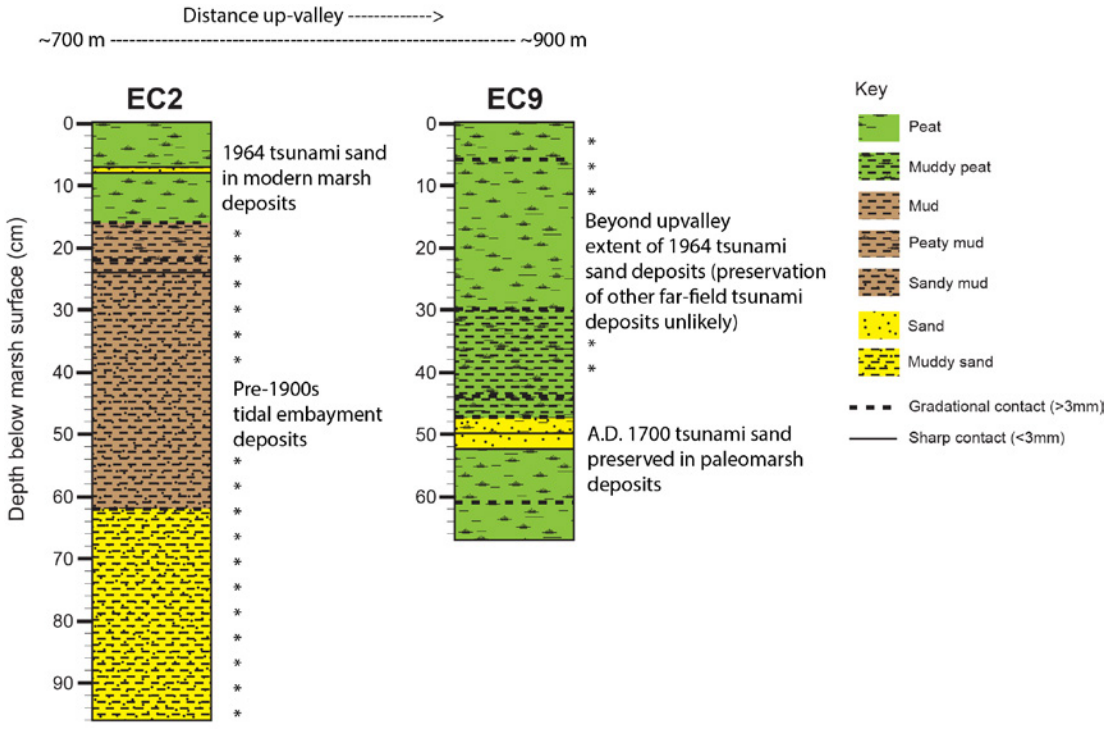

Figure 60. Core logs for Elk Creek cores EC2 and EC9. EC2 includes the 1964 tsunami deposit, but no older tsunami deposits are preserved in underlying estuarine/tidal embayment deposits. Core EC9, collected about 200 m further upvalley, includes a likely 1700 C.E. Cascadia Subduction Zone tsunami deposit preserved in paleomarsh deposits. The site was likely beyond the limit of sand deposition by any far-field tsunamis younger than 1700.

We infer that any pre-1900s distance-source tsunamis, in order to leave sedimentary deposit evidence, would have had to deposit material farther upvalley than the marsh fringe edge in the late 20th century (that is, farther inland than the 1964 tsunami, and in closer proximity to the downvalley extent of the marsh fringe in A.D 1700, see figure 59*B*). Because no evidence for anomalous sand deposits from possible distant-source tsunamis was observed in the peaty deposits above the A.D. 1700 tsunami deposit (for example, core E9, fig. 60), we infer that Elk Creek valley apparently lacks sedimentary evidence for tsunamis of distant origin between 1700 and 1964. This time window includes the 1788 tsunami from the vicinity of the hypothetical AASZ III source.

Therefore, it was concluded that no further work is warranted at Elk Creek because the locale within the Elk Creek valley that was susceptible to pre-1900s tsunami deposition does not contain any record of sand deposition younger than that ascribed to the A.D. 1700 Cascadia subduction zone earthquake. Peterson and others (2011) adequately described the distribution of the deposits—from sand to debris—for the 1964 tsunami, which is the one distant-source tsunami evident at the Elk Creek marsh locality.

Sand Mine Marsh.—Sand Mine marsh is a freshwater wetland about 1 km south of Crescent City (fig. 56). The field area was divided into two sections: an extensive marsh/swamp on the east side of Highway 101 and a small, back-berm marsh adjacent to Crescent Beach on the west side of the highway that is less than 50 m from the modern beach (fig. 61).

Figure 61. Vertical aerial photograph of Sand Mine Marsh showing gouge core locations. The 1964 tsunami deposited sand across the road and damaged buildings in this area.

The west-side field area and portions of the east-side area are within the inundation zone of the 1964 tsunami (Magoon, 1966, Dengler and Magoon, 2005). Geological evidence for the 1964 tsunami, and several near-field tsunamis from Cascadia subduction zone earthquakes, was previously documented in the Sand Mine marsh area (1998, unpublished, Investigation of paleotsunami evidence along the north coast of California, prepared for Pacific Gas and Electric Company; and Peterson and others, 2011). In addition to sand layers attributed to tsunamis, the unpublished 1998 report by Humboldt State University identified a few other thin sand deposits in several cores that were not correlated with any known event, either storm or tsunami. It was surmised that it would be possible for deposits from distant-source tsunami deposits, comparable to the 1964 event, to have been preserved at this site.

Three cores were evaluated in the east-side marsh area, each of which included a sand unit 5–10 cm thick capping a buried soil. We infer that this soil was buried as a consequence of coseismic subsidence during the A.D. 1700 Cascadia earthquake and that the overlying sand was deposited by a tsunami that accompanied that earthquake. Sand units correlative from core to core higher in the stratigraphic record than the AD 1700 sand were not identified, and therefore the rest of the coring focused on the back-berm wetland on the west side of the highway.

On the west side of the highway, a series of closely spaced cores were collected amongst a dense stand of cattails (fig. 61). The stratigraphy is complex, but a thin clay layer is a useful correlation unit in most cores. Age determinations and microfossil analyses are currently underway for several cores

collected in this area; these cores contain the best records of the 1964 and A.D. 1700 tsunami deposits. In core SM-11 (fig. 62) the results of ^{137}Cs analyses confirm that a 2-cm-thick unit of very fine sand near 10-cm depth is the 1964 tsunami deposit, as indicated by coincidence with the 1963–1964 ^{137}Cs peak caused by a peak in atmospheric atomic testing (Robbins and Edginton, 1975).

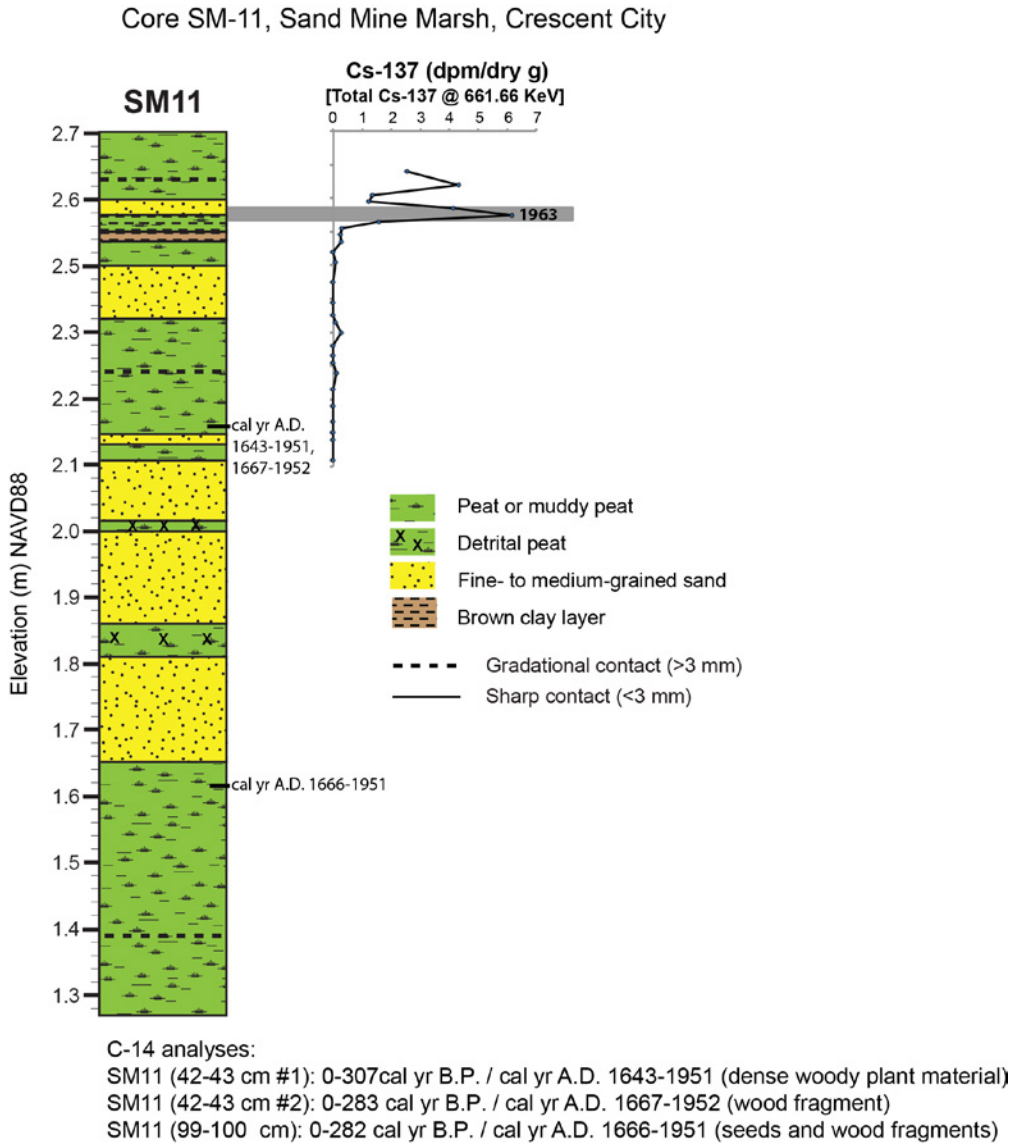

Figure 62. Core log showing stratigraphy and ^{137}Cs results for gouge core SM11, Sand Mine Marsh. The 1963 ^{137}Cs peak verifies that a 2-cm sand layer near 10-cm depth is the 1964 tsunami deposit. Three sand units with intervening detrital peaty deposits may have been deposited by the 1700 tsunami.

The sand was deposited by the tsunami into a wet, freshwater marsh or shallow pond, and therefore contains abundant and well-preserved freshwater diatoms. A few marine diatoms are present, but they are exceptionally rare compared to the freshwater taxa. Although sediment grading was not visually obvious in the sand grains of the thin (2-cm-thick) very fine grained unit, an upward trend from dominantly large to dominantly small diatom valves shows that the deposit is normally graded.

In addition to the 1964 deposit, there are several other prominent sand layers within about 1 m of the modern surface (>1.6 m NAVD88) that are correlative in the central part of the west-side marsh. Radiocarbon ages determined for seeds and small stems collected from peat above and below the lower four sand deposits show an age range that includes the A.D. 1700 earthquake and tsunami, although radiocarbon correlation age ranges are imprecise for the past few centuries (fig. 62, table 3). Although still preliminary, our current hypothesis is that the sand deposits between 50 and 92 cm in core SM-11 were deposited by the A.D. 1700 tsunami. This is based on two factors: (1) rooted (that is, in situ) peat deposits are found above (~45 cm depth) and below (~95–100 cm depth) the sand deposits, while plant-rich detrital deposits separate the individual sand layers; and (2) a paleoenvironmental change from fresh to brackish conditions is noted from the underlying peat to the overlying peat, based on diatoms. This change could be consistent with coseismic subsidence. Two additional sand deposits in the core include an 8-cm-thick fine- to medium-grained deposit at 20–28 cm depth, and a 2-cm-thick fine-grained sand layer a few centimeters above the proposed A.D. 1700 deposit. The 2-cm-thick unit contains a number of well-preserved marine diatoms; the 8-cm-thick unit is relatively coarse-grained, and diatoms are absent. Work is currently underway to further evaluate these units to better ascertain their mode of emplacement, whether storm or distant-source tsunami.

Conclusions

Three locations in the Crescent City area were evaluated for evidence of distant source tsunamis: McNamara marsh, Elk Creek marsh, and Sand Mine marsh. This was the first detailed search for possible paleotsunami deposits at McNamara marsh. Radiocarbon data from this marsh show that a widely correlatable sand unit about 1 m below the modern marsh is likely to be the A.D. 1700 tsunami deposit. At McNamara marsh, evaluation of several other sand units younger than A.D. 1700 observed in four cores about 100 m from the modern beach is being carried out to determine whether their mode of deposition would be better explained by tsunamis or large storms.

A thorough reconnaissance operation at Elk Creek marsh was completed, and it was determined that the pre-1900s environment for the lower valley, a tidal or estuarine embayment, was not conducive to preserving paleotsunami deposits. This study found no evidence for sandy deposits younger than the A.D. 1700 tsunami sand, except for the likely 1964 deposit preserved in relatively recent marsh deposits less than 800 m from the modern coastline.

At the Sand Mine locality, a series of cores from within the inundation zone of the 1964 tsunami were described and sampled, with the goal of finding deposits from previous distant-source tsunamis of comparable size. Initial results identify with certainty the 1964 tsunami deposit and support identification of the A.D. 1700 deposit. Work is currently underway to complete additional analyses including grain size, microfossils, and dating by ^{14}C, ^{210}Pb, and ^{137}Cs.

Because analyses of sediment in cores at both McNamara marsh and Sand Mine marsh are ongoing, it is premature to offer further conclusions. However, it is clear that a major question that will be addressed using the results of these analyses is the extent to which specific sand layers between the 1964 and A.D. 1700 sand layers can be attributed to a specific distant source tsunami or to a storm.

Pillar Point Marsh (primary summary by Bruce Jaffe and Bruce Richmond)

Introduction

Pillar Point marsh, located at the northern margin of Half Moon Bay (fig. 63), was chosen as a site to search for paleotsunami deposits from a distant-source tsunami for multiple reasons. In 1946 a tsunami generated by a M_w 8.1 earthquake in the eastern Aleutian Islands inundated more than 300 m (~1,000 ft) inland at Pillar Point, flooding the marsh (Bascom, 1946; Lander and others, 1993). Inundation modeling shows that an even larger tsunami, up to 8–9 m, would impact Pillar Point marsh if

a magnitude 9.2 earthquake occurred in the eastern Aleutian Islands (AASZ III tsunami model; Wilson and others, 2008; Barberopoulou and others, 2009). A tsunami striking the coast at this locality could pick up sand from the nearshore, beach, and dunes and transport it inland, creating a sandy tsunami deposit that could be identified in the mud and peat environment of the marsh and lagoon. The marsh is located in a pull-apart structure between two right-stepping strands of the San Gregorio Fault (SGF) (Koehler and others, 2005), which is a favorable environment for preservation. If coseismic subsidence occurred during a SGF earthquake, the lowered elevations in the marsh, and the lagoon within, would potentially facilitate deposition of postevent sediment, protecting any tsunami deposits that were present at that time.

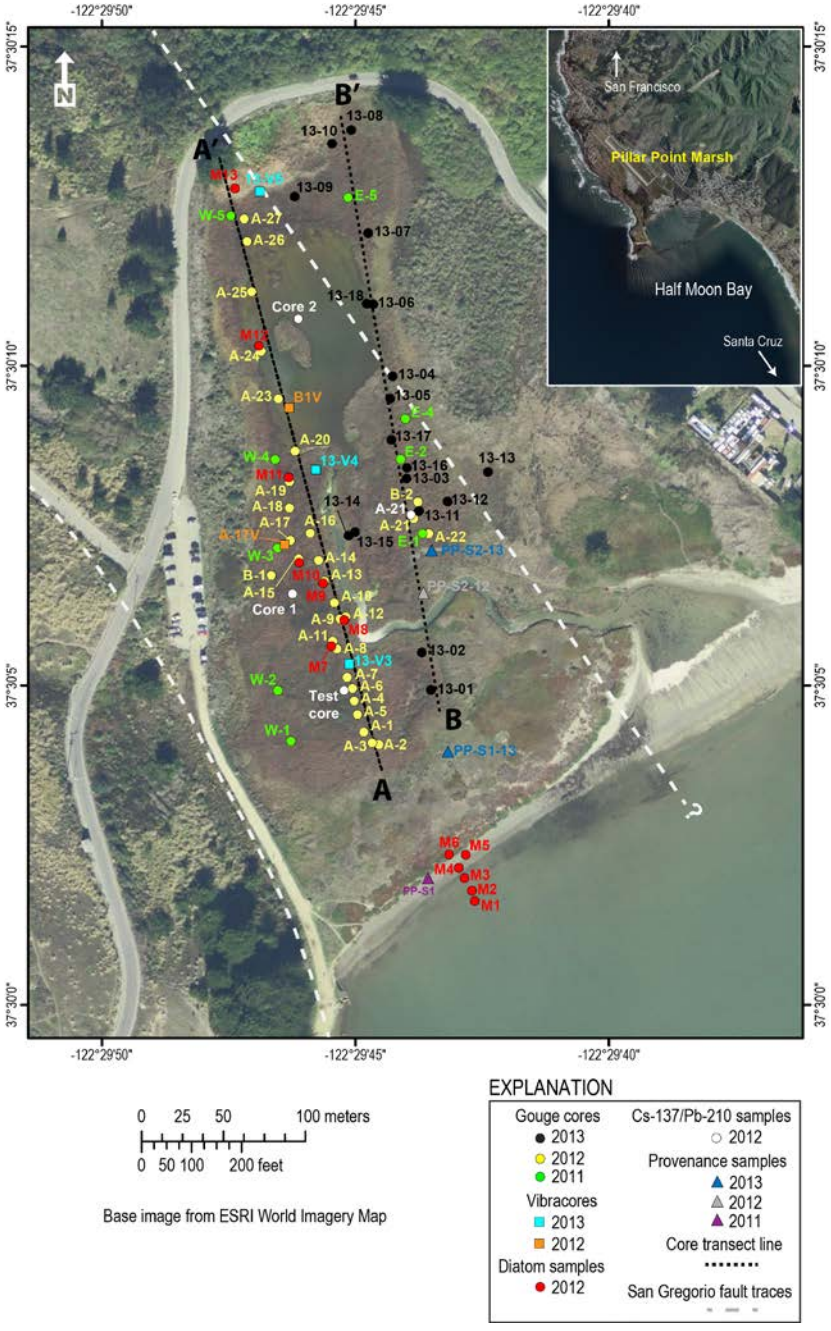

Figure 63. Vertical aerial photograph annotated to show locations of cores and samples collected at Pillar Point marsh, Half Moon Bay.

The paleoearthquake study by Koehler and others (2005) provides a framework for our paleotsunami work. However, because the goal of their study was to investigate faulting on the SGF, they collected cores along a transect normal to the fault strands and parallel to the shoreline. Shore-parallel orientation is not optimal for a paleotsunami study where shore-normal transects (roughly parallel to flow direction) can reveal changes in candidate tsunami deposits that can be used in conjunction with other characteristics (see, for example, Goff and others, 2012) to discriminate between tsunami and other event (and nonevent) deposits. For example, flow or shore-perpendicular deposit geometry and grading are two criteria used to identify tsunami deposits—tsunami deposits generally tend to thin and fine landward (Morton and others, 2007). The Koehler and others (2005) study was useful in that it confirmed our independent assessment of Pillar Point marsh as a good site for a paleotsunami investigation. The log for one of their cores located in the southwestern marsh noted the possibility that "a well sorted sand laminae between 24 and 24.5 cm" below the surface was formed either by a tsunami or storm surge. Core logs also noted clean sandy layers and sand laminae at depth that could possibly be tsunami deposits.

Field Studies

Pillar Point marsh consists of two types of marshes. A small freshwater stream marsh is present inland that drains coastward into a more extensive brackish water marsh (a mix of fresh and sea water), where plants are salt tolerant. This small but unique marsh system is an important habitat for local and migrating birds. The marsh is underlain by Holocene estuarine delta deposits consisting of a heterogeneous mixture of coarse and fine sediment (Brabb, 1980; Brabb and others, 1998) deposited in the delta at the mouth of the tidally influenced Denniston Creek. Road, airport, and building construction has greatly modified and constrained the natural flow of the creek. The western marsh boundary is bordered by the late Miocene to Pliocene sandstone and siltstone of the Purisima Formation, and the eastern boundary borders Pleistocene sand and gravel marine terrace deposits sediment (Brabb, 1980; Brabb and others, 1998). Denniston Creek, and the adjacent San Vincente Creek, drain through terrain dominated by Cretaceous granitic rocks of Montara Mountain capped with scattered Pleistocene marine terrace deposits.

The overall marsh stratigraphy consists of an upper modern peat, which includes both muddy peat and peaty mud and ranges in thickness between about 10 and 20 cm. The peat directly overlies a widespread sand unit that generally thins in a landward direction from nearly 50 cm near the coast to 1 cm or less in the northern marsh. The sand in turn overlies a near-continuous mud or peaty mud unit that is approximately 20 to 50 cm thick. Near the center of the marsh the mud unit contains layers of interbedded sand and mud (0.2–0.5 cm thick). In the western marsh, the mud unit rests on a thick (>50 cm) peat that in places contains mud interbeds. In the eastern marsh, the mud or peaty mud unit overlies a more complex stratigraphy that includes marsh, mud, and sand units. In some areas, particularly in the eastern marsh, our cores bottomed out in a poorly sorted coarse sand to fine gravel deposit.

Data were collected at Pillar Point marsh during four field efforts from October 2011 to March 2013. In all, 67 cores were collected, primarily along two shore-normal transects (fig. 63). Four types of cores were collected: (1) 30-mm-diameter gouge cores that allowed deep penetration (as much as 3.1 m); (2) 60-mm-diameter gouge cores useful for sampling, which gave a larger view of the subsurface but could only penetrate 1 m; (3) 7.6-cm-diameter vibracores; and (4) 10.2-cm-diameter and 15.2-cm-diameter push cores for dating. Most gouge cores were cleaned, photographed, and logged in the field; two were transported to the lab to subsample for ^{137}Cs and ^{210}Pb dating and diatom analysis. Vibracores and push cores were taken back to the lab for further analysis, including grain size and sand provenance for the vibracores, and ^{137}Cs and ^{210}Pb dating for the push cores. A differential GPS survey was conducted to determine elevation of core sites and the topography along transects and near the coast.

Clean sand deposits were observed in cores taken in the Pillar Point marsh and ephemeral lagoon/pond. For example, core PPE-1, which is located in the eastern marsh about 150 m inland from the present-day shoreline, contains 9 sand layers within 2 m of the surface, 5 of which are thicker than 2 cm (fig. 64). However, these sand layers may have been formed by a tsunami or by some other process, such as storm overwash. To determine if any of the observed sand deposits were formed by a tsunami, characteristics of the deposits were compared to known tsunami deposits. Criteria used as evidence of deposition by tsunami include deposit geometry (sheet-like, generally thinning landward), evidence of marine origin (sand similar to offshore or beach sands; presence of marine diatoms or foraminifera, marine geochemical indicators), grading (normal, suspension grading, landward fining), contacts (sharp erosive basal contact), and evidence of high-speed flow (rip-up clasts, erosive contacts) followed by still water (mud lamina, organic debris cap) (see, for example, Goff and others, 2004; Peters and others, 2007; Morton and others, 2007; Witter, 2008; Peters and Jaffe, 2010a; Chagué-Goff and others, 2011; Richmond and others, 2011; Goff and others, 2012; Jaffe and others, 2012; Richmond and others, 2012).

The sand layer 3–5 cm thick at about 10 cm below the surface in core PPE-1 has characteristics consistent with formation by tsunami. It has a sharp lower contact (fig. 64 photo of core), sand similar to beach sand, appears to have two normally graded intervals, contains mud rip-ups, and has an internal mud layer (not visible in photo in figure 64). A similar sand layer was found in the upper 10–20 cm in most of the cores taken in the marsh (figs. 65 and 66). A shore-normal transect shows that the sand-layer geometry (sheet-like and landward thinning, in general) is consistent with deposition from tsunami (figs. 65 and 66). In core A-21, well-preserved littoral marine diatoms (for example, *Diplomenora cocconeiformis*, *Cocconeis speciosa*) are found only in the candidate sand unit between 12 and 15 cm, supporting a marine source for the deposit.

The fine-scale (2-mm sections) vertical variation in grain size of the upper sand unit in core PPW-2 was analyzed to determine if there is suspension grading (see section on "Suspension Grading in Tsunami Deposits" above). The sand layer at PPW-2 contains an interval from 19.4 to 20.2 cm below the surface that is suspension graded (fig. 67). Suspension grading is common within tsunami deposits and rare in storm deposits and has not been searched for in deposits formed by other agents (for example, fluvial flooding).

Because the characteristics of the sand deposit are consistent with formation by tsunami and the deposit is near the present sediment surface, we hypothesized that it was formed by the 1946 tsunami. The 1946 tsunami arrived at Pillar Point marsh mid-morning on April 1, 1946 (Bascom, 1946). E.O. McMahon of the U.S. Army Engineering Division was conducting a survey in Half Moon Bay when the tsunami arrived. Bascom (1946) recounts McMahon's account that at approximately 10:30 a.m. the second and largest tsunami wave "rolled through the lagoon and crossed the road at the far end at an approximate elevation of 12.5 ft", which is 3.8 m above M.L.L.W. (fig. 63). The maximum height of the tsunami in the marsh is not known, but nearby at a pier it was 4.5 m (14.8 ft) above M.L.L.W. (3.1 m [10.1 ft] flow depth arriving at a tide of 1.4 m [4.7 ft]). The ^{137}Cs profile for core A-21 indicates that the top of the sand deposit is several centimeters below the 1963 peak (fig. 68). Deposition of several centimeters of sediment in the 17 years from 1946 to 1963 yields an average rate of about 2 mm/yr, which is reasonable for the brackish *Salicornia* marsh at Pillar Point (similar to the rate of eustatic sea level rise and in line with the observation that most marshes in San Francisco Estuary generally accrete sediment at a rate of 2–5 mm/yr [Callaway and others, 2012]). A sedimentation rate of about 2 mm/yr was confirmed for a nearby core by P.W. Swarzenski (written commun., 2013). The eyewitness accounts and ^{137}Cs constraints support the hypothesis that the upper sand deposit was formed by the 1946 tsunami.

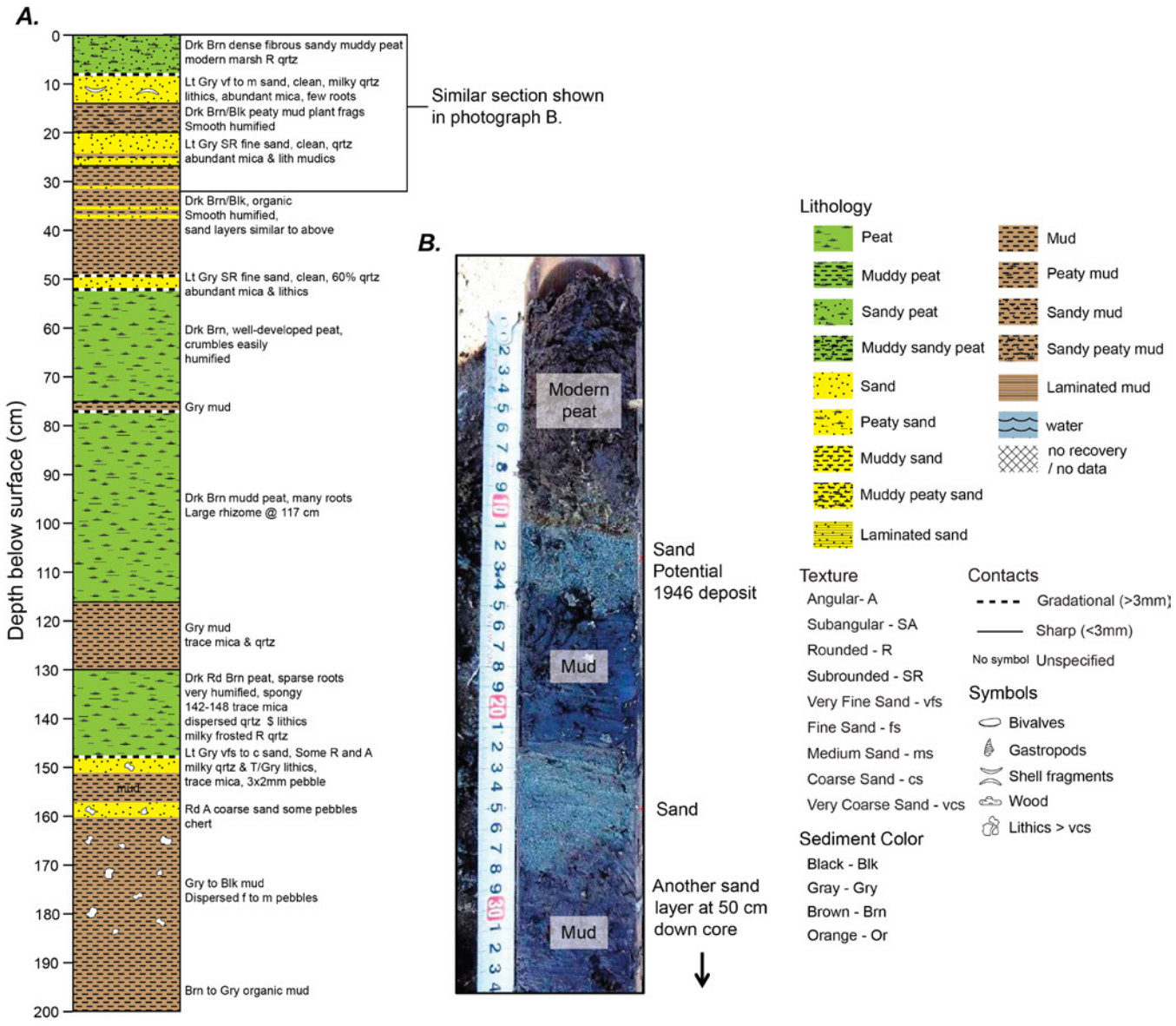

Figure 64. Log and photograph at gouge core location E-1, Pillar Point (see fig. 63 for location). *A*, Core log showing thin, anomalous sand layers in muddy marsh/lagoon sediment. *B*, Photograph of sand layers in upper 34 cm of a 60-mm-diameter gouge core located several meters from E-1. The upper sand is interpreted as deposited by the 1946 tsunami (see figures 65 through 67 and text for the basis of this interpretation).

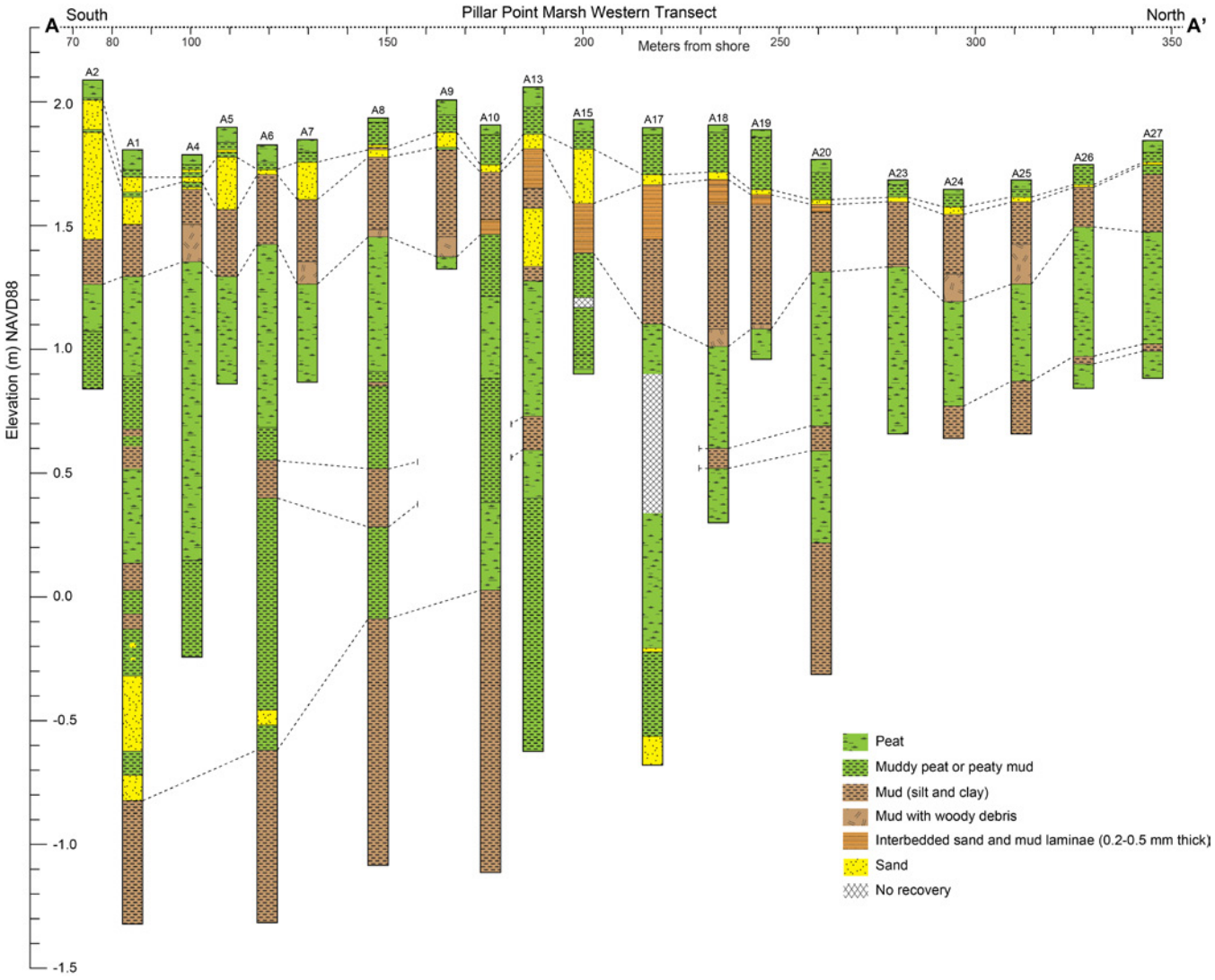

Figure 65. Correlation diagram of core logs along transect A-A' in the western part of Pillar Point marsh (see fig. 63 for location). This transect is oriented shore-normal to show correlations and inland changes in the upper sand layer, such as a general landward thinning, that are characteristic of tsunami deposits in coastal plain environments. The North American Vertical Datum of 1988 (NAVD88) is within a few centimeters of mean low low water (MLLW). The tide range at Pillar Point Marsh is about 2 m.

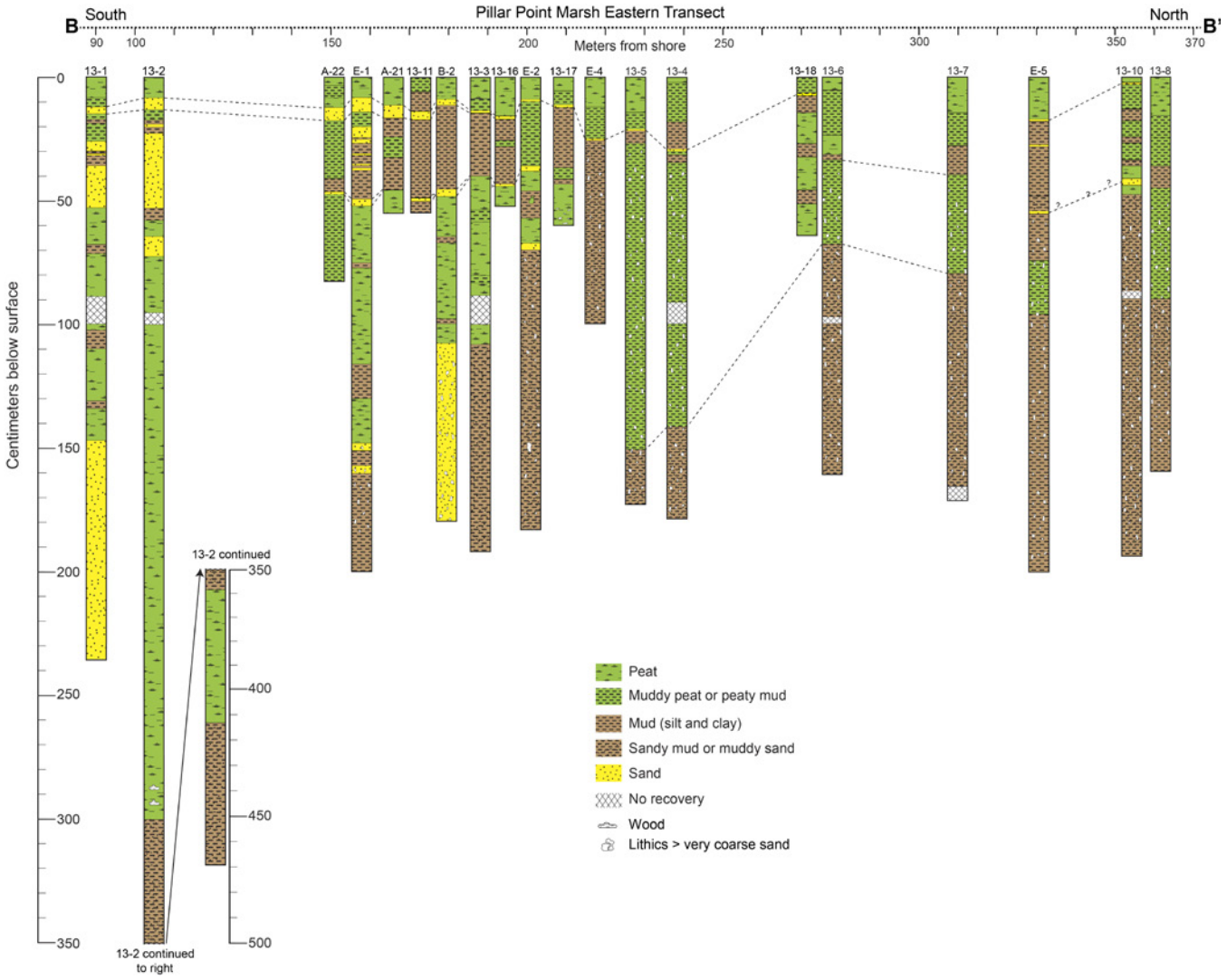

Figure 66. Correlation diagram of core logs along transect B-B' in the eastern part of Pillar Point marsh (see fig. 63 for location). This transect is oriented shore-normal to show correlations and inland changes in the upper sand layer, such as a general landward thinning, that are characteristic of tsunami deposits in coastal plain environments. Note that, unlike figure 13, where the elevations of the cores are relative to the North American Vertical Datum of 1988, cores on B-B' are here shown relative to the ground surface.

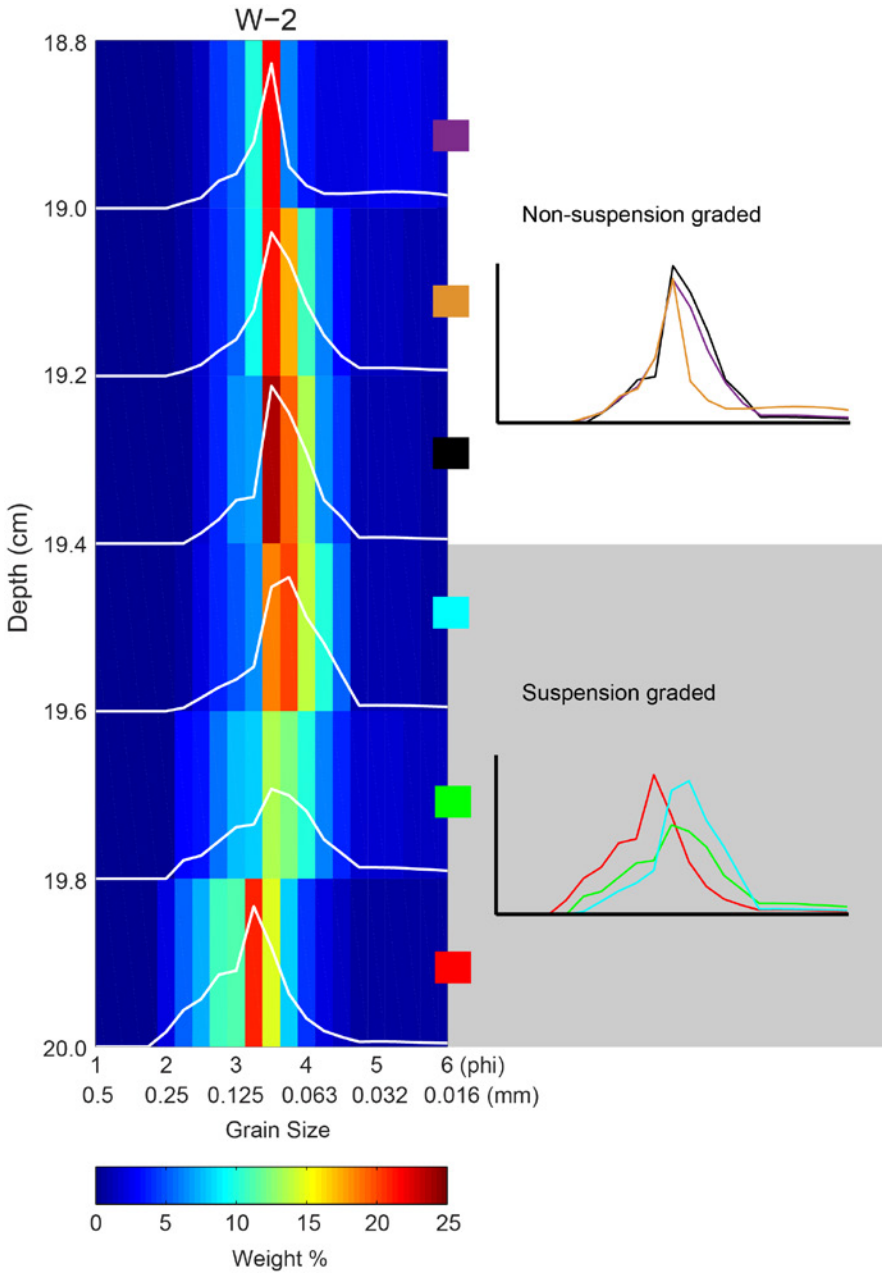

Figure 67. Graph showing fine-scale (2-mm) vertical grain-size variation of the upper sand layer in core W-2 at Pillar Point (see fig. 63 for location). The interval from 20.0 to 19.4 cm is suspension graded. Suspension grading is a specific type of normal grading formed by suspended sediment settling out of the water column that is found in modern tsunami deposits. The color of the little box in each depth interval matches the color of the diagrammatic distribution curve for that interval.

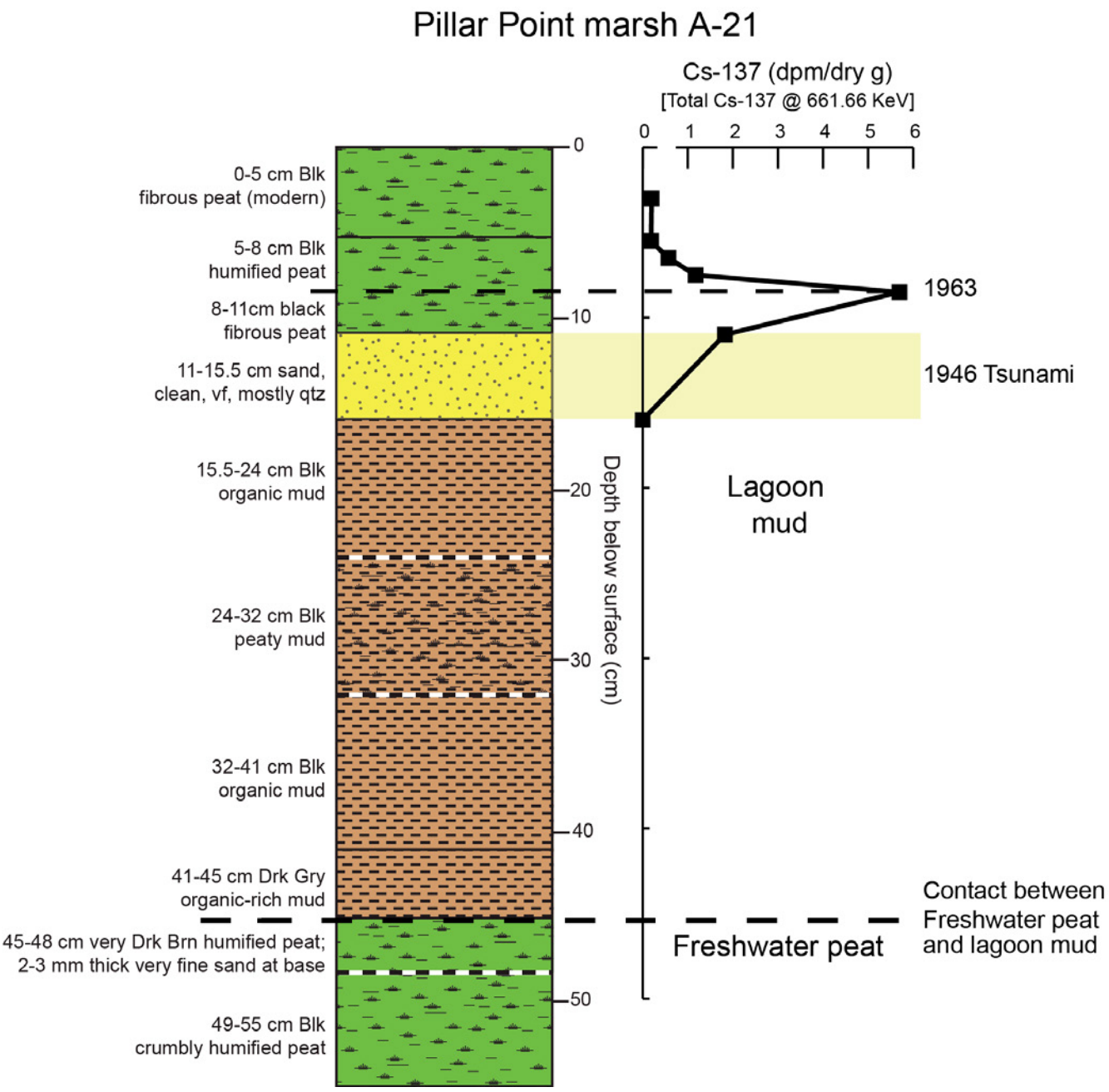

Figure 68. Core log and Cs-137 and Pb-210 profiles at gouge core site A-21 at Pillar Point.

Conclusions

A sand deposit was found near the surface of Pillar Point marsh that we interpret to be formed by the 1946 Aleutian Islands tsunami on the basis of sedimentological characteristics, deposit geometry, and ^{137}Cs dating. The sand deposits below this upper sand may or may not have been formed by a tsunami. Thus far, our study has not collected and analyzed the data necessary to attribute these deposits to tsunamis. In the eastern marsh along a transect B-B′ (fig. 66) there are sand deposits below the upper sand layer that may be correlated. If they are correlated, their geometry would be sheet-like, as would likely be formed in a tsunami. Preliminary analysis of the cores taken thus far suggests that some of these sand layers can be correlated. Additional coring may be warranted along the eastern transect. It may be that the location and history of the inlet and lagoon and the dune height control where a tsunami deposit would form and be preserved. It may also be possible that the 1946 tsunami has been the only tsunami to inundate Pillar Point marsh during its existence. Additional analyses, and interpretation of existing cores, may help answer this question. If analyses and the resulting interpretations are not able to unequivocally assign a tsunami or nontsunami origin to observed deeper sand layers, additional cores are warranted.

Carpinteria Salt Marsh (primary summary by Robert Peters)

Introduction

Carpinteria Salt Marsh is located at 34˚24.0′ N. and 119˚31.5′ W., about 19.4 km east of Santa Barbara in southern California (fig. 5). The marsh includes both intertidal estuarine wetlands and adjacent palustrine wetlands (Ferren and others, 1997). The predominant habitat is estuarine emergent wetland, and vegetation is dominated by pickleweed (*Salicornia virginica*). The watershed of Carpinteria Salt Marsh is confined to the watersheds of Santa Monica Creek and Franklin Creek, which enter the marsh in the southeast part, and a small, unnamed creek that enters from the northwest. These streams drain portions of the southern slope of the Santa Ynez Mountains and Carpinteria Valley, which are in the westernmost portion of the Transverse Ranges. Historically, Carpinteria Creek, to the east, and Arroyo Paridon, to the west, also flowed into the estuary but because of infilling of the marsh, they no longer do. However, sediments deposited in the marsh prior to infilling may include those derived from these drainages.

Investigations were conducted at Carpinteria Salt Marsh to study the geologic record of tsunamis along the Santa Barbara coast. Tsunamis in this region may be generated from offshore thrust or reverse faults in the Santa Barbara basin or from offshore landslides. Distant-source tsunamis may also impact the Santa Barbara coastline. The Santa Barbara coast has a history of small to medium tsunamis (Lander and Lockridge, 1989; Lander and others, 1993). However, the historical record for the Santa Barbara coast is relatively short. Written records from the region date back to October 1542, when the expedition led by Juan Rodriquez Cabrillo explored the California coast, and continuous records only began with the founding of Santa Barbara Presidio in 1782 (Senan and Vitoria, 1813). The first and largest recorded tsunami to impact the region during the historical period occurred on December 21, 1812. Trask (1856) reports that this tsunami inundated low-lying areas a little more than half a mile inland, reaching the lower part of the town of Santa Barbara at that time and destroying three small adobe buildings. Although runup was estimated at 3.5 m at El Refugio, and wave height was estimated at 2.0 m at Santa Barbara and at Ventura (Lander and Lockridge, 1989), there have been some questions about the validity of the size of the tsunami (Lander and others, 1993).

Field Studies

Field investigations looking for evidence of past tsunami inundation at Carpinteria Salt Marsh were begun in 2004 by the USGS and have continued through 2012. Over the course of these investigations, 115 cores have been collected (fig. 69). The 2004 Carpinteria survey was part of a reconnaissance of potential sites for future detailed tsunami sedimentation surveys and involved the examination of channel cutbanks and sediment collected in two shallow gouge core.

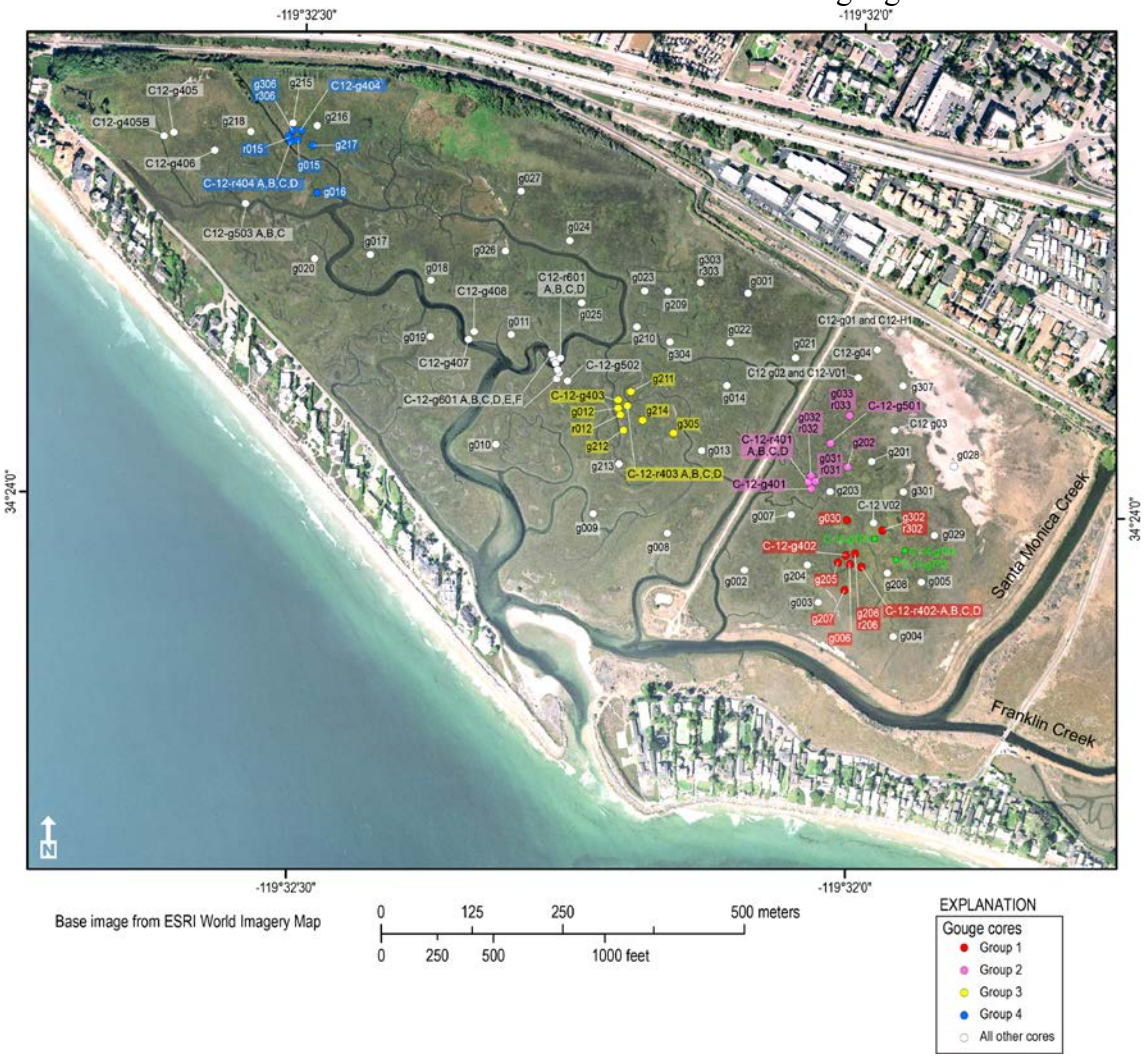

Figure 69. Vertical aerial photograph showing location of cores taken at Carpinteria Salt Marsh, with core groups that contain candidate tsunami deposits identified by color.

Results of this preliminary reconnaissance noted the presence of sand layers in the shallow stratigraphy, suggesting that the relatively undisturbed marsh environments might preserve a record of past tsunami inundation. In February 2008, a detailed field investigation was conducted at Carpinteria Salt Marsh, systematically coring across the marsh to identify sand layers consistent with tsunami deposition. Fifty-nine cores were taken using gouge augers to depths exceeding 2 m, and several cutbanks were examined. Sand layers showing characteristics consistent with tsunami deposition were sampled for grain size, composition, and textural analyses. Organic material was sampled for radiocarbon dating. In addition, eight Russian-style cores were collected targeting candidate tsunami deposits. Russian-style cores collect 0.5 m long undisturbed sediment samples for later analyses in a lab.

Surface sediment samples were taken from current marsh and surrounding environments, including the estuary, channels, beaches, and dunes.

Additional fieldwork was completed in February 2012 with an expanded project team. Twenty-one gouge cores were collected to enlarge coverage within the marsh, document the sedimentary characteristics of channels, and examine stratigraphic evidence for channel migration. Twenty Russian-style cores were retrieved from five locations (four at each location) for microfossil, grain size, and provenance analyses and to obtain additional material for radiometric dating. Sediments were also taken throughout the marsh to document current diatom and foraminiferal species within these environments. Cores collected prior to February 2012 rarely penetrated below 2 m, and the deepest recovery was 2.75 m. In October 2012, fieldwork was undertaken to obtain deeper cores in order to examine a longer record. Two vibracores were taken to a maximum depth of 3.7 m, and one hydraulic core penetrated to 4.5 m. Four gouge cores were also taken. Two of the gouge cores, using a 60-mm-diameter barrel, were taken to depths of 2.68 m and 2.88 m and transferred to D-tubes for storage and later examination and sampling in the lab.

Historical and Prehistoric Conditions at Carpinteria Salt Marsh

The extent of Carpinteria Salt Marsh and the depositional environments within the marsh have changed significantly both historically and prehistorically. Historically, Carpinteria Salt Marsh was once larger than at present and may have occupied more than three-quarters of the Carpinteria Valley (Clark, 1962). Infilling of the marsh has occurred both naturally and anthropogenically. Natural infilling occurs through erosion in the watersheds, transport of sediment by streams entering the marsh, and deposition within the marsh. At Carpinteria, the effect of the infilling is partly offset by subsidence of the Carpinteria Basin (Ferren and others, 1997). Infilling accelerated during the historical period as a result of anthropogenic changes in the watersheds. Several notable changes to native environments directly altered the extent of the marsh to accommodate agriculture and urban environments (Ferren and others, 1997). The eastern part of the marsh was filled to build the city of Carpinteria. Northern parts of the marsh have been filled for construction of Carpinteria Avenue, the Union Pacific Railroad, Highway 101, and other urban development. Road construction has fragmented the marsh into subbasins. The natural channels of Franklin and Santa Monica Creeks have been redirected to artificial channels lined with earthen berms, resulting in reduced sediment deposition on the natural alluvial fans and delta. In addition, the southern margins of the marsh adjacent to the sand spits have been altered to accommodate roads and residential development. A part of the marsh just north of the western dunes served as a borrow pit to provide fill for road and residential development along the dunes. Development on the dunes and armoring of the spits has also restricted the natural migration of the channel mouth.

Maps prepared in 1869 by the United States Coast Survey (Grossinger and others, 2011; Greenwell and Forney, 1869a,b) and a series of aerial photographs from 1929 to 1981 document historical changes to the marsh (Ferren and others, 1997). The channel patterns depicted in the 1869 maps are different from present-day channel patterns. By 1929, the marsh boundaries and channel patterns were similar to those in the present.

The watershed of the Carpinteria Salt Marsh is in one the highest sediment yield regions of California (Brownlie and Taylor, 1981; Inman and Jenkins, 1999; Warrick and Mertes, 2009), and because of this land sources may provide a major component of the sediment in this marsh. Debris basins were constructed in this watershed in the 1970s. Most coarse-grained sediment but only negligible fine-grained sediment is trapped by the debris basins (Barnard and others, 2009), and this could result in a change from sand-rich sediment to sand-poor sediments delivered to the marsh. The capture of sand and gravel by the debris basins in the upper watershed could cause a transition in sand sources from the upper watershed (which is primarily Eocene marine sedimentary rocks) to the lower watershed (which is primarily younger nonmarine sedimentary material). Hydraulic changes in the

Carpinteria Salt Marsh caused by levee and road construction and coastal armoring could also influence grain-size change in the wetland sedimentation. The creek channels were leveed in parts of the wetland, and a road cut off the direct flow between the creeks and the western wetland. Both of these would reduce the likelihood of fluvial sand from going overbank and depositing on the wetland surfaces. Furthermore, the armoring along the beach constrained the mouth of Carpinteria Salt Marsh, which may increase the residence time of creek water in the wetland, thereby increasing the likelihood for fine-grained sediment deposition. These anthropogenic changes to the marsh likely influence marsh sedimentation patterns and could account for changes from sand-rich to mud-rich deposition in the upper parts of the cores (Cole and Wahl, 2000).

Cores collected at Carpinteria Salt Marsh provide evidence that prehistoric conditions there were likely different from current or historic conditions. In most of the cores at Carpinteria, peat is present and well developed within the uppermost 0.5 m of core. this peat developed from the vegetated marsh surface. In most cores, at depths below 0.5 m, peat is rarely more than a few cm thick and commonly is absent. Below these upper peats, sediments are dominated by mud or sand, suggesting an initial tidal flat or open water environment.

Candidate Tsunami Deposits

Four groups of cores were identified that had sand layers with sedimentary properties consistent with tsunami deposition (figs. 69 through 73). These properties include the presence of sharp basal contacts, normal grading, rip-up clasts and sand layer thickness that ranged from 1.5 to 12 cm. Each group of cores had a sand layer that was laterally continuous within the group but discontinuous with the other groups. In some cases, the depth of the deposits and their ages also separated the groups (see "Radiocarbon Dating" section below). Several other cores contained anomalous sand layers, but they either lacked lateral continuity with sand layers in adjacent cores or were otherwise inconsistent with tsunami deposition.

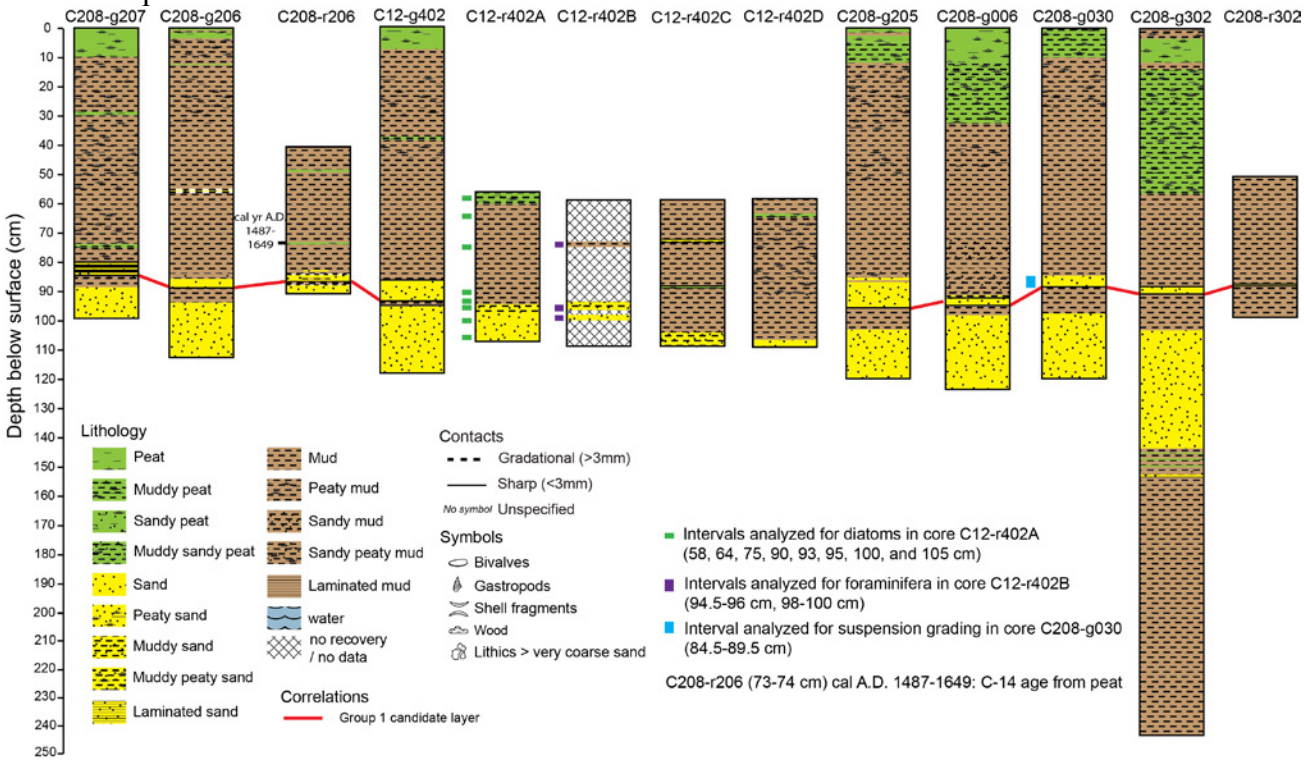

Figure 70. Core logs for gouge cores of group 1 at Carpinteria Salt Marsh, with correlations between candidate tsunami deposits shown by a solid red line.

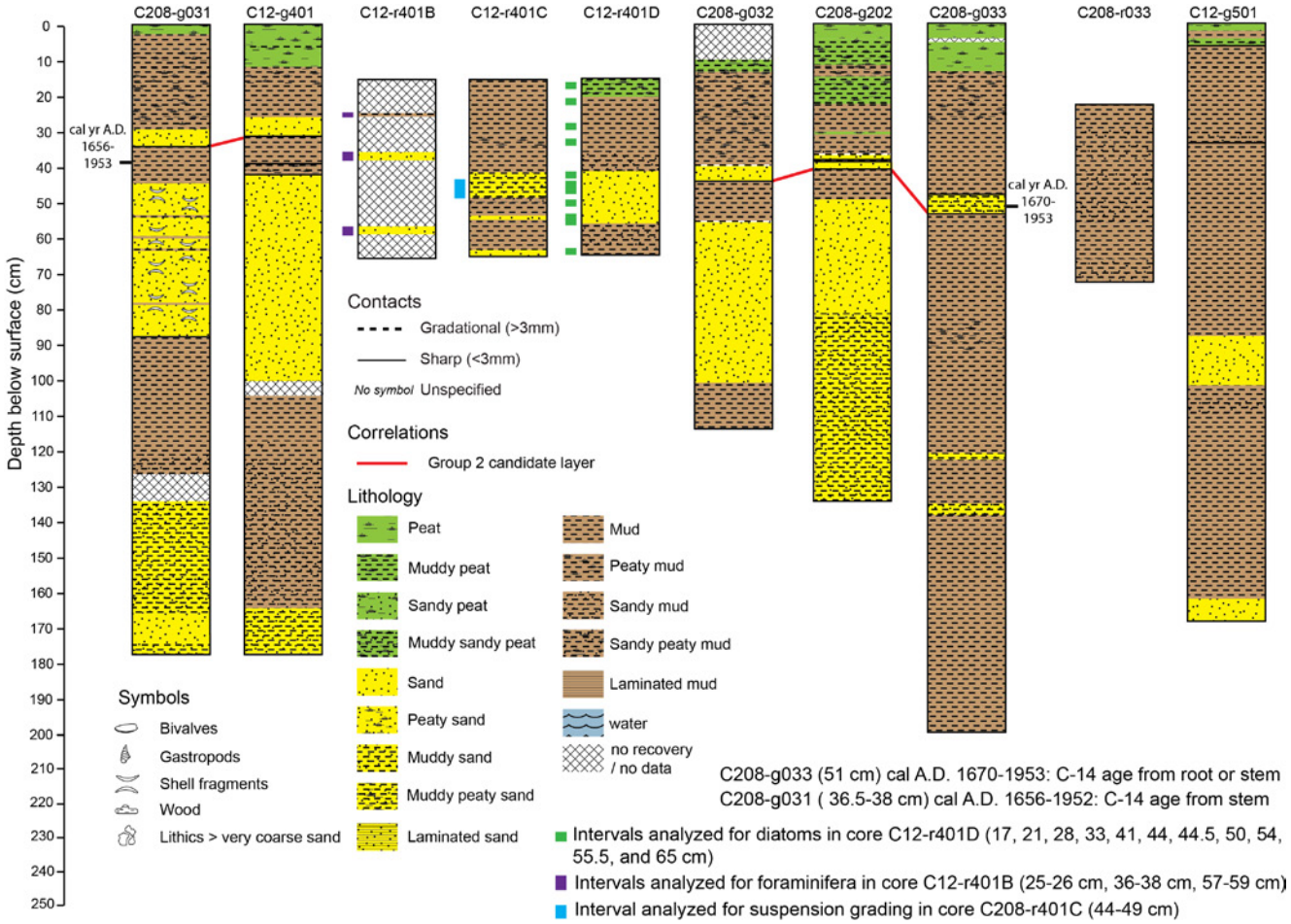

Figure 71. Core logs for gouge cores of group 2 at Carpinteria Salt Marsh, with correlations between candidate tsunami deposits shown by a solid red line. Core C12-r401A has not yet been described or sampled.

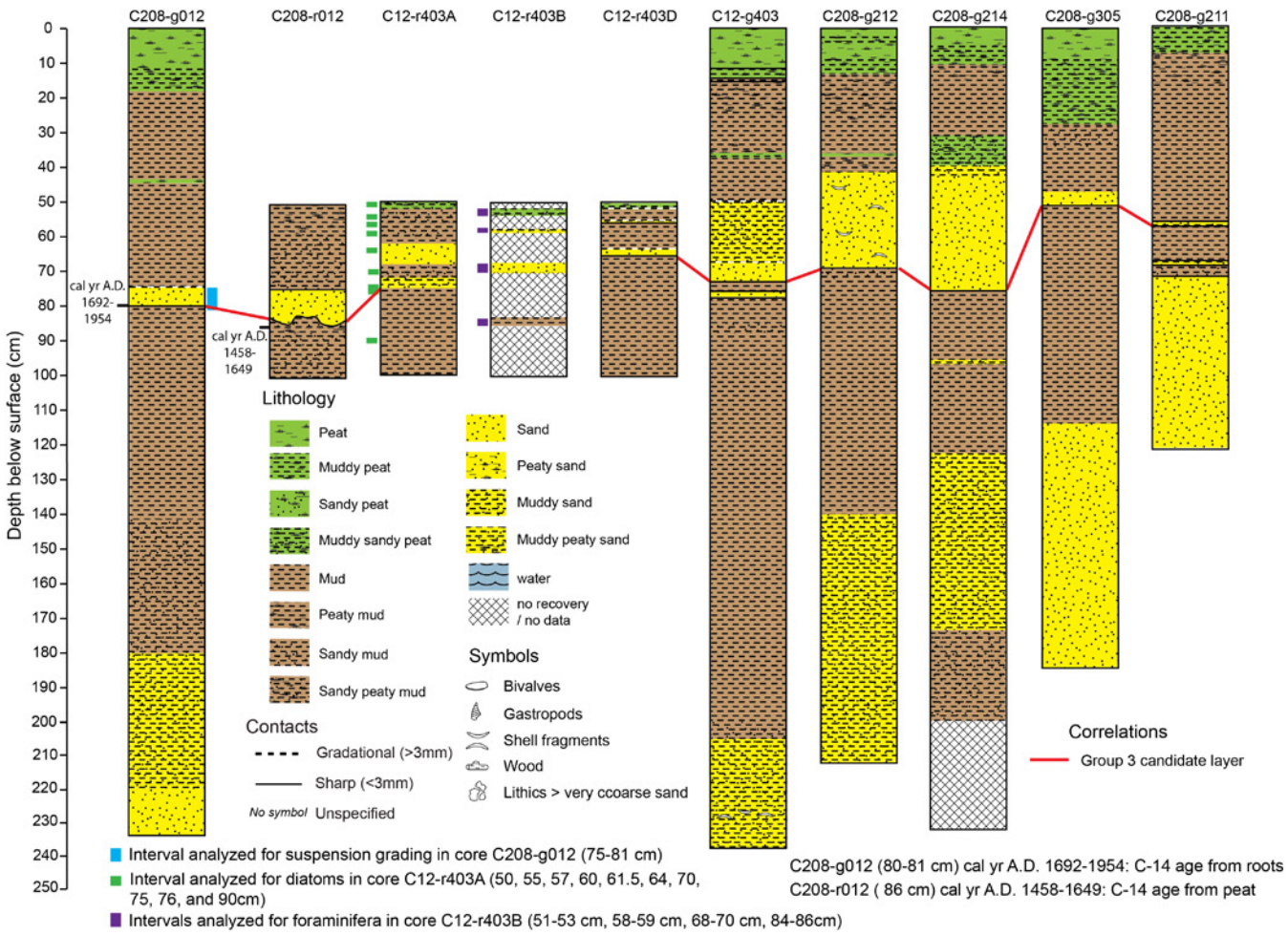

Figure 72. Core logs for gouge cores of group3 at Carpinteria Salt Marsh, with correlations between candidate tsunami deposits shown by a solid red line. Core C12-r403C has not yet been described or sampled.

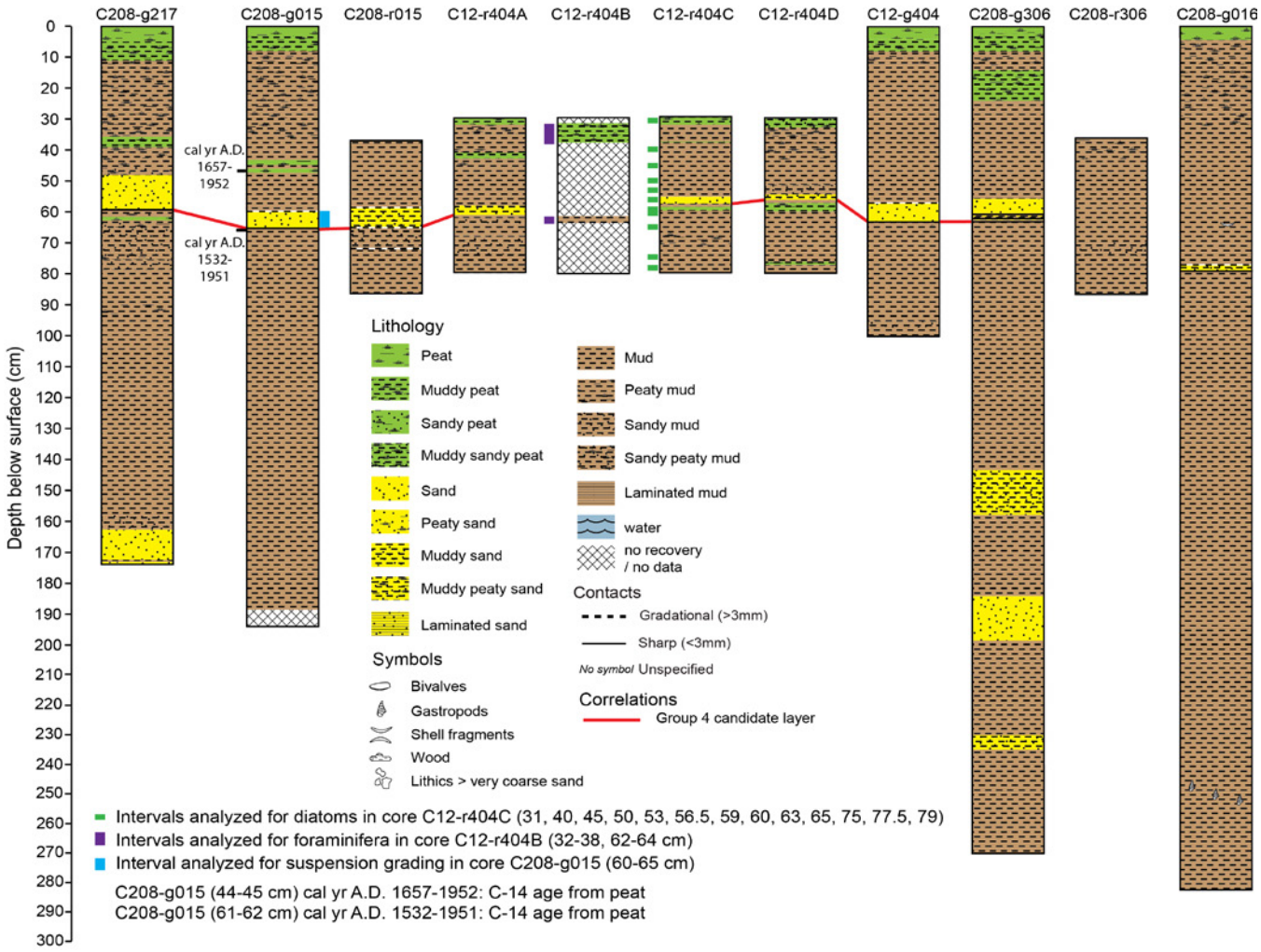

Figure 73. Core logs for gouge cores of group 4 at Carpinteria Salt Marsh, with correlations between candidate tsunami deposits shown by a solid red line.

- Group 1 consists of seven adjacent gouge cores (g207, g206 [r206], g205, g006, g030, g302 [r302] and g402 [r402]) (fig. 69). All gouge cores within the group have a sand layer from 1.5 to 10 cm thick with a sharp basal contact at depths between 85 and 96 cm. (fig. 70). Normal grading was observed in cores g207, g205, g030, and g006. The Russian cores r402 A, B, C, and D did not penetrate through the base of the sand layer at depths between 93 and 109 cm (fig. 70). It is not possible at this time to determine if this sand layer correlates with the candidate sand layer or the deeper sand layer found in all Group 1 gouge cores.
- Group 2 includes five adjacent gouge cores (g031, g032, g202, g033 [r033], g401 [r401] and possibly C12-g501 (fig. 69). Most cores within the group contain a sand layer from 4 to 5 cm thick with a sharp basal contact between 35 and 53 cm depth (fig. 71). Core C12-501 is located in the area of the Group 2 cores. It does not contain a sand layer in the depth range of other Group 2 cores, but has a layer of coarse silt with minor fine sand with a sharp basal contact at 34 cm.
- Group 3 consists of six adjacent gouge cores (g212, g012 [r012], g214, g305, g211, and g403 [r403]) (fig. 69). All cores have a sand layer with a sharp basal contact at depths between 51 and 80 cm (fig. 72). This sand layer is normally graded in cores g212 and g012. A sand-filled burrow was present at the base of core g212. A mud clast that may be a rip-up clast is present within the sand layer in core

r012. The sand layer in cores g211, g012, g403, and g305 is 5 cm thick or less, but in core g212 it is 28 cm thick and in g214 it is 35 cm thick, unusually thick for tsunami deposits.

- Group 4 includes four adjacent gouge cores (g217, g015 [r015], g306 [r306], g404 [r404]) and possibly the nearby g016 (fig. 69). The cores contain a sand layer from 5 to 12 cm thick with a sharp basal contact at depths between 59 and 65 cm (fig. 73). Normal grading is present in cores g217, g015, and g404, and in core g306 the sand layer is normally graded in the upper part while inversely graded in the lower part.

Normal and Suspension Grading

Normal grading was observed in sand layers from each of the four groups. Normal grading is often reported for tsunami deposits (see references in the section on "Identification of Tsunami Deposits"). In addition, a specific type of normal grading, termed suspension grading (see section on "Suspension Grading in Tsunami Deposits" above), was found in three of four cores for which detailed grain-size analysis was conducted.

Candidate tsunami sand deposits for each of the four groups were analyzed to determine if suspension grading was present. Samples were taken from cores where normal grading was observed in the field (g012, g015, g030, and r401C). Shifts in grain size for each of these four groups are shown in figure 74. A shift of the whole distribution to the right in an interval (towards higher phi numbers and, hence, smaller grain size) is considered a candidate for suspension grading. Consequently, three of the four groups appeared to have suspension-graded intervals (table 4, fig. 74). To test the hypothesis that these intervals formed by sediment settling out of suspension, we ran an inverse sediment transport model (Jaffe and Gelfenbaum, 2007). If the model is able to reproduce the observed fining upward of these intervals, then the hypothesis is supported.

Table 4. Results of inverse sediment transport model runs for intervals of Carpinteria deposits that exhibited suspension grading.

[Group refers to the candidate tsunami deposit group the core is associated with. SGL number refers to the suspension graded interval within the candidate layer. Int., depth interval in core. Flow depths were chosen to obtain a Froude number of approximately 0.7. RSE, the root square error, is a metric that quantifies the fit between the modeled and observed grain size distributions]

Core	Group	SGL no.	Int. (cm)	Flow Depth (m)	Avg. Speed (m/s)	Froude no.	RSE
g030	1	1	87.5–88.5	1.0	2.1	0.68	9.4
g030	1	2	85.5–86.5	1.0	2.2	0.71	8.4
g030	1	3	84.5–85.5	1.0	2.2	0.71	8.2
R401c	2	NONE					
g012	3	1	77–79	1.5	2.6	0.67	10.5
g015	4	1	63–65	2.0	3.4	0.76	7.1

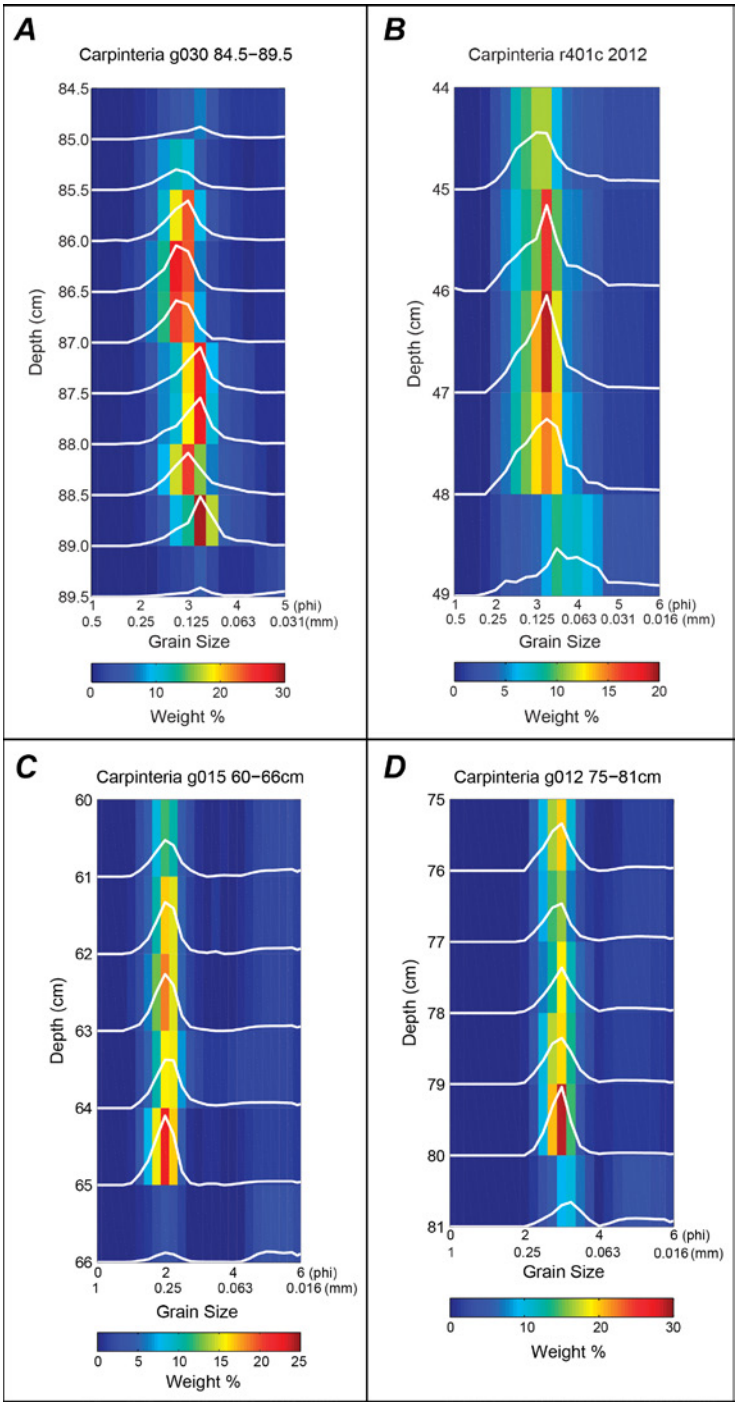

Figure 74. Fine-scale vertical grain-size variation of sand layers in Carpinteria Salt Marsh cores (*A*) g030 (group 1; see fig. 70), (*B*) r401C (group 2; see fig. 71), (*C*) g012 (group 3; see fig. 72), and (*D*) g015 (group 4; see fig. 73). See figure 69 for core locations. The intervals 87.5-88.5 cm, 85.5-86.5 cm, and 84.5-85.5 cm in core g030; 77-79 cm in core g012; and 63-65 cm in core g015 are suspension graded, showing a shift to the right (to finer grain sizes) up core. Suspension grading is a specific type of normal grading formed by suspended sediment settling out of the water column that is found in modern tsunami deposits. No intervals in core r401C appear to be suspension graded.

The root square error (RSE) between the observed and modeled distributions is a metric for whether the intervals were formed by sediment falling out of suspension (that is, suspension graded). The RSEs for the intervals for the Carpinteria candidate tsunami sand deposits ranged from 7.1 to 10.5. A RSE value in this range was found for about 30 percent of the suspension-graded intervals of deposits on the Sendai coastal plain in Japan formed by the 2011 Tohoku-oki tsunami (Jaffe and others, 2012). These values support the hypothesis that these intervals were formed by sediment settling out of suspension from a high-speed turbulent flow as it rapidly slowed, which is consistent with deposition by a tsunami. These patterns are not consistent with hurricanes or storms, which have not been found to create suspension grading—bedload deposition dominates for these deposits and creates a massive or inversely graded deposit. It may be possible that a process other than sediment falling out of suspension from a high-speed flow, or an agent other than tsunamis (for example, fluvial flooding), can produce the same vertical variation in grain size distributions as suspension grading, although this has not yet been tested. The RSE values for the intervals of the Carpinteria deposits analyzed support deposition by a tsunami, do not favor storm deposition, but, because suspension grading has not been looked for in all deposit types, do not rule out deposition by other processes or nontsunami agents.

If sediment settling out from a high-speed turbulent flow formed the suspension-graded intervals, such as would occur when a tsunami uprush slowed, then the inverse model of Jaffe and Gelfenbaum (2007) can be used to calculate flow speed. Derived flow speeds ranged from 2.1 to 3.4 m/s for the modeled suspension-graded intervals (table 4). The inverse model is not sensitive to flow depths except for very shallow flows and, as a result, does not constrain the flow depth, which is of interest. Flow depth may be calculated using the relationship that flow depth is equal to the Froude number squared times the gravitational constant (9.8 m/s^2) times the flow speed. For Froude numbers of ~0.7, a value at lower end of the range observed for overland flow in recent tsunamis (Fritz and others, 2006; Spiske and others, 2010), calculated flow depths range from 1 to 2 m. These speeds and flow depth are consistent with a small tsunami forming the deposit, but do not rule out other agents, such as fluvial flooding.

Microfossils

Diatoms and foraminifera were analyzed in 50-cm-long Russian cores, collected proximal to the cores used in the lithostratigraphic analyses, from each of the four core groupings having candidate tsunami deposits (groups 1–4, figs. 69–73). The goal of the microfossil analyses was to provide additional insight into the possible origin of the candidate tsunami deposits at Carpinteria, specifically to consider evidence for or against incursion from a marine source.

To support the downcore analyses, the distributions of diatoms and foraminifera were recorded for modern environments at Carpinteria Beach and in various estuarine benthic environments in the Carpinteria Salt Marsh Reserve. Beach samples included wet sand from the swash zone and beach seaward of the mouth of the estuary; sloughs and tidal stream channels within the estuary area; salt pans; and *Salicornia*- and *Frankenia*-dominated marsh surfaces. These observations provided baseline taxonomic data to compare with downcore samples, including the candidate tsunami deposits.

Diatoms and foraminifera were present in all marsh surface and slough channel samples, and consisted of cosmopolitan, brackish estuarine taxa typical of temperate salt marshes and tidal flats (Phleger, 1967, 1970; Patterson, 1990; Scott and Leckie, 1990; Jennings and Nelson, 1992; Vos and DeWolf, 1993; Witkowski and others, 2000; Hemphill-Haley, 2006). Diatoms were abundant on the marsh surface, both in vegetated areas (particularly *Diploneis bombus*, *D. smithii* var. *recta, Surirella fasciculata*, and *Nitzschia prolongata*) and in sparsely vegetated or open muddy areas (particularly *Caloneis westii*, *Surirella fasciculata*, *Navicula digitoradiata*, *Scoliopleura tumida*, *Gyrosigma eximium, G. balticum*, and *Fallacia subforcipata*). The most prominent foraminifera in the modern marsh environs were *Trochammina inflata* and *Miliammina fusca.* Diatoms were comparatively sparse in the slough and channel samples, and in addition to infrequent occurrences of some taxa observed in the marsh-surface

samples (for example, *C. westii*, *N. digitoradiata*, *S. tumida*), included a variety of pennate benthic taxa (*Nitzschia* spp., *Opephora* spp., *Amphora* spp.), as well as *Melosira moniliformis*, a cosmopolitan brackish epiphyte. Foraminifera were very rare in these locations as well, represented most often by the marsh species *Trochammina inflata* and *Miliammina fusca,* but occasionally including one or two specimens of the estuarine species *Ammonia tepida, Elphidium excavatum, Rosalina globularis,* and *Quinqueloculina bellatula*. The sand sampled from the beach consisted of wet sediment from the swash zone exposed at low tide, as well from the upper beach just east of the channel at the outlet of the estuary. Foraminifera were not observed in the beach sand. The beach sand was also devoid of diatoms with the exception of very small (<8 µm long) epipsammic taxa attached to mineral grains (for example, *Fallacia* cf. *cryptolyra, Amphicocconeis* sp.). None of the diatom taxa observed in the marsh and slough samples were observed in the beach samples. We did not have modern samples from the offshore area, but relied on published literature to predict the types of typical coastal marine diatoms (for example, *Coscinodicus* spp., *Thalassiosira* spp., *Actinocyclus* spp., *Thalassionema nitzschioides*, *Fragilariopsis doliolus*, *Chaetoceros* spp. resting spores) or foraminifera (for example, the benthic species *Bulimina denudata, Buliminella elegantissima, Trochammina pacifica, Nonionella* spp., *Uvigerina* spp., and *Cassidulina* spp., and the planktic species *Neogloboquadrina pachyderma* and *Globigerina bulloides*) that might be entrained from nearshore deposits (Cupp, 1943; Lankford and Phleger, 1973; Ingle, 1980; Hemphill-Haley, 1993a; Hemphill-Haley and Fourtanier, 1995; Kennett and others, 2000; McGann, 2009).

Of significance for this study, salinity and the presence of water are two important environmental factors controlling the distributions of diatoms and foraminifera. Diatoms are found in planktonic and benthic habitats and in freshwater to marine salinities, but they only grow where water is present and therefore are not indicative of upland soils that are dry for long periods of time (Stoermer and Stol, 1999). Foraminifera that form fossilizable hard parts are only found in brackish to marine environments, and they similarly are not found in upland environments (Loeblich and Tappan, 1964).

The results of the downcore microfossil analysis suggest that the candidate tsunami deposits in groups 1–4 did not originate from a coastal or marine source. We observed no marine taxa, which are often found in tsunami deposits (Dawson and others, 1996a,b; Dawson, 2007; Witter and others, 2009; see also the discussion of diatoms in the Pillar Point 1946 tsunami deposit in this report), and the array of microfossils observed in the candidate deposits are inconsistent with beach sands. For groups 1 and 2, in the eastern area of the marsh (fig. 69), the microfossil data suggest terrestrial flood deposits. For group 4, the data are consistent with accumulation in a low-energy brackish intertidal flat. The group 3 data are equivocal because of poor preservation in all but the near-surface, peaty deposits (fig. 71), but assemblages of both foraminifera and sparse, poorly preserved diatoms do not differ between the candidate deposit and other deposits in the cores, and as with the group 4 samples, are consistent with estuarine intertidal deposits.

The interpretation of upland flood deposits for groups 1 and 2 is based partly on the observation that brackish-marine diatoms and foraminifera are absent in the candidate deposits but present in similarly fine-grained (muddy), stratigraphically adjacent deposits. For group 1, diatoms and foraminifers were analyzed in cores C12-r402A and C12-r402B, respectively (fig. 70). It is difficult to correlate with certainty the sandy sediments in these Russian cores with the candidate sand layer, because the Russian cores did not penetrate the base of the sand layer (fig. 70), although the transition to muddy sand at the top of the deposit is comparable to what is observed in other cores. No intact diatoms or foraminifera were observed in the candidate tsunami deposit, a clean to organic-rich brown sand near 100–105 cm, nor in overlying brown muddy sand and mud between 90 and 100 cm. We interpret the entire interval of sand and mud between about 90 cm and the base of these cores at 105 cm to be flood deposits. In contrast to the nonfossiliferous flood deposits, diatoms and foraminifera are present in overlying silty mud and peaty mud, showing that the absence of microfossils between ~90 and 105 cm is

a function of the original sediment composition rather than the result of post-depositional processes. The group 1 candidate deposit also contains a few fragments of reworked Tertiary marine diatoms, which are identified by their darker, more heavily silicified appearance under a light microscope as compared with the translucent siliceous valves of the modern or subrecent diatoms at Carpinteria. The Tertiary fragments, also observed in the modern slough channel samples, are probably eroded out of fossiliferous rocks in the Santa Ynez Mountains above Carpinteria, some of which are found at or near the heads of drainages for the streams feeding into the marsh (Minor and others, 2009).

For group 2, diatoms and foraminifers were analyzed in cores C12-r401D and C12-r401B, respectively (fig. 71). The candidate deposit in r401D and r401B consists of brown mud underlying a thin layer of plant detritus, and correlates to a sand deposit overlain by detritus in other cores. Diatoms are absent in the muddy candidate layer with the exception of very rare freshwater soil diatoms and phytoliths (siliceous precipitates from grass species; Piperno, 1988; Mulholland and Rapp, 1992). In contrast, deposits above and below this interval contain common, well-preserved estuarine taxa consistent with the local intertidal environment. Foraminifera are present in a detritus-rich sample at 25–26 cm in core C12-r401B and consist entirely of the marsh-indicating species *Trochammina inflata*. The presence of rare soil diatoms and phytoliths is consistent with a terrestrial flood deposit, and the foraminifera associated with the detritus are consistent with reworked marsh plants.

Microfossils in the group 3 and 4 cores, from the western marsh area (fig. 69), are consistent with accumulation in a brackish intertidal environment. The analyses did not reveal any obvious evidence for tsunami deposition, such as allochthonous beach sand or coastal marine fossils. Neither diatoms nor foraminifera are well preserved in the group 3 cores (C12-r403A and C12-r403B; fig. 72), either within the candidate tsunami deposits or in other samples analyzed in the 50-cm core sections, and therefore the results for this site are less robust than for the other localities. Almost all diatom valves show evidence for dissolution, suggesting post-depositional chemical leaching of subsurface deposits at the core location. Although sparse and poorly preserved, the diatoms and foraminifera in the group 3 candidate deposit (near 65-75 cm; fig. 72) consist of estuarine species consistent with the local environment, which rules out redeposited beach sand or inland transport of coastal marine material. All core samples included fragments of reworked Tertiary marine diatoms.

In contrast to the group 3 cores, preservation of diatoms and foraminifera is excellent in the group 4 cores and provides valuable insight into the mode of deposition for the candidate deposit at this location. The candidate deposit in the group 4 cores (C12-r404D and C12-r404B; fig. 73) consists of fine-grained muddy sand or sandy mud at depths between 52 and 57 cm. Underlying the sandy candidate deposit is a 1-cm-thick mud deposit between 57 and 58 cm and a thin unit of muddy peat between 58 and 60 cm. Intertidal diatoms and foraminifera were observed in all samples, including frequent occurrences of the tidal flat and marsh foraminiferal species *Trochammina inflata* and *Miliammina fusca*. A few freshwater diatoms and chrysophyte stomatocysts (siliceous precipitates of freshwater algae; Adam and Mahood, 1981) in muddy deposits near 75 cm indicate minor freshwater input at this site prior to the emplacement of the candidate deposit, but a brackish environment persisted throughout the core record.

The exclusive occurrences of estuarine diatoms and foraminifera in the group 4 cores rule out redeposited beach sand or inland transport of offshore marine material. The diatom data additionally refute tsunami deposition for two reasons: (1) the prominence of large (>100 μm long) well-preserved taxa; and (2) lack of evidence for mixing of assemblages from different environments. Diatom preservation in tsunami deposits has been reported as both excellent (Hemphill-Haley, 1995, 1996; Sawai and others, 2009; Witter and others, 2009) and poor (Dawson and others, 1996a,b; Dominey-Howes and others, 1998; Dawson and Smith, 2001; Chagué-Goff and others, 2002, Sawai, 2002; Dawson, 2007; Kortekas and Dawson, 2007). But a closer examination of the various reports shows that diatom preservation in tsunami deposits is a function of several factors: (1) shape of the diatom valve,

whether round (centric) or elongate (pennate); (2) size of the valve, which depending on the species can range from <5 μm to >200 μm; and (3) siliceous structure of the valve, that is, whether densely or finely silicified, which will make the valve more or less easily susceptible to breakage. An agreement amongst all of these studies listed is that whereas small, sturdy pennate diatoms that live in sandy environments (epipsammic taxa), as well as larger densely silicified centric diatoms, may be found in good condition in tsunami deposits, large, elongate diatoms (>100 μm long) are not found intact. This is because the large pennate diatoms have a more delicate valve construction, and their elongate shape makes them more susceptible to breakage in turbulent flows (Dawson and Smith, 2001; Dawson, 2007; Witter and others, 2009). The group 4 candidate deposits contain numerous well-preserved valves of large elongate taxa (*C. westii, T. aspera*), including some specimens with the upper and lower valves still attached (as a complete shell or "frustule"). Other smaller taxa (~40–60 μm long) in the candidate deposits (*Tryblionella granulata, Navicula flagillifera*) are similarly pristine. Whereas elongate diatoms are overwhelmingly found as fragments in tsunami deposits, the group 4 candidate deposit contains few fragments relative to intact valves, and 60–80 percent of all valves in the samples are unbroken. In addition to the excellent preservation, which is inconsistent with transport and mechanical abrasion, the diatoms present in the group 4 candidate deposits are commonly found together in the same tidal flat habitat (Vos and DeWolf, 1993; Witkowski and others, 2000; Hemphill-Haley, 1993b,c, 2006), and there is no evidence for anomalous taxa mixed in from different environments, which is common in tsunami deposits (Sawai and others, 2009; Szczuciński and others, 2012).

In summary, the results of the microfossil analyses suggest that the candidate tsunami deposits in groups 1 and 2 cores are terrestrial flood deposits. The absence of estuarine diatoms and foraminifera in the candidate deposits is the result of deposition of upland sediment rather than post-depositional dissolution of the fossil deposits. The group 2 candidate deposit also contains a few occurrences of freshwater diatoms and phytoliths, further supporting a terrestrial origin for the sediment. The diatom and foraminifera data in the group 4 candidate deposit are consistent with accumulation in an intertidal environment, and inconsistent with incursion from a coastal or marine source. Excellent preservation of large (>100 μm long) elongate diatoms in the group 4 candidate deposits is inconsistent with turbulent flow, and there is no evidence for mixed material from different habitats, which is common in tsunami deposits. The results for the group 3 candidate are less informative because of poor preservation, but are more consistent with continuous deposition at the site than deposition of an allochthonous tsunami deposit.

Other Possible Depositional Processes

Several processes other than tsunami deposition were identified as possible sources for the anomalous sands layers in the Carpinteria cores. These processes include deposition by storm waves and storm surge, deposition by flooding from fluvial overwash, and deposition within channels by channel processes.

Large storm waves can deposit sand in coastal settings up to and sometimes exceeding 1 m in thickness (Morton and others, 2007), while tsunami deposits are typically less than 30 cm thick and form laterally continuous sheets (Peters and Jaffe, 2010a; Morton and others, 2007). Morton and others (2007) found normal grading and rip-up clasts to be consistent with tsunami deposition in coastal environments but rare or absent in storm wave or storm surge deposits. However, Shanmugan (2012) found that sedimentological criteria may be unreliable for distinguishing tsunami from storm deposits.

Overwash from flooding of the creeks entering the marsh may also result in sand deposited on the marsh surface. Comparison of the composition and texture of candidate tsunami deposits with fluvial and other sources was used to evaluate whether these deposits were formed by fluvial flooding. All candidate tsunami deposits contained a large component of quartz sand that was rounded to sub-rounded, and most had little to no feldspar and a minor component of rounded black lithics. Estuarine

sand was composed mainly of rounded quartz with black lithics. Beach sand was primarily quartz with black lithics but was less rounded. Creek sediment was sampled from a channel entering the northwest part of the marsh and from alluvial deposits in the southeast part of the marsh near where Santa Monica Creek enters the marsh. The sand component at both locations is angular to sub-angular and has a significant component of feldspar and abundant red, green, brown, and black lithics. However, sand sampled from the creek may not represent current or past fluvial inputs, as noted in the section on "Historical and Prehistoric Conditions at Carpinteria Marsh" above. There are many different sources of sand in the watershed, which all will be active under different times and processes. The colorful sands described here are likely from nonmarine sedimentary rocks of the lower watershed, which may not be the dominant geological formation of the watershed.

Creation of the candidate tsunami deposits by channel migration was evaluated using historical channel distributions and coring transects across present channels. Differences in channel patterns were evident between those shown on the 1869 coast survey maps (Grossinger and others, 2011; Greenwell and Forney, 1869a,b) and those seen in aerial photographs from 1929 and later, which more closely resemble current patterns (Ferren and others, 1997). If the changes in channel patterns were as large as the maps suggest, then there should be evidence for channel migration in the marsh. The candidate deposits were compared to core transects across a large and a medium channel and to sediments sampled from the channels. Observations from core transects across three channels show that the candidate deposits are inconsistent with deposits in large channels both in thickness and in occurrences of bivalve and gastropod shells; deposits in medium size channels are more consistent in thickness but still contain abundant shells. Shells were rare in the candidate tsunami deposits.

Radiocarbon Dating

Radiocarbon dates from within the sand layers or at depths close to them constrain the dates of the sand layers in the four groups (table 5, fig. 75). A 1-cm-thick peat layer from core r206 has a calibrated age range of A.D. 1487 to 1649. This suggests that the age of the candidate group 1 sand layer in core r206, 10 cm below the sampled peat layer, is older than A.D. 1649. However, if the bulk peat sample has an inbuilt age from incorporating older woody material, it could yield an age older than the underlying sand layer. Samples from two cores in group 2 are relatively consistent. In g033 a stem or root fragment within the sand layer was dated as A.D.1670 to modern, and in r031 a stem lying horizontally just below the sand layer was dated as A. D. 1656 to modern. This suggests that the age of the group 2 sand layer is A.D. 1670 or younger. Two samples were dated from group 3 cores. Bulk peat sampled from r012, 3 cm below the candidate sand layer, has a calibrated age of A.D.1458 to A.D.1649. Fine root hairs in core g012, taken directly from the candidate sand layer, yield an age range of A.D. 1692 to modern, suggesting that the deposit is younger than A.D.1692, although the roots may have penetrated the deposit a long time after deposition, giving a false young age. Two samples were taken from the group 4 core g015. A root or stem fragment taken from within the deposit has an age range of A.D.1532 to present and suggests that the deposit is younger than A.D. 1532. Peat sampled 10 cm above the candidate sand layer has an age range of A.D. 1657 to modern, consistent with this interpretation.

Table 5. Accelerator mass spectrometry (AMS) ^{14}C ages for samples from Carpinteria Salt Marsh.

[BP, before present (1950). Samples processed at Nation Ocean Sciences AMS laboratory (NOSAMS), Woods Hole Oceanographic Institute, Woods Hole, Massachusetts]

Core ID	Sample depth interval (cm)	Lab ID[a]	Conventional ^{14}C age (yr B.P.)[b]	$\partial^{13}C$	Calibrated calendric age (cal yr A.D.)[c]	Organic material used in analysis	Notes
r206	73–74	OS-72836	310 ± 30	-28.06	1487–1649	Peat	10 cm above sand layer
g033	51	OS-70762	140 ± 25	-27.01	1670–1953	Root or stem	Within sand layer
r031	36.5–38	OS-72815	185 ± 25	-28.96	1656–1952	Stem	Horizontal, below sand layer
g012	80–81	OS-72860	50 ± 35	-24.75	1692–1954	Fine root hairs	Within sand layer
r012	86	OS-72816	350 ± 30	-24.60	1458–1649	Peat	3 cm below sand layer
g015	44–45	OS-70675	175 ± 30	-25.55	1657–1952	Peat	10 cm above sand layer
g015	61–62	OS-70764	230± 30	-27.20	1532–1951	Peat	Within sand layer

[a]All analyses completed by the NOSAMS facility at Woods Hole Oceanographic Institute.

[b]Conventional lab-reported radiocarbon age with ± 1 sigma error.

[c]Calibrated calendric age range (± 2 sigma) in calibrated years A.D., calculated with the CALIB 6.0 program (http://calib.qub.ac.uk/calib/).

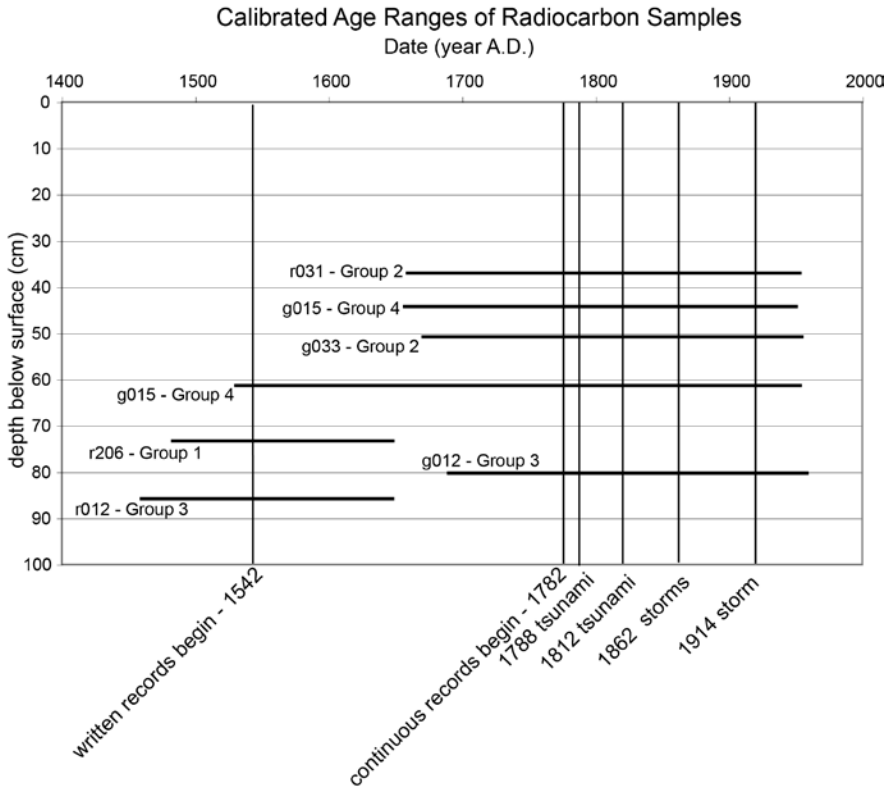

Figure 75. Radiocarbon age ranges for samples from cores representing each of the four core groups at Carpinteria Salt Marsh containing candidate tsunami deposits.

calibrated age range of A.D. 1487 to 1649. This suggests that the age of the candidate group 1 sand layer in core r206, 10 cm below the sampled peat layer, is older than A.D. 1649. However, if the bulk peat sample has an inbuilt age from incorporating older woody material, it could yield an age older than the underlying sand layer. Samples from two cores in group 2 are relatively consistent. In g033 a stem or root fragment within the sand layer was dated as A.D.1670 to modern, and in r031 a stem lying horizontally just below the sand layer was dated as A. D. 1656 to modern. This suggests that the age of the group 2 sand layer is A.D. 1670 or younger. Two samples were dated from group 3 cores. Bulk peat sampled from r012, 3 cm below the candidate sand layer, has a calibrated age of A.D.1458 to A.D.1649. Fine root hairs in core g012, taken directly from the candidate sand layer, yield an age range of A.D. 1692 to modern, suggesting that the deposit is younger than A.D.1692, although the roots may have penetrated the deposit a long time after deposition, giving a false young age. Two samples were taken from the group 4 core g015. A root or stem fragment taken from within the deposit has an age range of A.D.1532 to present and suggests that the deposit is younger than A.D. 1532. Peat sampled 10 cm above the candidate sand layer has an age range of A.D. 1657 to modern, consistent with this interpretation.

Our interpretation of these radiocarbon dates suggests that the sand layers in the four groups represent more than one event. The ages of the candidate tsunami deposit in two groups (groups 2 and 4) and possibly a third group (group 3, if a younger interpretation is used) may be consistent with deposition from the 1812 tsunami (fig. 75). However, the wide range of ages (~1700 to present) does not allow us to pinpoint the 1812 tsunami as the source for any of these sand layers. The age of one or more of these sand layers may also be consistent with the 1788 tsunami. However, there is no account of a significant tsunami in1788 in the records of the Presidio of Santa Barbara, which was established in 1782. Some of the deposits predate the historical record. The candidate layer in group 1 is older than the 1812 tsunami and may represent a prehistoric event. The candidate layer in group 3 may also represent a prehistoric event if an older interpretation is used for the sand layer. Portions of the age ranges from all of the groups predate the continuous historical record, and portions of the age ranges from core r206 (group 1), r012 (group 3) and g015 (group 4) predate the written record. It should be noted that age ranges of the candidate sand layers from groups 2, 4, and the younger interpretation for group 3, are also consistent with large storms that occurred in 1862 and 1914.

Deeper Sand Layers

Many cores penetrated deeper than 1 m, and a few cores penetrated below 2 m. Isolated sand layers were present at depth in some of these cores. For example, two long cores (C12-g04 and C12-H1) located in the northeast part of the marsh contain deeper sand layers (fig. 69). In core C12-g04 there is a sand layer with a sharp (but irregular) basal contact overlying peat at 185-cm depth. In core C12-H1, there is a sand layer overlying peat at 197-cm depth. The sand layers in these two cores likely correlate. A sand layer at this depth is not present in other nearby cores (for example, C12-g03 and C12-V02). However, vibracore C12-V02 contains two clean gray medium- to coarse-grained sand layers, at depths of 292–294 cm and 298–299 cm, separated by a layer of brown sand. They are overlain and underlain by brown sand deposits of likely nontsunami origin. The sand layer at 292–294 cm contains 1-cm scale mud clasts that could be rip-up clasts. Whether any of these deeper sand layers are of tsunami origin has not yet been determined. Several samples of charcoal, shells, and other organic material have been collected from these deeper cores for radiocarbon dating to determine if the ages correlate with other deeper sand layers in other parts of the marsh, but those analyses are not yet completed.

Conclusions

Identification of the candidate sand layers as tsunami deposits in Carpinteria Salt Marsh is still not certain. Sedimentary evidence from deposits within the uppermost meter indicates that sand layers found in four spatially isolated groups of cores were deposited from high-speed turbulent flows,

consistent with deposition by a tsunami. Candidate tsunamis include the 1812 Santa Barbara tsunami and a 1788 Aleutian Islands tsunami. The location has also been impacted by large storms in the past, particularly in 1862 and in 1914. Results of the microfossil analyses provide no evidence to support tsunami transport, and instead suggest flood deposits for the groups 1 and 2 cores, and intertidal deposits for groups 3 and 4. In addition, the thickness of sand layers in some cores is consistent with that found in small to medium-size channels. Deeper anomalous sand layers are present at Carpinteria as well, but their origin has not yet been determined. Further work remains to be done to determine the origin of the candidate sand layers and to constrain their age. Also, more work needs to be done to determine the origin and age of sand layers deeper in the cores.

Preliminary Results and Ongoing Work

This project is the most comprehensive tsunami-deposit field program ever completed for the 1,100-km length of California's coast. Twenty coastal wetland sites have been evaluated for the likelihood of containing tsunami deposits. Detailed analyses were performed for a number of sites showing the highest potential for historical and prehistoric tsunami deposits. Although the fieldwork and sampling portion of the project has been completed, not all laboratory results have been obtained and evaluated to date (May 18, 2013). With the data available at this time, the project collaborators draw the following preliminary findings from this work:

1. Although historical records in California are not extensive, the tsunami information collected over the past 70 years is a helpful resource for determining the impacts from distant-source tsunamis. Additional detailed analysis of these historical records would better define the potential impacts from future tsunamis.
2. Numerical modeling results from distant-source tsunami scenarios are useful to determine where tsunami deposits could exist. Tsunami deposits from distant events are more likely to be found in central and northern California based on larger modeled tsunami runups in those regions.
3. Because of typically smaller tsunami size and lack of coincident seismic subsidence, deposits from distant-source tsunamis are less likely to form, be preserved, or be identified than deposits from local source events.
4. The evidence from the evaluation, thus far, does not identify a distance-source tsunami similar in size to the AASZ III scenario tsunami statewide. However, other qualifying facts must be considered before concluding that such an event could not exist: (A) The findings of this evaluation are not yet complete. Additional sediment and age-dating analyses may provide more detailed information about the potential for other, larger Aleutian-Alaska source tsunamis. (B) Project team members could not core more than 1–2 m deep at many locations. For this reason, we were limited to making observations about a relatively brief paleo-record. (C) Because tsunami sediments in nonsubsiding marshlands are less likely to be preserved, the absence of evidence for past tsunamis does not preclude the potential that large, inundating distant-source tsunamis have occurred in California.
5. Site evaluations indicate that the potential for discovering tsunami deposits related to distant-source tsunamis is relatively low in southern California and the area of the Ports of Los Angeles and Long Beach compared to other parts of the state. Modeled tsunami heights there are relatively low (2–4 m), and most coastal wetlands have been disturbed by human activity. Reconnaissance work at Seal Beach Marsh south of the ports yielded no evidence for continuous or semi-continuous sand layers.
6. Evidence supports the inference that sand deposits from the 1946 and 1964 tsunamis were observed in Pillar Point and Crescent City marshes, respectively. This demonstrates that large

distant-source tsunamis originating from the Alaska-Aleutian Island region can result in tsunami deposits in California's coastal marshes. Detailed studies of these known tsunami deposits can be used to help identify similar deposits from distant-source tsunamis in the geological record.

7. Thus far, evidence is equivocal on whether the semi-continuous sand layer identified in the Carpinteria Salt Marsh has a tsunami origin. Although grain-size analysis indicates the deposit is consistent with tsunami-generated sands, microfossil evidence is inconsistent with tsunami deposits and instead supports deposition of the sand in a low-energy environment or deposition by flood.
8. Semi-continuous sand deposits similar to the known tsunami deposits were observed: (1) between the 1946 sand layer and the last San Gregorio Fault event (300 to 500 years before present; Koehler and others, 2004) in the Pillar Point Marsh; (2) between the 1964 sand the 1700 deposit in the Crescent City marshes; and (3) between sediments from the late 1600s and the present in Carpinteria Salt Marsh. Results of pending laboratory analyses could help determine if these deposits are potential tsunami deposits and of an age similar to known tsunamis, such as the 1788 event.
9. Although age-dating techniques like 210Pb and 137Cs are helpful for determining sediment ages from 0–100 years ago, and the 14C technique is useful for ages greater than 500 years ago, there is an age-dating "gap" between these time periods. This gap limits the success of determining the exact age of potential tsunami sands deposited by, for example, the 1788 event. Sedimentation rate calculations may be the only way to infer that a tsunami deposit representing the 1788 event, or other events, exists. Additional tools that could benefit the age-dating analyses include pollen analysis and optical stimulated luminescence (OSL) dating of sand units.
10. The absence of evidence for apparent tsunami deposits at many of the reconnaissance sites does not preclude the potential for those sites to contain evidence of past tsunamis. A more detailed evaluation of fine-grained layers in sediment cores may provide additional evidence of tsunami erosion or deposition.

All the data collected for this project will be added to the California Geological Survey tsunami deposit database to help form the background for future work. Project collaborators will evaluate additional laboratory results from the samples and data collected and develop more comprehensive conclusions. These additional test results include grain-size, microfossil, x-ray, and age-dating analyses. We hope to present these future findings in a more comprehensive report containing field data for all sites studied and identifying future work needs.

References

Abramson, H., 1998, Evidence for tsunami and earthquakes during the last 3500 years from Lagoon Creek, a coastal freshwater marsh, northern California: Arcata, Calif., Humboldt State University, Master's thesis, 75 p.

Adam, D.P., and Mahood, A.D., 1981, Chrysophyte cysts as potential environmental indicators: Geological Society of America Bulletin, v. 92, p. 839–844.

Admire, A.R., Dengler, L.A., Crawford, G.B., Uslu, B.U., and Montoya, J., 2012, Observed and modeled tsunami current velocities in Humboldt Bay and Crescent City Harbor, northern California: American Geophysical Union, Annual Fall Meeting, Poster presentation, available at http://fallmeeting.agu.org/2012/files/2012/12/AGU_2012_eposter.pdf.

Atwater, B.F., Cisternas V.M., Bourgeois, J., Dudley, W.C., Hendley, J.W. II, and Stauffer, P.H., 1999, Surviving a tsunami-Lessons from Chile, Hawaii, and Japan: U.S. Geological Survey Circular 1187, 18 p.

Atwater, B.F., Musumi-Rokkaku, S., Satake, K., Tsuji, Y., Ueda, K., and Yamaguchi, D.K., 2005, The orphan tsunami of 1700: U.S. Geological Survey Professional Paper 1707, 133 p.

Baher, S., Fuis, G., Sliter, R., and Normark, W.R., 2005, Upper-crustal structure of the inner continental borderland near Long Beach, California: Bulletin of the Seismological Society of America, v. 95, no. 5, p. 1957–1969.

Barberopoulou, A., Borrero, J.C., Uslu, B., Kalligeris, N., Goltz, J.D., Wilson, R.I., and Synolakis, C.E., 2009, Unprecedented coverage of the Californian coast promises improved tsunami response: Eos (American Geophysical Union Transactions), v. 90, no. 16, p. 137–138.

Barnard, P.L., Revell, D.L., Hoover, D., Warrick, J., Brocatus, J., Draut, A.E., Dartnell, P., Elias, E., Mustain, N., Hart, P.E., and Ryan, H.F., 2009, Coastal processes study of Santa Barbara and Ventura Counties, California: U.S. Geological Survey Open-File Report 2009–1029, 904 p., available at http://pubs.usgs.gov/of/2009/1029/.

Bascom, W., 1946, Effect of seismic sea wave on California Coast: University of California Berkeley, Department of Engineering, Fluid Mechanics Laboratory, Navy Department Bureau of Ships Contract NObs 2490, Laboratory Memorandum HE–116–204, 23 p.

Berquist, J.R., 1978, Depositional history and fault-related studies, Bolinas Lagoon, California: U.S. Geological Survey Open-File Report 78–802, 164 p.

Bourgeois, J., 2009, Geologic effects and records of tsunamis, *in* Bernard, E.N., and Robinson, A.L., eds., Tsunamis: Cambridge, Mass., Harvard University Press, The sea, v. 15, p. 55–91.

Brabb, E.E., 1980, Preliminary Geologic Map of the La Honda and Half Moon Bay Quadrangles, San Mateo County, California: U.S. Geological Survey Open-File Report 1980-0245, scale 1:24,000.

Brabb, E.E., Graymer, R.W., and Jones, D.L., 1998, Geology of the Onshore Part of San Mateo County, California: A Digital Database: U.S. Geological Survey Open-File Report 98–137, scale 1:62,500

Brownlie, W.R., and Taylor, B.D., 1981, Sediment management for Southern California mountains, coastal plains and shoreline—Part C, Coastal sediment delivery by major rivers in southern California: Pasadena, California Institute of Technology, Environmental Quality Lab., Technical Report 17–C, 314 p.

Bryant, W.A., 1988, Recently active traces of the Newport-Inglewood fault zone, Los Angeles and Orange Counties, California: California Department of Conservation, Division of Mines & Geology Open-File Report 88–14, 15 p., scale 1:24,000.

Byrne, R., Reidy, L., Kirby, M., Arthur, A., Watson, B., Schmidt, D., Krause, J., Sullivan, J., Borkowski, J., Yiu, A., and Menchaca, A., 2006, Recent (1850–2005) and Late Holocene (AD 400–

AD 1850) sedimentation rates at Bolinas Lagoon, Marin County, California: Marin County Parks, Open Space District, Final Report, 36 p.
California Seismic Safety Commission, 2005, The tsunami threat to California: Ad Hoc Committee on Tsunami Safety, CSSC 05-03, 24 p.
Callaway, J.C., Borgnis, E.L., Turner, R.E., and Milan, C.S., 2012, Carbon sequestration and sediment accretion in San Francisco Bay tidal wetlands: Estuaries and Coasts, v. 35, no. 5, p. 1163–1181, doi:10.1007/s12237-012-9508-9.
Casagrande, J., 2006, Wetland habitat types of the Carmel River Lagoon: California State University Monterey Bay, The Watershed Institute, Report No. WI–2006–05, 15 p.
Casagrande, J., and Watson, F., 2003, Hydrology and water quality of the Carmel and Salinas Lagoons, Monterey Bay, California 2002/2003: California State University Monterey Bay, The Watershed Institute, Report No. WI–2003–14, 118 p., Available at http://science.csumb.edu/~ccows/pubs/reports/CCoWS_LagoonBreaching2002-2003_030630.pdf.
Central Coast Regional Water Quality Control Board, 2002, Morro Bay total maximum daily load for sediment, including Chorro Creek, Los Osos Creek, and the Morro Bay Estuary: State of California, Central Coast Regional Water Quality Control Board, 83 p.
Chagué-Goff, C., Schneider, J.-L., Goff, J.R., Dominey-Howes, D. & Strotz, L., 2011. Expanding the proxy toolkit to help identify past events: Lessons from the 2004 Indian Ocean Tsunami and the 2009 South Pacific Tsunami. Earth-Science Reviews 107, 107-122.
Chagué-Goff, C., Dawson, S., Goff, J.R., Zachariasen, J., Berryman, K.R., Garnett, D.L., Waldron, H.M., and Mildenhall, D.C., 2002, A tsunami, ca. 6300 years BP, and other Holocene environmental changes, northern Hawke's Bay, New Zealand: Sedimentary Geology, v. 150, p. 89–102.
Chagué-Goff, C., Schneider, J.-L., Goff, J.R., Dominey-Howes, D., and Strotz, L., 2011, Expanding the proxy toolkit to help identify past events—Lessons from the 2004 Indian Ocean tsunami and the 2009 South Pacific tsunami: Earth-Science Reviews, v. 107, p. 107–122.
Chagué-Goff, C., Goff, J., Nichol, S.L., Dudley, W., Zawadzki, A., Bennett, J.W., Mooney, S.D., Fierro, D., Heijnis, H., Dominey-Howes, D., and Courtney, C., 2012, Multi-proxy evidence for trans-Pacific tsunamis in the Hawai'ian Islands: Marine Geology, v. 299–302, p. 77–89, doi:10.1016/j.margeo.2011.12.010.
Choowong, M., Murakoshi, N., Hisada, K., Charusiri, P., Charoentitirat, T., Chutakositkanon, V., Jankaew, K., Kanjanapayont, P., and Phantuwongraj, S., 2008, 2004 Indian Ocean tsunami inflow and outflow at Phuket, Thailand: Marine Geology, v. 248, p. 179–192.
Clague, J.J., Bobrowsky, P.T., and Hamilton, T.S., 1994, A sand sheet deposited by the 1964 Alaska tsunami at Port Alberni, British Columbia: Estuarine, Coastal and Shelf Science, v. 38, p. 413–421.
Clark, A.M., 1962, From grove to cove—A brief history of Carpinteria Valley, California: A.M. Clark, 93 p.
Clark, J.C., and Brabb, E.E., 1997, Geology of the Point Reyes National Seashore and vicinity, Marin County, California: U.S. Geological Survey Open-File Report 97–456, available at http://pubs.usgs.gov/of/1997/of97-456/.
Cole K.L., and Wahl, E., 2000, A late Holocene paleoecological record from Torrey Pines State Reserve, California: Quaternary Research, v. 53, p. 341–351.
Cupp, E., 1943, Marine plankton diatoms of the west coast of North America: Bulletin of the Scripps Institute of Oceanography, Technical Series, v. 5, no. 1, 238 p.
Dawson, A.G., and Shi, S., 2000, Tsunami deposits: Pure and Applied Geophysics, v. 157, p. 875-897.
Dawson, A.G., Shi, S., Dawson, S., Takahashi, T., and Shuto, N., 1996a, Coastal sedimentation associated with the June 2nd and 3rd, 1994 tsunami in Rajegwesi, Java: Quaternary Science Reviews, v. 15, p. 901–912.

Dawson, S., 2007, Diatom biostratigraphy of tsunami deposits—Examples from the 1998 Papua New Guinea tsunami: Sedimentary Geology, v. 200, p. 328–335.
Dawson, S., and Smith, D.E., 2001, The sedimentology of mid-Holocene tsunami facies in northern Scotland: Marine Geology, v. 170, p. 69–79.
Dawson, S., Smith, D.E., Ruffman, A., and Shi, S., 1996b, The diatom biostratigraphy of tsunami sediments—Examples from recent and middle Holocene events: Physics and Chemistry of the Earth, v. 21, no. 12, p. 87–92.
Dengler, L.A., and Magoon, O., 2005, The 1964 tsunami in Crescent City, California—A 40-year retrospective: American Society of Civil Engineers, Solutions to Coastal Disasters, Proceedings, p. 639–648.
Dengler, L., Uslu, B., Barberopoulou, A., Borrero, J., and Synolakis, C., 2008, The vulnerability of Crescent City, California to tsunamis generated by earthquakes in the Kuril Islands region of the northwestern Pacific: Seismological Research Letters, v. 79, no. 5, p. 608–619.
Dominey-Howes, D.T.M., Dawson, A.G., and Smith, D.E., 1998, Late Holocene coastal tectonics at Falasarna Harbour, western Crete, Greece—A sedimentary contribution, *in* Stewart, I., and Vita-Finzi, C., eds., Coastal tectonics: London, Geological Society Special Publication, v. 146, p. 341–350.
Donnelly, J.P., Bryant, S.S., Butler, J., Dowling, J., Fan, L., Hausmann, N., Newby, P., Shuman, B., Stern, J., Westover, K., and Web, T., 2001. 700 yr sedimentary record of intense hurricane landfalls in southern New England. Geological Society of America Bulletin, v. 113, p. 714-727.
Ferren, W.R., Jr., Page, H.M., and Saley, P., 1997, Management plan for Carpinteria Salt Marsh Reserve—A southern California estuary: University of California, Santa Barbara, Museum of Systematics and Ecology, Environmental Report no. 5.
Forney, S., 1883–84, Coast of California, Moro [sic] Bay to Toro Point, California [map]: National Oceanographic and Atmospheric Adminisjtration (NOAA), Office of Coast Survey, Topographic Register Number T1662, scale 1:10,000, available from NOAA's Historical Map and Chart Collection at http://historicalcharts.noaa.gov/historicals/preview/image/T01662-00-1883.
Forrestel, A.B., Moritz, M.A., and Stephens, S.L., 2011, Landscape-scale vegetation change following fire in Point Reyes, California, USA: Fire Ecology, v. 7, no. 2, p. 114–128.
Fritz, H.M., Borrero, J.C., Synolakis, C.E., and Yoo, J., 2006, 2004 Indian Ocean tsunami flow velocity measurements from survivor videos: Geophysical Research Letters, v. 33, L24605, doi:10.1029/2006GL026784.
Fryer, G.J., Watts, P., and Pratson, L.F., 2004, Source of the great tsunami of 1 April 1946—A landslide in the upper Aleutian forearc: Marine Geology, v. 203, p. 201–218.
Fujino, S., Naruse, H., Matsumoto, D., Sakakura, N., Suphawajruksakul, A., and Jarupongsakul, T., 2010, Detailed measurements of thickness and grain size of a widespread onshore tsunami deposit in Phang-nga Province, southwestern Thailand: Island Arc, v. 19, no. 3, p. 389–398.
Galloway, A.J., 1977, Geology of the Point Reyes peninsula, Marin County, California: Sacramento, California Division of Mines and Geology, Bulletin, v. 202, 72 p., map scale 1:48,000.
Garrison-Laney, C.E., 1998, Diatom evidence for tsunami inundation from Lagoon Creek, a coastal freshwater pond, Del Norte County, California: Arcata, Calif., Humboldt State University, Masters thesis, 97 p.
Gelfenbaum, G., and Jaffe, B.E., 2003, Erosion and sedimentation from the 17 July 1998 Papua New Guinea tsunami: Pure and Applied Geophysics, v. 60, p. 1969–1999.
Gillespie, A., Schaffner, A., Watson, E., and Callaway, J., 2011, Morro Bay sediment loading update: Morro Bay National Estuary Program, 48 p.
Goff, J., McFadgen, B.G., and Chagué-Goff, C., 2004, Sedimentary differences between the 2002 Easter storm and the 15th-century Okoropunga tsunami, southeastern North Island, New Zealand: Marine Geology, v. 204, p. 235–250.

Goff, J., Chagué-Goff, C., Nichol, S., Jaffe, B.E., and Dominey-Howes, D., 2012, Progress in paleotsunami research: Sedimentary Geology, v. 243–244, p. 70–88, doi:10.1016/j.sedgeo.2011.11.002.

González, F.I., Geist, E.L., Jaffe, B., Kanoglu, U., Mofjeld, H., Synolakis, C.E., Titov, V.V., Arcas, D., Bellomo, D., Carlton, D., Horning, T., Johnson, J., Newman, J., Parsons, T., Peters, R., Peterson, C., Priest, G., Venturato, A., Weber, J., Wong, F., and Yalciner, A., 2009, Probabilistic tsunami hazard assessment at Seaside, Oregon, for near- and far-field seismic sources: Journal of Geophysical Research, v. 114, C11023, doi:10.1029/2008JC005132.

Greene, H.G., Murai, L.Y., Watts, P., Maher, N.A., Fisher, M.A., Paull, C.E., and Eichhubl, P., 2006, Submarine landslides in the Santa Barbara Channel as potential tsunami sources: Natural Hazards and Earth System Sciences, v. 6, p. 63–88.

Greenwell, W.E., and Forney, S., 1869a, Map of part of the coast of California, Santa Barbara channel, from Sand Point to Point Gorda: Washington D.C., U.S. Coast Survey, Topographic Register Number T1127 [map], scale 1:34,000, available from National Ocean Service, Silver Spring, Md.

Greenwell, W.E., and Forney, S., 1869b, Map of part of the coast of California, Santa Barbara channel, from Santa Barbara to Sand Point: Washington D.C., U.S. Coast Survey, Topographic Register Number T1128 [map], scale 1:34,000, available from National Ocean Service, Silver Spring, Md.

Grossinger, R.M., Stein E.D., Cayce K., Dark, S., Askevold, R., and Whipple, A., 2011, Historical wetlands of the southern California coast—An atlas of U.S. coast survey t-sheets, 1851–1889: San Francisco Estuary Institute, available at http://www.sfei.org/projects/SoCalTSheets.

Haltiner, J., 1988, Sedimentation processes in Morro Bay, California: San Francisco, Calif., Philip Williams and Associates Report 437, 94 p.

Hawkes, A.D., Bird, M., Cowie, S., Grundy-Warr, C., Horton, B.P., Hwai, A.T.S., Law, L., Macgregor, C., Nott, J., Ong, J.E., Rigg, J., Robinson, R., Tan-Mullins, M., Sa, T.T., Yasin, Z., and Aik, L.W., 2007, Sediments deposited by the 2004 Indian Ocean tsunami along the Malaysia–Thailand Peninsula: Marine Geology, v. 242, p. 169–190.

Hayes, S.A., Bond, M.H., Hanson, C.V., Freund, E.V., Smith, J.J., Anderson, E.C., Ammann, A.J., and MacFarlane, R.B., 2008, Steelhead growth in a small central California watershed—Upstream and estuarine rearing patterns: Transactions of the American Fisheries Society, v. 137, p. 114–128.

Hemphill-Haley, E., 1993a, Distribution and taxonomy of late Quaternary diatoms from gravity cores L13-81-G117, L13-81-G138, L13-81-G145, and TT197-G330, northern California continental slope: U.S. Geological Survey Open-File Report 93-340, 108 p.

Hemphill-Haley, E., 1993b, Occurrences of recent and Holocene intertidal diatoms, *Bacillariophyta* in northern Willapa Bay, Washington: U.S. Geological Survey Open-File Report 93-284, 94 p.

Hemphill-Haley, E., 1993c, Taxonomy of recent and fossil, Holocene, diatoms, *Bacillariophyta*, from northern Willapa Bay, Washington: U.S. Geological Survey Open-File Report 93-289, 151 p.

Hemphill-Haley, E., 1995, Diatom evidence for earthquake-induced subsidence and tsunami 300 years ago in southern coastal Washington: Geological Society of America Bulletin, v. 107, no. 3, p. 367–378.

Hemphill-Haley, E., 1996, Diatoms as an aid in identifying late Holocene tsunami deposits: The Holocene, v. 6, no. 4, p. 439–448.

Hemphill-Haley, E., 2006, Diatoms, *Bacillariophyta*, from salt marshes and intertidal flats of Tomales Bay, California: A report to the National Park Service, Tomales Bay Biodiversity Inventory [TBBI], 30 p., 17 plates.

Hemphill-Haley, E., and Fourtanier, E., 1995, A diatom record spanning 114,000 years from Site 893, Santa Barbara Basin: Proceedings of the ocean drilling program, Scientific Results, v. 146, pt. 2, p. 233–249.

Hemphill-Haley, E., Graehl, N., Jaffe, B., Kelsey, H., Leeper, R., Peters, R., and Wilson, R., 2011, Evaluation of potential paleotsunami deposits along the California coast to determine the tsunami threat from distant sources [abs.]: American Geophysical Union Fall Meeting, Abstract NH21C-1524, available at http://eposters.agu.org/epostersearch/?search=1&search1=1&posters=1&final_id=NH21C-1524&x=20&y=16.

Hill, M.R., 1970, Barrier beach: California Geology, v. 23, no. 12, p. 231–233.

Hoirup, D.F., 2006, Suspect tsunami deposits, Point Reyes National Seashore, California [abs.]: American Geophysical Union Fall Meeting, Abstract PP43B-1243.

Hori, K., Kuzumoto, R., Hirouchi, D., Umitsu, M., Janjirawuttikul, N., and Patanakanog, B., 2007, Horizontal and vertical variation of 2004 Indian tsunami deposits—An example of two transects along the western coast of Thailand: Marine Geology, v. 239, p. 163–172.

Ingle, J.C., Jr., 1980, Cenozoic paleobathymetry and depositional history of selected sequences within the southern California continental borderland: Cushman Foundation for Foraminiferal Research, Special Publication no. 19, p. 161–195.

Inman, D.L., and Jenkins, S.A., 1999, Climate change and the episodicity of sediment flux of small California rivers: Journal of Geology, v. 107, no. 3, p. 251–270.

Jaffe, B.E., and Gelfenbaum, G., 2007, A simple model for calculating tsunami flow speed from tsunami deposits: Sedimentary Geology, v. 200, p. 347–361, doi:10.1016/j.sedgeo.2007.01.013.

Jaffe, B., Gelfenbaum, G., Rubin, D., Peters, R., Anima, R., Swensson, M., Olcese, D., Bernales, L., Gomez, J., and Riega, P., 2003, Tsunami deposits—Identification and interpretation of tsunami deposits from the June 23, 2001 Peru tsunami, *in* Proceedings of the International Conference on Coastal Sediments 2003: Corpus Christi, Texas, World Scientific Publishing Corp and East Meets West Productions, CD-ROM, ISBN 981-238-422-7, 13 p.

Jaffe, B.E., Borrero, J.C., Prasetya, G.S., Dengler, L., Gelfenbaum, G., Hidayat, R., Higman, B., Kingsley, E. Lukiyanto, M.B., Moore, A., Morton, R., Peters, R., Ruggiero, P., Titov, V., Kongko, W., and Yulianto, E., 2006, The December 26, 2004 Indian Ocean tsunami in northwest Sumatra and offshore islands: Earthquake Spectra, v. 22, no. S3, p. S105–S136.

Jaffe, B.E., Buckley, M.L., Richmond, B.M., Strotz, L., Etienne, S., Clark, K., and Gelfenbaum, G., 2011, Flow speed estimated by inverse modeling of sandy sediment deposited by the 29 September 2009 tsunami near Satitoa, east Upolu, Samoa: Earth-Science Reviews, v. 107, p. 23–37, doi:10.1016/j.earscirev.2011.03.009.

Jaffe, B.E., Goto, K., Sugawara, D., Richmond, B.M., Fujino, S., and Nishimura, Y., 2012, Flow speed estimated by inverse modeling of sandy tsunami deposits—Results from the 11 March 2011 tsunami on the coastal plain near the Sendai Airport, Honshu, Japan: Sedimentary Geology, v. 282, p. 90–109, doi:10.1016/j.sedgeo.2012.09.002.

Jagodziński, R., Sternal, B., Szczuciński, W., Chagué-Goff, C., and Sugawara, D., 2012, Heavy minerals in the 2011 Tohoku-oki tsunami deposits—Insights into sediment sources and hydrodynamics: Sedimentary Geology, v. 282, p. 57–64.

Jennings, A.E., and Nelson, A.R., 1992, Foraminiferal assemblage zones in Oregon tidal marshes—Relation to marsh floral zones and sea level: Journal of Foraminiferal Research, v. 22, p. 13–29.

Kennedy, M.P., and Peterson, G.L., 1975, Geology of the San Diego metropolitan area, California: California Division of Mines and Geology Bulletin 200, 56 p.

Kennett, J.P., Rozo-Vera, G.A., and Machain Castillo, M.L., 2000, Latest Neogene planktonic foraminiferal biostratigraphy of the California margin, *in* Lyle, M., Koizumi, I., Richter, C., and Moore, T.C., Jr., eds., California margin: Proceedings of the ocean drilling program, Scientific Results, v. 167, p. 41–62.

Knudsen, K.L., Witter, R.C., Garrison-Laney, C.E., Baldwin, J.N., and Carver, G.C., 2002, Past earthquake-induced rapid subsidence along the northern San Andreas fault—A paleoseismological method for investigating strike-slip faults: Bulletin of the Seismological Society of America, v. 92, no. 7, p. 2612–2636.

Koehler, R.D., Simpson, G.D., Witter, R.C., Hemphill-Haley, E., and Lettis, W.R., 2004, Paleoseismic investigation of the Northern San Gregorio Fault at Pillar Point Marsh near Half Moon Bay, California: U.S. Geological Survey National Earthquake Hazards Reduction Program, Award 02HQGR0071, Final Technical Report.

Koehler, R., Witter, R., Simpson, G., Hemphill-Haley, E. and Lettis, W., 2005, Paleoseismic investigation of the northern San Gregorio fault, Half Moon Bay, California: U.S. Geological Survey, National Earthquake Hazards Reduction Program, Award 04HQGR0045, Final Technical Report.

Kortekaas, S.S., and Dawson, A.G., 2007, Distinguishing tsunami and storm deposits—An example from Martinhal, SW Portugal: Sedimentary Geology, v. 200, p. 209–222.

Kowalik, Z., Horrillo, J., Knight, W., and Logan, T., 2008, Kuril Islands tsunami of November 2006—1. Impact at Crescent City by distant scattering: Journal of Geophysical Research, v. 113, 11 p.

Kuenen, P.H., Menard, H.W., 1952, Turbidity currents, graded and non-graded deposits: Journal of Sedimentary Petrolology, v. 22, p. 83–96.

Lander, J.F., and Lockridge, P.A., 1989, United States tsunamis, Including United States Possessions, 1690–1988: Boulder, Colo., National Oceanic and Atmospheric Administration, National Geophysical Data Center, Publication 41-2, 265 p.

Lander, J., Lockridge, P.A., and Kozuch, J., 1993, Tsunamis affecting the west coast of the United States 1806–1992: Boulder, Colo., National Oceanic and Atmospheric Administration, National Geophysical Data Center, Key to Geophysical Research Documentation No. 29, v. 29, 242 p.

Lankford, R.R., and Phleger, F.B., 1973, Foraminifera from the nearshore turbulent zone, western North America: Journal of Foraminiferal Research, v. 3, p. 101–132.

Larson, J., Watson, F., Masek, J., Watts, M., and Casagrande, J., 2005, Carmel River lagoon enhancement project—water quality and aquatic wildlife monitoring, 2004–05: California State University Monterey Bay, The Watershed Institute, prepared for the California Department of Parks and Recreation, no. WI-2005-12, 130 p.

Lawson, A.C., (chairman), 1908 [reprint 1969], The California earthquake of April 18, 1906—Report of the State earthquake investigation commission: Washington, D.C., Carnegie Institution of Washington Publication, 451 p.

Leeper, R., Graehl, N., Hemphill-Haley, E., Hoirup, D., Jaffe, B., Kelsey, H., Peters, R., and Wilson, R., 2011, Probing California's coastline to unearth traces of paleotsunamis—Implications for the next USGS multi-hazards scenario: Southern California Earthquake Center Annual Meeting, September 11–14, Palm Springs, poster B-086.

Loeblich, R., Jr., and Tappan, H., 1964, Sarcodina chiefly "thecamoebians" and *foraminiferida*, *in* Moore, R.C., ed., Treatise on invertebrate paleontology, Part C, Protista 2, v. 1–2: Geological Society of America and University of Kansas Press, p. C1–C900.

López, A.M., and Okal, E.A., 2006, A seismological reassessment of the source of the 1946 Aleutian "tsunami" earthquake: Geophysical Journal International, v. 165, p. 835–849.

Ludwin, R., Dennis, R., Carver, D., McMillan, A., Losey, R., Clague, J., Jonientz-Trisler, C., Bowechop, J., Wray, J., and James, K., 2005, Dating the 1700 Cascadia earthquake—Great coastal earthquakes in native stories: Seismological Research Letters, v. 76, no. 2, p. 140–148.

Magoon, O.T., 1966, Structural damage by tsunamis, *in* Coastal engineering Santa Barbara specialty conference October 1965: New York, American Society of Civil Engineers, p. 35–68.

McCulloch, D.S., 1985, Evaluating tsunami potential, *in* Zoiny, J., Evaluating earthquake hazards in the Los Angeles region—An earth science perspective: U.S. Geological Survey Professional Paper 1360, p. 375–413.

McGann, M., 2009, Review of impacts of contaminated sediment on microfaunal communities in the southern California bight, *in* Lee, H., and Normark, W.R., eds., Earth science in the urban ocean—The southern California continental borderland: Geological Society of America Special Paper 454, p. 413–455.

Middleton, G.V., 1967, Experiments on density of turbidity currents III—Deposition of sediment: Canadian Journal of Earth Sciences, v. 4, p. 475–503.

Minor, S.A., Kellogg, K.S., Stanley, R.G., Gurrola, L.D., Keller, E.A., and Brandt, T.R., 2009, Geologic map of the Santa Barbara coastal plain area, Santa Barbara County, California: U.S. Geological Survey Scientific Investigations Map 3001, scale 1:25,000, 1 sheet, pamphlet, 38 p.

Minoura, K., Imamura, F., Takahashi, T., and Shuto, N., 1997, Sequence of sedimentation processes caused by the 1992 Flores tsunami—Evidence from Babi Island: Geology, v. 25, p. 523–526.

Moore, A., Nishimura, Y., Gelfenbaum, G., Takanobu, K., and Triyono, R., 2006, Sedimentary deposits of the 26 December 2004 tsunami on the northwest coast of Aceh, Indonesia: Earth Planets Space, v. 58, p. 253–258.

Moore, A.L., McAdoo, B.G., and Ruffman, A., 2007. Landward fining from multiple sources in a sand sheet deposited by the 1929 Grand Banks tsunami, Newfoundland: Sedimentary Geology, 200 (3-4), 336-346.

Morton, R.A., Gelfenbaum, G., and Jaffe, B.E., 2007, Physical criteria for distinguishing sandy tsunami and storm deposits using modern examples: Sedimentary Geology, v. 200, p. 184–207, doi:10.1016/j.sedgeo.2007.01.003.

Morton, R.A., Gelfenbaum, G., Buckley, M.L., and Richmond, B.M., 2011, Geological effects and implications of the 2010 tsunami along the central coast of Chile: Sedimentary Geology, v. 242, p. 34–51.

Monterey Peninsula Water Management District, 2013, Planning documents for Carmel River Beach and Lagoon: accessed April 2013 at http://www.mpwmd.dst.ca.us/mbay_irwm/irwm_library/LCR/LCRproject.pdf [and] http://www.mpwmd.dst.ca.us/Mbay_IRWM/IRWM_library/CarmelBay/LongTermStudyPlanFinal2007-04-17.pdf.

Mulholland, S.C., and Rapp, G., Jr, 1992, A morphological classification of grass silica-bodies, *in* Rapp, G., Jr, and Mulholland, S.C., eds., Phytolith systematics: New York and London, Plenum Press, Advances in Archaeological and Museum Science, v. 1: p. 65–89.

Nanayama, F., Shigeno, K., Satake, K., Shimokaka, K., Koitabashi, S., Miyasaka, S., and Ishii, M., 2000. Sedimentary differences between the 1993 Hokkaido-nansei-oki tsunami and the 1959 Miyakojima typhoon at Taisei, southwestern Hokkaido, northern Japan: Sedimentary Geology, v. 135, p. 255-264.

National Geophysical Data Center, 2013, Global historical tsunami database: Boulder, Colo., National Oceanic and Atmospheric Administration, National Geophysical Data Center, World Data Service (NGDC/WDS).

Nelson, A.R., Briggs, R.W., Engelhart, S.E., Gelfenbaum, G., Dura, T., Bradley, L., and Vane, C.H., 2012, Holocene tsunami recurrence along the eastern Aleutian-Alaskan megathrust, Chirikof Island, Alaska [abs.]: Geological Society of America Annual Meeting, Charlotte, N.C., Paper 119–8.

Nelson. A.R., Shennan, I., and Long, A.J., 1996. Identifying coseismic subsidence in tidal-wetland stratigraphic sequences at the Cascadia subduction zone of Western North America. Journal of Geophysical Research, v. 101, n. B3, p. 6115-6135.

Nyman, J.A., Crozier, C.R., and Delaune, R.D., 1995, Roles and patterns of hurricane sedimentation in an etuarine marsh landscape: Estuarine, Coastal and Shelf Science, v. 40, p. 665–679.
Patterson, R.T., 1990, Intertidal benthic foraminiferal biofacies on the Fraser River Delta, British Columbia—Modern distribution and paleoecological importance: Micropaleontology, v. 36, p. 229–244.
Patton, J.R., 2004, Late Holocene coseismic subsidence and coincident tsunamis, southern Cascadia subduction zone, Hookton Slough, Wigi [Humboldt Bay], California: Arcata, Calif., Humboldt State University, Masters thesis, 84 p.
Peters, R., and Jaffe, B.E., 2010a, Identification of tsunami deposits in the geologic record—Developing criteria using recent tsunami deposits: U.S. Geological Survey Open-File Report 2010-1239, 39 p., http://pubs.usgs.gov/of/2010/1239/.
Peters, R., and Jaffe, B.E., 2010b, Database of recent tsunami deposits: U.S. Geological Survey Open-File Report 2010-1172, 12 p. and database, http://pubs.usgs.gov/of/2010/1172/.
Peters, R., Jaffe, B.E., Gelfenbaum, G., and Peterson, C.D., 2003, Cascadia tsunami deposit database: U.S. Geological Survey Open-File Report 03-13, 24 p.
Peters, R., Jaffe, B.E., and Gelfenbaum, G., 2007, Distribution and sedimentary characteristics of tsunami deposits along the Cascadia margin of western North America: Sedimentary Geology, v. 200, p. 372–386, doi:10.1016/j.sedgeo.2007.01.015.
Peters, R., Jaffe, B.E., Buckley, M., and Watt, S.G., 2008, Candidate tsunami deposits at Carpinteria Salt Marsh, Southern California [abs.]: American Geophysical Union, Fall Meeting 2008, abstract OS53A-1292.

Petersen, M.D., Bryant, W.A., Cramer, C.H., Cao, T., Reichle, M.S., Frankel, A.D., Lienkaemper, J.J., McCrory, P.A., and Schwartz, D.P., 1996, Probabilistic seismic hazard assessment for the State of California: Division of Mines and Geology Open-File Report 96-08 and U.S. Geological Survey Open-File Report 96-706, 64 p., http://pubs.er.usgs.gov/pubs/ofr/ofr96706.
Peterson, C.D., Carver, G.A., Cruikshank, K.M., Abramson, H.F., Garrison-Laney, C.E., and Dengler, L.A., 2011, Evaluation of the use of paleotsunami deposits to reconstruct inundation distance and runup heights associated with prehistoric inundation events, Crescent City, southern Cascadia margin: Earth Surface Processes and Landforms, v. 36, no. 7, p. 967–980.
Phleger, F.B., 1967, Marsh foraminiferal patterns, Pacific coast of North America: Anales de Instituto Biolología Universidad Nacional Autónoma de México 38, Series Cienco Del Mar y Limnolologie, v. 1, p. 11–38.
Phleger, F.B, 1970, Foraminiferal populations and marine marsh processes: Limnology and Oceanography, v. 15, p. 522–534.
Pilarczyk, J.E., Horton, B.P., Witter, R.C., Vane, C.H., Chagué-Goff, C., and Goff, J., 2012, Sedimentary and foraminiferal evidence of the 2011 Tohoku-oki tsunami on the Sendai coastal plain, Japan: Sedimentary Geology, v. 208, p. 78–89.
Piperno, D.R., 1988, Phytolith analysis—An archaeological and geological perspective: San Diego, Calif., Academic Press, 280 p.
Porter, K., Byers, W., Dykstra, D., Lim, A., Lynett, P., Ratliff, J., Scawthorn, C., Wein, A., and Wilson, R., 2013, The SAFRR tsunami scenario—Physical damage in California, chap. E *of* Ross, S.L., and Jones, L.M., eds., the SAFRR (Science Application for Risk Reduction) tsunami scenario: U.S. Geological Survey Open-File Report 2013–1170 and California Geological Survey Special Report 229, 168 p., http://pubs.usgs.gov/of/2013/1170/e/.
Richmond, B.M., Buckley, M., Etienne, S., Chagué-Goff, C., Clark, K., Goff, J., Dominey-Howes, D., and Strotz, L., 2011, Deposits, flow characteristics, and landscape change resulting from the

September 2009 South Pacific tsunami in the Samoan islands: Earth Science Review, v. 107, p. 38–51.
Richmond, B.M., Szczucinski, W., Chagué-Goff, C., Goto, K., Sugawara, D., Witter, R., Tappin, D.R., Jaffe, B., Fujini, S., Nishimura, Y., and Goff, J., 2012, Erosion, deposition and landscape change on the Sendai coastal plain, Japan, resulting from the March 2011 Tohoku-oki tsunami: Sedimentary Geology, v. 282, p. 27–39.
Robbins, J.A., and Edgington, D.N., 1975, Determination of recent sedimentation rates in Lake Michigan using Pb-210 and CS-137: Geochimica et Cosmochimica Acta, v. 39, p. 285–304.
Ross, S.L., Boore, D.M., Fisher, M.A., Frankel, A.D., Geist, E.L., Hudnut, K.W., Kayen, R.E., Lee, H.J., Normark, W.R., and Wong, F.L., 2004, Comments on potential geologic and seismic hazards affecting coastal Ventura county, California: U.S. Geological Survey Open-File Report 2004-1286, 20 p.
Satake, K., Wang, K.L., and Atwater B.F., 2003, Fault slip and seismic moment of the 1700 Cascadia earthquake inferred from Japanese tsunami descriptions: Journal of Geophysical Research, v. 108, p. 2535, doi:10.1029/2003JB002521.
Sawai, Y., 2002, Evidence for 17th century tsunamis generated on the Kuril–Kamchatka subduction zone, Lake Tokotan, Hokkaido, Japan: Journal of Asian Earth Science, v. 20, p. 903–911.
Sawai, Y., Jankaew, K., Martin, M.E., Prendergast, A., Choowong, M., and Charoentitirat, T., 2009, Diatom assemblages in tsunami deposits associated with the 2004 Indian Ocean tsunami at Phra Thong Island: Marine Micropaleontology, v. 73, p. 70–79.
Schlichting, R.B., and Peterson, C.D., 2006. Mapped overland distance of paleotsunami high-velocity inundation in back-barrier wetlands of the central Cascadia margin, U.S.A.: Journal of Geology, v. 114, no. 5, p. 577-592.
Scott, D.K., and Leckie, R.M., 1990, Marsh foraminifera of Prince Edward Island—Their recent distribution and application for former sea level studies: Maritime Sediments and Maritime Geology, v. 17, p. 98–129.
Senan, F.J., and Vitoria, F.M.A., 1813, Baptismal Entries: Santa Barbara Mission Archives Document CMD, 943a.
San Francisco Estuary Institute, 2009, Historical wetlands of the southern California coast—An atlas of US Coast Survey T-sheets 1851–1889: San Francisco Estuary Institute, available at http://www.sfei.org/node/2873.
Shanmugam, G., 2012, Process-sedimentological challenges in distinguishing paleo-tsunami deposits: Natural Hazards, v. 63, p. 5–30.
Shi, S., Dawson, A.G., and Smith, D.E., 1995, Coastal sedimentation associated with the December 12th, 1992 tsunami in Flores, Indonesia: Pure and Applied Geophysics, v. 144, p. 525–536.
Soloviev, S.L., 1968, The Sanak Kodiak Island tsunami of 1788 [in Russian]: Moscow, Nauka, The Tsunami Problem, Moscow, Nauka, p. 232–237. [English translation in Science of Tsunami Hazards, v. 8, no. 1, p. 34-38, 1990.]
Soulsby, R.L., Smith, D.E., and Ruffman, A., 2007. Reconstructing tsunami run-up from sedimentary characteristics – a simple mathematical model: Coastal Sediments 2007, p. 1075-1088.
Spiske, M, Weiss, R., Bahlburg, H., Roskosch, J., and Amijaya, H., 2010, The TsuSedMod inversion model applied to the deposits of the 2004 Sumatra and 2006 Java tsunami and implications for estimating flow parameters of paleo-tsunami: Sedimentary Geology, v. 224, p. 29–37, doi:10.1016/j.sedgeo.2009.12.005.
Stoermer, E.F., and Stol, J.P., 1999, The diatoms—Applications for the environmental and earth sciences: Cambridge University Press, 469 p.
Striplen, C.J., Grossinger, R.M., and Collins, J.N., 2004, Wetland habitat changes in the Rodeo Lagoon watershed, Golden Gate National Recreation Area, Marin County, CA: San Francisco Estuary

Institute, Technical Report of the Historical Ecology and Wetland Programs, SFEI Contribution 116, 36 p.
Szczuciński, W., Chaimanee, N., Niedzielski, P., Rachlewicz, G., Tepsuwan, T., Lorenc, S., and Siepak, J., 2006, Environmental and geological impacts of the 26 December 2004 tsunami in coastal zone of Thailand—Overview of short and long-term effects: Polish Journal of Environmental Studies, v. 15, no. 5, p. 793–810.
Szczuciński , W., Kokociński, M., Rzeszewski, M., Chagué-Goff, C., Cachão, M., Goto, K., and Sugawara, D., 2012, Sediment sources and sedimentation processes of 2011 Tohoku-oki tsunami deposits on the Sendai Plain, Japan—Insights from diatoms, nannoliths and grain size distribution: Sedimentary Geology, v. 282, p. 40–56.
Thio, H.K., 2010, Probabilistic tsunami hazard in California: URS Corporation report for CalTrans/Pacific Earthquake Engineering Research Center, January 5, 2010, 61 p.
Torrey Pines State Natural Reserve, 2013, Geology of Torrey Pines State Natural Reserve: available at http://www.torreypine.org/index.html.
Trask, J.B., 1856, On earthquakes in California, 1812 –1855: San Francisco, Proceedings of the California Academy of Natural Sciences, series 1, v. 1, no. 2, p. 80-82.
Tuttle, M.P., Ruffman, A., Anderson, T., and Jeter, H., 2004. Distinguishing tsunami from storm deposits in Eastern North America: the 1929 Grand Banks tsunami versus the 1991 Halloween storm: Seismological Research Letters, v. 75, p. 131-177.
U.S. Fish and Wildlife Service, 2013, National wetlands inventory—California, Region 3: Washington, D.C., United States Department of the Interior, Fish and Wildlife Service, Project ID: RO1Y07P11_So_CA-grant_area_3 http://www.fws.gov/wetlands/Wetlands-Mapper.html.
U.S. Geological Survey, 2004, Quaternary fault and fold database of the United States: U.S. Geological Survey, available at http://earthquakes.usgs.gov/hazards/qfaults/.
U.S. Army Corps of Engineers, 2002, Bolinas Lagoon Ecosystem Restoration Project, Draft Feasibility Study: Marin County, California, U.S. Army Corps of Engineers, San Francisco Division.
University of Southern California Tsunami Research Center, 2013, 1964 Alaskan tsunami: Accessed January 2013 at http://www.usc.edu/dept/tsunamis/alaska/1964/webpages/index.html.
Uslu, B., 2008, Deterministic and probabilistic tsunami studies in California from near and farfield sources: University of Southern California, Department of Civil Engineering, Ph.D. dissertation, 194 p.
Vos, P., and de Wolf, H., 1993, Diatoms as a tool for reconstructing sediment environments in coastal wetlands—Methodological aspects: Hydrobiologia, v. 269–270, p. 285–296.
Warrick, J.A., and Mertes, L.A.K., 2009, Sediment yield from the tectonically active semi arid Western Transverse Ranges of California: Geological Society of America Bulletin, v. 121, no. 7–8, p. 1054–1070.
Watson, E.B., Wasson, K., Pasternack, G.B., Woolfolk, A., Van Dyke, E., Gray, A.B., Pakenham, A., and Wheatcroft, R.A., 2011, Applications from paleoecology to environmental management and restoration in a dynamic coastal environment: Restoration Ecology, v. 19, p. 765–775, doi:10.1111/j.1526-100X.2010.00722.x.
Wilson, R.I., Barberopoulou, A., Miller, K.M., Goltz, J.D., and Synolakis, C.E., 2008, New maximum tsunami inundation maps for use by local emergency planners in the State of California, USA [abs.]: Eos (American Geophysical Union Transactions), v. 89, no. 53, Fall meeting supplement, abs. OS43D-1343.
Wilson, R.I., Barberopoulou, A., Borrero, J.C., Bryant, W.A., Dengler, L.A., Goltz, J.D., Legg, M.R., McGuire, T., Miller, K.M., Real, C.R., Synolakis, C.E., and Uslu, B., 2010, Development of new databases for tsunami hazard analysis in California [abs.], *in* Lee, W.H.K., Kirby, S.H., and Diggles,

M.F., compilers, Program and abstracts of the second tsunami source workshop, July 19–20, 2010: U.S. Geological Survey Open-File Report 2010-1152, p. 31.
Wilson, R., Admire, A., Borrero, J., Dengler, L., Legg, M., Lynett, P., Miller, K., Ritchie, A., Sterling, K., McCrink, T., and Whitmore, P., 2013, Observations and impacts from the 2010 Chilean and 2011 Japanese tsunami in California (USA): Pure and Applied Geophysics, v. 170, no. 6-8: p. 1127-1147.
Wilson, R.I., Hemphill-Haley, E., and Admire, A., 2012, A robust tsunami deposit database for California [abs.]: American Geophysical Union Fall Meeting, abs. NH33A-1642.
Witkowski, A., Lange-Bertalot, H., and Metzeltin, D., 2000, Diatom flora of marine coasts I, Lange-Bertalot, H., ed.: Vaduz, Liechtenstein, A.R.G. Gantner-Verlag, Iconographia Diatomologica (Annotated diatom monographs, ed. by Lange-Bertalot, H.), v. 7, 925 p.
Witter, R.C., 2008, Prehistoric Cascadia tsunami inundation and runup at Cannon Beach, Oregon: Oregon Department of Geology and Mineral Industries, Open-File Report O-08-12, 36 p. plus appendix.
Witter, R.C., Hemphill-Haley, E., Hart, R., and Gay, L., 2009, Tracking prehistoric tsunami deposits at Nestucca Bay, Oregon: U.S. Geological Survey National Earthquake Hazards Reduction Program [NEHRP] Final Technical Report 08HQGR0076, 92 p.
Witter, R.C., Jaffe, B.E., Zhang, Y., and Priest, G., 2012, Reconstructing hydrodynamic flow parameters of the 1700 tsunami at Cannon Beach, Oregon, USA: Natural Hazards, v. 63, no. 1, p. 223–240, doi:10.1007/s11069-011-9912-7.
Wood, N., Ratliff, J., Peters, J., and Shoaf, K.,, 2013, Population vulnerability and evacuation challenges in California for the SAFRR tsunami scenario, chap. I *of* Ross, S.L., and Jones, L.M., eds., the SAFRR (Science Application for Risk Reduction) tsunami scenario: U.S. Geological Survey Open-File Report 2013–1170 and California Geological Survey Special Report 229, 168 p., http://pubs.usgs.gov/of/2013/1170/i/.
Wright, T.L., 1991, Structural geology and tectonic evolution of the Los Angeles Basin, California, *in* Biddle, K.T., ed., Active margin basins: American Association of Petroleum Geologists Memoir 52, p. 35–134.
Zoback, M.L., Jachens, R.C., and Olson, J.A., 1999, Abrupt along-strike change in tectonic style—San Andreas fault zone, San Francisco Peninsula: Journal of Geophysical Research, v. 104, p. 10719–10742.